Motion Artifact Reduction of Electrocardiograms Using Multiple Motion Sensors

A Thesis Submitted to the College of
Graduate Studies and Research
In Partial Fulfillment of the Requirements
For the Degree of Master of Science
In the Department of Electrical Engineering
University of Saskatchewan
Saskatoon

by

Joseph Schneider

Permission to Use

In presenting this thesis in partial fulfilment of the requirements for a Postgraduate degree from the University of Saskatchewan, I agree that the Libraries of this University may make it freely available for inspection. I further agree that permission for copying of this thesis in any manner, in whole or in part, for scholarly purposes may be granted by the professor or professors who supervised my thesis work or, in their absence, by the Head of the Department or the Dean of the College in which my thesis work was done. It is understood that any copying or publication or use of this thesis or parts thereof for financial gain shall not be allowed without my written permission. It is also understood that due recognition shall be given to me and to the University of Saskatchewan in any scholarly use which may be made of any material in my thesis.

Requests for permission to copy or to make other use of material in this thesis in whole or part should be addressed to:

Head of the Department of Electrical Engineering
57 Campus Drive
University of Saskatchewan
Saskatoon, Saskatchewan
S7N 5A9

Abstract

An electrocardiogram (ECG) is a measurement of the electrical signal produced by the heart as it beats. This is a signal very commonly used by medical professionals, as it gives an indication of an individual's heart rate and can further be used to detect specific abnormalities within the heart. There are a number of sources of noise that can corrupt the ECG signal, the most problematic being that of motion artifacts. As an individual wearing a surface ECG moves, their movements will add noise to the signal. This noise is particularly difficult to remove, as it will change depending on the movements of the user and will often fall in the same spectrum as the ECG signal itself.

The effectiveness of the adaptive filtering method in reducing motion artifacts is investigated using multiple motion sensors on key locations of the body and by combining the motion data through the use of various blind source separation methods. An adaptive filter is a filter that can use a reference signal in order to readjust itself to a constantly changing noise signal and is commonly used to clean ECG signals. The adaptive filter uses noise estimations based on the reference signal as well as previous noise estimations in order to continually clean the noisy signal. Since motion artifacts are based directly off the movements of the user, collected motion data will be directly correlated with the noise being introduced to the ECG, and can therefore be used in the adaptive filter to produce a desirable ECG signal.

Acknowledgements

I would like to express my gratitude for my supervisor, Prof. Daniel Teng, for his support and immense patience throughout my work. This thesis would not have been possible without his continued guidance. I would like to thank Dr. Jenny Basran. Her medical insights provided a very important perspective that would have been sorely lacking otherwise. I would also like to extend my thanks to my defense examiners, Prof. Ron Bolton, Prof. Denard Lynch, and Prof. Fangxiang Wu, for their invaluable critiques and feedback.

I would like to show my appreciation to Dr. Vanina Dal Bello-Hass and Xiaoye Xia, who I worked closely with in putting together the experiments in this work, and to Zheng Qian, who selflessly assisted with data collection. They helped make this work possible.

Finally, I would like to show my deepest gratitude for my family and, in particular, my significant other Heather Beaulieu. I would not have been able to complete this work without their continuous encouragement and their bottomless patience.

Table of Contents

List of Figures

List of Tables

List of Abbreviations

BSS	Blind Source Separation
ECG	Electrocardiogram
EMG	Electromyogram
FANFARE	Fall and Near Falls Assessment and Research Evaluation
ICA	Independent Component Analysis
LMS	Least Mean Square
PCA	Principal Component Analysis
RLS	Recursive Least Square

1 Introduction

Healthcare is a continuously developing field, constantly offering new obstacles and challenges. As healthcare improves, life expectancy increases and the general population grows, both of which ultimately place higher demands on the healthcare system. An easier lifestyle has led to increases in obesity, itself leading into an increase in such diseases as diabetes. Altogether, the healthcare industry has much more to deal with than ever before and a limited amount of resources with which to handle it all. This has all led to the need for technological solutions to ease the burden on the current system.

A body area network is a planned method to assist medical professionals in the monitoring of large quantities of patients while improving the quality of life for those that need ambulatory monitoring. A body area network opens new possibilities in how much data one can realistically have available to work with and how the data can be combined. One opportunity allowed by the system is how one can approach motion artifact reduction in electrocardiograms.

1.1 Body Area Network

A body area network is a planned system for wireless medical applications. The essential premise behind a body area network is that patients will wear a variety of sensor nodes distributed on their body, collecting necessary data from their vital signs. This data is wirelessly transmitted for use by medical professionals. This system has two major benefits. First, it provides more information for medical professionals, allowing for more accurate diagnosis. Second, it can better allow for patients to be monitored within their own homes, both increasing patient comfort and reducing the demands on hospitals and other healthcare establishments.

The data provided by a body area network could be used to monitor any developing conditions, provide early warnings to the patient for sudden threats such as fainting or seizures, provide an alarm to the appropriate organizations in the event of an accident, or

generally provide data for analysis among medical researchers. As the system develops, it could further be used to offer direct medical assistance over extensive periods of time, such as automatically injecting insulin when a diabetic's blood level calls for it [1]. Broadly speaking, its intention is to make monitoring and body regulation less intrusive for the patients while still securely providing all necessary information for the medical professionals.

One of the promising aspects of a body area network is that each node can collect data from multiple vital signs simultaneously, all ultimately transmitted to a single destination. This not only means that the medical professional will have more data to work with, but that the data can be used alongside each other in real time to improve the quality of the received data itself. One particular example that will be discussed is that of using motion data in order to improve the data provided by an electrocardiogram. The proposed FANFARE project is a body area network that would benefit from the use of motion data in improving electrocardiogram quality while using strictly the data already needed to directly achieve the goals of the project.

1.2 FANFARE

The FANFARE (Fall and Near-Falls Assessment and Research Evaluation) project is a project designed around the concept of determining what may be the causes of unexpected falls, particularly among the elderly [2]. The aim of the project is to develop a system of sensor nodes that can detect falls and near-falls, as well as recording various vitals involved at the time of the incident. A recent study under the project involved the use of multiple motion sensors worn over the body in order to help determine a fall or near-fall incident.

While the immediate goal of the project is to detect falls and near-falls, it ultimately aims to determine the causes of falls and near-falls through an analysis of the vitals during these events. The activity of the heart is one of the most important vitals to investigate, meaning that use of an ECG within the project will assist in the understanding of falls. The data from the various motion sensors can be used on the ECG data in order to reduce the amount of noise introduced by motion.

1.3 Electrocardiogram

The electrocardiogram (ECG) is a recording of the signal produced by the electrical activity of the heart. Abnormalities in the heart rhythm are indicative of a variety of medical issues, many of which are very serious. As such, the ECG is very commonly used in diagnosis.

Accurate diagnosis of an ECG requires it to be largely free of noise. Noise can corrupt an ECG signal to the degree that it becomes largely unreadable and may lead to incorrect diagnosis for the patient. Motion artifacts, caused by disruption of the contact between ECG electrodes and the skin, are one of the most problematic sources of noise in an ECG. This is due to the fact that traditional filters cannot be used to remove the motion artifacts without removing part of the desired ECG signal itself.

One method investigated in research to remove motion artifacts from an ECG is to apply an adaptive filter with the use of motion data from an accelerometer. The goal of this work is to expand that research by more thoroughly investigating adaptive filtering with motion sensors, particularly with respect to the location of the motion sensor on the body. From there, the possibility of combining motion data from multiple sensors to improve the effectiveness of the filtering will be pursued. For a clearer understanding of how this goal will be achieved, the broad objectives of this work will be discussed, followed by an overall outline of the rest of this thesis.

1.4 Objectives

The goals of this work can be broken down as follows.

1. To select the best single motion sensing device and axis for use in standard single input adaptive filtering of ECGs.
2. To investigate the differences in adaptive filtering methods on ECGs using motion data.
3. To compare the results of adaptive filtering of ECG based on location of the motion sensor on the body.
4. To analyze the results of adaptive filtering with respect to the motion being performed, the degree of skin preparation prior to applying the ECG, the

difference in user performing the motions, and the frequency of ECG and motion data collection.

5. To attempt to improve on single motion sensor adaptive filtering by combining motion data using blind source separation methods for preprocessing.

1.5 Outline

This work will begin with a look at existing literature in Chapter 2, delving into the technical aspects of the electrocardiogram to better understand the challenges of filtering and why it is needed. An examination of adaptive filtering and blind source separation will follow, including their prior uses in filtering ECGs and their intended use in this work's performed experiments. Chapter 3 will discuss the performed experiment, including the sensors used, the overall process for the data collection, and some of the challenges that may have an impact on the results. Chapter 4 follows with some early tests performed to justify certain decisions made during analysis as well as to verify the use of the selected algorithms. Chapter 5 presents the results of both filtering with the use of single sensors and filtering through the combination of multiple sensors. The results are examined from the perspective of the motions being performed, the degree of skin preparation prior to applying the electrodes, the sampling frequency used in motion and ECG data collection, and the use of different test subjects in collecting the data. Finally, Chapter 6 summarizes the results as well as discussing future work that could yet be accomplished.

2 Background

Additional information is necessary to understand the performed experiments and the results of their analysis. Three major areas must be examined in depth. First, a closer look at the details of the ECG is necessary. Second, the adaptive filter and its major algorithms must be explored. Finally, an understanding of blind source separation and a number of its methods is required.

2.1 ECG Info

Before methods for reducing noise in an ECG can be discussed, a better understanding of the ECG itself is required. ECG devices are examined in order to provide a clearer picture of how the signal is collected and the situations where noise reduction is required. The ECG signal itself is examined, describing how the signal is created by the heart's activity and how the signal is typically described. Finally, the sources of noise in an ECG are examined to explain how the signal can be corrupted, how they interfere with the signal itself, and how they are typically handled.

2.1.1 ECG Devices

ECG devices generally collect data using a series of electrodes. These electrodes are secured to the body using a pad and gel. The pads are typically disposable, offering a simple attachment for the leads of the ECG device. The number of electrodes can vary. 12-lead is the customary clinical ECG, using a total of ten electrodes. Some go as few as 1-lead. The number of electrodes is a balance between patient convenience and reliability. 1-lead is yet generally unusable, simply due to its unreliability [3]. 12-leads are highly accurate and provide the most data, but the sheer number of electrodes can be too inconvenient for the patient, particularly if they are expected to wear the device for extended periods of time or even to regularly take off and put on the device themselves.

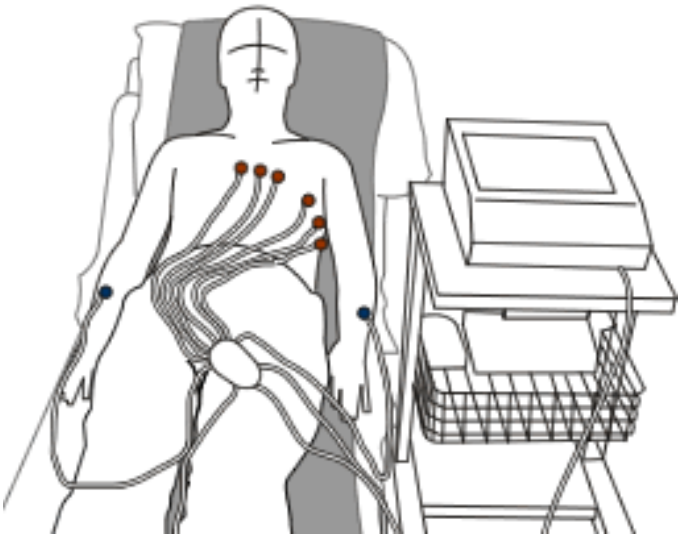

Figure 2.1: Patient wearing 12-lead ECG [4]

A number of steps must be taken in preparation for electrode application in order to ensure the most accurate results are obtained [5]. The skin must be shaved and cleaned. Hair and dirt can both impede the results and lead to noisier data. In addition, the later removal of the electrodes will lead to significant discomfort for the patient if hair was present during application. Finally, an abrasive should be used to remove part of the outer layer of skin to further improve the signal.

There are a number of different ECG devices available for use. In the case of short-term use, as when undergoing a stress test or during events of medical emergency, the 12-lead devices are best used. An example of a patient wearing a 12-lead ECG is depicted in Figure 2.1. Medical professionals are available during these periods and the inconvenience to the patient is minimal. These generally provide simple real time data. However, when going into long term use of ECG, there are a number of devices available for use. The need for these devices occurs when a patient has infrequent symptoms that may not necessarily occur during their stay in a medical environment. They need to wear ECG devices as they go about their daily lives. For these situations there are three different possibilities available. These are the Holter Monitors, Loop Recorders, and Implantable Loop Recorders [6].

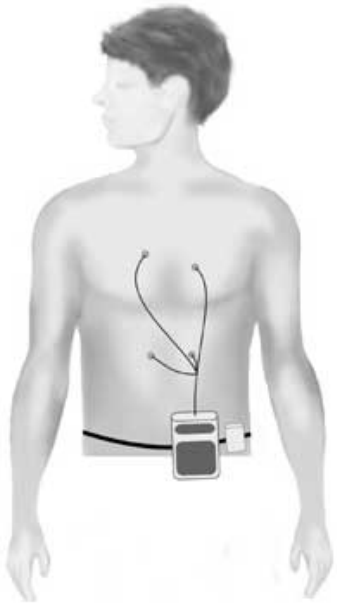

Figure 2.2: Patient wearing Holter monitor [7]

Holter Monitors are portable devices that record ECG data over the entire period of time they are being used. They use surface electrodes as previously discussed, ranging from 3-lead to 12-lead. Figure 2.2 depicts an example of a patient wearing a 3-lead Holter monitor. Loop Recorders are similar devices, only they do not store all data over time. Rather, they only store a particular window of data. When the patient suffers the medical symptom under investigation, they press a button on the device. The device then properly stores data from a brief time before the event to a brief time after the event. Implantable Loop Recorders are devices that are surgically placed inside the patient. Similar to the Loop Recorders, they need to be activated by the patient in order to store the data upon undergoing the medical symptom.

The main differences between the three devices are that of battery life, reliability, and convenience. Holter Monitors and Loop Recorders both require the patient to be able to apply the electrodes properly as they both are used over long periods of time. Wearing the devices can be an inconvenience for two reasons. The first is simply the bulk of the device and the electrodes that hang from the body. The other is the potential irritation to the skin, from the gel securing the electrodes or the preparation needed for accurate results. The battery life of a Holter Monitor is relatively short due to the fact it is constantly storing data. As a result, it needs periodic recharging. However, Loop

Recorders collect only a short window of data and require the patient to remember to activate it, reducing their reliability in terms of capturing the desired event. Implantable Loop Recorders have the longest battery life and don't have the inconveniences of external electrodes, but the simple fact they require surgery to be used can be a significant obstacle.

2.1.2 ECG Signals

A single heartbeat starts with the depolarization of cells located in the right atrium of the heart, travelling through to the ventricles. The depolarization of the heart muscles causes them to contract. The electrical activity therefore controls the beating of the heart. This electrical activity can be detected with an ECG, with the resulting signal representing the activity of the heart [8].

The ECG representation of a heartbeat can be divided into three main periods of activity, each separated by a period of silence. Figure 2.3 provides an example of an ECG of a single heartbeat. The P wave represents the depolarization of the atriums. The repolarization of the atriums is not detected by the ECG. The following pause is known as the PR segment. This is then followed by the depolarization of the ventricles, which creates the QRS complex. This is notably larger than the P wave, due to the significantly larger size of the ventricles when compared to the atriums. Another pause follows, known as the ST segment. Finally, the repolarization of the ventricles results in the T wave. The process will repeat the next time the heart beats.

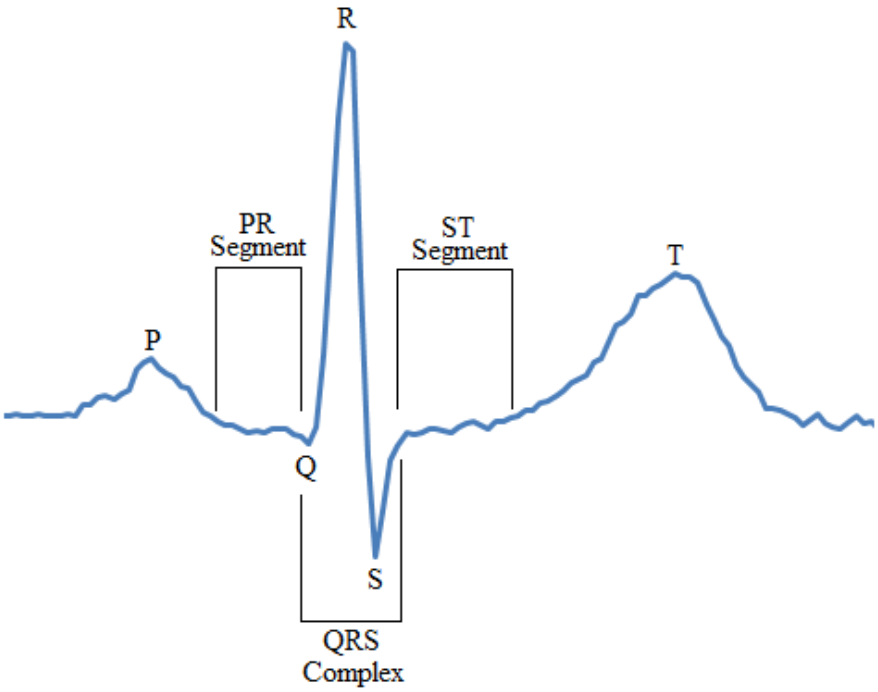

Figure 2.3: Components of an ECG signal

The signal has two major uses for medical professionals. First, the peaks of the signal can be used to determine the wearer's heart rate. Secondly, the shape of the signal demonstrates how the heart is beating. Abnormalities in the signal indicate an abnormality within the heart. An understanding of the various potential medical issues allows a medical professional to make an accurate diagnosis for the patient using the ECG. If the data during a medical event is corrupted by noise, proper diagnosis becomes difficult.

The best way to avoid motion artifacts is simply proper preparation and application of the ECG's electrodes. However, this cannot always be relied on in the events of long term monitoring where the patient is expected to apply the ECG themselves While medical professionals can be relied on for proper application of the ECG, the patient may be considerably less thorough, particularly when they must use the ECG for several days or even weeks. In these cases, successful reduction in motion artifacts will allow for successful readings of the ECG when they would have otherwise been unreadable. Further, successful elimination of motion artifacts means that the step of abrasion in preparation for an ECG can potentially be removed, meaning less distress for the patient when an ECG is to be applied.

2.1.3 Sources of Noise in ECGs

The primary sources of noise for an ECG are baseline wander, power line interference, electromyogram (EMG), and motion artifacts [9]. The power line interference is electrical noise that occurs at 50 or 60 Hz, depending on the country of use. The EMG signal is caused by the electrical activities of the muscles during motion and typically occurs at high frequencies, from 50 Hz to 10 kHz. Baseline wander is caused by respiration and movement, typically at low frequencies at 0.3 Hz and lower [10]. Motion artifacts are caused by the disruption of contact between the electrode and the skin and are found most significantly between 1 to 7 Hz [11].

Power line interference, baseline wander, and EMG noise can largely be solved with the use of traditional filters. A notch filter can remove the power line interference at 50/60 Hz. A low pass filter can remove the EMG noise. A high pass filter can remove the baseline wander, though it may remain in the spectrum of the ECG depending on its severity. The high pass and low pass filters are typically placed respectively at 0.05 Hz and 100 Hz for general diagnosis and at 0.05 Hz and 35 Hz for patient monitoring [12]. However, this will still leave motion artifacts, as its noise is found entirely within the ECG spectrum. Traditional filtering is not sufficient to remove motion artifacts, so other methods must be explored to solve this problem.

Figure 2.4 demonstrates the effects of motion artifacts and remaining baseline wander in an ECG that has already been put through a low pass filter and a high pass filter. The motion artifacts severely corrupt the ECG signal, often making the P and T waves difficult to distinguish. The original baseline is noted in the figure to demonstrate how significantly the ECG can be affected by baseline wander, the wander in this particular case starting at the third full ECG signal.

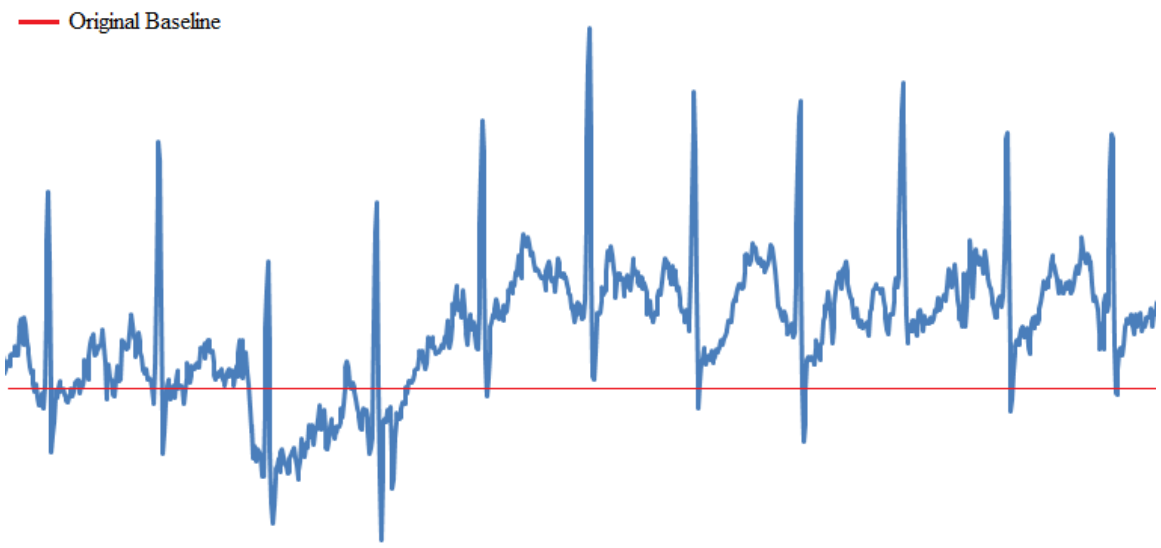

Figure 2.4: Example of ECG motion artifacts and baseline wander

One of the larger areas of modern research in reducing motion artifacts is that of adaptive filtering. Generally speaking, adaptive filtering is a filter that uses either feedback or an additional source of input in order to continuously adjust the filter being applied. This is especially useful in cases where the noise does not have any single model but is rather continuously changing. Noise introduced due to motion will change in a manner directly related to that motion, due to both the nature of the motion itself and the intensity of that motion [13]. The motion of the human body is the cause of the contact disruption between the body and the electrodes. Therefore, it is intuitive to say that adaptive filters should be particularly effective at suppressing motion artifacts.

2.2 Adaptive Filtering

Adaptive filters can be used in a wide range of applications. For the case of removing motion artifacts from an ECG, the desired format for use is that of noise cancellation. The block diagram for this approach can be seen in Figure 2.5, where d represents the desired signal corrupted with noise, x represents the reference signal used to remove the noise, y represents the corrected signal, and e represents the estimated error. Filter weights are updated iteratively based on the reference signal input and the estimated error.

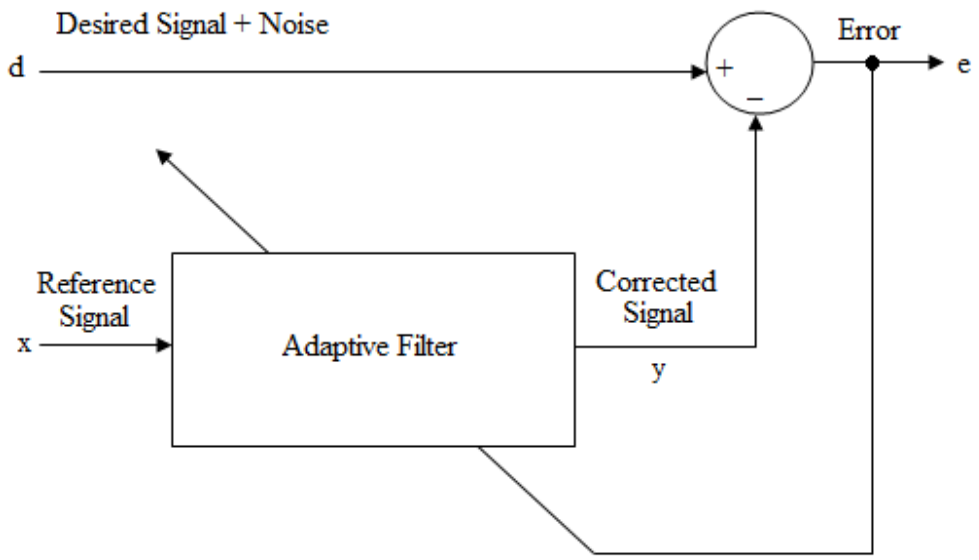

Figure 2.5: Block diagram of noise cancellation in adaptive filtering

The system works when the original input signal is uncorrelated with the noise while the reference signal is correlated with the noise. All input signals are statistically stationary and have zero means. The output of the system is defined as in Eq. 2.2.1.

$$e^2 = s^2 + (q - y)^2 + 2s(q - y) \tag{2.2.1}$$

where s denotes the original signal and q denotes the noise. The expectation of Eq. 2.2.1 reduces as follows.

$$E\{e^2\} = E\{s^2\} + E\{(q - y)^2\} + 2E\{s(q - y)\} = E\{s^2\} + E\{(q - y)^2\} \tag{2.2.2}$$

Adapting the filter to minimize the error energy will not affect the signal. Therefore, as Eq. 2.2.3 demonstrates, minimizing the total output energy will minimize the noise energy, which is generally done using numerical methods.

$$E_{min}\{e^2\} = E\{s^2\} + E_{\min}\{(q - y)^2\} \tag{2.2.3}$$

The most significant part of adaptive filtering is the selection of the reference signal. An adaptive filter operates by using a reference signal to change the filter weights over time. If the reference signal is well correlated with the noise introduced to the desired

signal while being entirely uncorrelated with the desired signal itself, it can be used by the adaptive filter to remove the noise from the desired signal.

A good deal of previous work has been done analyzing various approaches to using adaptive filters to remove motion artifacts from ECG signals. The most intuitive reference signal to use in removing motion artifacts is motion data as collected by a sensor such as an accelerometer. Raya *et al.* investigated the use of a single accelerometer attached to the subject's lower back [14]. Tong used an accelerometer attached to the electrodes of the ECG, creating motion artifacts by manipulating the electrode, its wire, and the skin around the electrode [15]. Accelerometer research since includes work focusing on using all of the data from a single 3-axis accelerometer to its fullest. Yoon *et al.* investigates adaptive filtering in an electro-conductive fabric, rotating the axes of the motion data in order to use the motion data normal to the chest plane [16]. Pandey combined all 3 axes of a 3-axis accelerometer by summing their individual power spectrums [17].

Another signal considered for use in adaptive filtering is one that measures skin stretch. The stretching of the skin around the electrodes is the fundamental cause of noise, meaning a signal that properly represents the skin stretch can be an effective reference signal. Hamilton *et al.* uses a displacement sensor on the ECG in order to detect skin stretch [18]. Liu *et al.* makes use of an optical sensor integrated into an electrode to more effectively represent skin stretch [19]. Finally, Lee *et al.* uses a strain gauge to measure skin stretch. In this final case, an accelerometer is used alongside the strain gauge to more effectively reduce noise [20].

A third approach in the use of adaptive filtering to reduce motion artifacts investigates the use of measured electrode-tissue impedance as a reference signal. Buxi *et al.* investigates the correlation between electrode-tissue impedance and motion artifacts in order to validate its use in adaptive filtering [21]. Kim *et al.* directly applies electrode-tissue impedance to the adaptive filtering of motion artifacts [22]

The work using accelerometers in reducing motion artifacts in ECGs have so far only made use of a single accelerometer on the torso. Applying the concept of skin stretch to motion data, one can note that motion artifacts may be induced while the torso remains stationary. Movements of the arms while the torso remains stationary will cause

the skin on the chest to stretch, resulting in motion artifacts in the ECG. Use of a single accelerometer on the torso is therefore an incomplete picture of the motions producing the noise in the ECG. A more thorough investigation of accelerometer placement may lead to an improvement in adaptive filtering using accelerometers.

While the selection of reference signal is crucial to the success of the adaptive filter, the specific algorithm of adaptive filtering used will also have a significant impact on the results. The two most commonly used algorithms in adaptive filtering are Least Mean Squares (LMS) and Recursive Least Squares (RLS). Generally speaking, the LMS algorithm is computationally simpler and so expected to perform quicker of the two, while the RLS algorithm typically converges faster and is expected to provide better filtering results. A more in-depth discussion of each algorithm follows.

2.2.1 Least Mean Squares

The Least Mean Squares algorithm is an adaptive filter that uses a gradient descent method in order to minimize the mean square error [23]. The gradient descent method itself is an iterative method that uses a weight vector to filter the input. The filtered output is updated according to Eq. 2.2.4.

$$y[n] = \mathbf{w}^{\mathrm{T}}\mathbf{x} \tag{2.2.4}$$

where y is the filtered output, $\mathbf{x}$ is the reference signal, and $\mathbf{w}$ is the weight vector. The weight vector is updated every iteration as seen in Eq. 2.2.5.

$$\mathbf{w}[n+1] = \mathbf{w}[n] - \mu\Delta \tag{2.2.5}$$

where Δ is the gradient of the mean square function and μ is a small positive gain factor. Single samples of square error are used to estimate the mean square error. The instantaneous gradient of this estimation can be used, leading to a simplification of the gradient as in Eq. 2.2.6.

$$\Delta = -2e[n]\mathbf{x}[n] \tag{2.2.6}$$

where e is the estimated error.

Substituting Eq. 2.2.6 into Eq. 2.2.5 leads to the final weight update equation as seen in Eq. 2.2.9 and, in turn, the LMS algorithm to filter noisy input d in full. The weight vector is initialized to $\mathbf{w}[0] = 0$.

$$y[n] = \mathbf{w}^{\mathrm{T}}\mathbf{x}[\mathrm{n}] \tag{2.2.7}$$

$$e[n] = d[n] - y[n] \tag{2.2.8}$$

$$\mathbf{w}[n+1] = \mathbf{w}[n] + \mu e[n]\mathbf{x}[n] \tag{2.2.9}$$

The variable of interest in this algorithm is the gain factor μ, as it controls the stability and the convergence of the algorithm. A well chosen gain factor is crucial for the success of the LMS algorithm.

2.2.2 Recursive Least Squares

The essential premise behind the Recursive Least Squares algorithm is that the filter coefficients are updated using both the new sample of information and the past samples of information. The effectiveness of the algorithm is measured against how well the filter coefficients perform for both previous and current times, leading to Eq. 2.2.10.

$$\xi(n) = \sum_{k=0}^{n} \lambda^{n-k} \left| d[k] - \mathbf{w}^{\mathrm{T}}[n]\mathbf{x}[k] \right|^2 \tag{2.2.10}$$

where ξ is the error function, λ is the forgetting factor, d is the noisy input, $\mathbf{w}$ is the weight vector, and $\mathbf{x}$ is the reference signal.

The forgetting factor controls how much weight is given to recent error estimations over older error estimations. It is desirable for more recent errors to have a greater impact on the error function than older errors, in order to more quickly react to changes in the input and the reference signal. As such, the forgetting factor is a positive value close to but less than 1.

The algorithm is developed by taking the derivative of the error function with respect to the weight vector and setting it to 0. Through algebraic manipulation, the resulting iterative algorithm is produced.

$$\mathbf{k}(n) = \lambda^{-1}\mathbf{P}(n-1)\mathbf{x}[n] / (1 + \lambda^{-1}\mathbf{x}^{\mathrm{T}}[n]\mathbf{P}(n-1)\mathbf{x}[n]) \tag{2.2.11}$$

$$e(n) = d[n] - \mathbf{w}^{\mathrm{T}}[n-1]\mathbf{x}[n] \tag{2.2.12}$$

$$\mathbf{w}[n] = \mathbf{w}[n-1] + e(n)\mathbf{k}(n) \tag{2.2.13}$$

$$\mathbf{P}(n) = \lambda^{-1}[\mathbf{P}(n-1) - \mathbf{k}(n)\mathbf{x}^{\mathrm{T}}[n]\mathbf{P}(n-1)] \tag{2.2.14}$$

Similar to LMS, the algorithm is initialized by setting weight vector **w** to 0. The variable **P**, which is in fact the inverse of the autocorrelation of reference signal **x**, must also be initialized. This is done through Eq. 2.2.15.

$$\mathbf{P}(0) = \delta^{-1}\mathbf{I} \tag{2.2.15}$$

where δ is a small positive constant less than 1 and **I** is an identity matrix. This ensures the correlation remains nonsingular [23].

2.3 Blind Source Separation

Adaptive filtering, as described above, can only use a single reference signal as input. In order to use multiple signals at once, as desired with the multiple accelerometers, they must be combined into a single input. Multiple reference single input adaptive filtering, as discussed by Tu [24], describes how multiple reference signals can be summed for use as a single reference signal, so long as they are all uncorrelated with each other. The human body is connected, so while motion sensors on different parts of the body will collect unique information, there will still be shared information between sensors as the trunk of the body moves. Before the motion data can be combined, the individual motions of each individual body part must be separated.

A possible solution can be found in blind source separation (BSS). The aim of BSS is to take a group of signals, known to contain some mixture of desired signals, and to separate them without knowledge of exactly how they are mixed or what their statistical attributes may be. A common example of this is described through the cocktail party problem. In this example, there are a number of individuals in a room talking at the same time. A number of microphones are set up around the room, each one receiving all of the unique conversations but at different volumes due to the locations of each microphone. For the sake of the example, the issue of sound traveling is ignored and the conversations are assumed to reach each microphone at the same time. BSS is then a method that can take the mixed data recorded by each individual microphone and use them together to separate the individual conversations.

The basics of BSS can be described broadly by defining the desired source signals as matrix **S** and the measured mixed data as matrix **X**. For successful operation, there must be at least as many mixed signals $x(t)$ as there are source signals $s(t)$, though this work will work with the assumption that there are n vectors of each. There will then be an unknown n x n matrix **A** mixing the source signals into the measured mixed signals.

$$\mathbf{X} = \mathbf{AS} \tag{2.3.1}$$

Therefore, there must exist a matrix **W** that can unmix the signals and retrieve the desired source signals.

$$\mathbf{Y} = \mathbf{WX} \tag{2.3.2}$$

$$\mathbf{W} = \mathbf{A}^{-1} \tag{2.3.3}$$

$$\mathbf{Y} = \mathbf{S} \tag{2.3.4}$$

The case of body movement can potentially be solved through BSS. The motions of the arms are going to be mixed with the motion of the torso due to how they are inherently connected. Their motion data will need to be separated before they can be summed for use in adaptive filtering. BSS is a large grouping of many different approaches. Two possible methods within BSS that will be examined are independent component analysis (ICA) and principal component analysis (PCA).

The use of ICA starts with an assumption that every set of data under investigation is statistically independent of each other. This leads to the question of whether it is safe to assume that the motion of the torso and the motion of the arms can be considered independent. Fortuna *et al.* suggests that it is safe to assume that 3D point measurements on a body can be considered independent [25]. Sigalas *et al.* proposes that tracking the movement of one arm is statistically independent of the track of the other arm, with the orientation of the torso being independent of the track of the arm [26]. Taken together, it appears to be safe to move forward on the assumption that the movement of the torso and arms can be considered independent of each other.

ICA has been used in various biomedical applications, including uses in conjunction with ECGs. It has been implemented in order to separate the ECG signals of a fetus and their mother [27, 28]. It has been used to separate the ECG signal from an

electroencephalography signal [29]. It has additionally been used as a method to remove noise from ECGs, applying ICA between the signals provided from multiple electrodes. One case did so using electrodes integrated into clothing [30] and another using standard electrodes implemented within a custom patch [31].

Prior work has been done in regards to ICA applied to motion. One such example measured pose parameters, defined in angles, over 17 parts of the human body. ICA is applied to the pose parameters in order to break down motions of the human body as a whole into a fewer number of independent components [32].

There are multiple methods that fall under the definition of ICA. Two commonly used algorithms are FastICA and Infomax. FastICA is an algorithm used to separate non-Gaussian data while Infomax can be implemented to work with source signals that are either sub-Gaussian or super-Gaussian. The overall goal of ICA is to maximize the independence of the source signals and each algorithm is developed by approaching this goal in different ways. FastICA maximizes the independence of its source signals by aiming to maximize the non-Gaussianity of each source signal. Infomax maximizes the independence of its source signals by minimizing their mutual information [33].

While ICA has been the focus so far, PCA is an additional method used in BSS. The key difference between ICA and PCA is that ICA aims to separate the source signals into independent signals while PCA aims to separate the source signals on the weaker condition of uncorrelation. PCA assumes the signals it is separating are Gaussian. It aims to separate the signals by maximizing their variance [33].

2.3.1 FastICA

FastICA begins with some preprocessing. The mixed data must be centered and whitened. It then aims to determine the unmixing matrix $\mathbf{W}$ that will produce the separated source signals from the mixed data $\mathbf{X}$ through use of an appropriate contrast function *f(u)*. For FastICA, $\mathbf{W}$ is determined column by column. For the first column, $\mathbf{w_1}$ is initialized to a random vector and Eq. 2.3.5 and 2.3.6 are repeated until it converges.

$$\mathbf{w}^{+} = E(\mathbf{X} f\left(\mathbf{w}^{\mathrm{T}}\mathbf{X}\right)) - E\left(f'\left(\mathbf{w}^{\mathrm{T}}\mathbf{X}\right)\right)\mathbf{w} \tag{2.3.5}$$

$$\mathbf{w} = \mathbf{w}^{+}/\left\|\mathbf{w}^{+}\right\| \tag{2.3.6}$$

For every column i after the first, two more steps are added to the above equations before checking for convergence in order to prevent the same signal from being extracted repeatedly.

$$\mathbf{w}_i^+ = \mathbf{w}_i - \sum_{j=1}^{i-1} \mathbf{w}_i^{\mathrm{T}} \mathbf{w}_j \mathbf{w}_j \tag{2.3.7}$$

$$\mathbf{w}_i = \mathbf{w}_i^+ / \left\| \mathbf{w}_i^+ \right\| \tag{2.3.8}$$

The contrast function $f(u)$ is necessary for convergence. There are contrast functions which work for virtually all distributions of independent components, leaving the choice between them strictly a matter of optimization [34]. Two examples of such contrast functions are listed in equations 2.3.9 and 2.3.10.

$$f_1(u) = \tanh(u) \tag{2.3.9}$$

$$f_2(u) = u^3 \tag{2.3.10}$$

2.3.2 Infomax

Similar to FastICA, Infomax requires the mixed data to be centered and whitened before the algorithm is used. The unmixing matrix $\mathbf{W}$ is initialized with random values. From there, Eq. 2.3.11 is repeated until convergence, where $\mathbf{I}$ is an identity matrix, $\mathbf{X}$ is the mixed data, and $g(u)$ is a function depending on whether the data is super-Gaussian or sub-Gaussian. The step size value α is typically set to 0.01 [35].

$$\mathbf{W}^+ = \mathbf{W} + \alpha\left(\mathbf{I} - g(\mathbf{X})\mathbf{X}^{\mathrm{T}}\right)\mathbf{W} \tag{2.3.11}$$

For super-Gaussian data, the function $g(u)$ is set as seen in Eq. 2.3.12.

$$g(u) = \tanh(u) \tag{2.3.12}$$

For sub-Gaussian data, the function $g(u)$ is set as seen in Eq. 2.3.13.

$$g(u) = u - \tanh(u) \tag{2.3.13}$$

2.3.3 PCA

The whitening preprocessing step used in the ICA algorithms is a form of PCA [36]. This can be accomplished through eigenvalue decomposition [37]. The eigenvalues and

eigenvectors of the mixed data's covariance matrix can be combined as in Eq. 2.3.14, where **D** is the diagonal matrix of eigenvalues and **V** is the matrix of eigenvectors.

$$\mathbf{Q} = \mathbf{V}\mathbf{D}^{-1/2}\mathbf{V}^{\mathrm{T}} \tag{2.3.14}$$

The resulting matrix with uncorrelated source signals is then produced by Eq. 2.3.15 and 2.3.16.

$$\mathbf{x} = E(\mathbf{X}) \tag{2.3.15}$$

$$\mathbf{Y} = \mathbf{Q}\mathbf{x} \tag{2.3.16}$$

2.4 Summary

Noise removal of ECGs is important to ensure accurate diagnosis of problems relating to the heart. Motion artifacts are the most problematic source of noise in ECGs due to the fact that they reside in the same spectrum as the ECG itself. Adaptive filtering is one possible technique for the removal of motion artifacts, with LMS and RLS filtering being the most commonly used algorithms.

The goal is to expand the use of motion data in adaptive filtering by making use of multiple motion sensors on the body. For the use of multiple reference single input adaptive filtering, the motion sensors must be uncorrelated before being summed for use. Blind source separation is a technique that can be used to separate the source motions prior to use. FastICA, Infomax, and PCA are specific algorithms of BSS that all work with different data characteristics. They will be investigated as possible candidates for preprocessing the motion data prior to use in filtering.

3 Experiments and Data Collection

In order to test out the planned method for reducing motion artifacts, data must first be collected through performed experiments. The discussion of how the data was collected will be broken into three parts. First, the sensor node selected for use in the experiments and its significant properties will be discussed. The experiments performed with the sensor nodes will then be detailed. Finally, the specifics of how the data was collected with the sensor nodes during the experiments and how the data was prepared for analysis will be presented.

3.1 Shimmer

A quality sensor node for a wearable sensor network must meet a number of important criteria. It must be reasonably small and lightweight, as users are expected to wear them for a significant amount of time. They must have wireless communication capabilities, as wires would be inconvenient for the user. They must also be designed with low power consumption in mind, as they must be used for long periods of time. One commercial example of a sensor node suitable for a wearable sensor network is the Shimmer node.

The Shimmer node, selected for use in the ECG motion experiments, was developed by Shimmer Research. The sensor node was developed specifically with biomedical applications in mind and, as such, the nodes meet the criteria desired for a wearable sensor network. The nodes are expandable with a number of prebuilt sensors for measuring various physiological data as well as a unit for attaching one's own sensors readily available. These expansions, along with the programmable capabilities of the nodes, make them flexible for experiment use. Figure 3.1 shows a single Shimmer Node while Figure 3.2 demonstrates its system diagram.

Figure 3.1: Shimmer node [38]

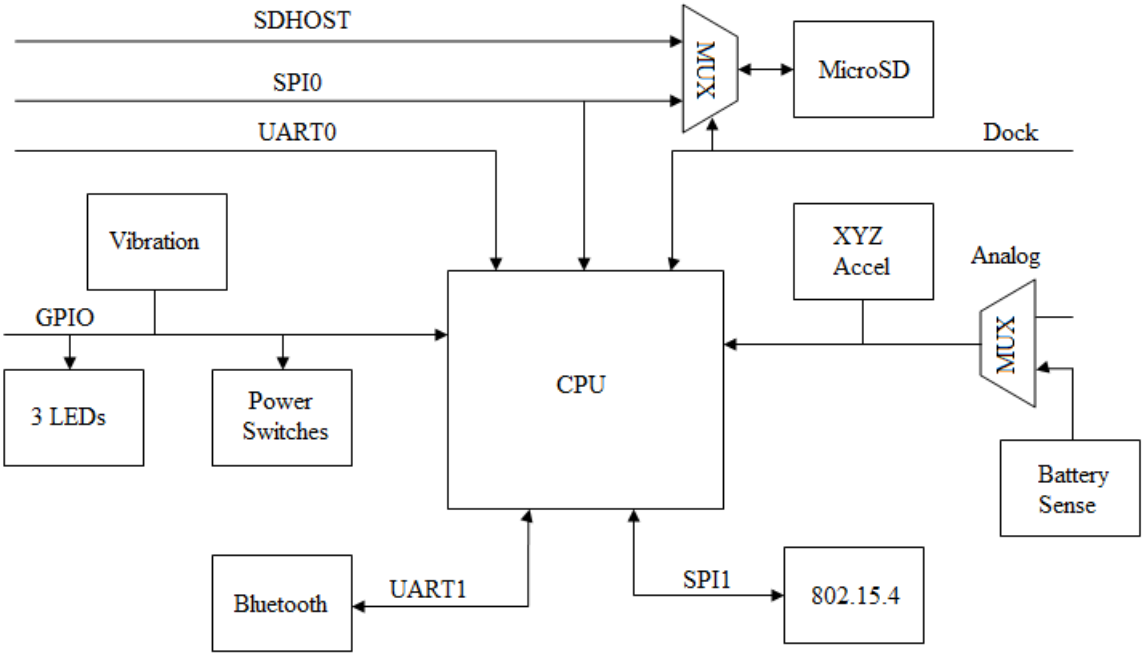

Figure 3.2: Block diagram of a Shimmer node [39]

The base Shimmer sensor node is a unit 53mm × 32mm × 15mm in size, weighing 22g. It runs on Texas Instruments' 16-bit MSP430f1611 low power microprocessor, which operates up to 8 Mhz with 10kB of RAM and 48 kB of flash. It is powered by a 450 mAh battery. It has two radios to communicate with: an 802.15.4 radio and a Bluetooth radio. Every unit has a built in 3-axis Freescale MMA7351 1.5//6g MEMs accelerometer. Available for the user are three individual LEDs that can provide status information and a power button that can either reset or turn off an active node [40, 41].

Available for local file storage on a node is a memory card slot allowing for up to 2GB of memory on a microSD card. Files are all stored in FAT format [42].

Two of the sensor expansions for the base sensor unit are the gyro module, increasing the motion sensing capabilities of the unit, and the ECG module, allowing for the recording of the patient's heart activity. The Shimmer node can only connect to one expansion at a time, so any single sensor node can only use one of either the gyro or the ECG expansion. The gyro expansion increases the size of the sensor node to 53mm x 32mm x 19mm and its weight to 27g. It makes use of the InvenSense 500 series MEMS gyro, which offers ±500°/s with a sensitivity of 2mv/°/s [43]. The ECG expansion increases the size of the sensor node to 53mm x 32mm x 23mm and its weight to 32g. It uses four electrodes and provides information from three leads. Leads II and III are provided directly as outputs while Lead I is computed by subtracting Lead III from Lead II. The frequency of the ECG ranges from 0.05 Hz to 159 Hz [44, 45].

A number of prebuilt firmware applications are available for use with the Shimmer nodes. Users can develop their own custom applications to better suit their individual research goals. The operating environment is TinyOS, an event based environment made for use in low-power wireless systems [46]. It is designed specifically for resource-limited and low-power devices, making it particularly suitable for wearable sensor networks. The language of the coding is nesC. Since the code is based around hardware events, pre-emption occurs regularly. Variables must be appropriately protected to prevent errors.

3.2 Experiment

The broad goal of the experiment is to record the ECG of a user alongside motion data from parts of the body most expected to cause motion artifacts in order to provide sufficient data for analyzing the effects of adaptive filtering. A number of decisions must be made to put together the experiment. Namely, where the sensors will be placed, what data each sensor will collect, and what variables are desired to be tested.

As discussed in Section 2.2, one can intuitively determine that the areas expected to provide the most information for motion artifacts are the torso and the arms. Further, motion data is desired from 3-axis accelerometers and 3-axis gyroscopes, so that the best

axis on the best sensor can be determined for use in adaptive filtering. Together, this leads to a 4 sensor node setup. The first node is on the chest for collecting ECG data. The second and third nodes are placed on the left and right upper arms, both collecting accelerometer and gyroscope data. The fourth and final node is placed on the back, also collecting accelerometer and gyroscope. The node on the back is necessary for use as the node receiving ECG data cannot collect gyroscope data. Figure 3.3 demonstrates the locations of the sensor nodes on a human body.

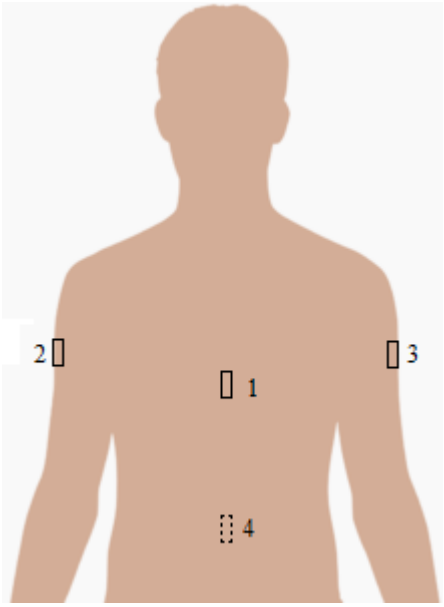

Figure 3.3: Locations of sensor nodes

It is naturally expected that different motions will have different impacts on the amount of motion artifacts introduced into the ECG. Motion selection is therefore an important part of the experiment. Motions are selected to represent a wide variety of motions expected to be performed in day to day activity. This is due to the fact that, as part of the FANFARE project, the sensors are expected to be worn by the elderly over an average day. In order to cover a full range of activities in terms of intensity, each experiment includes at least one trial with a heavier degree of activity.

One variable that needs to be taken into consideration is skin preparation. As discussed in Section 1.3.2, the best way to eliminate motion artifacts is proper skin preparation. Proper cleaning of the area where the electrodes are to be applied has a

significant effect on the amount of motion artifacts that will result in the ECG. Therefore, it is desired to analyze the results of filtering both with proper skin preparation and without proper skin preparation.

Another variable to be looked at is that of sampling frequency. The sampling frequency used tends to vary depending on whether the ECG is being used for diagnostic or for monitoring purposes. Since frequency monitoring of the ECG may vary, it is desired to examine how much of an impact sampling frequency may have on the adaptive filtering process.

Finally, everyone's hearts are shaped differently and everyone moves differently. ECG and motion results will vary from person to person. Since this data is the core of the analysis, it is important to collect data from different users and compare the results.

In the end, data was collected across two experiments. The first experiment was performed on a single test subject with the goal of analyzing the effects of sampling frequency changes and the differences between testing without proper skin preparation and with proper skin preparation. Table 3.1 lists the motions performed in this experiment.

Table 3.1: List of motions in Experiment 1

Trial No.	Motion
1	Sit down, stand up
2	Bend down (from sitting)
3	Walking in place
4	Bend down (from standing)

Trial No.	Motion
5	Reach forward (right arm)
6	Reach up (right arm)
7	Jogging in place

Each trial was performed eight times. Electrodes were attached without proper preparation of the skin at the electrode sites. Each motion was performed with sampling at 50 Hz, 100 Hz, 166 Hz, and 200 Hz. The electrodes were removed and the skin properly prepared with abrasion. Electrodes were then reattached and the motions all repeated at all four of the different sampling frequencies. Each trial involves the motion being performed five times with breaks in between with the exception of the final trial, which was performed as thirty seconds of uninterrupted jogging.

The second experiment was performed on multiple test subjects to see how results may vary across different users. Sampling frequency was kept constant in this experiment. Table 3.2 lists the motions performed in this experiment.

Table 3.2: List of motions in Experiment 2

Trial No.	Motion	Trial No.	Motion
1	Lie down, stand up	6	Reach forward (right arm)
2	Sit down, stand up	7	Reach up (right arm)
3	Bend down (from sitting)	8	Step onto and off stool
4	Walking	9	Climb stairs
5	Bend down (from standing)	10	Trials 1 to 8, continuous

Three test subjects were selected due to a combination of limited resources and time constraints. The test subjects were given instructions on how to prepare the skin at the electrode sites and apply the ECG themselves. All data was sampled at 50 Hz. In each trial the motions were performed five times by each test subject, with the exception of the final trial which was performed three times. Appendix C can be referred to for a more detailed breakdown of every performed motion and how they can be grouped by variable.

It is difficult to quantify motion intensity. However, the motions can be roughly sorted by intensity through rough qualitative analysis. The heaviest motions for each experiment are jogging in place and climbing stairs respectively. Both involve the whole body moving for a regular period of time and are expected to result in increased breathing and heart rate. The next heaviest would be walking in place, again with the whole body moving continuously for a regular period of time, but without increased breathing and heart rate. Progressing further in lesser intensity is lying down/standing up, sitting/standing, and stepping on/off a stool. Again, the whole body is involved, though for a smaller period of time before completion compared to walking. The lightest are the bending and reaching motions, which involve strictly the upper body.

3.3 Data Collection

Data collection was controlled over two different programs. One program was found on every sensor node and controlled how each individual sensor operated. The second

program communicated with the sensor nodes and sent commands as needed. It was decided that the sensor nodes should communicate through Bluetooth due to ease of use and due to the fact that Bluetooth usage is common in the medical field.

The experiment was performed alongside body motion capture research, leading to a total of 11 sensor nodes used in the experiment. Bluetooth is limited by a maximum of seven simultaneous connections with a single machine. As a result, each sensor node stored the collected information on the local memory card rather than having the central computer record all information in real time. Communications with each node was solely to start and stop the recording of the information.

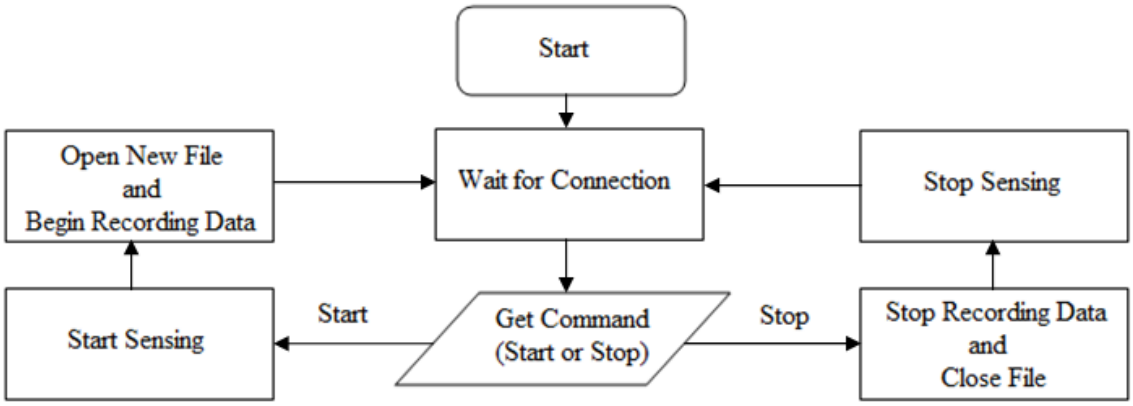

Figure 3.4: Flow diagram of sensor node program

The flow diagram for the sensor node program is demonstrated in Figure 3.4. Each individual sensor was programmed identically. Each one ran with the radio continuously on, awaiting a connection from the computer controlling the experiment. When it received a connection and a command to start running, it started each sensor available on the unit and stored timestamps and sensor information in a new data file on the memory card. It would continue to do so until it received a command to stop running. Using this method, the data of each trial was recorded in its own individual file on the sensor node for future analysis.

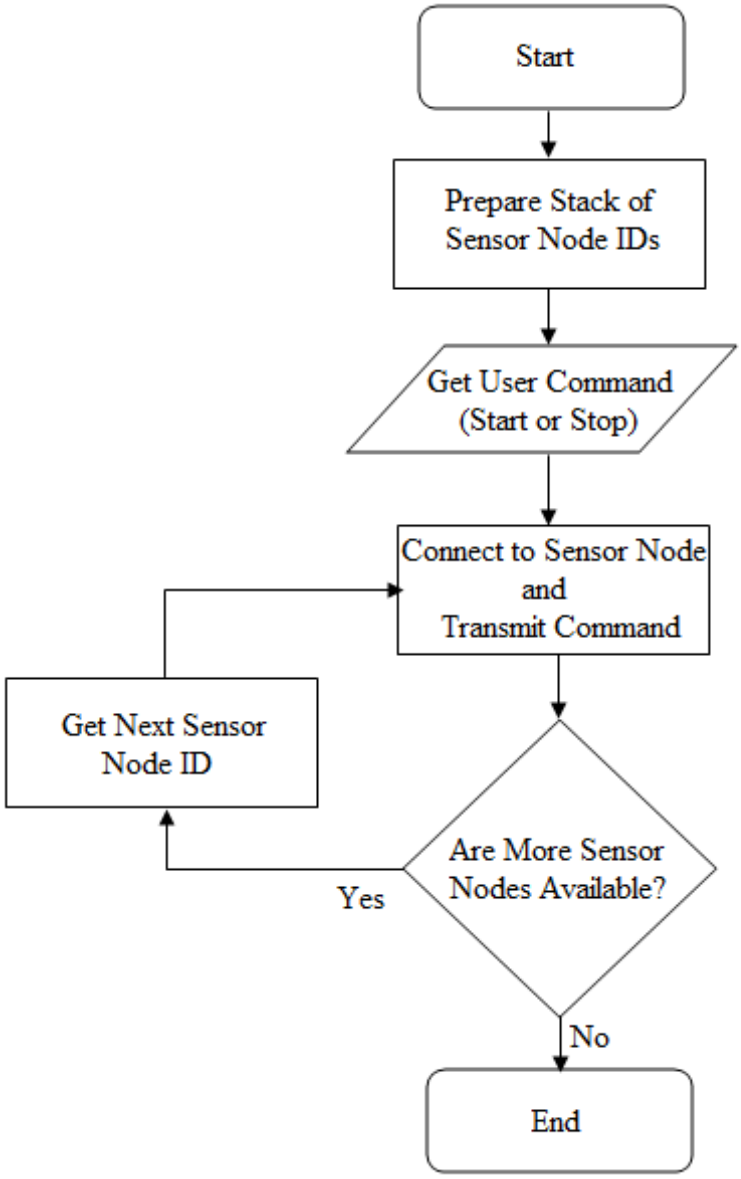

Figure 3.5: Flow diagram of Visual Studio program

A Visual Studio program controlled the experiment as a whole as demonstrated in Figure 3.5. To start a trial for an experiment, the user would order the program to start a trial. The program contained a list of all sensor node IDs in the experiment, each ID giving enough information for the program to be able to establish a connection to each sensor node. It would connect to a sensor node, transmit a command to start recording, disconnect, and repeat for each sensor node until the list of nodes was exhausted. At this point it would wait for further user commands. When ordered to stop a trial, it would act

in a similar manner, only it would send a different command that would instruct each sensor node to stop recording.

3.3.1 Synchronizing Data

One problem brought up by the above process is that of synchronization. The sensor nodes cannot all be activated to start recording at the same time due to the connection limitations of Bluetooth. This means the stored motion and ECG data files among different sensor nodes must be synchronized after having created them. This is achieved through two methods. First, all sensors store accelerometer information, including the ECG sensor. Since all trials start with a period of inaction where the user is completely stationary, the first major motion incident within each data file is a coarse point where they can be roughly aligned. Secondly, all sensors record timestamps, and these timestamps can be synchronized by resetting each sensor node simultaneously.

Figure 3.6: Shimmer multigang charger [47]

Figure 3.6 shows Shimmer's multigang charger, the unit that makes resetting several sensor nodes at once a reliable task. Along with charging multiple Shimmer nodes at once, the multigang charger will simultaneously reset all attached Shimmer nodes when one is manually reset.

The timestamps alone are not sufficient to fully synchronize the data as they will regularly overflow during motion performances. The use of the initial movement as a coarse starting point allows for a precise area where the timestamps can be used to more finely synchronize the data. While this process successfully synchronizes the sensor nodes, this issue could be more easily resolved in future experiments by increasing the memory size of the timestamp variable when coding the Shimmer node program, ensuring the timestamps do not overflow during motion tests.

3.3.2 Noiseless ECGs

With the experiments performed and all data collected and synchronized, one final issue must be handled. The results require a noiseless ECG to compare with in order to be able to quantify the noise being removed by each filtering process. Any additional ECG recordings would suffer similar motion artifacts beyond making use of implantable loop recorders. Requiring the volunteers to undergo surgery was simply not a feasible option for this experiment. Instead, noiseless ECG data sets need to be created artificially.

Every ECG file begins with a period of inactivity before the test subject begins the motion being tested and ends with a period of inactivity after the test subject ends the motion being tested. Since there is no motion during these periods, they are free of motion artifacts. A single sample of ECG can be taken from a period of inactivity in a file and used as a noiseless sample across every occurrence of a heartbeat throughout the rest of that file. The very distinctive peak of the QRS complex is used to align the ECG properly in every instance.

One possible error in this method arises in how the ECG shape may change under exertion. According to a paper published by the American Heart Association, the ECG waveform sees minor changes during and after exercise [48]. A sample taken before motion has started may therefore have normal differences to the true noiseless ECG unrelated to error. Trials that involve more intensive activity therefore use an ECG sample during the period of inactivity after the motions have finished.

3.4 Summary

The Shimmer sensor node was selected for use due to its small size, its ability to expand easily to use the sensors desired for the FANFARE project, and its ability to be easily programmed. The ECG sensor was worn on the chest while data was collected from sensor with accelerometers and gyroscopes worn on the arms and the small of the back. Data was collected over two experiments. The first focused on differences in skin preparation and sampling frequency. The second focused on differences in multiple test subjects who had abrased themselves prior to the experiment. Motions were selected over a variety of intensities to see how motion can impact the results.

Data was collected through a central computer sending commands directing the sensor nodes to start and stop recording appropriately, with all data being stored locally on microSD cards. This led to some extra steps necessary to ensure proper synchronization of the data between sensor nodes. Finally, noiseless ECGs were simulated due to the inability to directly record a noiseless ECG alongside the recording of a properly noisy ECG.

4 Preliminary Tests

Before proper analysis of the data can begin, a few preliminary tests must be performed. First, it must be determined which motion sensor and which axis is most appropriate for use in filtering. Second, the adaptive filtering algorithms must be tested to ensure proper operation. Finally, the source separation methods must be tested to ensure they are functioning as expected.

4.1 Correlation Tests

As discussed in Section 2.2, adaptive filtering for noise cancellation relies on the premise that the noise is correlated with the reference signal and uncorrelated with the source signal. The suitability of adaptive filtering for ECGs using motion data must be established through an investigation of the correlation between the motion data and the ECG noise and between the motion data and the noiseless ECG.

The recorded motion data is readily available. The motion data available is an accelerometer and gyroscope on each sensor node, with three axes on each. Prior to use, each set of motion data must be centered and rescaled. This means subtracting the mean value of the motion data to produce a new mean value of 0 and then dividing the entire motion set by its maximum absolute value to produce a new maximum absolute value of 1. This is a necessary preprocessing step for the use of the motion data as the reference signal in adaptive filtering.

Noiseless ECG representations have already been created as discussed in Section 3.3.2. The noise can be produced by subtracting the noiseless ECG from the original noisy ECG. The result is imperfect, due to the fact that the ECG data is digital. The created noiseless ECG will not be perfectly aligned with every original ECG as the sampling of each heartbeat will differ slightly every time. The results are worse at lower sampling rates, with the biggest problem being found at the steep R wave.

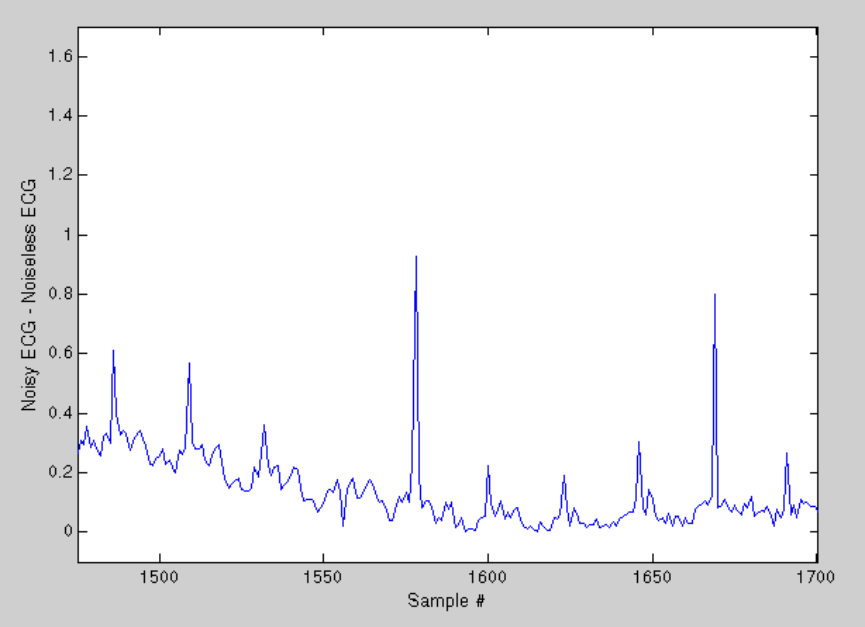

Figure 4.1: Example of calculated noise at 50 Hz sampling frequency

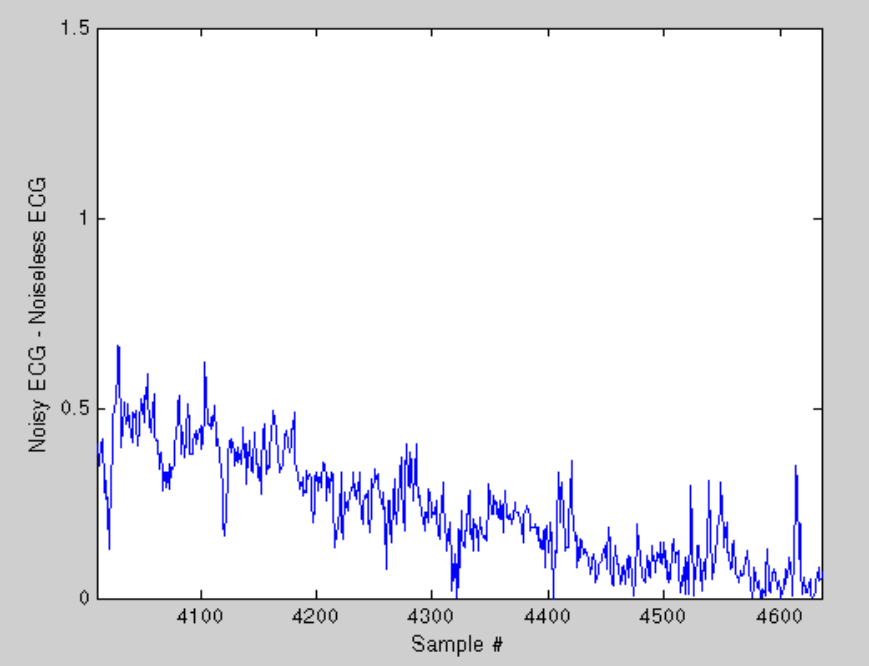

Figure 4.2: Example of calculated noise at 200 Hz sampling frequency

Figure 4.1 demonstrates this issue with an example of noise calculated from Trial 7 from Experiment 1, jogging in place, sampled at 50 Hz. Figure 4.2 demonstrates the noise from Trial 28 of Experiment 1, jogging in place, sampled at 200 Hz. The periodic peaks are due to the R wave of the ECG.

These peaks can be removed through the implementation of a moving average filter. The result after the moving average has been applied to the data in Figure 4.1 can be seen in Figure 4.3. Similarly, the result of applying the moving average filter to Figure 4.2 can be seen in Figure 4.4. A 70 sample window is used for the moving average filter for data sampled at 50 Hz while a 300 sample window is used for data sampled at 200 Hz.

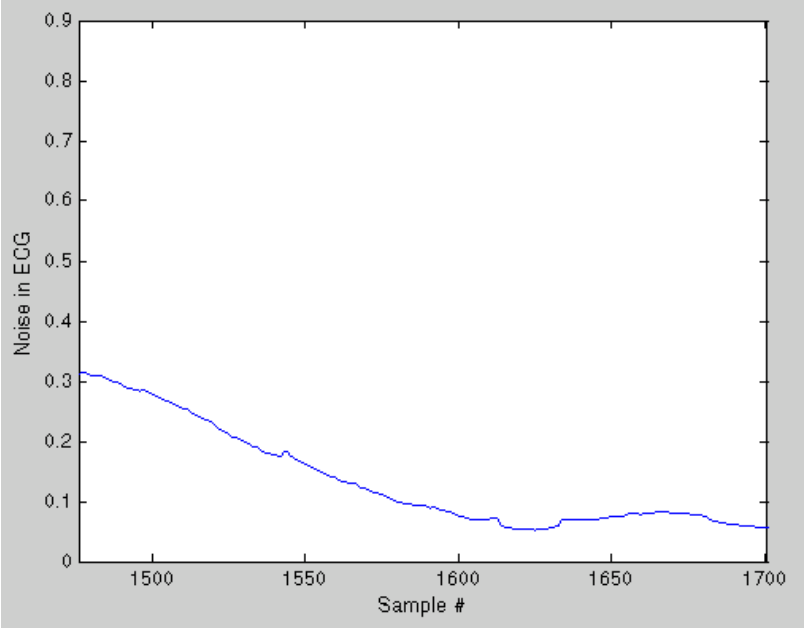

Figure 4.3: ECG noise after applying moving average filter, 50 Hz example

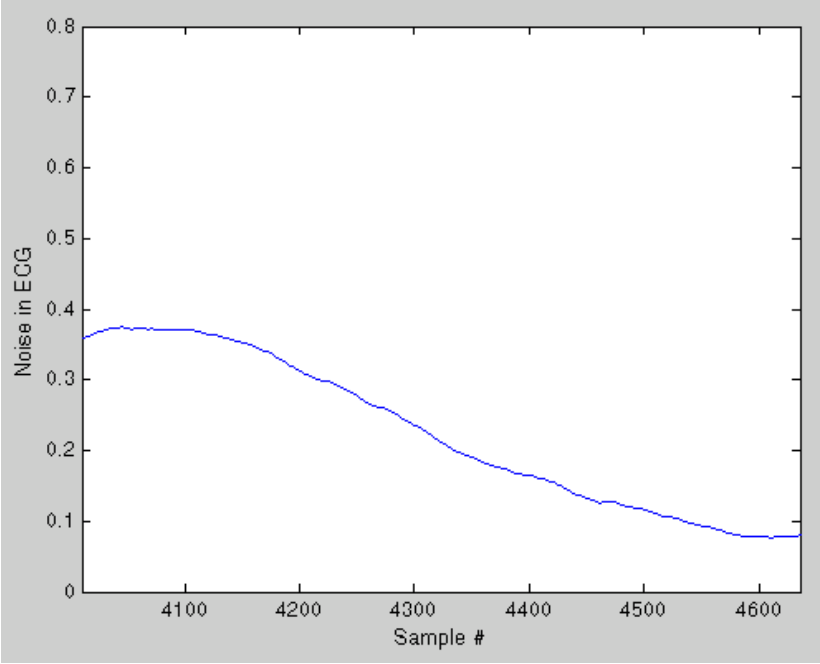

Figure 4.4: ECG noise after applying moving average filter, 200 Hz example

With a usable ECG noise representation now available, the correlation between the motion data and the noise can be investigated. The correlation coefficient r between vectors x and y of length n is calculated as shown in Eq. 4.1. The correlation coefficient between the averaged noise and the motion data is taken for every motion trial performed.

$$r_{xy} = \left(\sum xy - \frac{(\sum x)(\sum y)}{n}\right) \Bigg/ \sqrt{\left(\sum x^2 - \frac{(\sum x)^2}{n}\right)\left(\sum y^2 - \frac{(\sum y)^2}{n}\right)} \tag{4.1}$$

The average correlation coefficient of all trials for each axis of each sensor is shown in Figure 4.5. A higher correlation is desired as the better the reference signal is correlated with the noise, the better the adaptive filter will perform. The accelerometers are better correlated with the noise than the gyroscopes. Among the accelerometers, the Z axis performs best among all three sensors. Adaptive filtering of the ECG using motion data will therefore make use of the Z axis on the accelerometer as the reference signal.

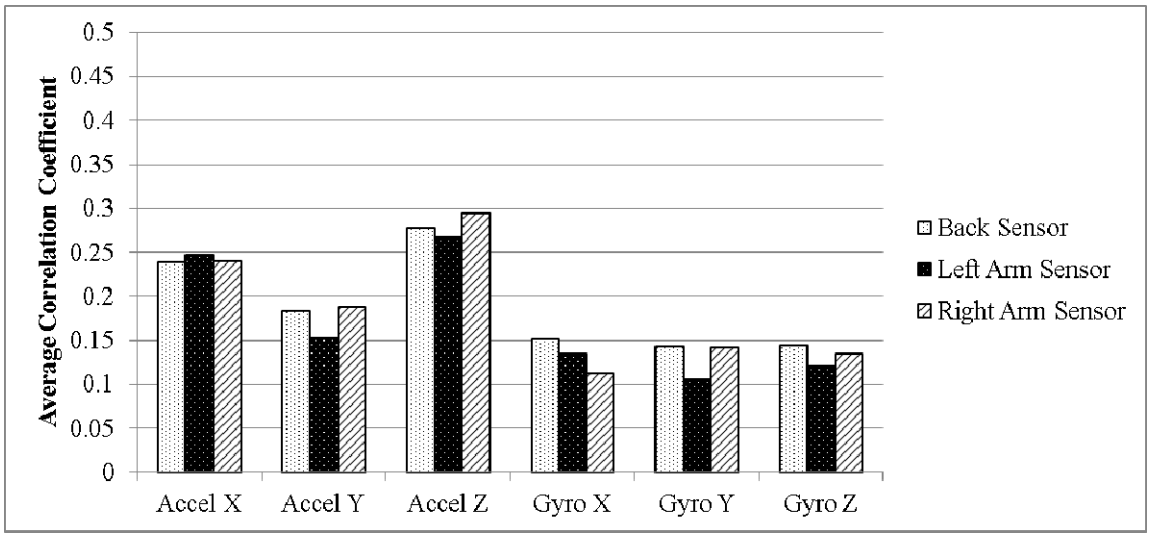

Figure 4.5: Correlation between motion and noise

The motion data is correlated with the noise and therefore usable as a reference signal. However, it must still be demonstrated that the noiseless ECG is uncorrelated with the noise. It should be intuitive that the noiseless ECG will be uncorrelated with motion data. The heart beats more rapidly when more intensive activity is prolonged and there

are slight changes to the ECG shape during and after exercise, but the overall shape of the ECG signal remains largely constant regardless of the specifics of the motion.

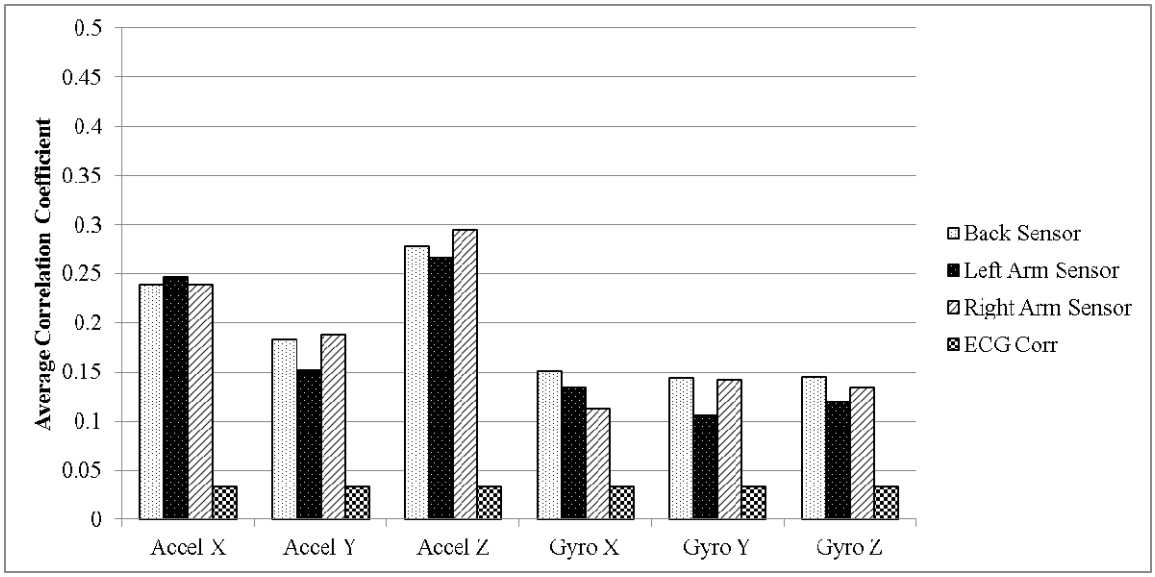

Figure 4.6: Comparison of correlation of motion vs. ECG

The correlation coefficient between the noiseless ECG and the motion data is taken for every trial performed. Figure 4.6 includes the average ECG correlation coefficient beside the motion vs. noise results previously shown in Figure 4.5. The maximum correlation coefficient between the noiseless ECG and the motion data is 0.0517, with an average of 0.0331 across all trials. The noiseless ECG is visibly uncorrelated, particularly relative to the correlation between the motion data and the noise. Based on these results, noise cancelling through adaptive filtering should be a viable method.

4.2 Adaptive Filtering of Simulated Noise

It is desired to test the adaptive filters before directly applying them to the data. In order to accomplish this, artificial noise that is highly correlated with motion data is created and added directly to the created noiseless ECG data. The adaptive filters can then be applied to the artificial noisy ECGs using the motion data as a reference signal.

The goal is to create noise that resembles muscle noise and is very highly correlated with the motion data. The simulated noise must be created based on the motion data to ensure high correlation with it. To make it a better representation of noise, random

elements must be included. The average quantity of noise as previously produced in Section 4.1 is examined to find an appropriate range of values. The average amount of noise during high motion activity is selected to act as the maximum average noise value in the simulated noise. The average amount of noise during no motion activity is selected to act as the minimum average noise value in the simulated noise. The rescaled motion data is used to determine the expected quantity of noise at any given moment of time with all noise samples being subject to a small but random amount of variation.

$$\mathbf{v} = (M - m)\mathbf{u} + m - \mathbf{r} \tag{4.2}$$

Using m to depict the minimum average noise during no motion, M to depict the maximum amount of noise expected during high amounts of motion, $\mathbf{r}$ to be a vector of uniformly distributed random values between $\pm m$, $\mathbf{u}$ to represent the rescaled motion vector, and $\mathbf{v}$ to depict the simulated noise vector, the creation of the noise is demonstrated in Eq. 4.2.

Similar to Section 4.1, the correlation between the artificial noise and the motion data is tested to ensure the results meet the expectations. Table 4.1 shows the minimum, maximum, and average correlation coefficients between the noise and motion for each sensor among all trials. The correlation of the simulated noise with the motion data ranges from 0.64 to 0.95, with an average of about 0.87. There is no significant difference in the results based on the sensor used.

Table 4.1: Correlation coefficients of simulated noise vs. motion

	Left Arm Sensor	Right Arm Sensor	Back Sensor
Min	0.6426	0.6821	0.6389
Max	0.9507	0.9479	0.9501
Mean	0.8644	0.8810	0.8732

The artificially created noise is added to the noiseless ECGs. Adaptive filtering methods can now be applied to this new noisy ECG data. The Matlab™ code used in the implementation of both LMS and RLS filtering is available in Appendix A.

4.2.1 Least Mean Squares- Simulated Noisy ECGs

Two factors influence the success of the Least Mean Squares algorithm. The first factor is the filter length used. In all cases, a filter length of 16 is used. A more formal analysis of the filter length and an explanation for the selected filter length will be investigated in Chapter 5. The second factor is the gain factor μ, as discussed in Section 2.2.1.

Results are compared on the basis of the average percentage of noise remaining. The noiseless ECG data is subtracted from the output of the LMS filter, producing a vector of the remaining noise left in the system after filtering. The percentage of noise remaining is therefore determined as in Eq. 4.3.

$$e_{per} = \sum_{i=0}^{n-1}(|\mathbf{y} - \mathbf{s}|) \Big/ \sum_{i=0}^{n-1}|\mathbf{q}| \tag{4.3}$$

with e_{per} being the percentage of remaining noise, **y** depicting the output of the filter, **s** being the noiseless ECG vector, **q** being the noise vector, and n being the length of vectors **y**, **s**, and **q**. For $e_{per} < 1$, noise has successfully been filtered, with smaller e_{per} values indicating better performance. A result of $e_{per} > 1$ means the filter isn't converging fast enough and it is instead corrupting the input instead of cleaning it.

Every motion trial for each motion sensor is tested with gain factors ranging from 0.01 to 0.5 in increments of 0.01. All best results for all trials are found when the gain facto is less than 0.1. For more accurate results, the trials are repeated for gain factors of 0.001 to 0.1 in increments of 0.001. The gain factors that produce the best results for each individual trial and sensor combination, as well as the resulting percentage of remaining noise, are recorded.

The results of filtering the numerous trials can be approached from a number of variables. They can be grouped by motion, by test subject, by frequency, and by whether or not skin had been properly prepared for electrode placement beforehand. For the case of manufactured ECGs with simulated noise added, the only variable examined is that of motion performed. The two experiments performed use the motions as discussed in tables 3.1 and 3.2. For each trial where the motion is repeated a number of times, the end result of the trial is the average results of each motion.

The results of the gain factor analysis can be approached in one of two ways. First, the results can be looked at with each and every motion using its optimal gain factor, as in the gain factor constant that produces the best possible result for the selected data set. This is not a realistic approach for practical applications, but it gives the best possible results. The second approach is to determine an average gain factor based on a particular variable, as in the gain factor constant that produces the best average result for multiple data sets grouped by a particular shared feature. The use of the optimal gain factor in every trial will be referred to as the Optimal Variable approach, while the use of a shared gain factor based on grouping of trials will be referred to as the Shared Variable approach. These approaches will be referred to throughout both the simulation results and the full data analysis in Chapter 5.

In order to demonstrate the difference between the two approaches, consider the fictitious example in Table 4.2. The gain factor results are analyzed for a particular motion as performed by test subjects 1 through 3, finding the optimal gain factors and the resulting remaining amount of noise. Due to the difficulty in predicting the best possible gain factor in a real time situation, it is decided to use the results to estimate the best gain factor based on the motion performed. As all test subjects are performing the same motion, the same gain factor must be shared among them. By using this approach, there is less fine tuning on the used gain factor, but there is also more noise remaining in the trials performed by test subjects 1 and 3.

Table 4.2: Example of optimal variable approach vs. shared variable approach

	Opt. Gain Factor	% remaining noise	Shared Gain Factor	% remaining noise
Test Subject 1	0.018	55%	0.016	58%
Test Subject 2	0.016	60%	0.016	60%
Test Subject 3	0.014	50%	0.016	56%

For quick reference, abbreviations representing each motion are included in the motion trials for each experiment. The motions and their corresponding abbreviations are presented in Table 4.3.

Table 4.3: Listing of all motions and their abbreviations

Sit down, stand up (SDSU)	Jogging in place (JiP)
Bend down from sitting (BDSi)	Lie down, stand up (LDSU)
Walking in place (WiP)	Walking (W)
Bend down from standing (BDSt)	Step on and off stool (SOOS)
Reach forward with right arm (RF)	Climb stairs (CS)
Reach up with right arm (RU)	Trials, continuous (TC)

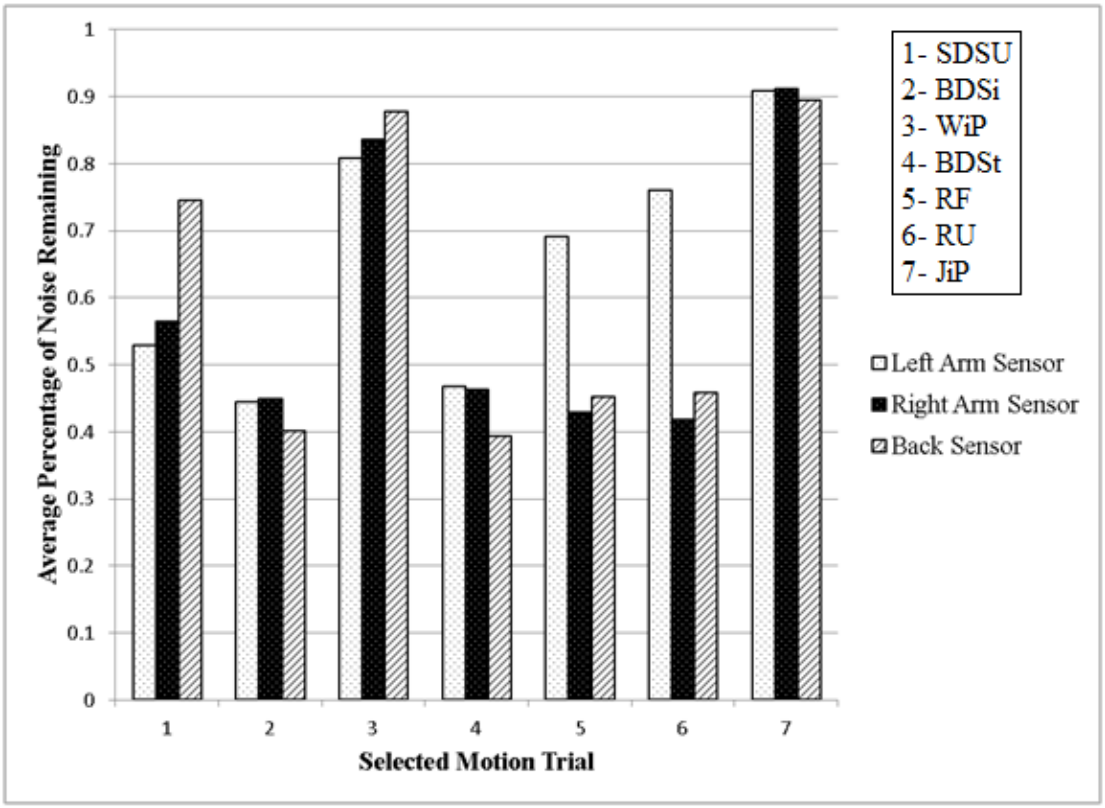

Figure 4.7: LMS motion experiment 1, optimum variable

Figure 4.7 shows the results for the applications of the Least Mean Squares filter to the simulated noisy ECGs of experiment 1. The results are the averaged outcomes of each identical motion trial, using the optimum gain factor for each individual recorded performance of that trial.

The best results are found in trials 2 and 4, as well as the right arm and back sensors for trials 5 and 6. These are the lightest motions performed, being bending down from sitting, bending down from standing, reaching forward, and reaching up respectively. In

these cases, 55%-60% of the noise is removed on average. The arm sensors perform comparatively well for trials 2 and 4 while the back sensor performs about 5% better than the arm sensors. The left arm sensor performs drastically worse for trials 5 and 6, leaving an additional 25%-30% noise after filtering compared to the right arm and back sensors.

The next best results are found in the left arm and right arm sensors of trial 1, being sitting down and standing up. In this trial, 45%-50% of the noise is removed on average. The back sensor performs notably worse than the arm sensors here, leaving an additional 20% of noise on average.

The worst results are found in trials 3 and 7. These are the heaviest motions performed, being walking in place and jogging in place respectively. Only 10%-20% of the noise is removed on average. The back sensor performs slightly worse than the arm sensors for trials 3, leaving an additional 5% of noise. All sensors perform comparatively for trial 7.

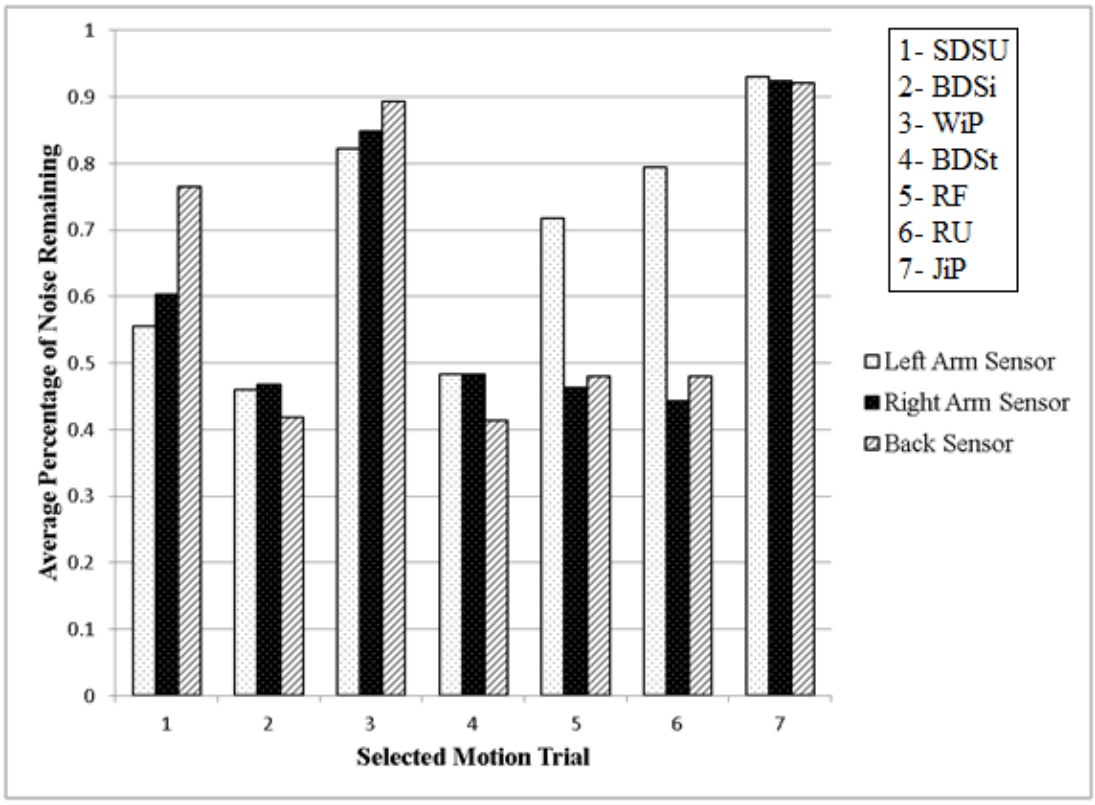

Figure 4.8: LMS motion experiment 1, shared variable

Figure 4.8 shows the results for the application of the Least Mean Squares filter to the simulated noisy ECGs of experiment 1. The results are the averaged outcomes of each

identical motion trial with each trial sharing a single gain factor across all recorded performances of that trial.

As would be expected, all sensors for all trials perform worse for shared gain factors than for optimum gain factors. However, the differences are not particularly notable. The results for shared gain factors all see 5% or less additional noise remaining when compared against the results for optimum gain factors.

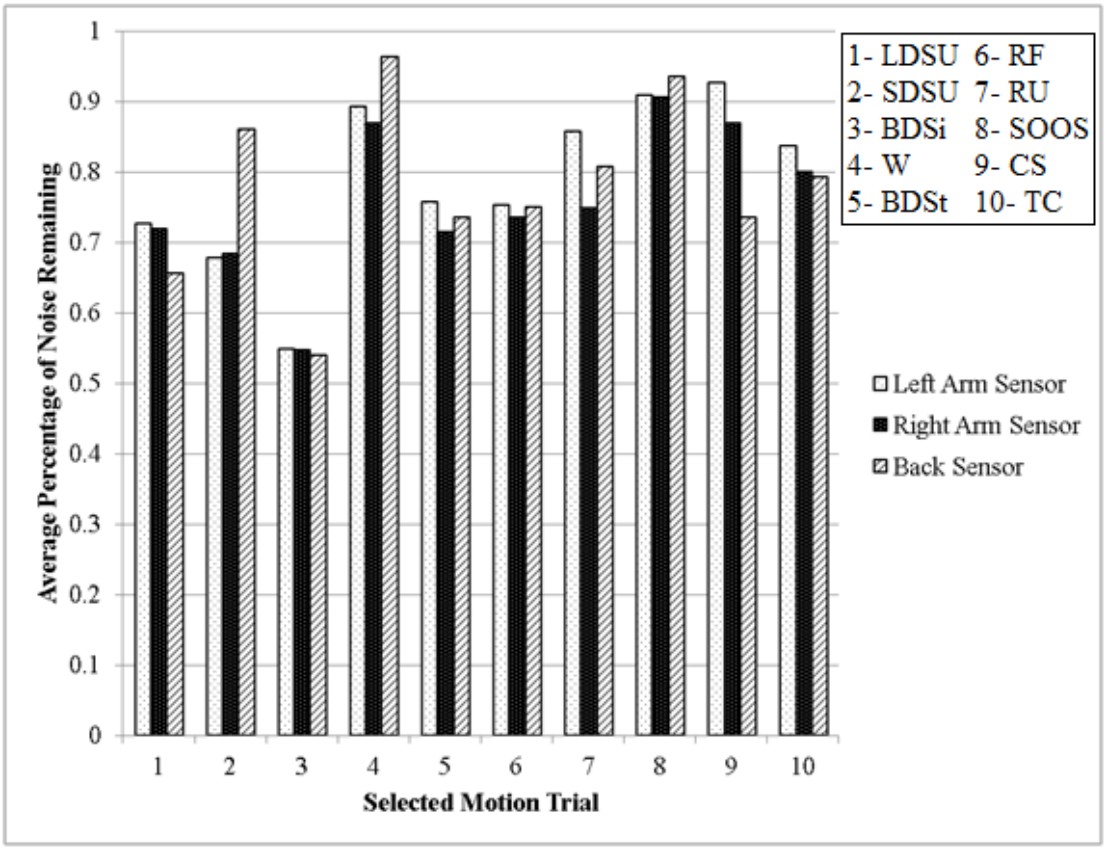

Figure 4.9: LMS motion experiment 2, optimum variable

Figure 4.9 shows the results for the applications of the Least Mean Squares filter to the simulated noisy ECGs of experiment 2. The results are the averaged outcomes of each identical motion trial, using the optimum gain factor for each individual recorded performance of that trial.

The best result is found in trial 3, bending down from sitting, with 45% of noise removed on average. Next best trials are trials 1, 5, and 6, being laying down and standing up, bending down from standing, and reaching forward. They see roughly 25%-30% of noise removed on average. The best performing sensors for trials 2, 7, and 9, being sitting down standing up, reaching up, and climbing stairs, all perform similarly

well. Trial 10, the continuous performance of multiple trials, follows closely with roughly 20% of noise removed on average.

The worst results are found in trials 4 and 8, being walking and stepping on and off a stool respectively. Roughly 10% of the noise is removed on average for the arm sensors on these trials.

There remains a general tendency for lighter motions to perform better than heavier motions. The worst results are found in walking, stepping on and off a stool, and the arm sensors of climbing stairs, followed by the continuous trial. The primary anomalies are the back sensor for climbing stairs, which performs as well as the lighter motions, and the left arm and back sensor of reaching up, which performs as badly as the heavier motions.

There is less consistency in what sensor performs best for each trial compared to experiment 1. The back sensor performs 15% worse than the arm sensors for trial 2, 10% worse than the right arm sensor for trial 4, and 5% worse than the right arm sensor for trial 7. It performs 5% better than the right arm sensor for trial 1 and 15% better than the right arm sensor for trial 9. The left arm sensor performs 10% worse than the right arm sensor for trial 7 and 5% worse than the right arm sensor for trial 9. The arm sensors typically perform comparatively well against each other otherwise.

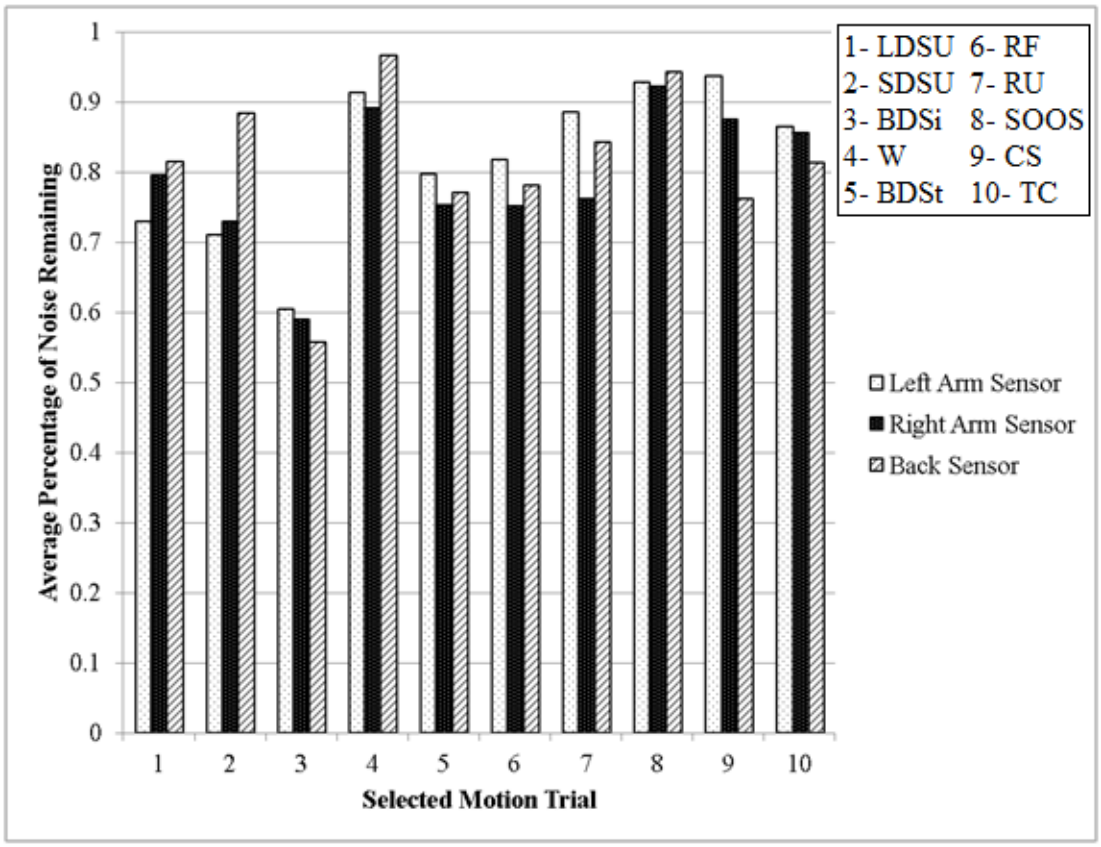

Figure 4.10: LMS motion experiment 2, shared variable

Figure 4.10 shows the results for the application of the Least Mean Squares filter to the simulated noisy ECGs of experiment 2. The results are the averaged outcomes of each identical motion trial with each trial sharing a single gain factor across all recorded performances of that trial.

As with the shared gain factor results of experiment 1, all results are worse than the optimal gain factor results by at least some degree, as expected. The majority of results leave no more than 5% additional noise compared against the optimal gain factor results. The exceptions are the right arm and back sensor results of trial 1. The right arm sensor result has an additional 10% of noise on average remaining compared against the optimal gain factor results. The back sensor has an additional 15% of noise on average remaining compared against the optimal gain factor results.

Overall, across both experiments, lighter trials appear to perform better overall than heavier motions. The heaviest motions of walking, jogging, and stair climbing see the poorest performances across both experiments, with the single exception of the back

sensor filtering of stair climbing. This indicates that the motion under investigation has a significant impact on the results of adaptive filtering.

Individual trials see individual sensors doing significantly better than others in many cases. As a general rule across both experiments, the right arm sensor tends to perform either roughly as well as the left arm sensor, if not substantially better. This may have to do with the right handedness of the test subjects, as indicated by the especially large difference in results between use of the right arm sensor and the left arm sensor in the right hand focused reaching trials. There are multiple trials where there is a significant difference between the results of the arm sensors compared against the result of the back sensor. Overall, the differing results in sensor choice support the idea that the use of multiple motion sensors could improve adaptive filtering over the use of a single motion sensor.

While the optimum variable results are naturally better than the shared variable results in every instance, it is typically not by a significant margin, with the exceptions of the right arm and back sensor of trial 1 for experiment 2. While the selection of the gain factor is important, optimizing the results for every individual set of data typically does not offer a significant improvement over a more coarsely selected value based on the motion being performed. This is partly due to the selection of the filter length, which took into account sensitivity of LMS to variations in gain factor. This will be discussed further in Section 5.1.

4.2.2 Recursive Least Squares – Simulated Noisy ECGs

There are three variables of concern in the performance of the RLS algorithm. Similar to the LMS algorithm, the first variable is the filter length, which is chosen to be 2 as will be detailed in Section 5.1. Second is the forgetting factor λ, which similar to the gain factor of LMS, is the primary determination of how fast the filter will converge to the desired result. The third variable is δ, the initial value set for the iterative calculation of the inverse autocorrelation of the reference signal.

Preliminary tests find that the initial value of δ does not significantly impact the results, so long as it is set to a value somewhere between 10 and 1000. A value of $\delta = 100$

is found to be the best result on average across all trials, and will be used without further fine-tuning through the rest of the simulated noise RLS tests.

Similar to the approach of analyzing the optimal gain factor for LMS, the forgetting factor was tested on all trials across the range of 0 to 1. The forgetting factor was ultimately found to operate best for all trials within the range of $\lambda = 0.9$ to $\lambda = 1$. Filtering is performed on each trial from 0.9 to 1 in increments of 0.001 with the best forgetting factor for each individual trial stored for use.

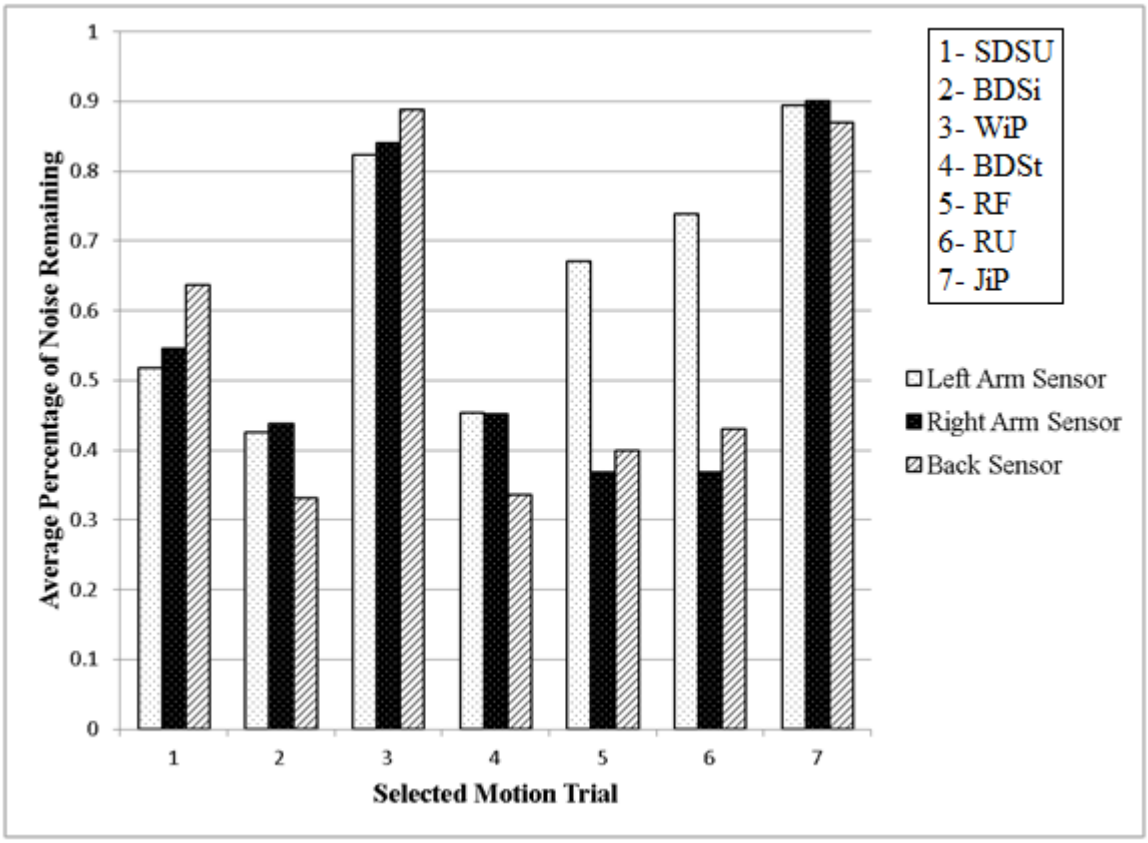

Figure 4.11: RLS motion experiment 1, optimum variables

Figure 4.11 shows the results for the applications of the Recursive Least Squares filter to the simulated noisy ECGs of experiment 1. The results are the averaged outcomes of each identical motion trial, using the optimum forgetting factor for each individual recorded performance of that trial.

The best results are found in trials 2, 4, 5, and 6, with 60%-65% noise removed on average through each best performing sensor. Next best is trial 1 with 45%-50% of noise removed on average through its best performing sensors. The worst results are found in trials 3 and 7, with 10%-20% of noise removed on average.

Results are generally similar to the results of the LMS optimal gain factor results. The notable differences are found in the back sensor results for trials 1, 2, 4, 5, and 6, where RLS removes an additional 5%-10% of noise compared against LMS. All other results are improved by less than 5%

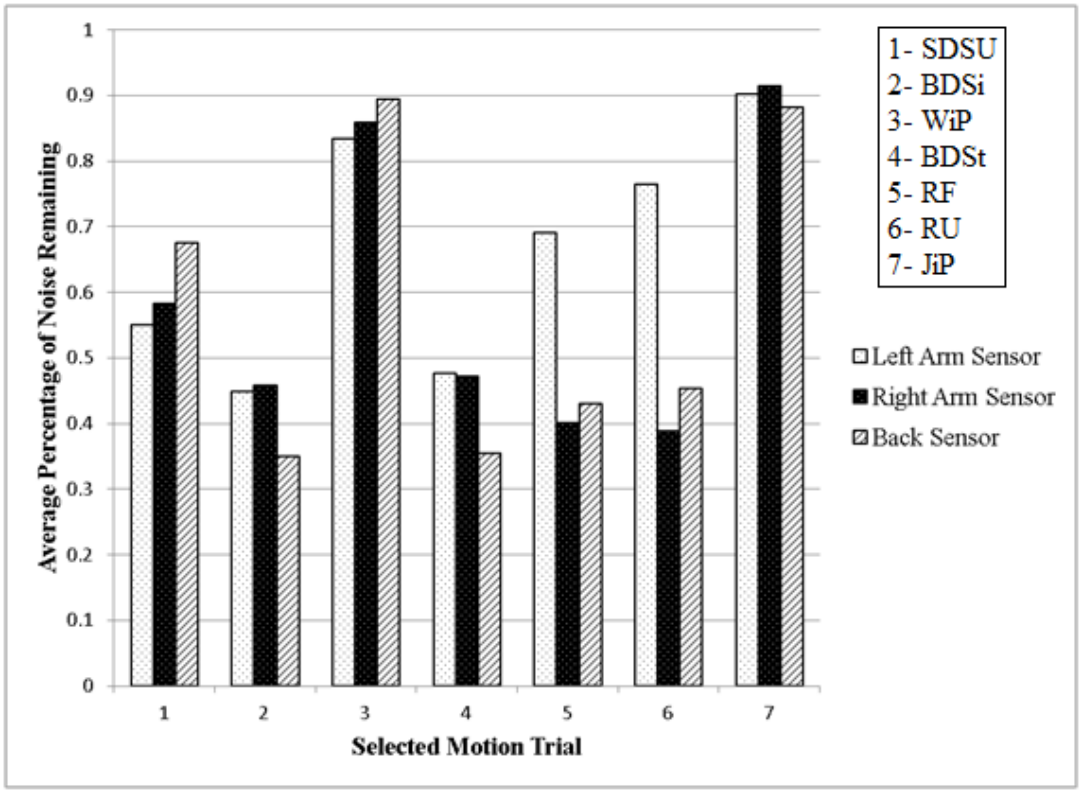

Figure 4.12: RLS motion experiment 1, shared variables

Figure 4.12 shows the results for the application of the Recursive Least Squares filter to the simulated noisy ECGs of experiment 1. The results are the averaged outcomes of each identical motion trial with each trial sharing a single forgetting factor across all recorded performances of that trial.

As with optimal vs. shared gain factors in the LMS filtering results, results for shared forgetting factors all leave an additional amount of noise compared to the optimal results, as expected. Once again, there are no particular trials that are heavily affected, with no more than an additional 5% of noise left across all results compared against the optimal forgetting factor results.

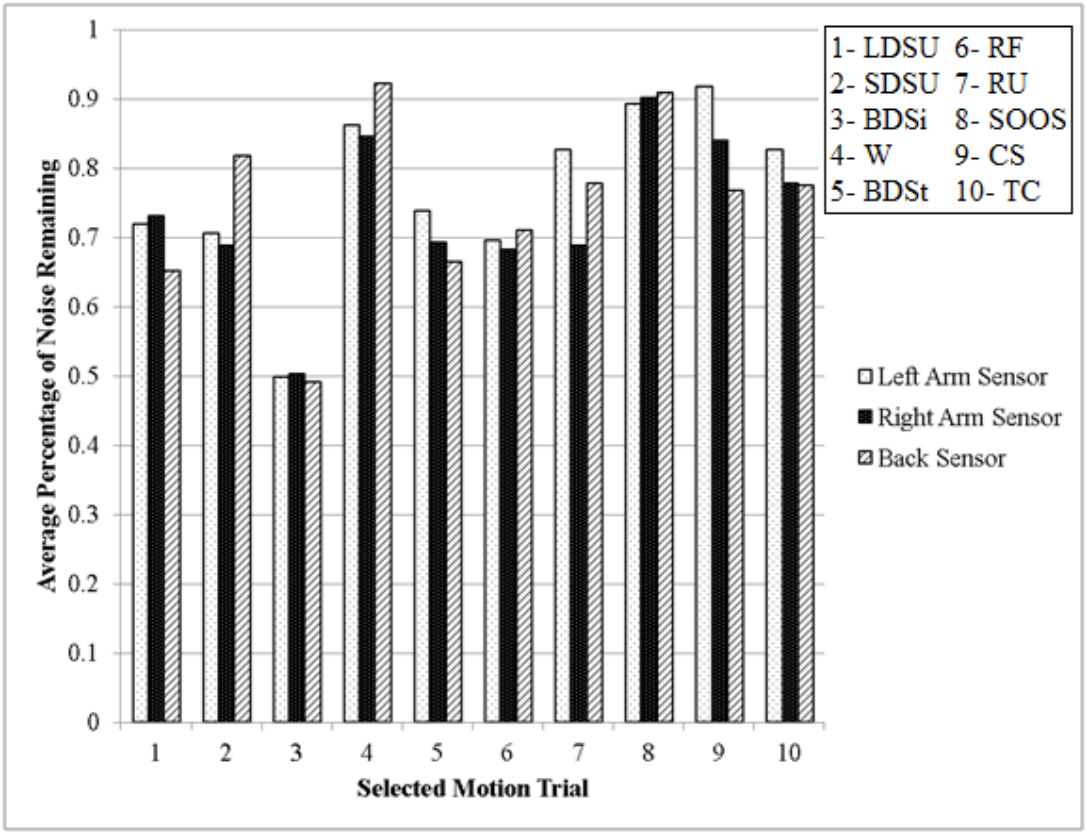

Figure 4.13: RLS motion experiment 2, optimum variables

Figure 4.13 shows the results for the applications of the Recursive Least Squares filter to the simulated noisy ECGs of experiment 2. The results are the averaged outcomes of each identical motion trial, using the optimum forgetting factor for each individual recorded performance of that trial.

The best result is found in trial 3, with 50% of noise removed on average for all sensors. The next best results are found in the best sensor performances of trials 1, 2, 5, 6, and 7, with 30%-35% of noise removed on average. The worst results are found in trials 4, 8, 9, and 10, with 10%-20% of noise removed on average.

As with experiment 1, the results are again largely comparable to the LMS results. Unlike experiment 1, there are no truly notable improvements between the two results, with RLS typically removing an additional 5% or less. There is a single instance where LMS outperforms RLS, being the right arm sensor of trial 1, though it is not by a significant amount.

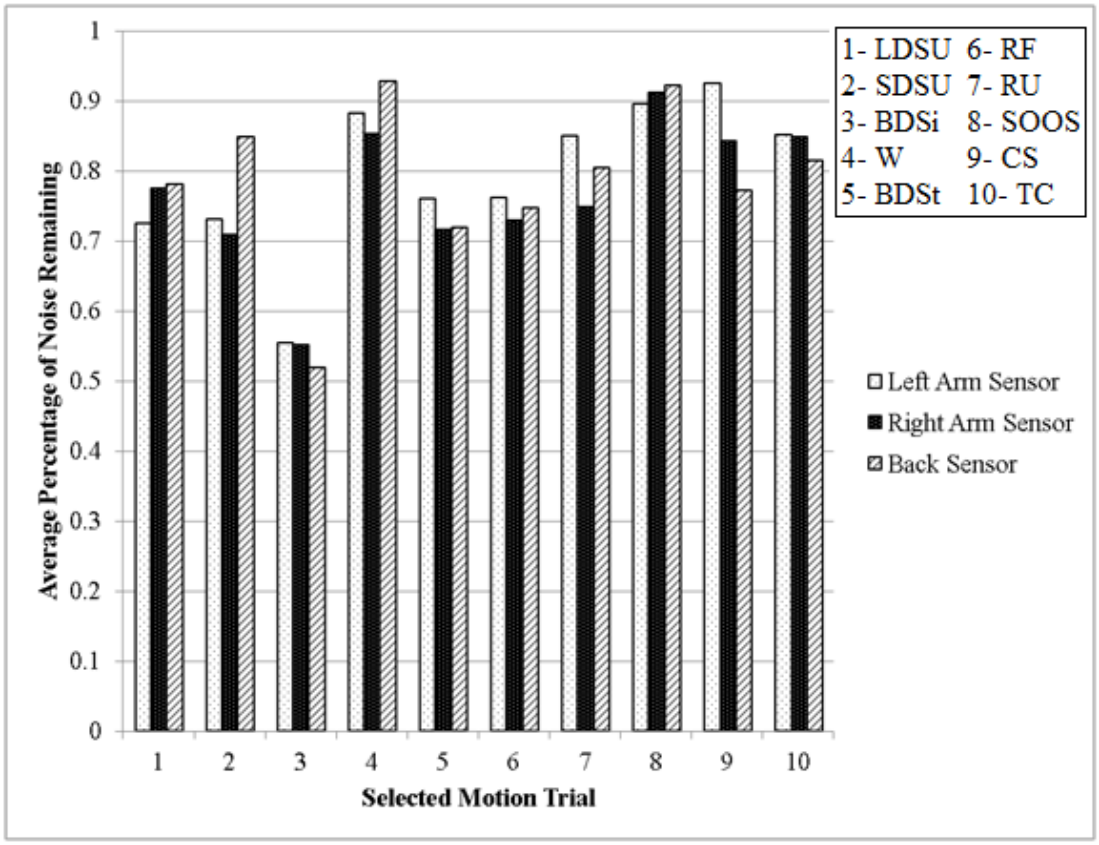

Figure 4.14: RLS motion experiment 2, shared variables

Figure 4.14 shows the results for the application of the Recursive Least Squares filter to the simulated noisy ECGs of experiment 2. The results are the averaged outcomes of each identical motion trial with each trial sharing a single forgetting factor across all recorded performances of that trial.

As with prior comparisons between optimal and shared variable results, all shared forgetting factor results are expectedly leaving an additional amount of noise compared to the optimal results. Once again, the results see an additional 5% of noise or less left in the majority of trials. The single exception is the back sensor of trial 1, where the use of shared forgetting factors sees an additional 10% of noise remaining compared to the use of optimal forgetting factors.

Overall, RLS performs marginally better than LMS across the majority of the results. RLS filtering is expected to have superior performance compared to LMS filtering at the cost of additional computation time, so this is not a surprising result. RLS typically removes an additional 5% of noise compared against LMS, though there are instances in both experiments where it removes upwards of an additional 10% of noise. There is only

a single instance where LMS removes more noise than RLS, though it is not at all by a significant amount and can be regarded as an anomaly.

Broadly speaking, the RLS results do not differ significantly from the LMS results in terms of sensor result comparisons or amount of noise removal between specific kinds of movements. Similarly to LMS, the optimization of the forgetting factor does not result in significant improvements beyond the more coarse use of shared forgetting factors between motions.

4.3 Separation of Simulated Signals

Some brief testing is done with each ICA method to ensure proper operation. The successful operation of the ICA methods cannot be verified by using them directly on the motion data. It is unknown how the motion data should appear once successfully separated or the extent of the mixing between the arm motion data and the torso motion data for specific motions. As such, one would not be able to determine whether the results of ICA used on motion data is performing correctly. Tests are therefore done more broadly with simpler signals that are manually mixed. The Matlab^{TM} code used for Infomax and PCA are available in Appendix A. The FastICA algorithm is implemented through Gavert's FastICA software package [49].

The FastICA is tested by mixing together a sine wave and a quadratic function as in Eq. 2.3.1, using a randomized mixing matrix **A**. Figure 4.15 demonstrates the results. Column 1 contains the original, unmixed signals. Column 2 shows the signals after they have been mixed. Column 3 is the output of FastICA. Notably, after unmixing the signals, the scales of the outputs are off compared to the original. This is due to ICA's inability to recover the exact amplitude of the original source signals. As a result, the motion data will need to be rescaled after being unmixed with FastICA.

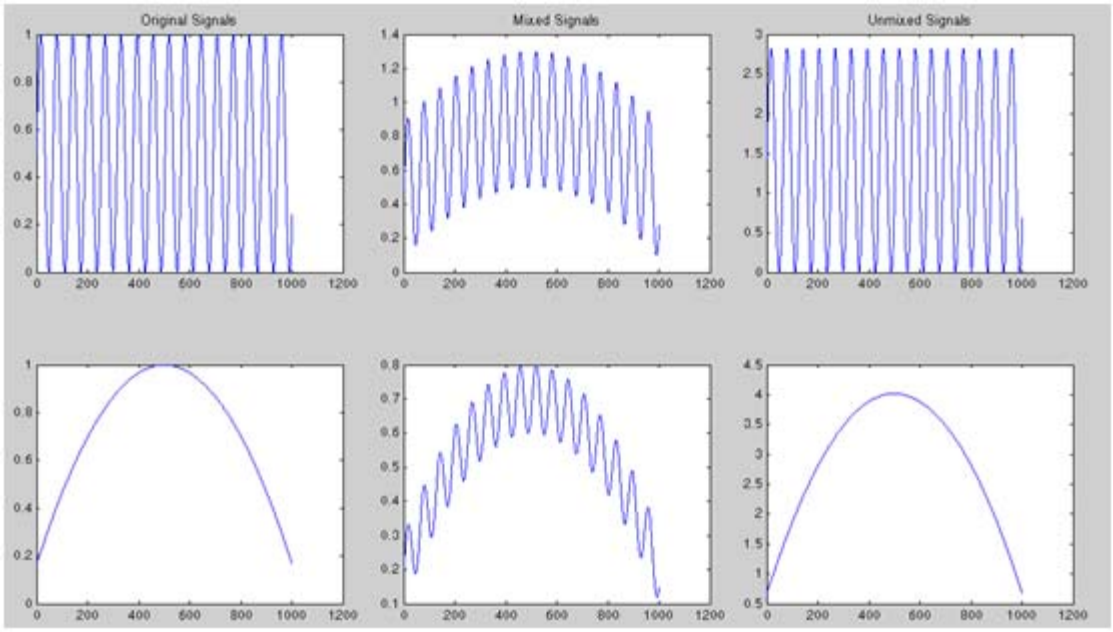

Figure 4.15: FastICAunmixing

The Infomax algorithm for unmixing subgaussian signals is tested using a mixed sine wave and sawtooth wave. Different signals are selected to satisfy the different conditions required of the source signals for success. The results are seen in Figure 4.16. Similar to FastICA's demonstration, column 1 contains the original unmixed signals, column 2 contains the mixed signals, and column 3 contains the output after unmixing by Infomax.

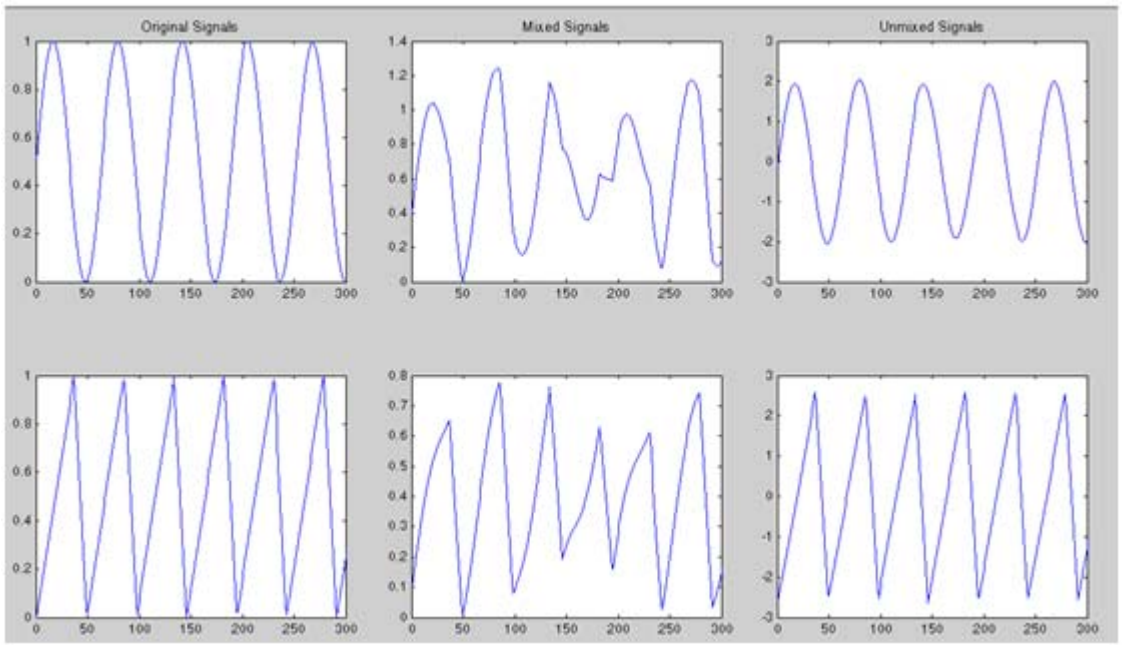

Figure 4.16: Subgaussian Infomax unmixing

These quick tests validate the use of FastICA and Infomax for unmixing signals. PCA and the supergaussian version of Infomax are more difficult to produce appropriate source signals. However, PCA is a preprocessing step to the two ICA algorithms, and so is indirectly verified. The supergaussian version of Infomax requires only a small change to the subgaussian Infomax, as demonstrated in Section 2.3.2, and so can be used safely based on the success of the subgaussian Infomax.

4.4 Summary

This chapter has discussed the approach for collecting and quantifying the filtering results. The correlation between the used data and the noise has been examined to ensure that the prerequisite conditions for use of adaptive filtering have been met. An adaptive filtering test using real motion data and a noiseless ECG combined with simulated noise has been performed to verify the used LMS and RLS algorithms. Tests with known combined source signals have been used to verify the use of the selected ICA algorithms. With the approach for examining the results discussed and the various algorithms verified for use, the full results of applying the algorithms to real data can be analyzed.

5 Results

Motion data on three different sensors have been collected alongside ECGs across a variety of motions. The effectiveness of their use in reducing the noise in ECGs can be compared on several different bases. Most broadly, it is desired to investigate the results in terms of filtering by the sensors individually and in filtering after having combined the source components of the motion sensors. Each instance of filtering is performed over two algorithms, that of LMS and RLS. Within each algorithm, the variables that most influence the results are compared in terms of the optimal variable for each individual data set and in terms of a shared variable that best operates for a grouped number of data sets that share some feature. Finally, comparisons are made most specifically from the perspectives of the motion performed, the degree of skin preparation prior to application of the ECG, the individual wearing the sensors, and the data frequency.

5.1 Determining Filter Length

In adaptive filtering, the filter length indicates the number of past samples and weight coefficients available for use. The filter length is the least reasonable variable to alter in a real-time application of an adaptive filter compared to the gain factor of LMS or the forgetting factor of RLS. As such, a constant filter length must be selected prior to full analysis of the results. An appropriate filter length can be selected through testing of the LMS and RLS algorithms across differing filter lengths on all sets of motion data while varying the gain factor and forgetting factor.

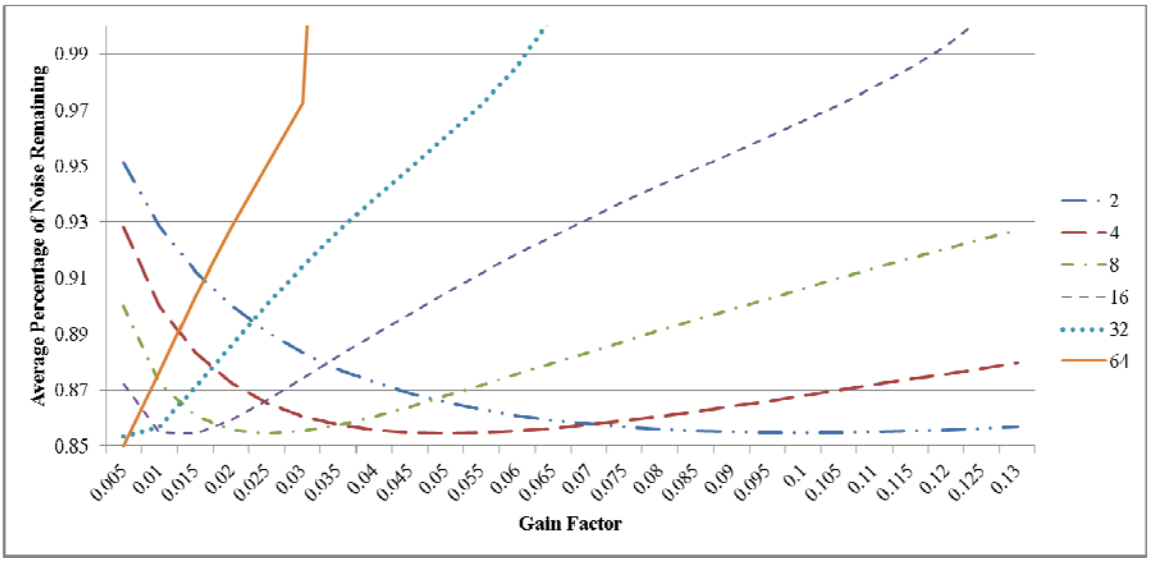

Figure 5.1: LMS comparison of differing filter lengths

Figure 5.1 demonstrates the average performance of the LMS algorithm as gain factor is altered for numerous filter lengths. The results are all using the data from the back sensor. The filter lengths examined are from 2 to 64, increasing exponentially from 2. The gain factor is altered in increments of 0.005 from 0.005 to 0.13. The results are compared on the basis of the percentage of noise remaining, as discussed in 4.2.1. The noise remaining is taken as the average of results across all performed motion trials.

As filter length increases, the best gain factor for optimal results decreases. The amount of noise removed at the optimal result also improves as filter length increases. However, higher filter lengths more rapidly deteriorate as gain factor increases. A filter length of 64 fails to converge entirely for some data sets beginning at a gain factor of 0.03. A filter length of 16 is used in all performances of the LMS filter, being a compromise between best removal performance and slower deterioration due to increasing gain factor.

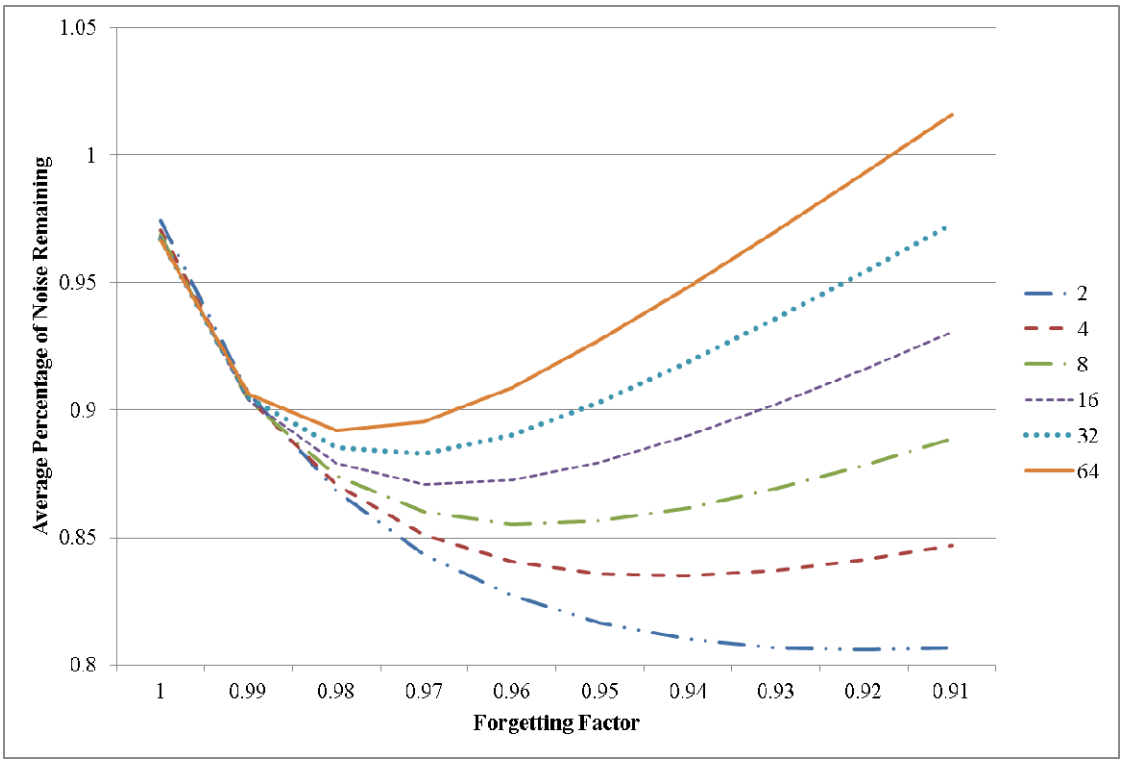

Figure 5.2: RLS comparison of differing filter lengths

Figure 2 demonstrates the impact of altering filter length on the RLS algorithm. Initialization of the inverse autocorrelation is set with $\delta = 100$. δ can be kept constant as testing it at different filter lengths and forgetting factors ultimately proved it had minimal impact on the results, with the value of 100 specifically selected as $\delta = 100$ roughly provided the best results. The main activity desired to analyze is the impact of filter length as the forgetting factor changes. The forgetting factor is tested from 1 to 0.91, decreasing in intervals of 0.01.

As the filter length decreases, the optimal amount of noise removed improves significantly. As such, a lower filter length is highly desirable for this work's use of the RLS algorithm. A filter length of 2 is used for all subsequent RLS work.

5.2 Adaptive Filtering of Individual Sensors

Analysis of adaptive filtering on ECGs using motion data as reference will begin with an examination of the use of each sensor individually. The three sensors in use are the left arm, the right arm, and the back. Each will be used as a reference signal in

filtering the corresponding ECG data. The approach is identical to that of Section 4.2.1, only the filtering is performed on the recorded ECG data rather than on simulated noisy ECG.

5.2.1 LMS – Optimal Gain Factor

Figure 5.3 depicts the LMS results for each individual sensor, using the optimal gain factor for each motion trial of experiment 1. The lightest motions, bending down from sitting (2), bending down from standing (4), reaching forward (5), and reaching up (6) see an average noise removal of 35%-40%. The heaviest motions, walking in place (3) and jogging in place (7) see the worst results with only an average of about 5%-10% noise removed. Sitting down and standing up (2) falls in the middle with an average of 20%-25% of the noise removed.

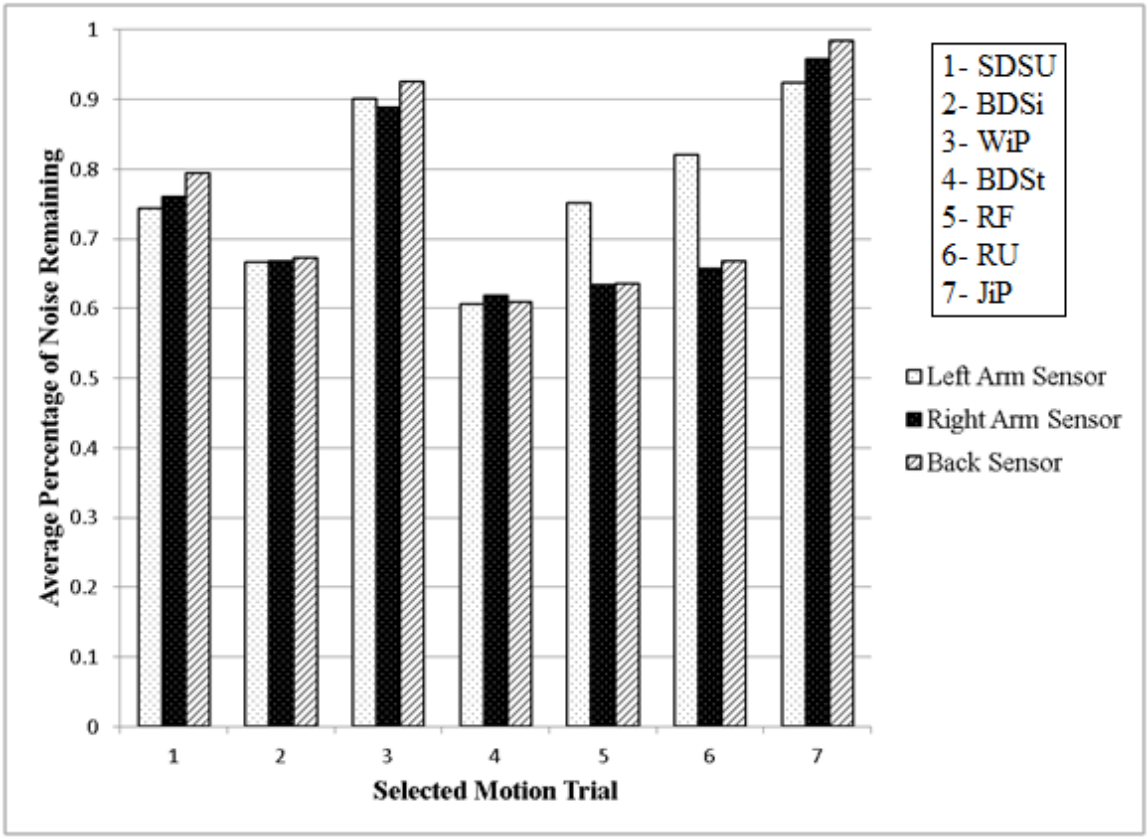

Figure 5.3: LMS motion experiment 1, optimum variables

The results between the sensors tend to be largely comparable with the exceptions of reaching forward and up (5, 6) where the left arm performs worse on average than the

other sensors by about 10%-15%. This is likely due to the fact that the reaching forward and reaching up trials are performed solely with the right arm. Overall, the right arm sensor gets the best results, though not by a significant amount compared to the back sensor.

All in all, the results strongly indicate that the amount of noise removed is related to the intensity of the motion. The least intensive motions, being reaching and bending down, see the best performance. The most intensive motions, being jogging in place and walking in place, see the worst performance. The difference in remaining noise between the light motions and heavy motions is roughly 25%-30%.

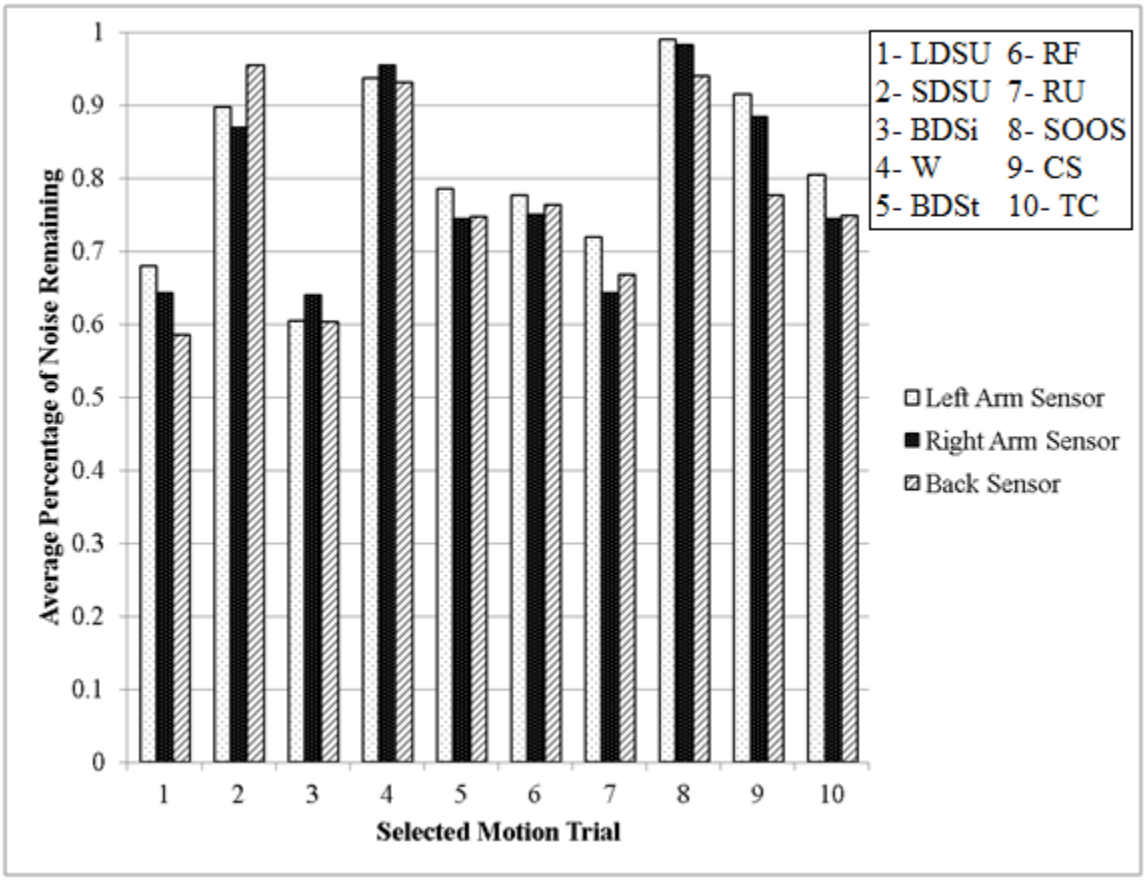

Figure 5.4: LMS motion experiment 2, optimum variables

Figure 5.4 depicts the LMS results for each individual sensor, using the optimal gain factor for each motion trial of experiment 2. Similar to the experiment 1 results, the left arm sensor regularly removes the least amount of noise, consistently being outpaced by the performance of either the right arm or the back sensor, and frequently both. The back sensor performs on average 5-10% better than right arm for lying down (1), stepping on

and off a stool (8), and climbing stairs (9). Right arm only performs notably better for sitting down (2).

Best results are in lying down (1), bending down from sitting (3), and reaching up (7), with about 35%-40% noise removed on each. Next best performances are bending down from standing (5), reaching forward (6), the combined movement trials (10), and the back sensor of stair climbing (9) with about 25% noise removed. Worst performances are sitting down and standing up (5), walking (4), stepping on and off a stool (8), and the arm sensors of climbing stairs (9), with 5%-15% of noise removed. Generally speaking, lighter movements still generally perform better than heavier movements, though given that assumption, lying/standing (1) performs comparatively well while sitting/standing (2) and stool stepping (8) performs comparatively poor.

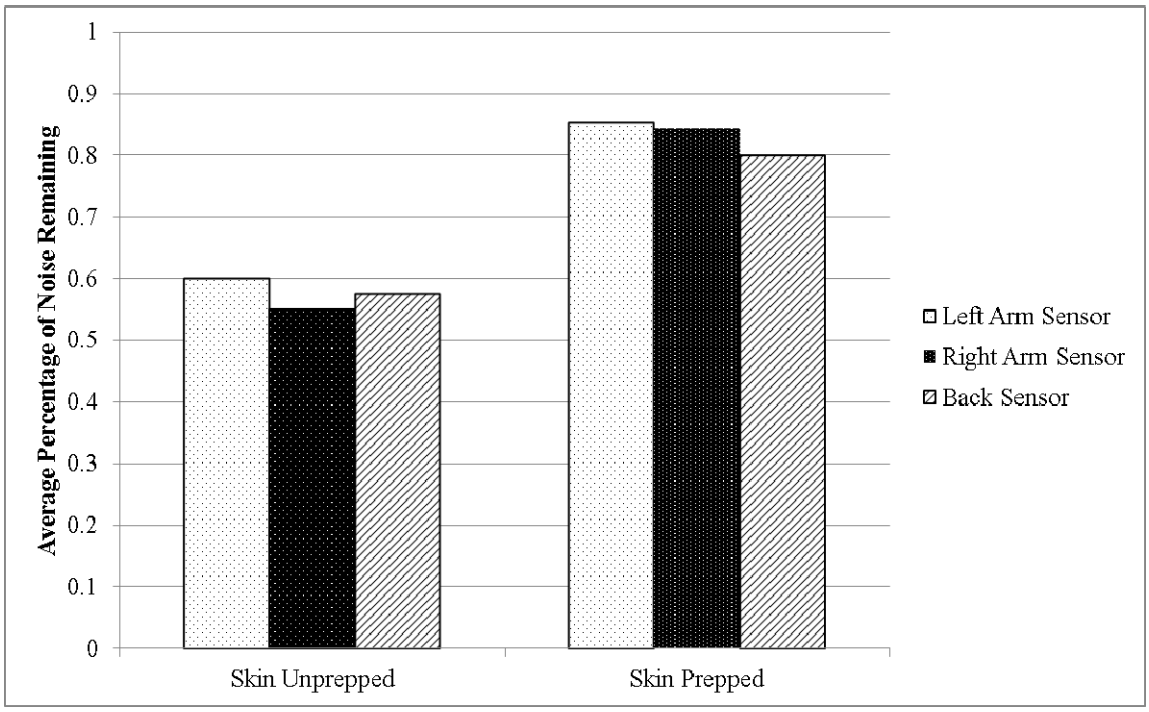

Figure 5.5: LMS skin preparation, optimum variables

The difference in results between ECG data collected on untreated skin and results collected on skin that underwent proper abrasion, as seen in Figure 5.5, is notable. An average of 40%-45% of noise is removed when skin hasn't been properly prepared against the 15%-20% average removed on abrased skin. The left arm sensor performs the worst while the right arm sensor performs best for untreated skin and the back sensor performs best for abrased skin. This matches the motion experiment 1 data, where the left

arm sensor performs the worst and the right arm and back sensors are reasonably close in performance. Overall, the results demonstrate a significant difference in the effectiveness of adaptive filtering depending on whether or not the skin has been properly treated prior to application of the ECG electrodes.

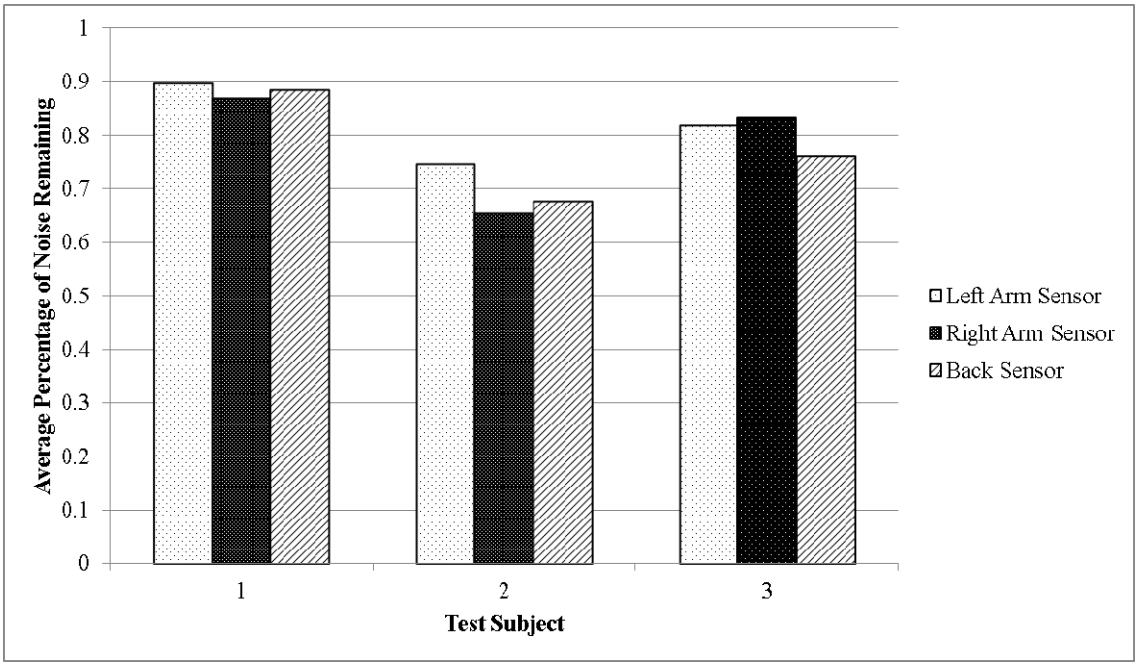

Figure 5.6: LMS multiple users, optimum variables

Figure 5.6 demonstrates a significant variance in results depending on user. As each user abrased and applied the electrodes themselves, this may be due to variance in skin preparation. Test Subject 1 had an average of 10%-15% noise removed, Test Subject 2 had an average of 30%-35% noise removed, and Test Subject 3 had an average of 20%-25% noise removed.

The right arm sensor performs notably worse than the back sensor for Test Subject 3. This is likely associated with how the results between the right arm sensor and back sensor were more varied overall for the motion experiment 2. The reason for the more varied sensor results may be due to the natural variance in how individuals move as a whole.

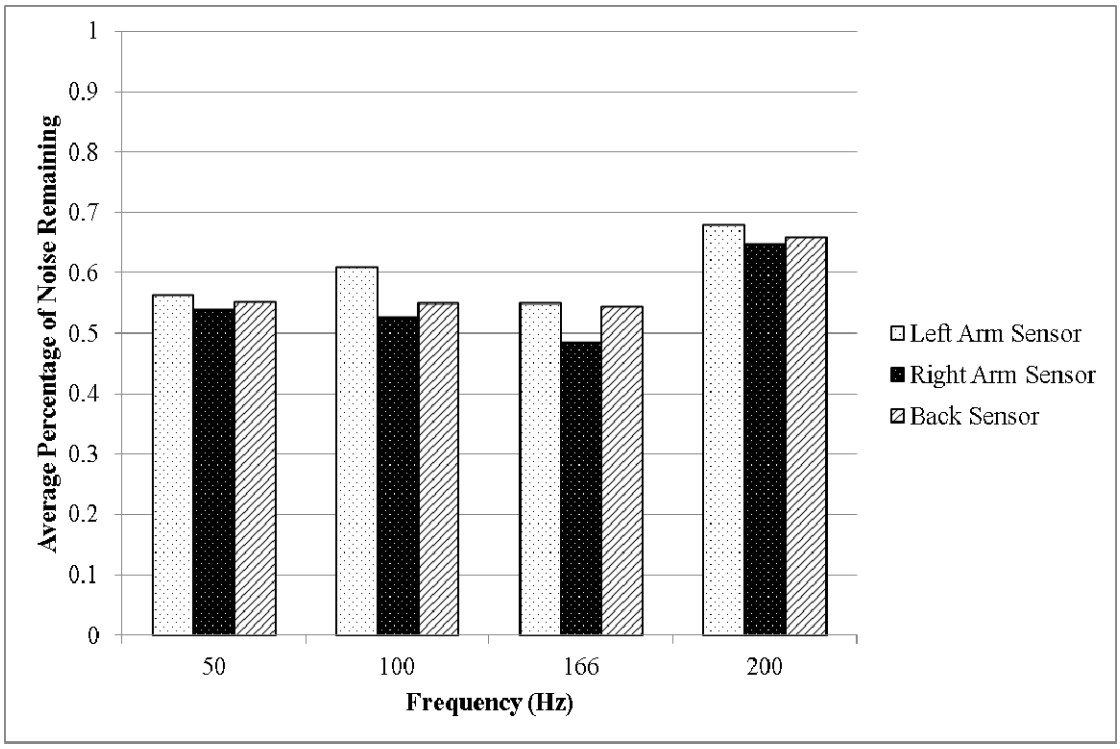

Figure 5.7: LMS sampling frequencies, optimum variables

Figure 5.7 depicts results based on sampling frequency. Data is used from experiment 1, strictly from unprepared skin. The results by sensor are similar to that of the unprepared skin result from figure 5.5. This, again, makes sense as the sensor best suited for filtering should come down to motion above all else. Results for 50 Hz to 166 Hz are largely similar, with roughly 45%-50% of noise removed across all trials on average. 200 Hz appears to be an anomaly with about 35% of noise removed, 10%-15% less than the others. From these results, the performance of the filter does not appear to be directly tied to sampling frequency.

5.2.2 LMS – Shared Gain Factor

The work so far has focused on the use of LMS with optimum gain factors. While this achieves the best possible results, it is unrealistic to expect to be able to constantly achieve the optimum gain factor in a real time scenario. The shared gain factor approach is a more realistic approach that applies the same single gain factor based on a particular variable. More specifically, the assumption is made that an appropriate gain factor can be estimated based on the motion being performed, and so a single gain factor is used across

all performances of a single motion. The gain factor used on a motion trial is that which eliminates the most noise on average across all of the samples within that trial.

The results will typically be the same in terms of which sensor is the best to use, so the focus will be on how the noise removal is impacted relative to the optimum results. Grouping the results by skin preparation, test subject, and frequency leads to redundant results, so only the shared variable results as grouped by motion trials are presented. These additional graphs, along with future redundant graphs left out, are available for viewing in Appendix B.

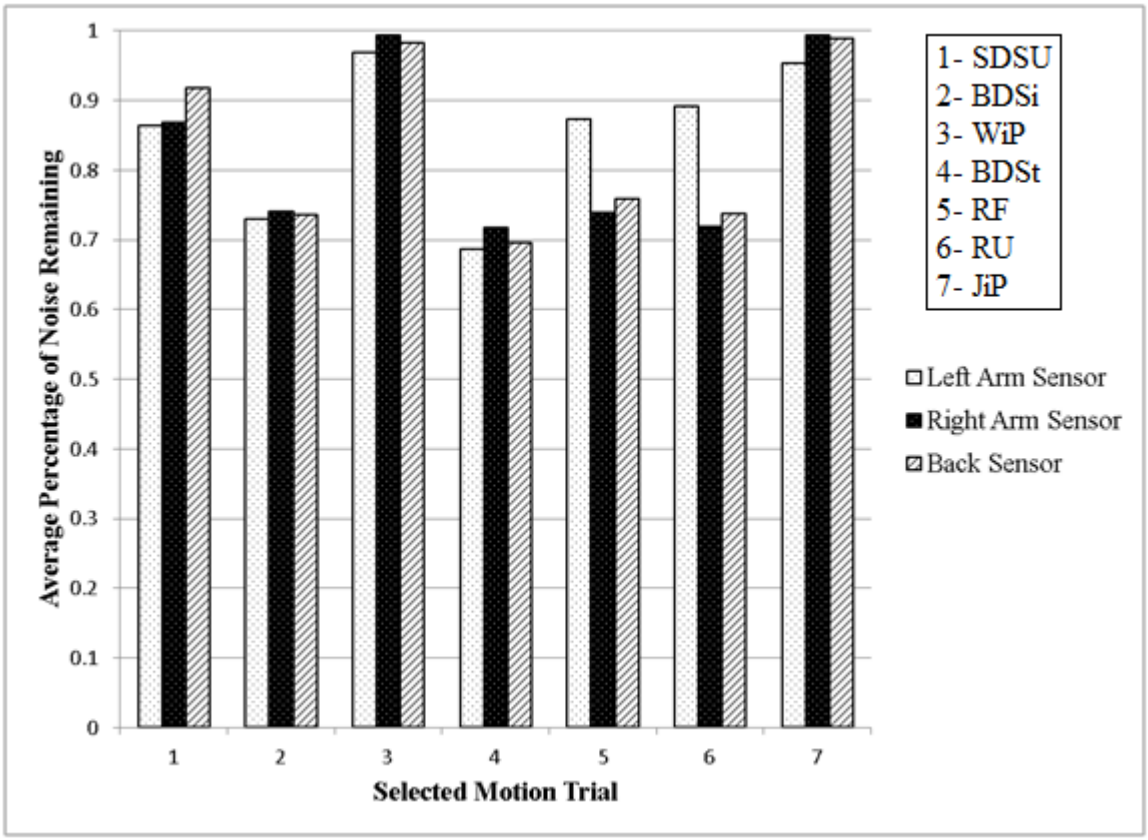

Figure 5.8: LMS motion experiment 1, shared variables

Figure 5.8 demonstrates the results of using a single gain factor within each motion trial for experiment 1. Trials 2, 4, 5, and 6 all see about 25%-30% of the noise removed. Compared to the noise removal with optimum gain factors, there is about 10% extra noise remaining. Trial 1 sees about 10%-15% of the noise removed, also about 10% extra noise remaining compared against the optimum result. Trials 3 and 7 remove 0%-5% of the noise, about 5% extra noise left compared against the optimum results.

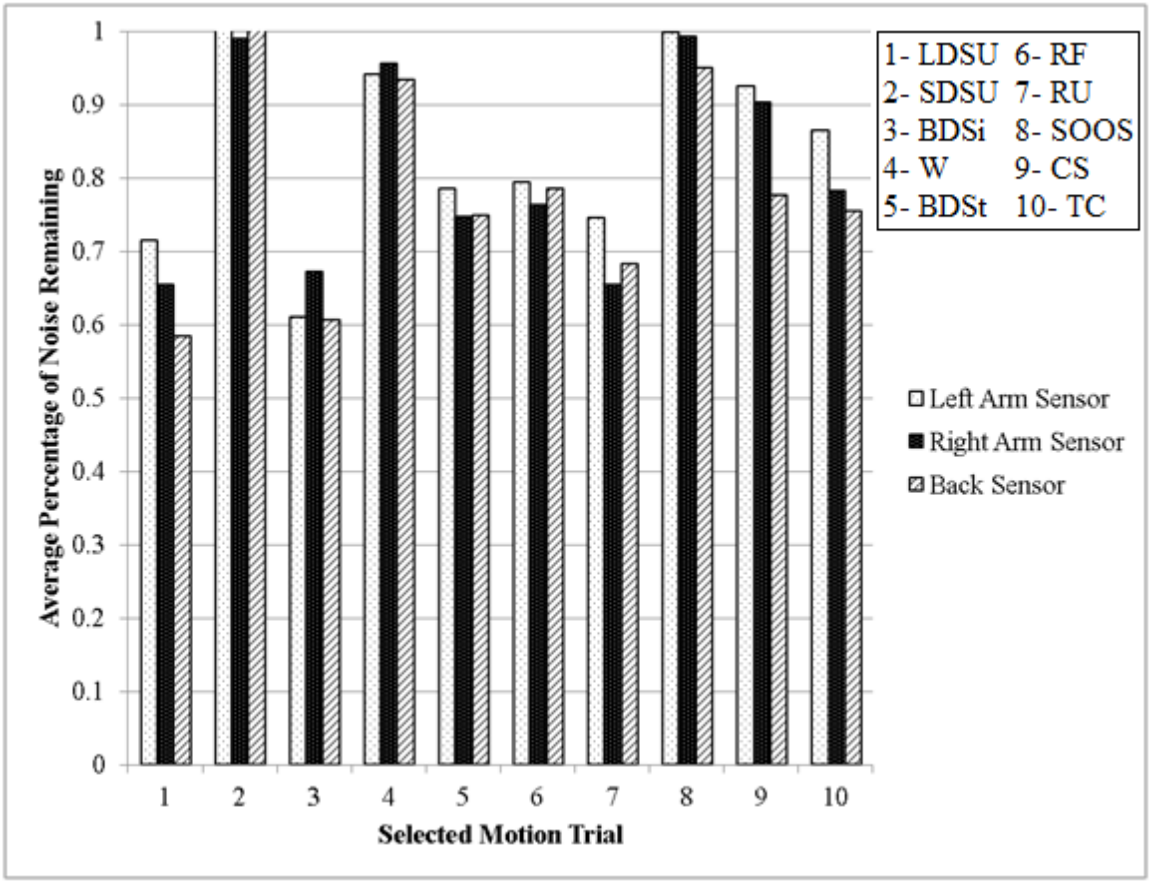

Figure 5.9: LMS motion experiment 2, shared variables

Figure 5.9 uses the same approach, but for the motion trials of experiment 2. Overall, the results are very comparable with the optimum results, with one exception. With shared variables, trial 2 has little to no improvement offered by filtering, when it was previously removing 5-10% of the noise.

Overall, experiment 2 sees less additional noise introduced in using shared variables over optimum variables than experiment 1. Only one trial of experiment 2 is significantly impacted by the use of shared variables, while experiment 1 saw 5%-10% more noise left unfiltered across all trials. The most likely reason for this is that experiment 1 has variations in both sampling frequency and skin preparation among the tested motions while experiment 2 contends only with different test subjects performing each motion.

5.2.3 RLS – Optimal Forgetting Factor

Figure 5.10 demonstrates the results of RLS applied to the motion trials of experiment 1 with optimum forgetting factors used for every dataset. Trials 2, 4, 5, and 6 see an average of 30%-40% of the total noise removed, ignoring the left arm sensors for trials 5 and 6. Trial 1 removes roughly 25% of the total noise. Trials 3 and 7 remove about 10%-15% of the noise.

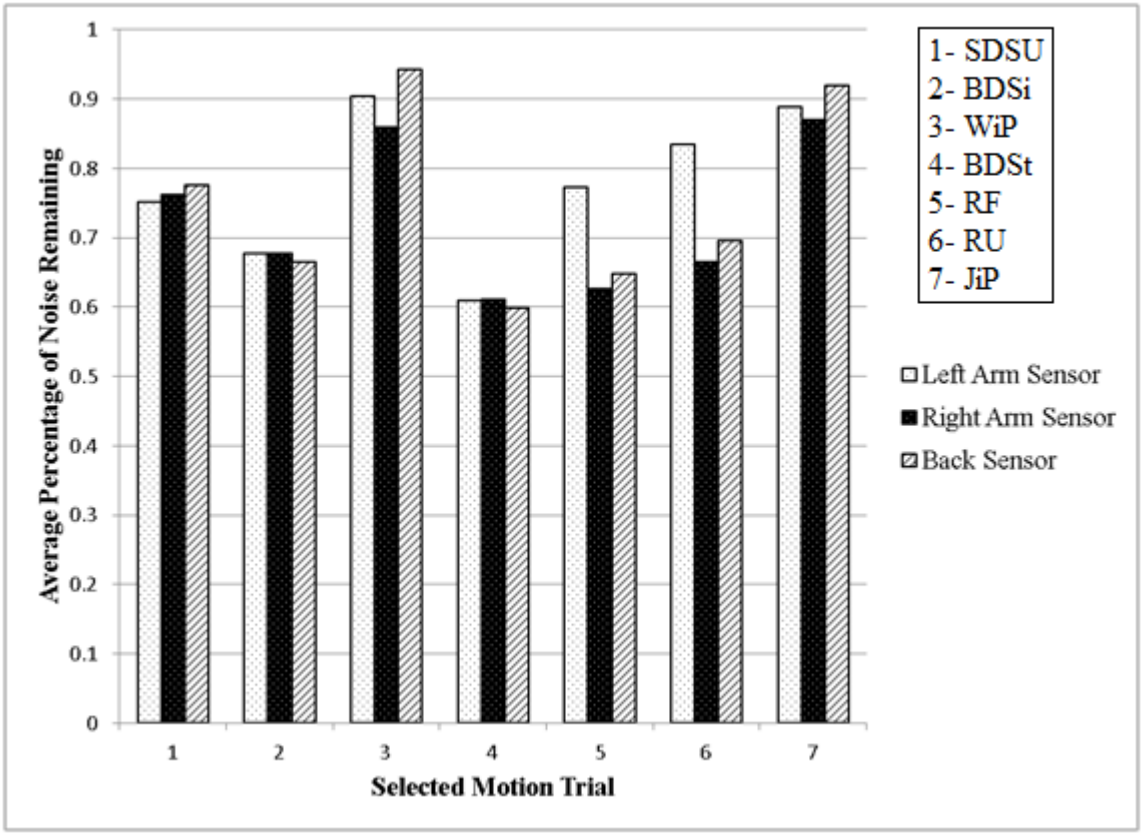

Figure 5.10: RLS motion experiment 1, optimum variables

The left arm sensor rarely proves to be the best sensor of choice. It is notably ineffective in trials 5 and 6, where it removes about 15% less noise on average than its back and right arm sensor counterparts. The results using the right arm and back sensors tend to be fairly close, with a notable exception of trial 3, where the right arm sensor is roughly 5% better than the back sensor. The right arm sensor is the best sensor in this experiment on average, with only trials 2 and 4 seeing it outperformed, and even then by a negligible amount. The broad results in terms of motion intensity and sensor selection

are similar to that of LMS. The comparison in performance will be explored in Section 5.2.5.

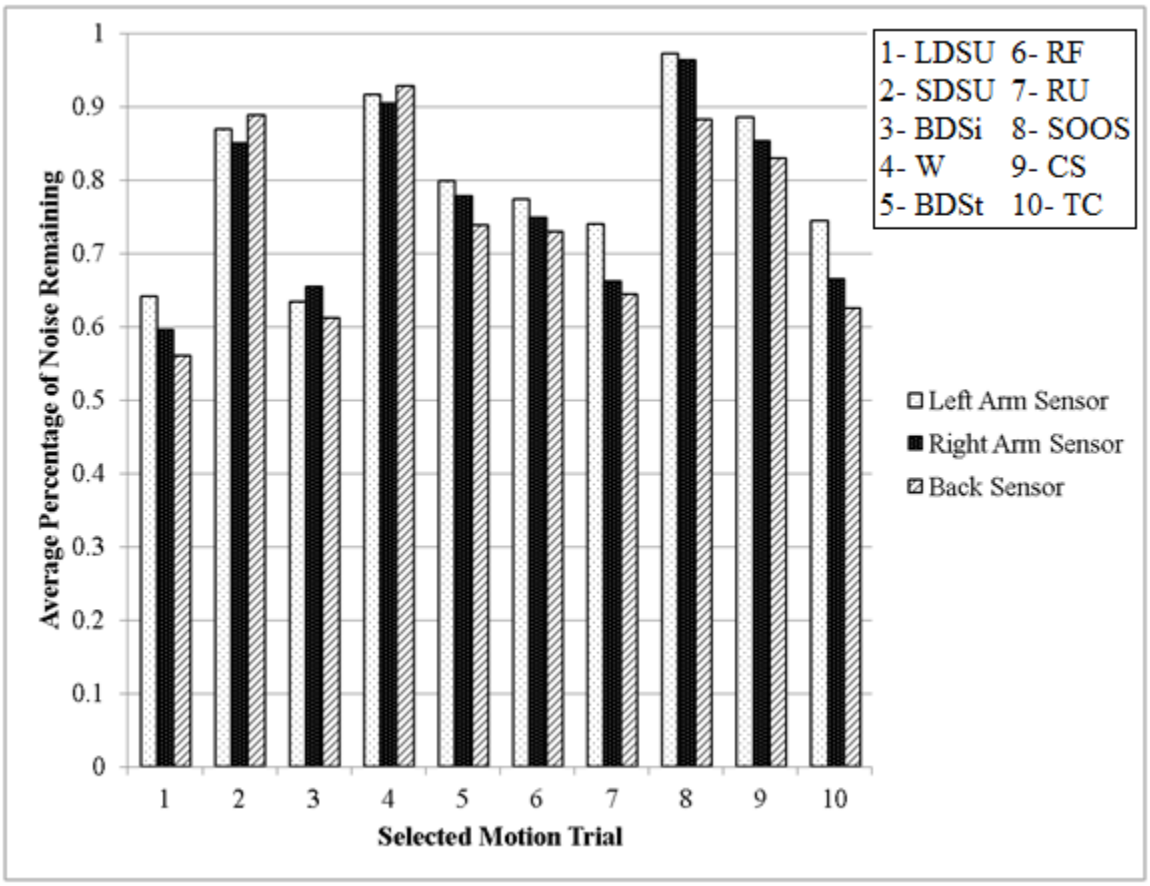

Figure 5.11: RLS motion experiment 2, optimum variables

Figure 5.11 demonstrates the results of RLS applied to the motion trials of experiment 1 with optimum forgetting factors used for every dataset. Trials 1, 3, 7, and 10 see 35%-45% of the average noise removed. Trials 5 and 6 have about 25%-30% of the noise removed. Trials 2, 4, and 9 see about 10%-20% of the noise removed. Trial 8 has about 5%-10% of the noise removed.

The left arm sensor performs poorly compared to the back sensor and right arm sensor in the majority of trials. It is at not the best choice of sensor for any single trial in experiment 2. Results between right and back sensor tend to be reasonably close, with the exception of trial 8 where the back performs better by a little over 5%. Overall, the back

sensor is the best sensor of choice in this experiment with only trials 2 and 4 seeing it outperformed by the right arm sensor, and by less than 5% in each case.

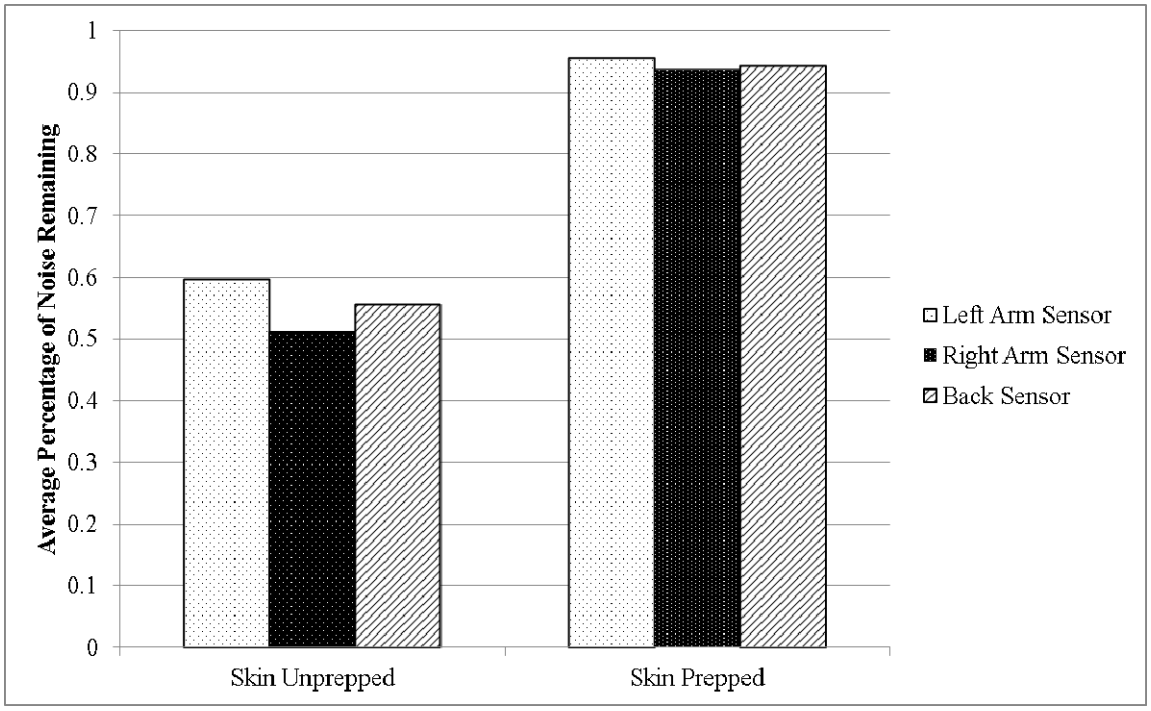

Figure 5.12: RLS skin preparation, optimum variables

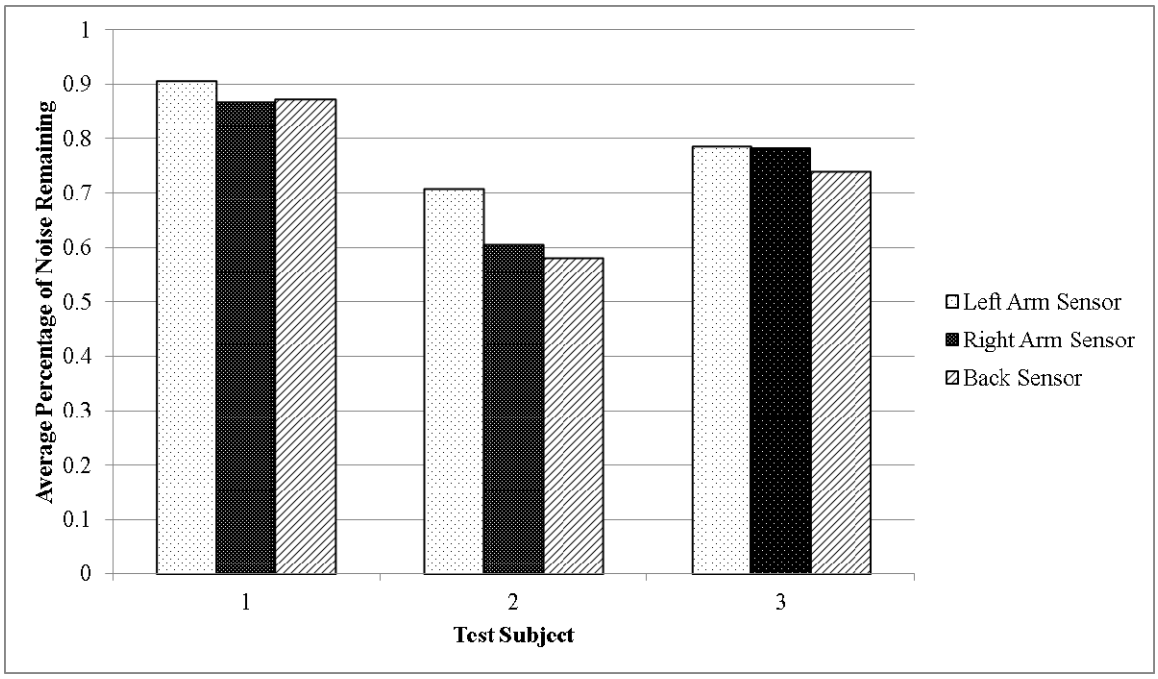

Figure 5.13: RLS multiple users, optimum variables

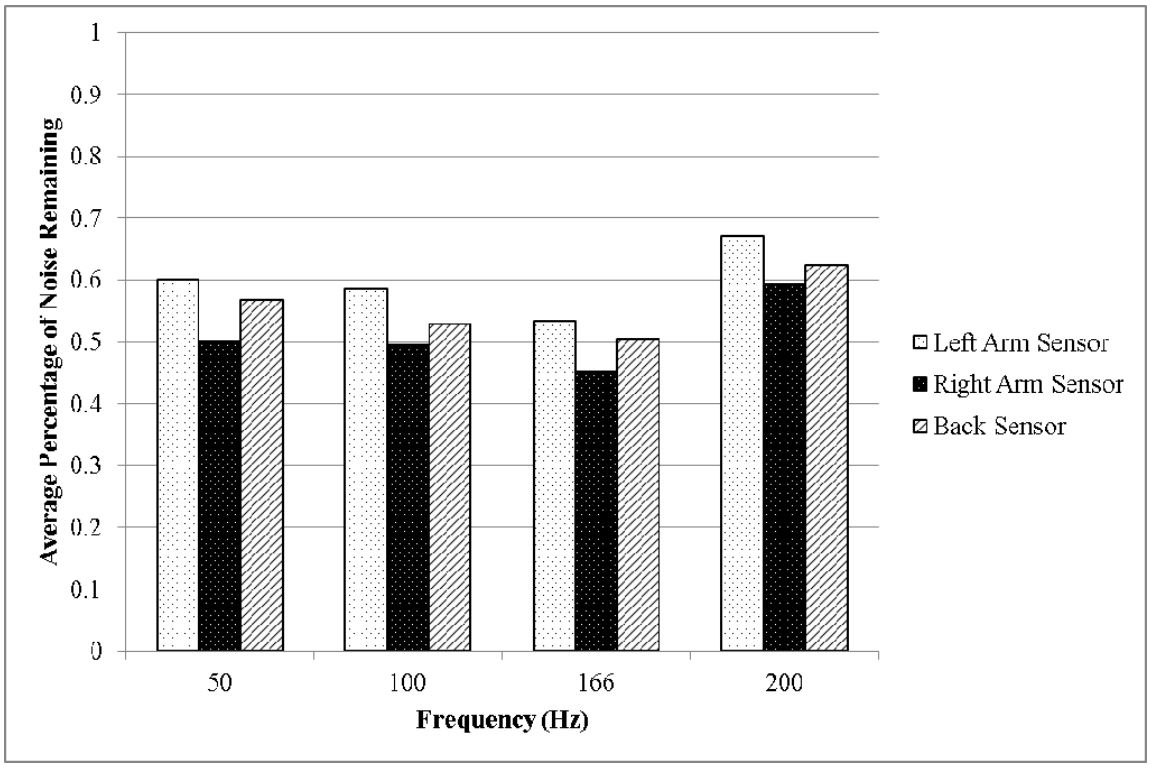

Figure 5.14: RLS sampling frequencies, optimum variables

Figure 5.12, Figure 5.13, and Figure 5.14 show the average RLS results for groupings of skin preparation, test subjects, and frequency respectively. The broad results discussed with LMS have not changed. There is a significant difference in noise removal between unprepared skin and properly abrased skin. The results for each test subject vary significantly. Altering frequency does not have a consistent impact on the performance of the filter.

5.2.4 RLS – Shared Forgetting Factor

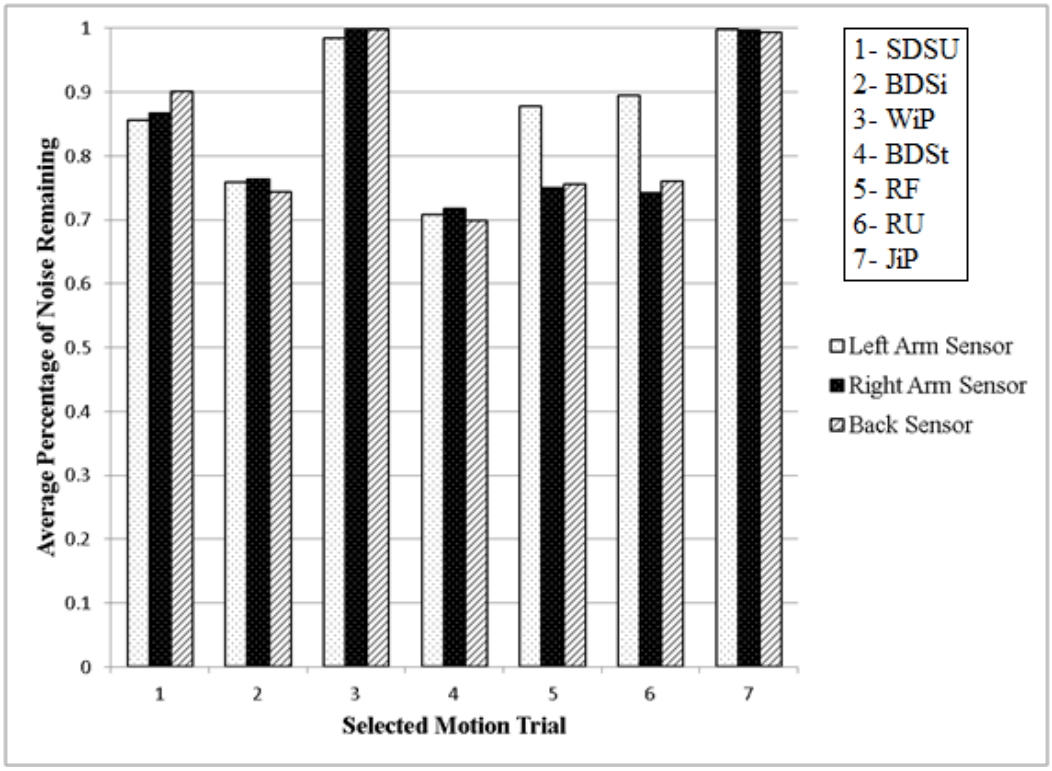

Figure 5.15: RLS motion experiment 1, shared variables

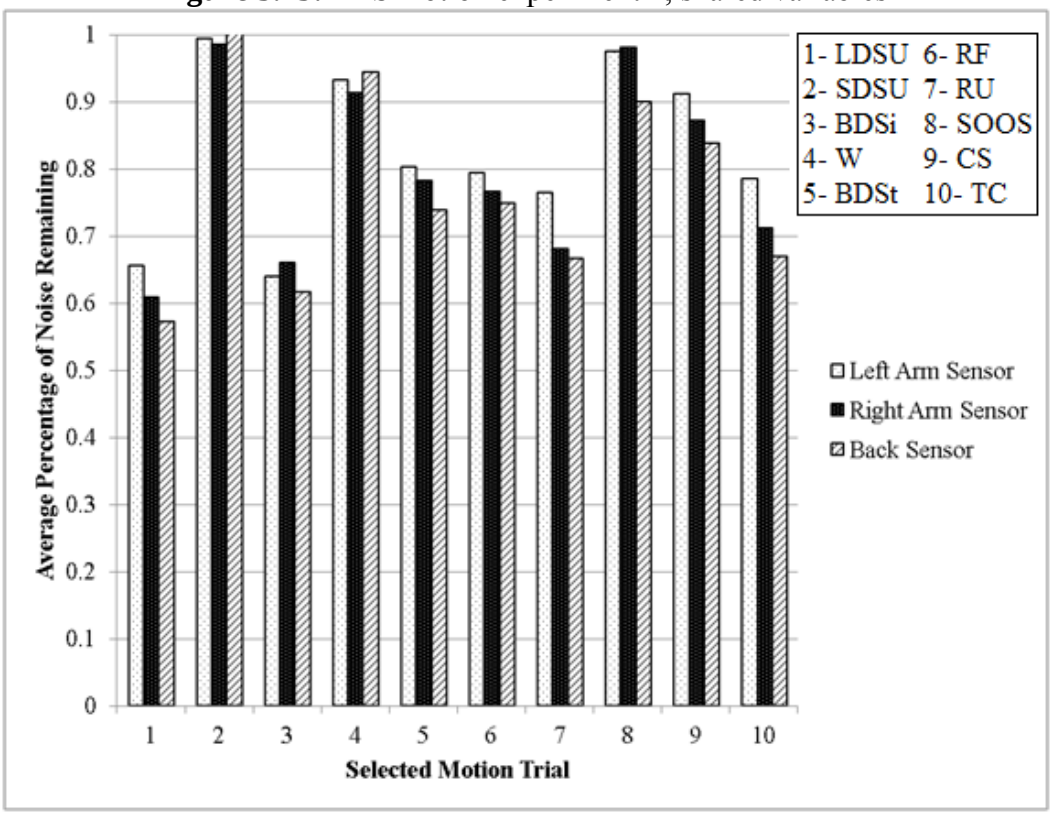

Figure 5.16: RLS motion experiment 2, shared variables

Figure 5.15 and Figure 5.16 show the results for having a single forgotten factor used for every dataset within the motion trials of experiment 1 and experiment 2 respectively. The results are similar to that of going from optimal to shared gain factors in LMS. Experiment 1 sees an additional 10% noise remaining on average across all trials. The results for experiment 2 remain close to the results of the optimal variables, outside of trial 2 which performs 10% worse on average.

5.2.5 LMS vs RLS – Optimal Variables

It is important to analyze the performance of the two different filtering approaches side by side. When comparing the two algorithms, the best results of the individual sensors are of the most interest. This will be examined in two ways. The first approach, best of all sensors, always uses the best result between all three sensors for each individual performance of a trial. The second approach, single sensor result, selects the best sensor on average for use in all performances of a trial. The main purpose of this is to determine the value in having multiple sensors available as opposed to simply selecting the single best location for a sensor and using it alone.

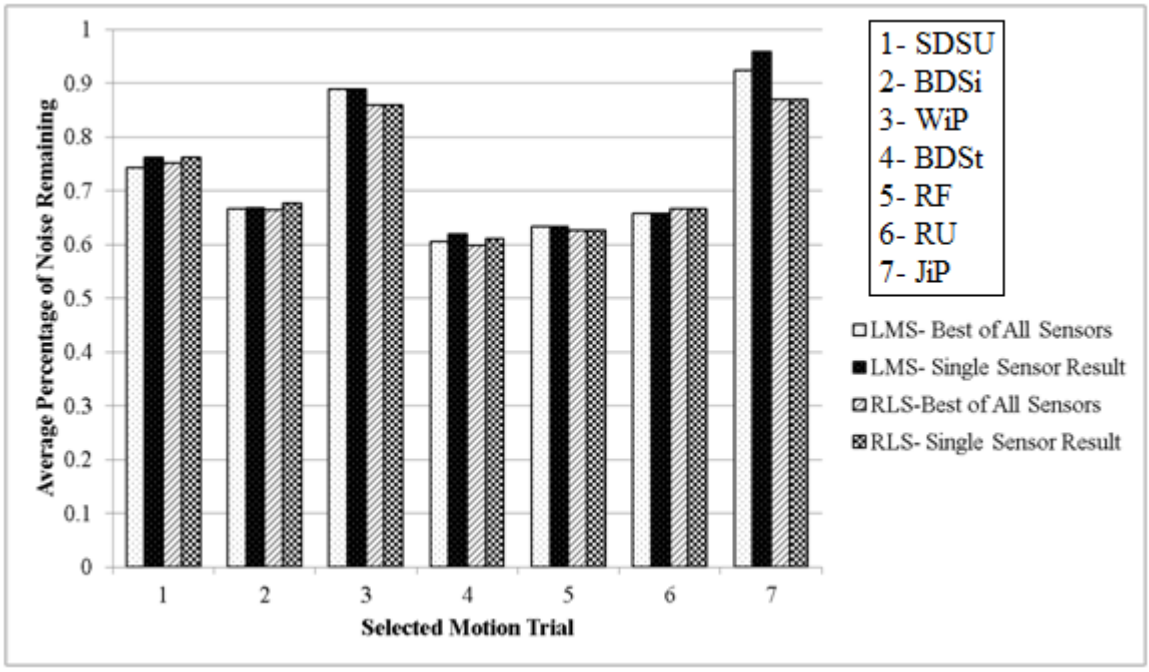

Figure 5.17: LMS vs RLS motion experiment 1, optimum variables

In Figure 5.17, LMS vs. RLS can be seen performing comparatively well in the lighter trials. RLS performs slightly better for walking and about 5% better for jogging in place. As a rule, selecting the best result among different sensors over simply choosing a single generally well performing sensor does not offer much benefit in any trial.

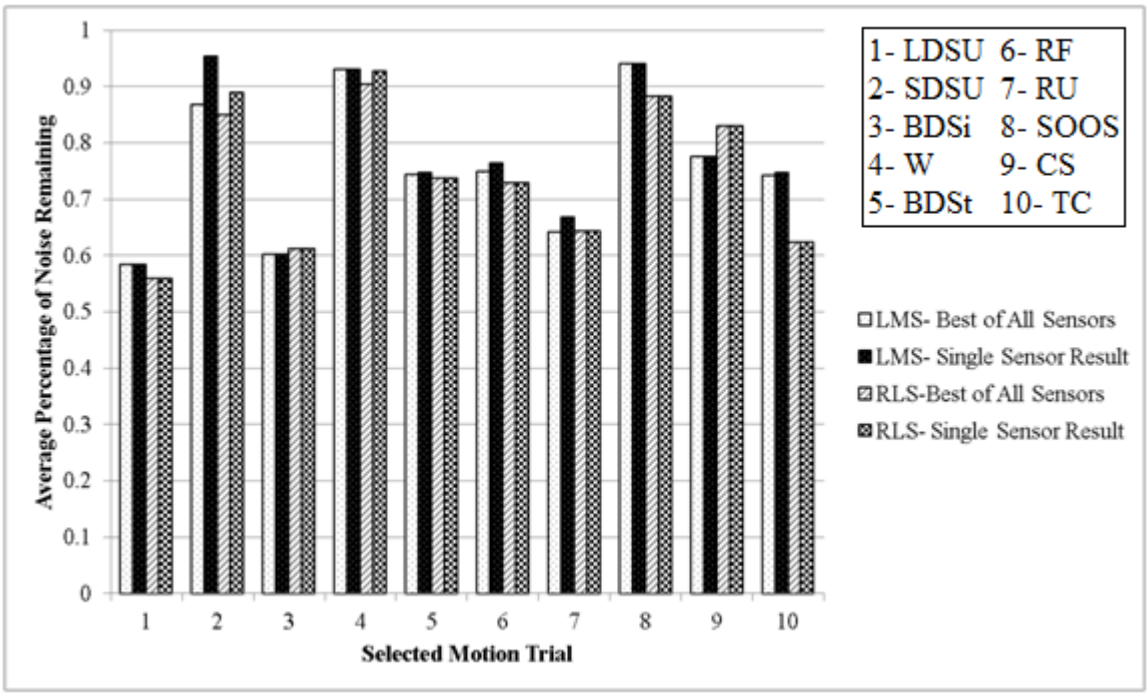

Figure 5.18: LMS vs RLS motion experiment 2, optimum variables

In Figure 5.18, RLS can be seen performing better than LMS through most of the experiment 2 trials, the exceptions being bending down from sitting (3) and climbing stairs (9). Trial 3 is a negligible difference, while trial 9 appears to be an anomaly. The most notable differences are where RLS performs 5% better in trial 8, stepping on and off a stool, and where RLS performs 10% better than LMS in trial 10, where multiple different movements are strung together in sequence.

Having multiple sensors available to choose from once again does not offer significant improvement over choosing a single quality location, with a single exception for LMS in trial 2. Committing to a single sensor results in a failure to remove an additional 5% of the noise for sitting down and standing up.

Overall, while RLS generally performs better than LMS, the degree by which it does so is rarely by a significant amount. It is notable that it does perform better in trial 10 of experiment 2, which indicates that RLS is better at adjusting to changing motions.

5.2.6 LMS vs RLS – Shared Variables

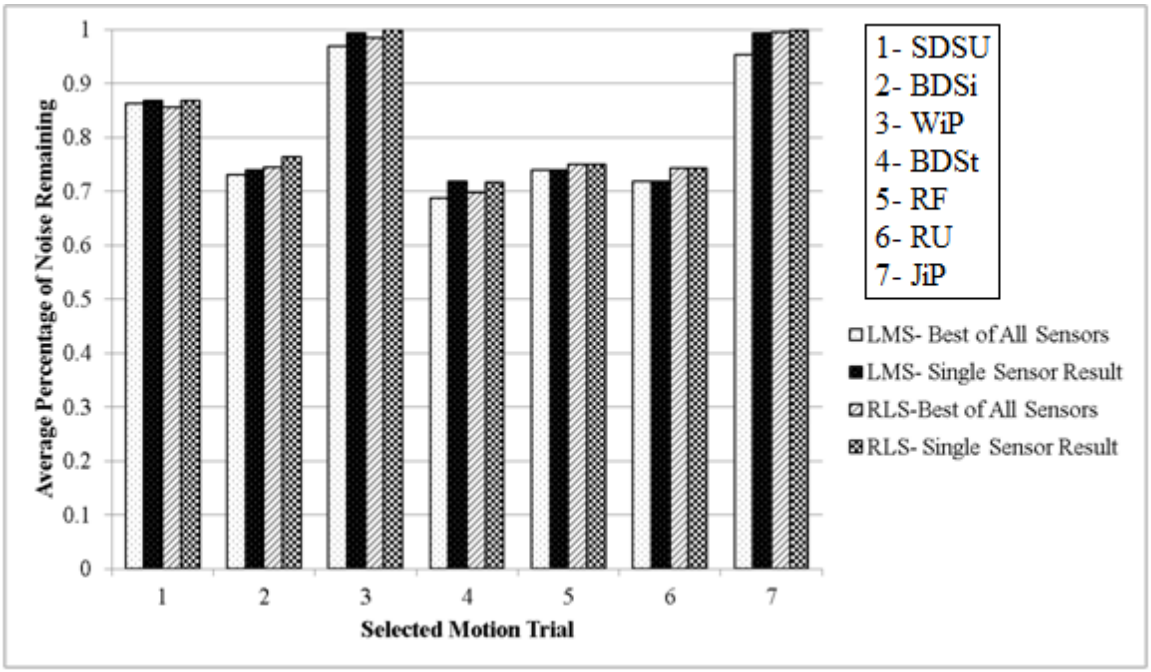

Figure 5.19: LMS vs RLS motion experiment 1, shared variables

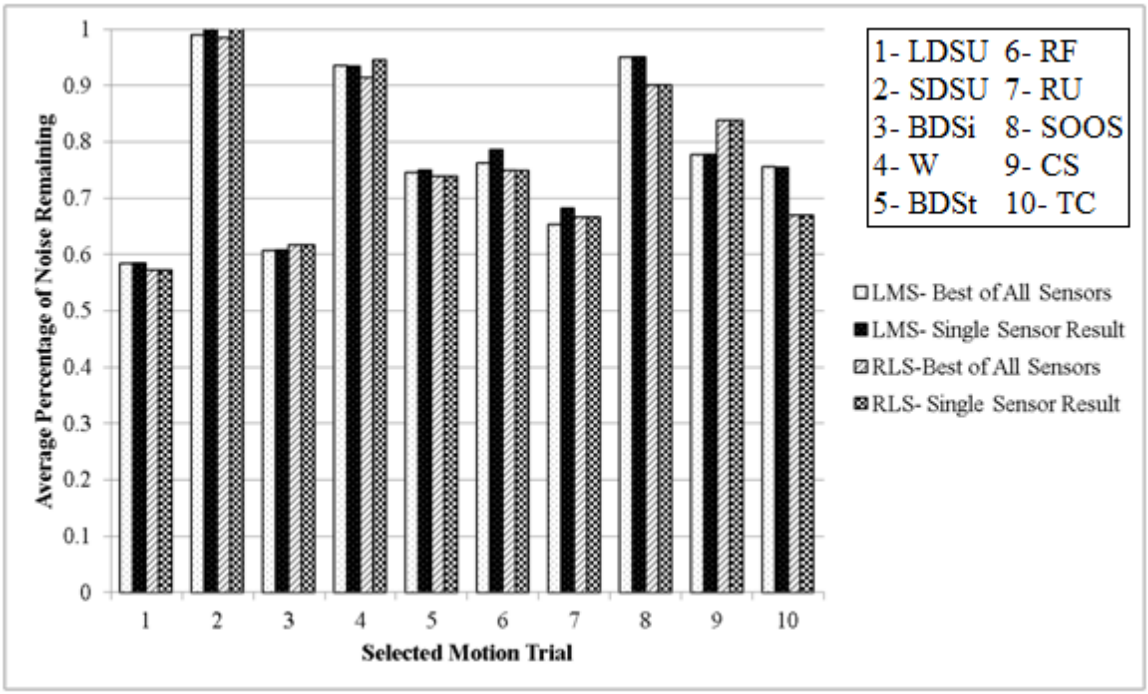

Figure 5.20: LMS vs RLS motion experiment 2, shared variables

As seen in Figure 5.19 and Figure 5.20, when sharing variables within individual motion trials, the differences between LMS and RLS become negligible. The biggest

differences are encountered in trials 8, 9, and 10 of experiment 2. RLS performs about 5% better on trial 8, LMS performs about 5% better on trial 9, RLS performs a little under 10% better on trial 10.

Overall, it does not appear to make a truly significant difference whether multiple sensors are used or just one well located sensor. RLS generally performs better than LMS when the forgetting factors and gain factors are optimized, but the performance difference diminishes when they must be more roughly approximated. This is most notable in experiment 1, where the 5% improvements in trials 3 and 7 are lost.

5.3 Adaptive Filtering of All Sensors via ICA

The next step is to investigate combining motion data from multiple sensors. This is done by first separating them to ensure they are uncorrelated and then summing them together for use as the reference signal in an adaptive filter. The methods for source separation under investigation are FastICA, Infomax, and PCA. Once the sensors are combined, they will be tested through the LMS and RLS adaptive filters in the same process as the individual sensors were analyzed. Whenever multiple motion sensors have been separated and then summed for use in adaptive filtering, the results of the filtering will be referred to as combined sensor results.

The FastICA will be tested under both its Gradient and its Symmetric approach. In the Gradient approach, each independent signal is extracted one after another. In the Symmetric approach, all signals are extracted at the same time. For each approach, two different contrast functions will be tested. For Infomax, the Supergaussian approach will be tested with step sizes $\mu = 0.01$ and $\mu = 0.001$. The Subgaussian approach was tested, but filtering the results could not guarantee convergence for all datasets. As such, it is unsuitable for use and excluded wholly from the results. Analysis will focus on comparisons between the results of the tested BSS approaches. The combined sensor results will be compared against the individual sensor results in Section 5.4.

5.3.1 LMS- Optimum Gain Factors

Figure 5.21 depicts the results of experiment 1 for using FastICA to separate the motion data from the three different sensors before summing them and applying the LMS filter under optimal gain factors. Trials 1, 2, 3, 4, and 6 perform the best of the tested motion trials, similar to the best trials when using a single sensor for the filtering, with 25% to 30% of the noise removed on average. Trials 3 and 7 perform substantially worse, with only 5 to 10% of the noise removed.

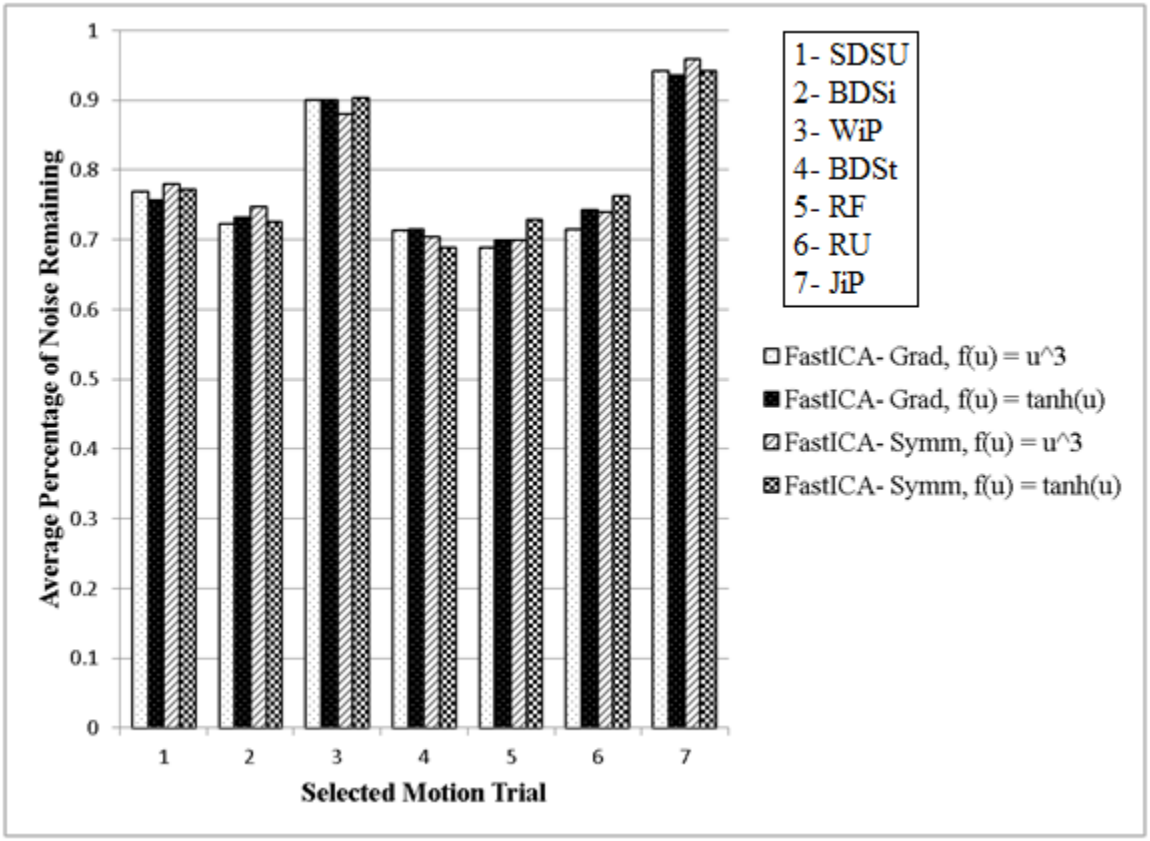

Figure 5.21: FastICA LMS motion experiment 1, optimal variables

There is no single approach that regularly produces the best results, whether in terms of using the gradient or symmetrical FastICA or by the selection of the convergence function. However, the results are all reasonably close to each other, so the selection of a single approach is trivial.

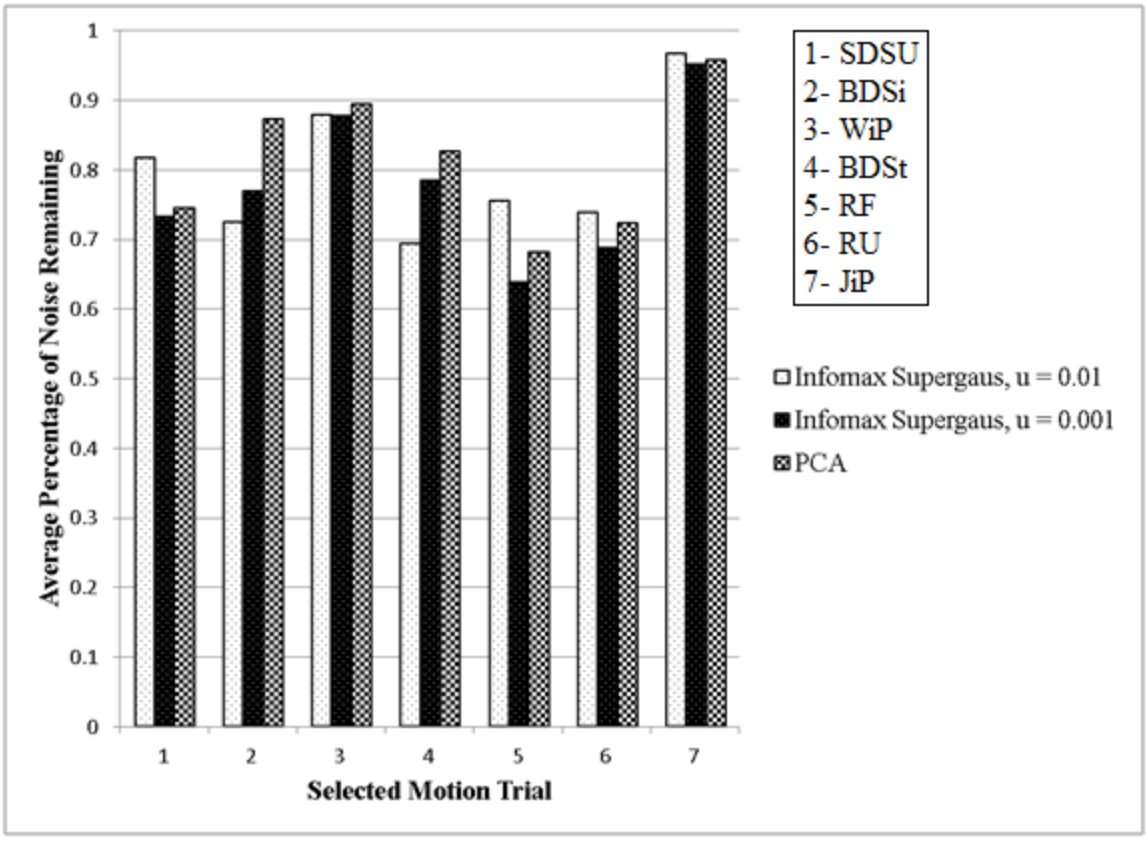

Figure 5.22: Infomax & PCA LMS motion experiment 1, optimum variables

The use of Infomax, as demonstrated in Figure 5.22, shows little in the way of consistency. The best results are still found within the less motion intensive trials 1, 2, 4, 5, and 6, though the average amount of noise removed varies greatly between 20% and 35%. Trial 3 sees a little over 10% of noise removed on average while trial 7 sees roughly 5% removed. A step size of 0.001 sees 10% more noise unfiltered over a step size of 0.01 for trials 1 and 5 while a step size of 0.01 sees 10% more noise unfiltered over a step size of 0.001 for trial 4.

The best results for the use of PCA are in trials 1, 5, and 6, with an average of 25% to 30% of the noise removed. The average noise removal of trials 2, 3, and 4 are roughly 10% to 20%, with trials 2 and 4 in particular performing notably poorly compared to the FastICA and Infomax methods. Trial 7 performs the poorest, with only about 5% removal.

Overall, the best approach tends to be found when using Infomax, so long as the best step size is always selected. However, the selection of step size can lead to significance

differences in the Infomax results. If only a single step size is selected for use, its results become much more inconsistent, leaving FastICA as the better choice overall.

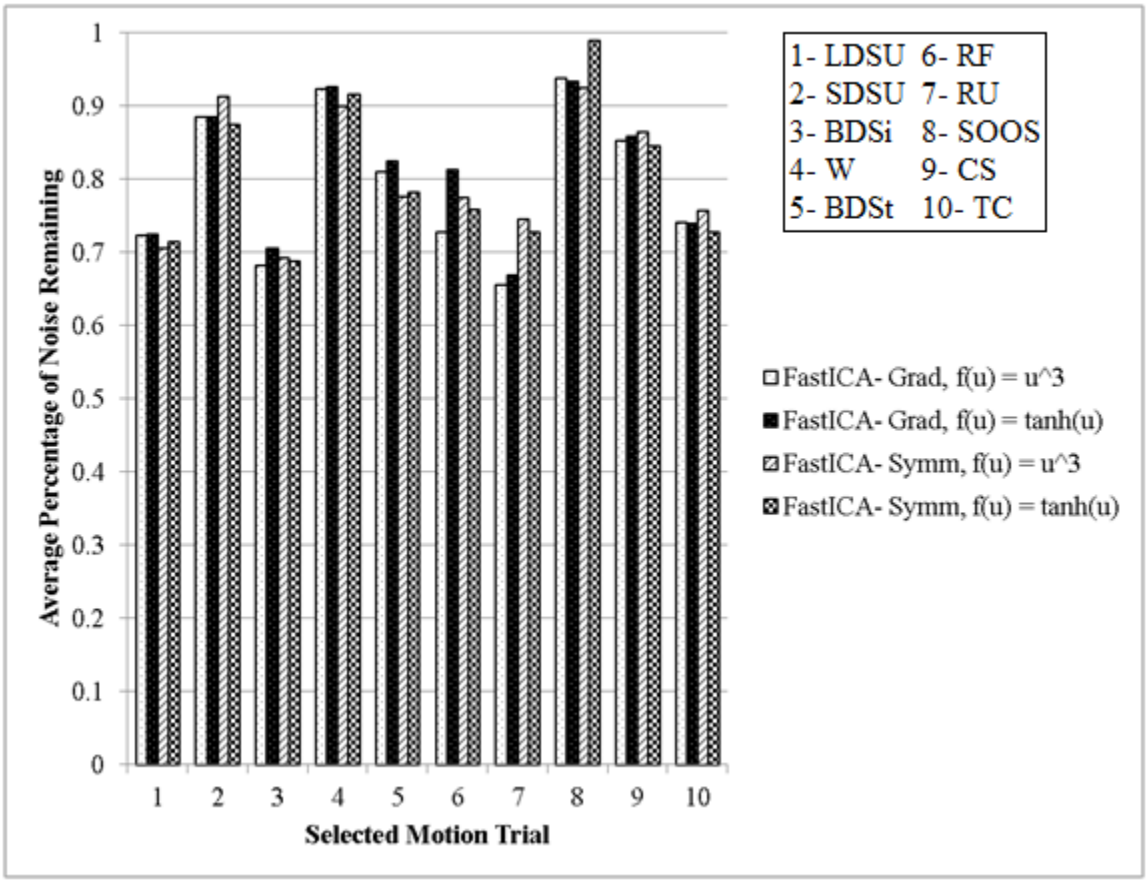

Figure 5.23: FastICA LMS motion experiment 2, optimum variables

Figure 5.23 depicts the results of experiment 2 for using FastICA to separate the motion data from the three different sensors before summing them and applying the LMS filter under optimal gain factors. The best performing test trials are 1, 3, 5, 6, 7, and 10, with an average of 20% to 35% noise removal. The worst performing trials are 2, 4, 8, and 9, with an average of 5% to 15% noise removal.

Results are fairly uniform across the different approaches, with a few exceptions. The *tanh(u)* contrast function performs 10% worse in trial 6 for the gradient approach and a little over 5% worse for the symmetric approach in trial 8. Trial 7 sees the gradient approach generally removing about 5% to 10% more noise than the symmetrical approach.

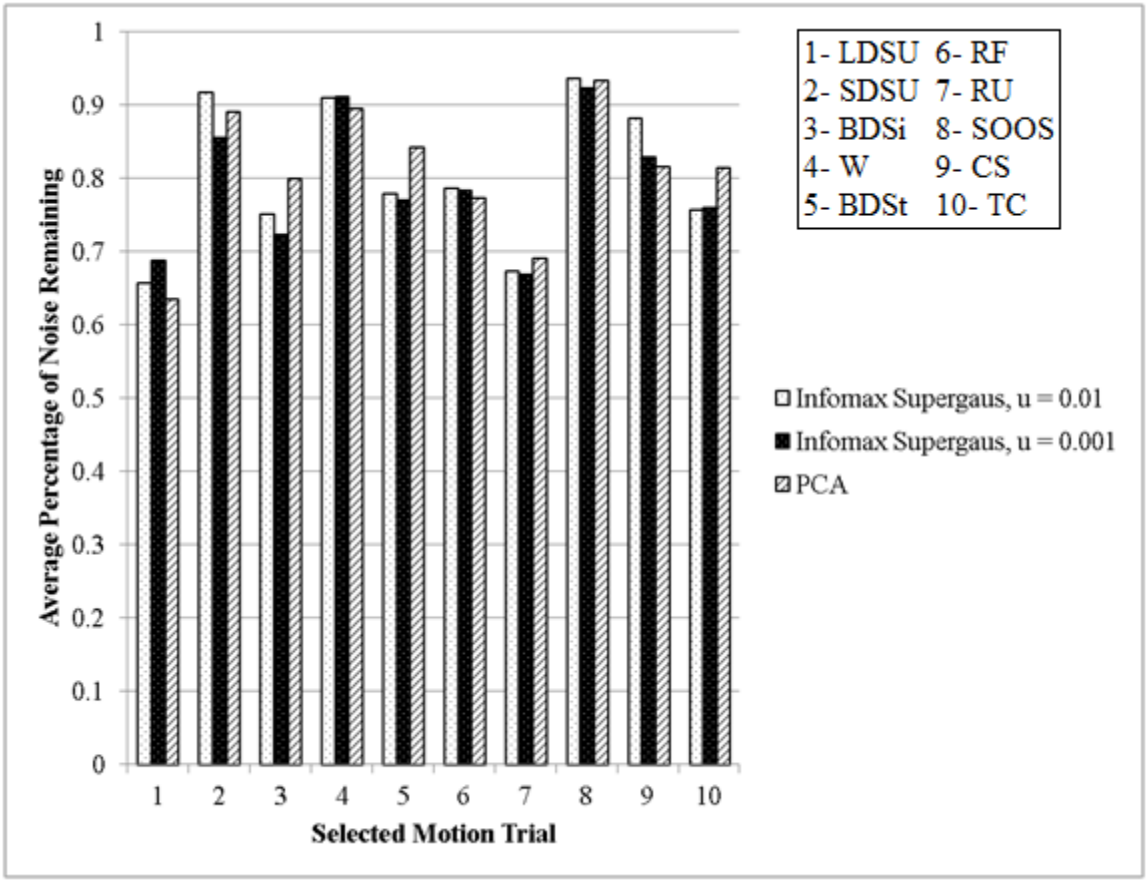

Figure 5.24: Infomax & PCA LMS motion experiment 2, optimum variables

Figure 5.24 demonstrates the results of experiment 2 with the use of Infomax and PCA. Similar to FastICA, best trials are 1, 3, 5, 6, 7, and 10 with roughly 25% to 35% of noise removed on average. Trials 2, 4, 8, and 9 see roughly 10%-15% of noise removed.

There's more consistency here in the better choice of step size. Infomax with a step size of 0.001 performs better than with a step size of 0.01 in the majority of trials and performs reasonably close in the two instances it doesn't. The most notable differences have the step size of 0.01 leaving on average an additional 5% of noise in trials 2 and 9.

PCA performs closely to that of Infomax with the exception of trials 3, 5, and 10, where it leaves an additional 5%-10% of noise.

The best selection for FastICA is gradient with a convergence function of u^3 while the best selection for supergaussian Infomax is utilizing a step size of 0.001. Infomax performs best in trials 1, 2, 4, 5, 8, and 9. None of the differences are particularly substantial, with each method removing within 5% of the other. PCA rarely outperforms either method and too often performs notably worse.

The results when combined in terms of skin preparation, test subject, and frequency offer no new information that hasn't been discussed previously. The broad results by variable follow similarly to the results of the individual sensors, with more intensive movements typically performing worse than the lighter movements. Between the methods themselves, PCA is the most inconsistent and performs poorly compared against FastICA and Infomax more often than not. FastICA and Infomax continue to perform competitively, with FastICA largely seeing no significant differences between approaches and the supergaussian Infomax with step size 0.001 most frequently performing best.

5.3.2 LMS – Shared Gain Factors

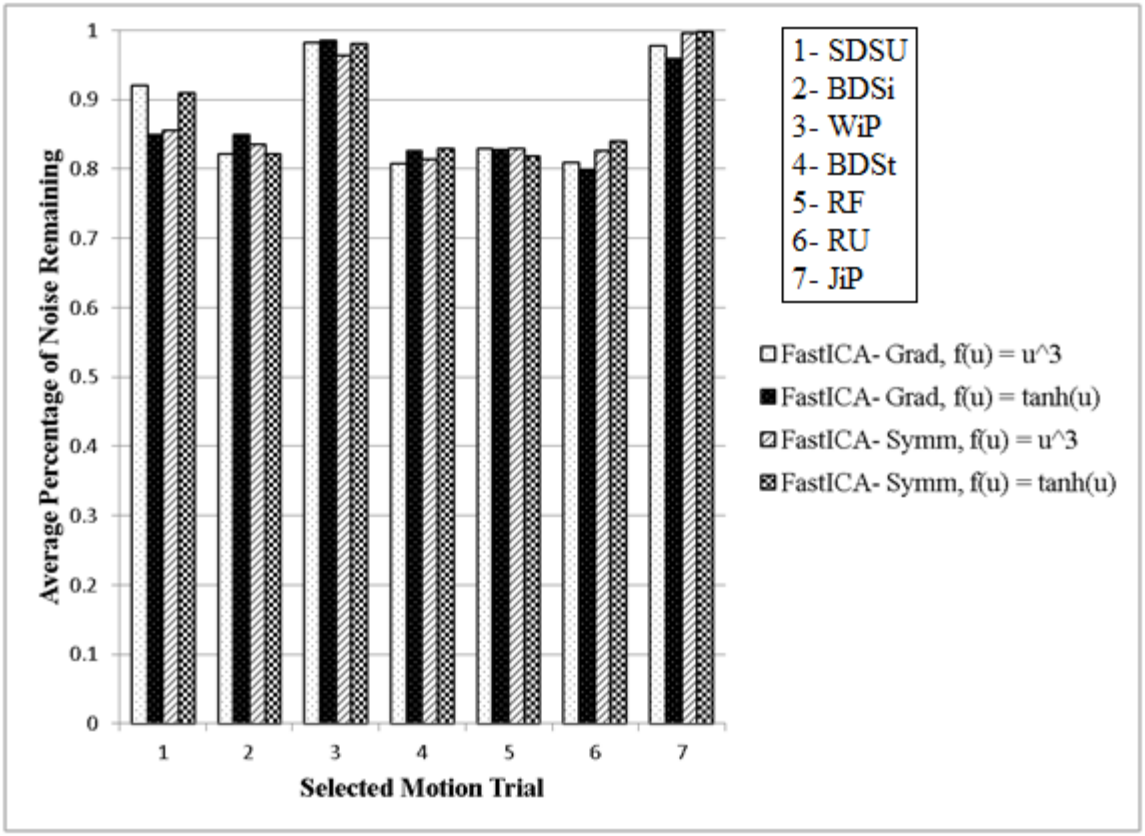

Figure 5.25: FastICA LMS motion experiment 1, shared variables

Figure 5.25 depicts the results of experiment 1 for using FastICA to separate the motion data from the three different sensors before summing them and applying the LMS filter under shared gain factors. FastICA sees roughly 15%-20% of noise removed for trials 1, 2, 4, 5, and 6, ignoring the worst case approaches for trial 1. Trials 3 and 7 see

0%-5% noise removed on average. Overall, there is 5% to 10% additional noise left unfiltered on average when compared against the optimum results.

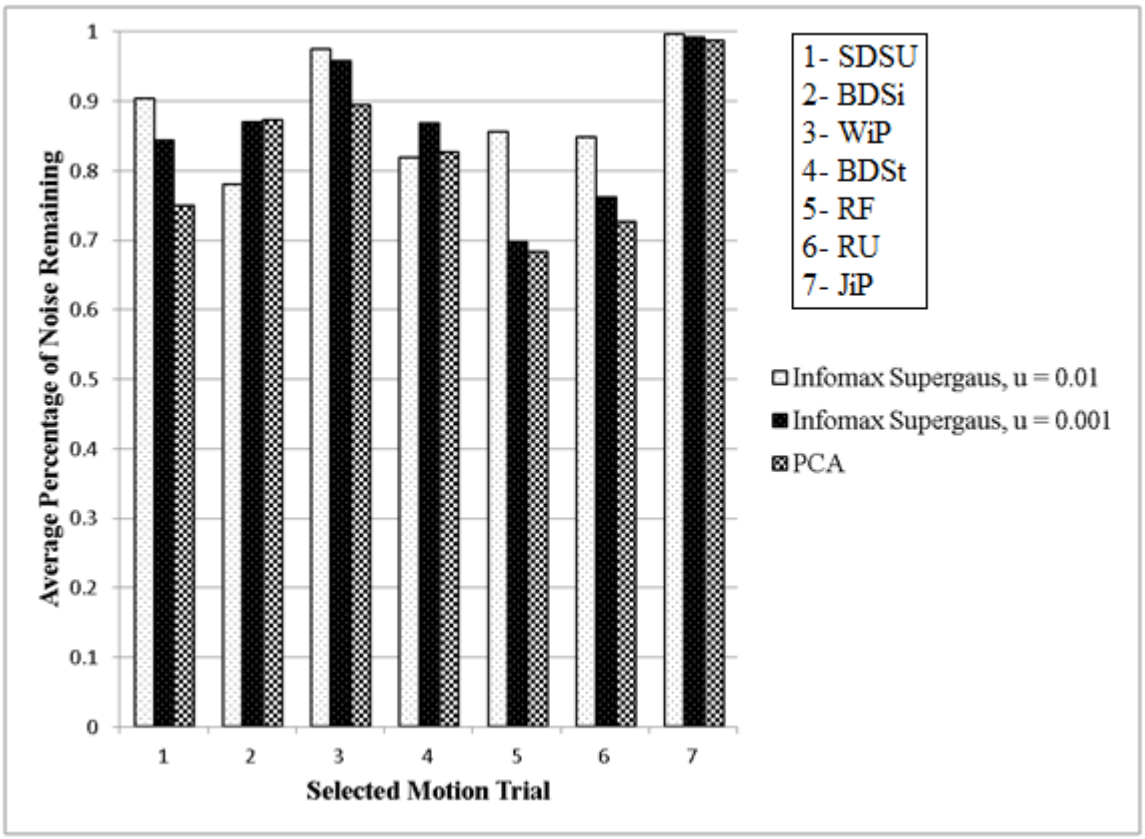

Figure 5.26: Infomax & PCA LMS motion experiment 1, shared variables

Figure 5.26 shows the results when the motion data is processed through Infomax and PCA. Infomax sees identical deteriorations in performance with the use of shared gain factors as FastICA, leaving behind an additional 5% to 10% noise on average when compared against the results using optimum gain factors.

The data processed by PCA appears to better find a gain factor that can be shared across the datasets of a trial, seeing insignificant change across all but trial 7, which worsens by less than 5%. This leaves PCA the best method for all but trial 2, contrasting with it being the worst method when optimum gain factors are used.

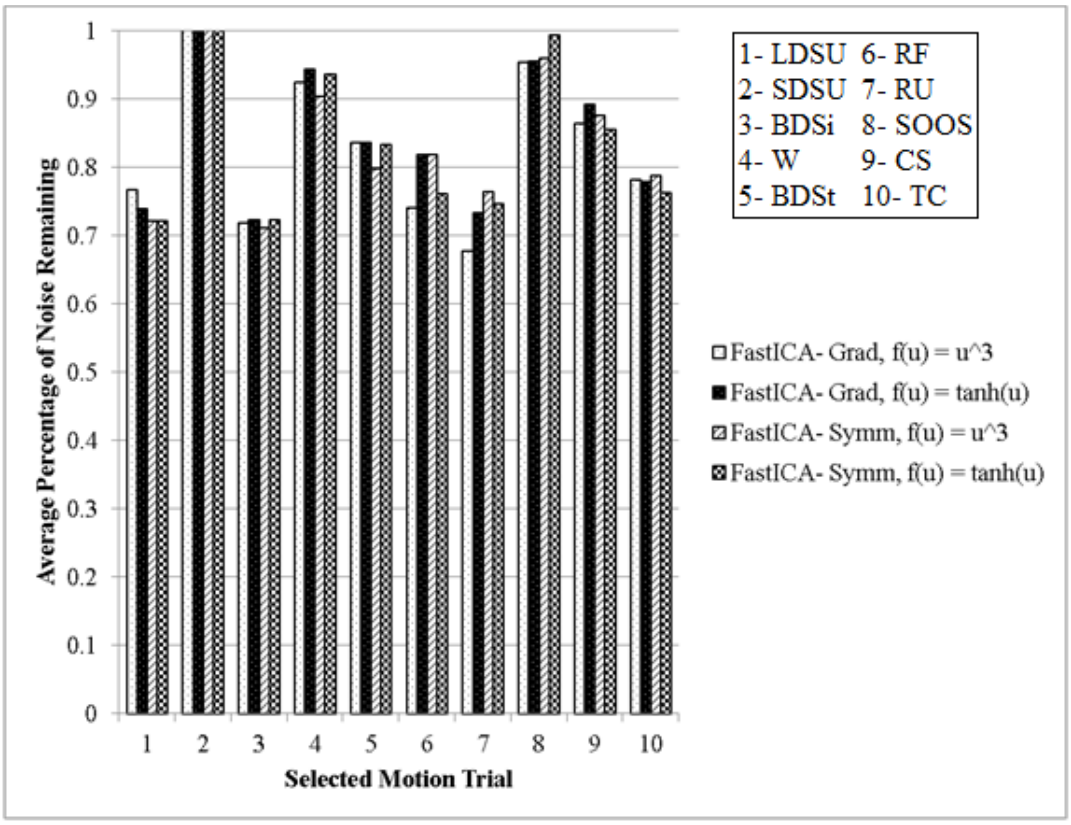

Figure 5.27: FastICA LMS motion experiment 2, shared variables

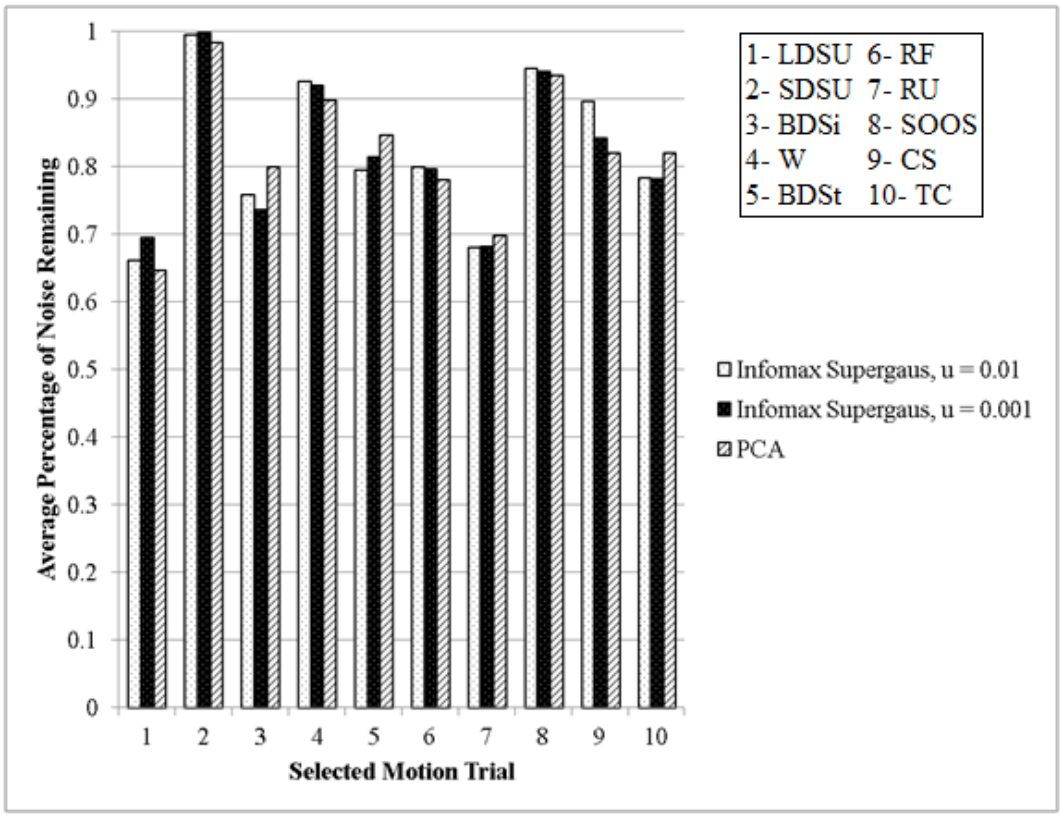

Figure 5.28: Infomax & PCA LMS motion experiment 2, shared variables

Figure 5.27 depicts the results of experiment 2 for using FastICA to separate the motion data prior to summing and applying the LMS filter under shared gain factors. Figure 5.28 depicts the results for using Infomax and PCA. The methods all largely see reasonably comparable results to the optimum results, seeing a worse performance of no more than about 5% across the majority of the trials. The single exception is trial 2, which in all cases goes from 10% to 15% noise removal in optimum gain factors to negligible amounts of noise removal in shared gain factors.

When shared forgetting factors are used, PCA becomes the best approach overall. FastICA and Infomax see 5%-10% worse results for the majority of trials in both experiment 1 and 2 while PCA only sees significantly worse results in experiment 2. Generally, after using ICA, finding a common gain factor for data without significantly worsening results is difficult.

5.3.3 RLS – Optimum Forgetting Factors

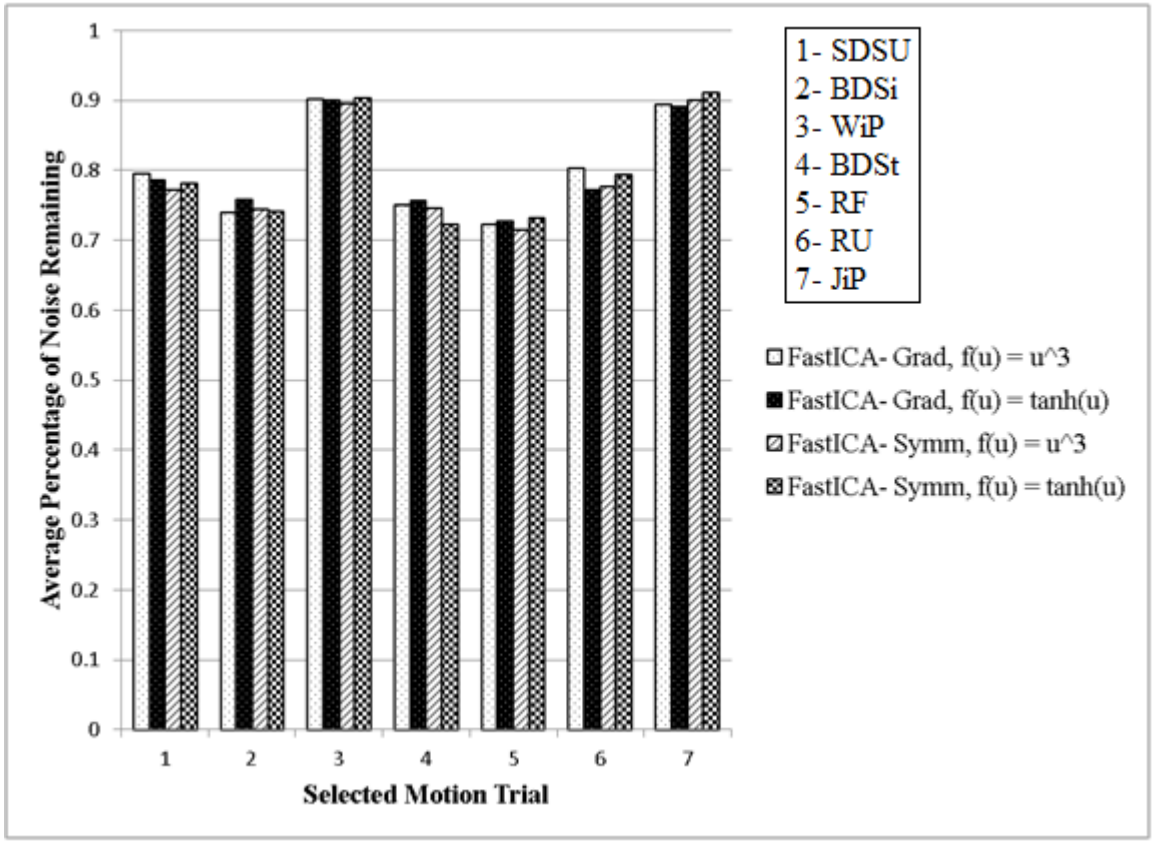

Figure 5.29: FastICA RLS motion experiment 1, optimum variables

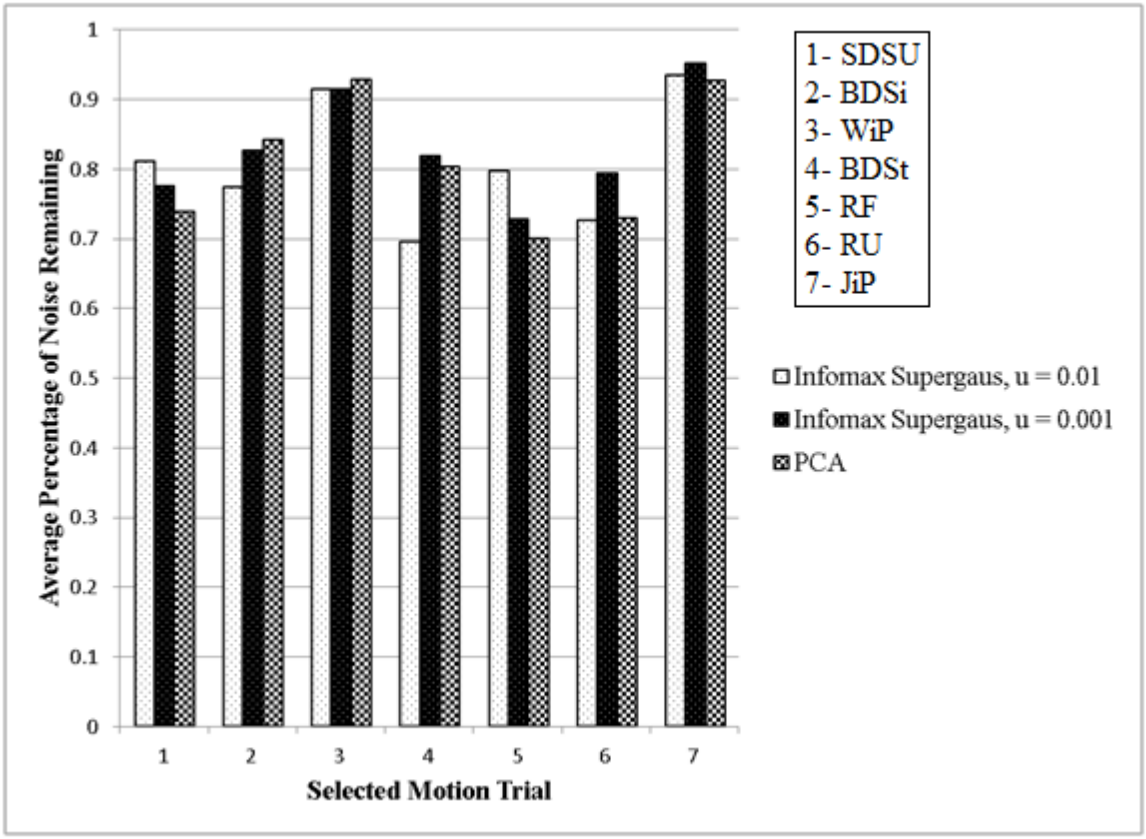

Figure 5.30: Infomax & PCA RLS motion experiment 1, optimum variables

Figure 5.29 depicts the results of experiment 1 for using FastICA to separate the motion data prior to summing and applying the RLS filter under optimum forgetting factors. Figure 5.30 depicts the results using Infomax and PCA. All methods see roughly similar results. Trials 1, 2, 4, 5, and 6 all have 20% to 30% of noise removed on average. Trials 3 and 7 see roughly 10% of noise removed on average.

FastICA has no particular approach performing consistently better than the others. In the end, all are reasonably close to each other in each individual trial.

As was the case when applying the LMS filter, Infomax has no consistently superior step size. A step size of 0.01 outperforms a step size of 0.001 by about 10% for trial 4 and by about 5% for trial 6, while a step size of 0.001 outperforms a step size of 0.01 by about 5% for trial 5.

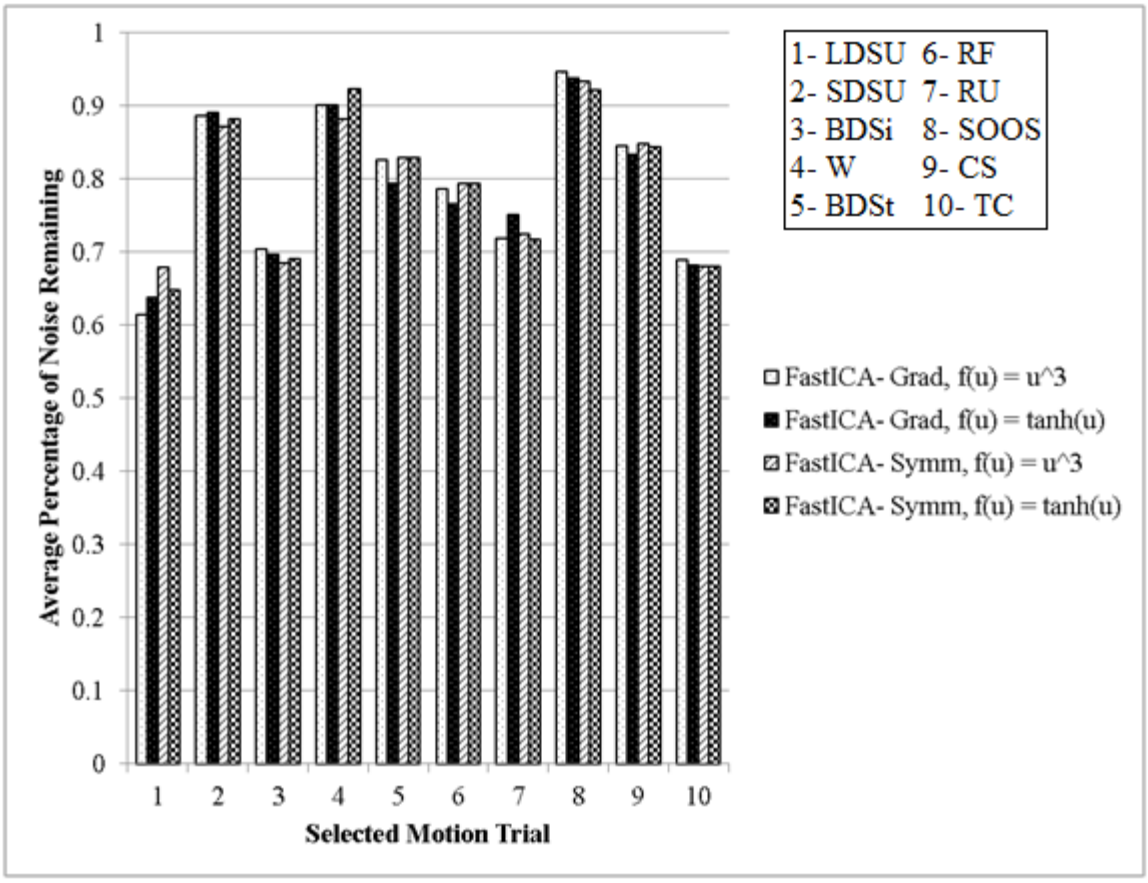

Figure 5.31: FastICA RLS motion experiment 2, optimum variables

Figure 5.31 depicts the results of experiment 2 for using FastICA to separate the motion data prior to summing and applying the RLS filter under optimum forgetting factors. Trials 1, 3, 7, and 10 all see roughly 25% to 40% of the noise removed on average. Trials 5, 6, and 9 see roughly 15% to 25% of the noise removed. Trials 2, 4, and 8 all see roughly 5% to 15% of the noise removed.

Once again, there is no consistently better performing FastICA approach. The largest difference is in trial 1, where the Gradient approach using contrast function u^3 performs a little over 5% better than the Symmetrical approach using contrast function u^3. All other trials see results that are all reasonably close to each other.

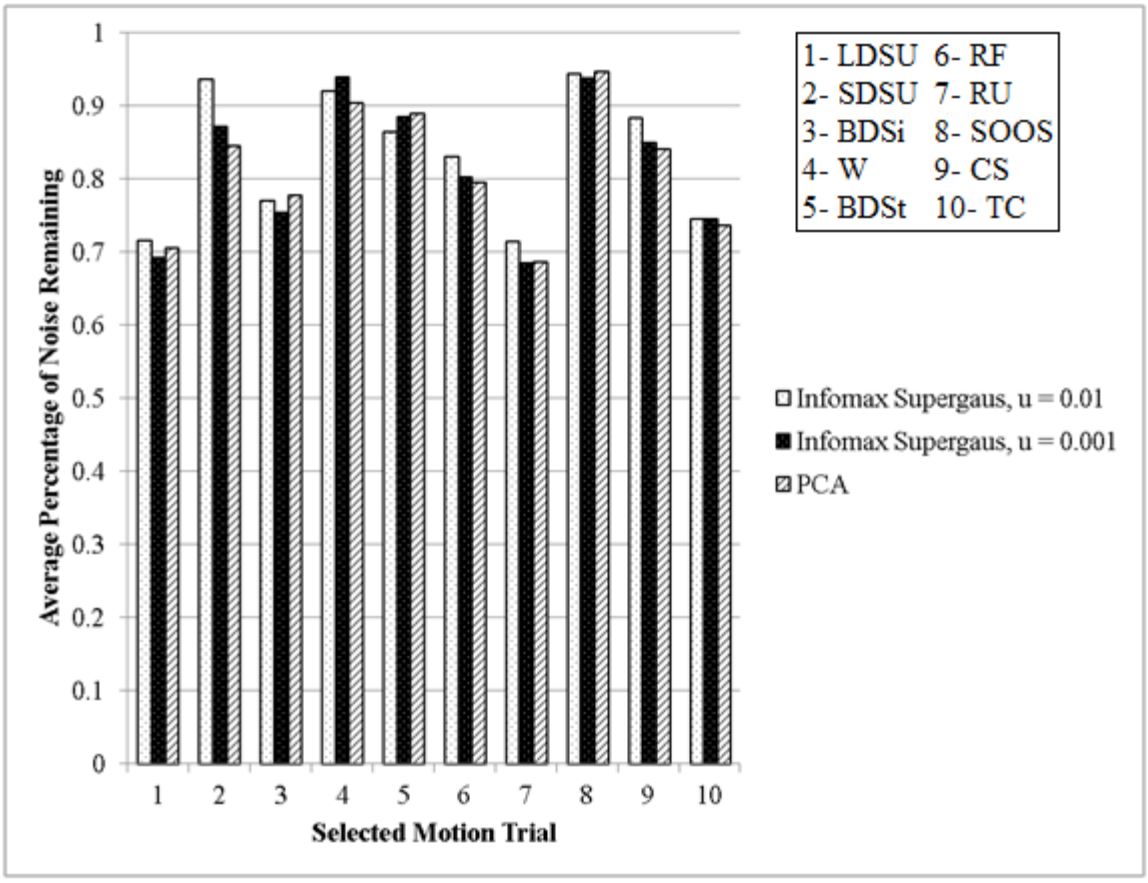

Figure 5.32: Infomax & PCA RLS motion experiment 2, optimum variables

Figure 5.32 shows the results when the motion data is processed through Infomax and PCA. Outside of the Infomax approach with step size of 0.01 in trial 2, the results are all roughly similar. Trials 1, 3, 7, and 10 see an average removal of roughly 25% to 30% of the noise. Trials 2, 5, 6, and 9 see an average removal of roughly 10% to 20%. Trials 4 and 8 see the removal of roughly 5% to 10%.

A step size of 0.001 works better overall for the Infomax approach. A greater number of trials perform better with it, particularly in trial 2, while the results are not significantly worse in those cases it doesn't.

FastICA performs about 5% better than Infomax and PCA in trials 1, 3, 5, and 10, and is roughly comparable to them in all other trials. Overall, it would be the preferable method of choice for RLS under optimal conditions.

5.3.4 RLS – Shared Forgetting Factors

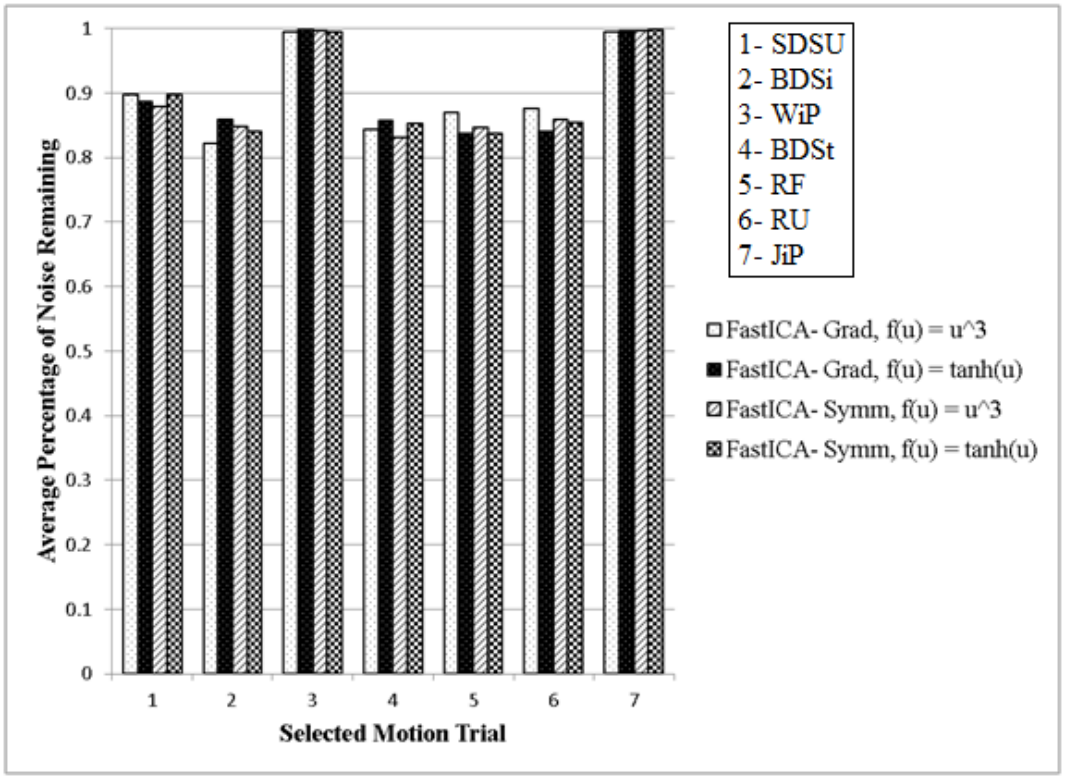

Figure 5.33: FastICA RLS motion experiment 1, shared variables

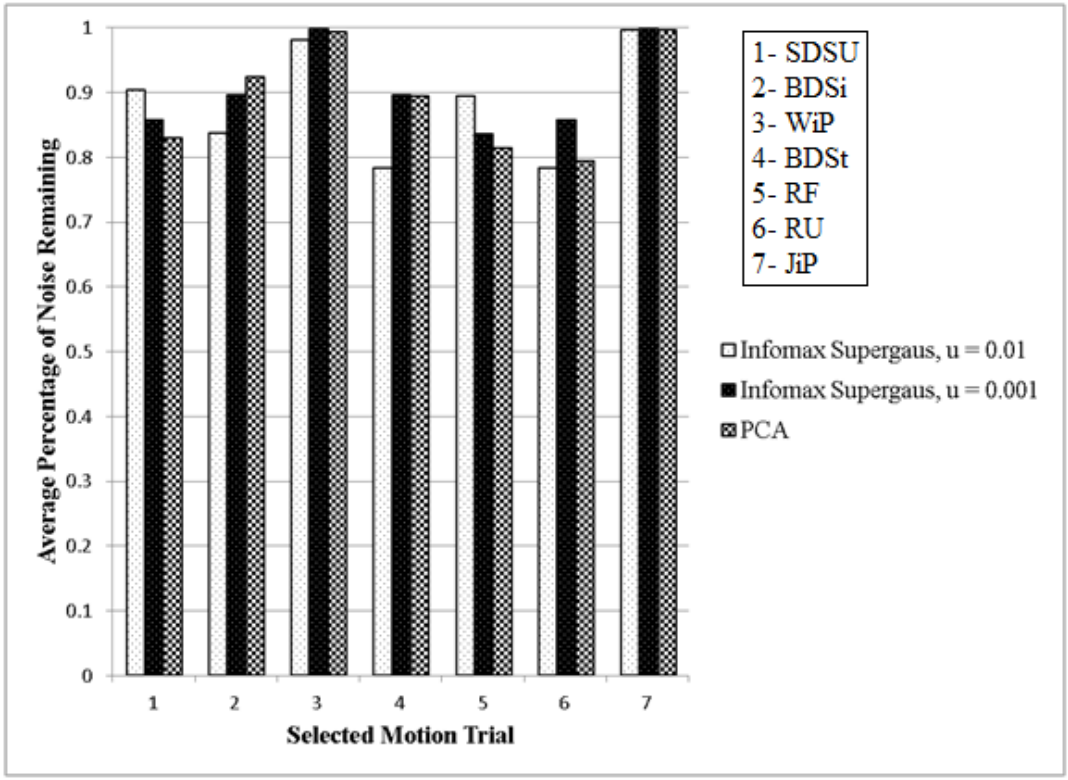

Figure 5.34: Infomax & PCA RLS motion experiment 1, shared variables

Figure 5.33 depicts the results of experiment 1 for using FastICA to separate the motion data prior to summing and applying the RLS filter under shared forgetting factors. Figure 5.34 depicts the results using Infomax and PCA. All methods see roughly similar results. Trials 1, 2, 4, 5, and 6 see roughly 10% to 20% noise removed on average. Trials 3, 7 see no significant improvement at all. Overall, results are roughly 10% worse for every trial compared against optimal forgetting factors.

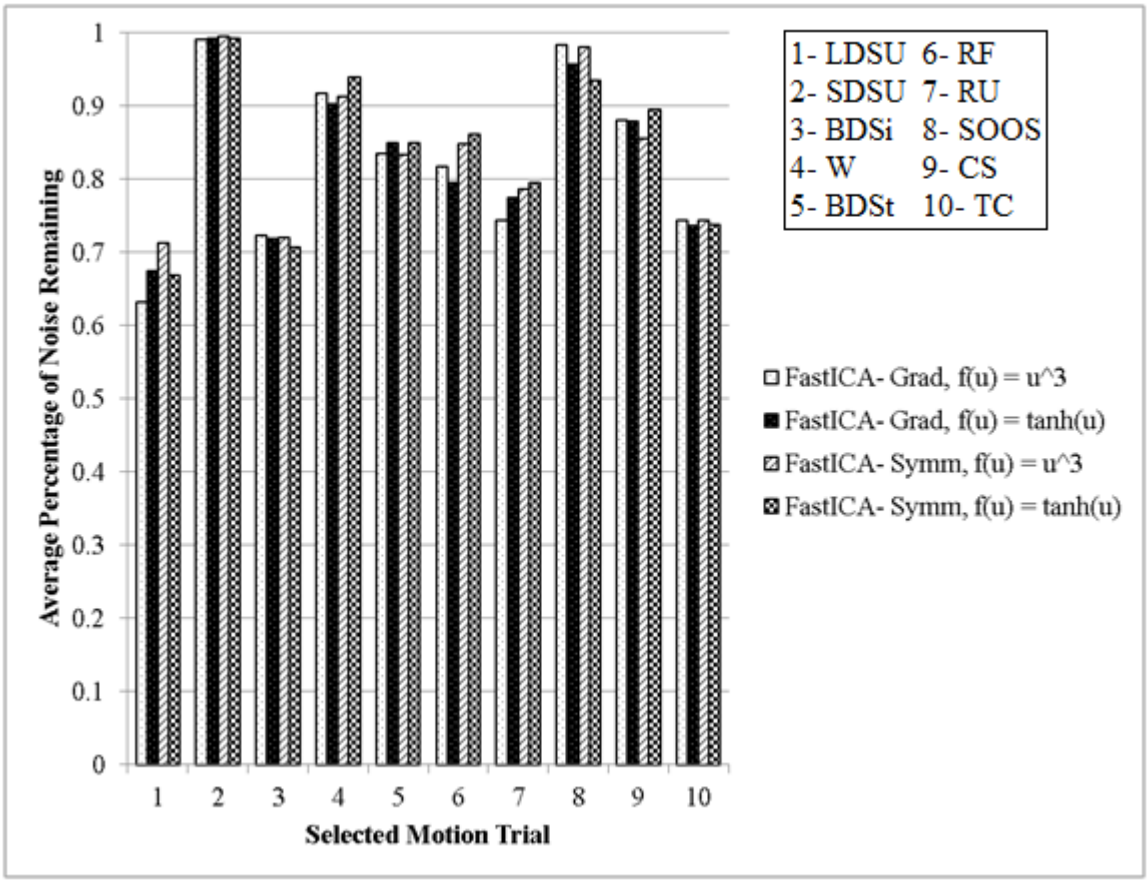

Figure 5.35: FastICA RLS motion experiment 2, shared variables

Figure 5.35 depicts the results of experiment 2 for using FastICA to separate the motion data prior to summing and applying the RLS filter under shared forgetting factors. Trials 1, 3, 7, and 10 see an average of roughly 20% to 35% of noise removed. Trials 5, 6, and 9 have roughly 10% to 20% of the noise removed. Trials 2, 4, and 8 have roughly 0% to 10% of the noise removed.

Trial 2 suffers the worst compared to the optimum results, going from a little over 10% of noise removed on average to an insignificant amount. Trials 7, 9, and 10 all increase by roughly 5% on average. All other increases are for less.

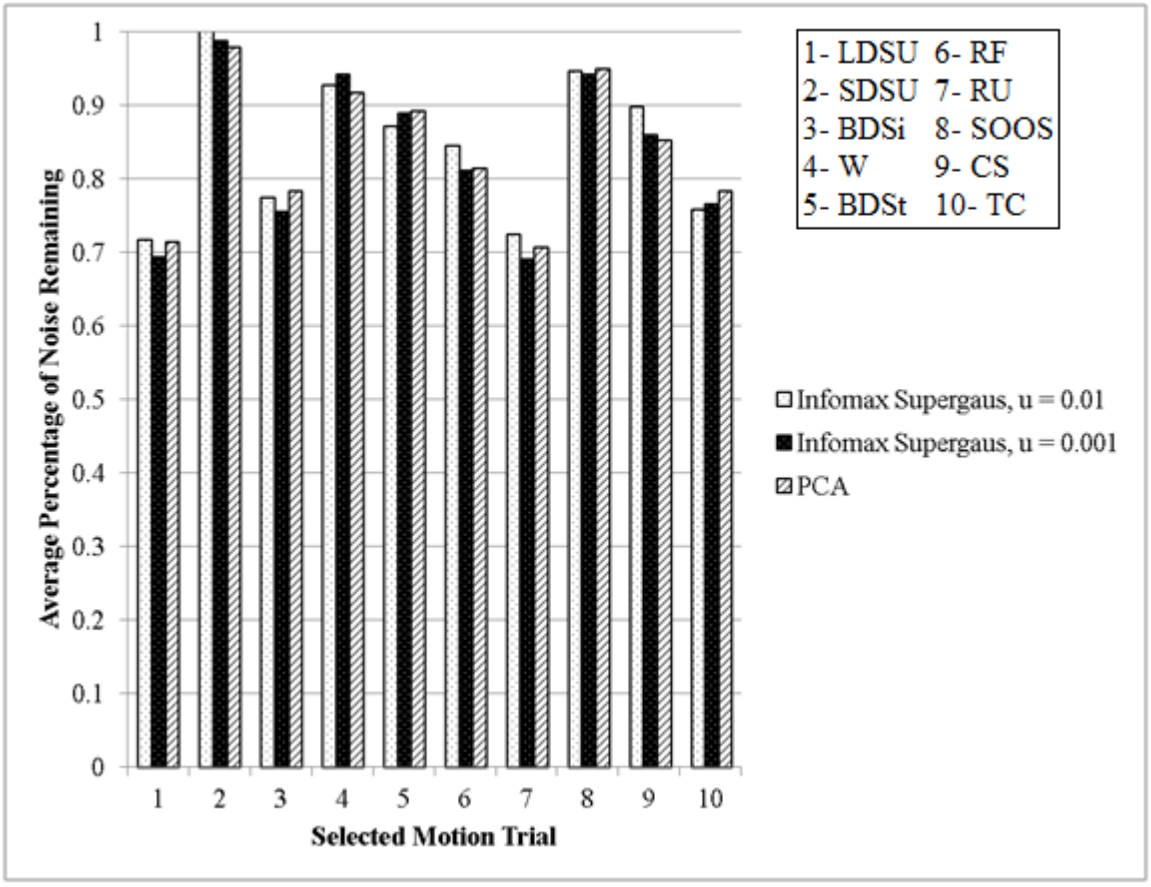

Figure 5.36: Infomax & PCA RLS motion experiment 2, shared variables

Figure 5.36 shows the results when the motion data is processed through Infomax and PCA. Trials 1, 3, 7, and 10 see roughly 25% to 30% of the noise removed on average. Trials 5, 6, and 9 have about 10% to 20% removed. Trials 2, 4, and 8 have roughly 0% to 10% removed.

Infomax and PCA see minimal changes between shared forgetting factors and optimum forgetting factors. The exception is once again trial 2, which goes from removing roughly 15% of total noise on average to an insignificant amount of noise removed.

While FastICA had been largely the best choice for RLS under optimal conditions, it ended up deteriorating more than Infomax and PCA with the shared forgetting factors. Overall, the results are mixed and no method stands out as best for RLS under shared forgetting factor conditions.

5.3.5 LMS vs. RLS – Optimum Variables

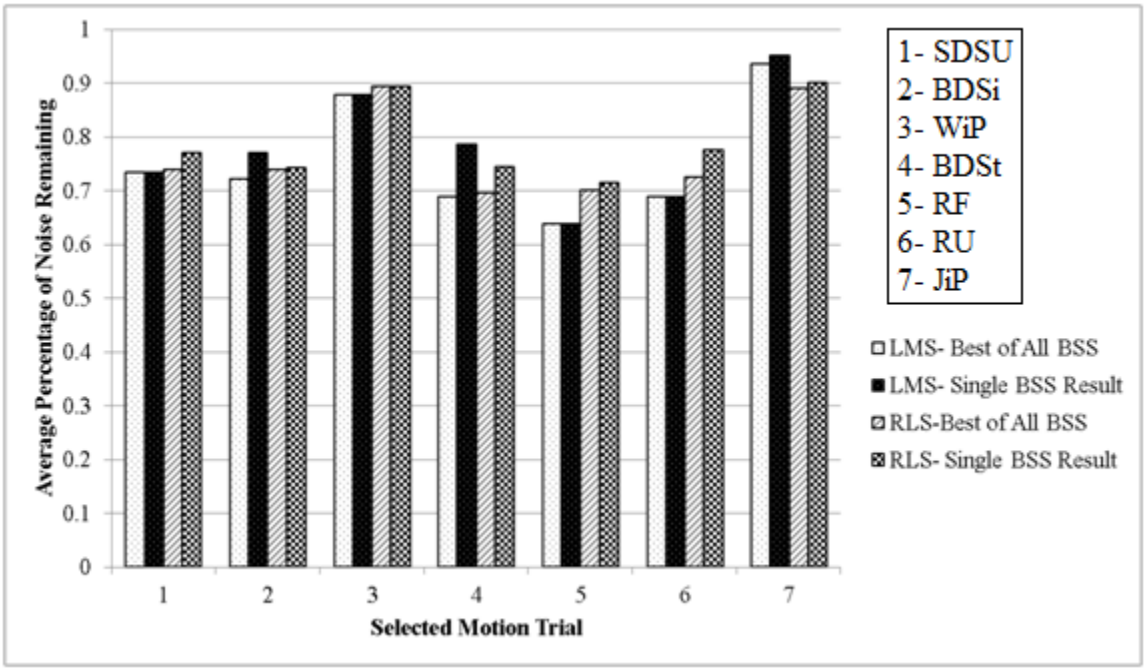

Figure 5.37: LMS vs RLS motion experiment 1, optimum variables

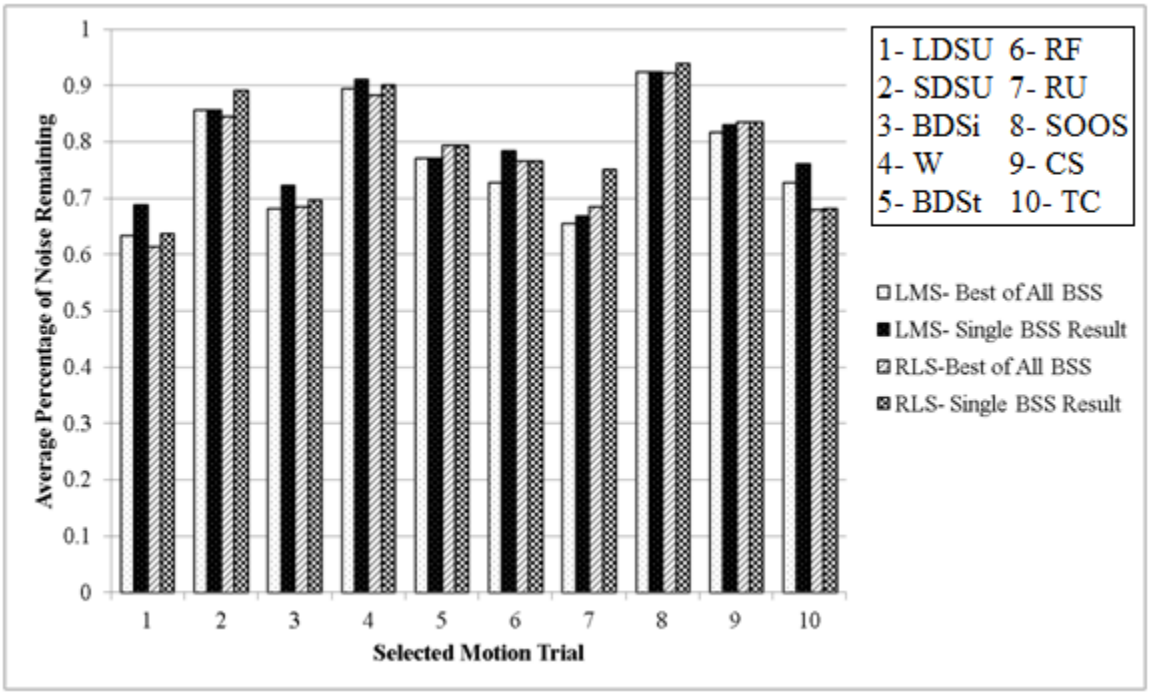

Figure 5.38: LMS vs RLS motion experiment 2, optimum variables

Figure 5.37 and Figure 5.38 compare the best results of experiments 1 and 2 respectively among the combined sensor approaches for both the LMS and RLS filters

under optimum variables. In a side by side comparison, it can be seen that the LMS filter is performing better than the RLS filter more often than expected.

For trials 1 through 6 of experiment 1, the best of all BSS results end up with the LMS filters removing more noise than the RLS filters. Overall, the results between the two aren't particularly large, with the biggest difference being trial 5 with LMS removing a little over 5% noise on average, but the frequency with which LMS outperforms RLS on average is concerning, given that it is expected for RLS to perform better than LMS. LMS performs better than RLS for trials 3, 5, 6, 7, and 9 for experiment 2. RLS only achieves a significantly better performance in trial 10, with an average of about 5% additional noise removed on average.

The lack of a single consistently strongly performing separation method results in the differences between the best of all methods and the best average method results, as seen in trial 4 of experiment 1 and in trials 1 and 7 of experiment 2. This demonstrates how no single method is performing well for separating the motion data.

5.3.6 LMS vs. RLS – Shared Variables

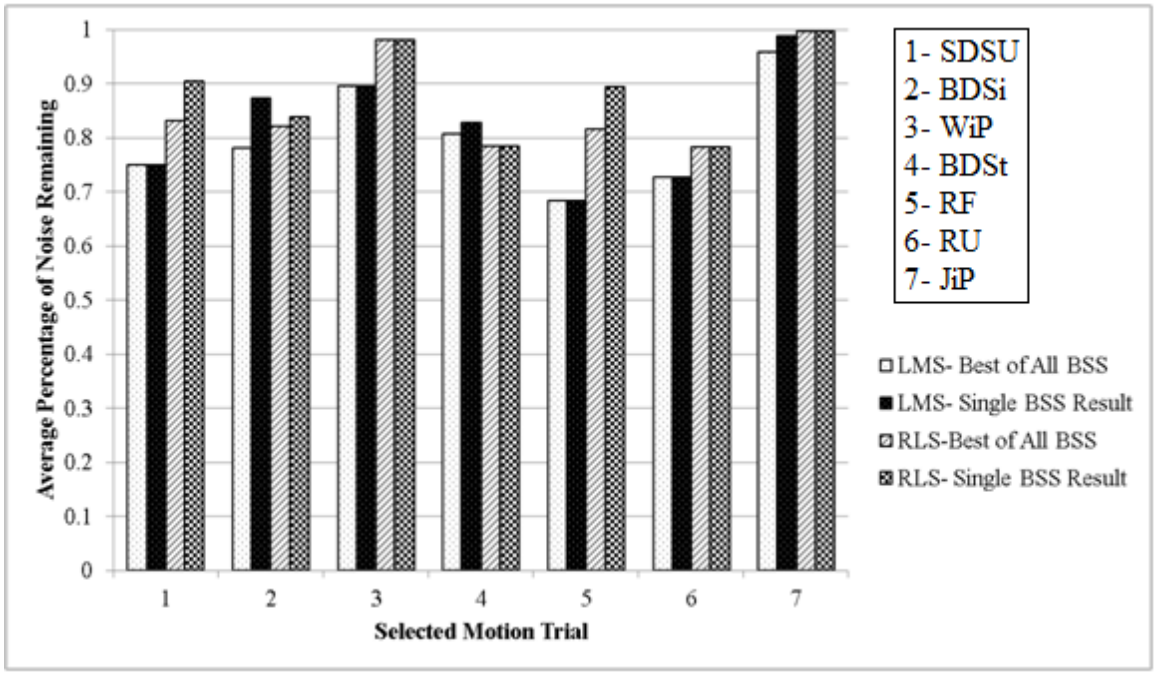

Figure 5.39: LMS vs RLS motion experiment 1, shared variables

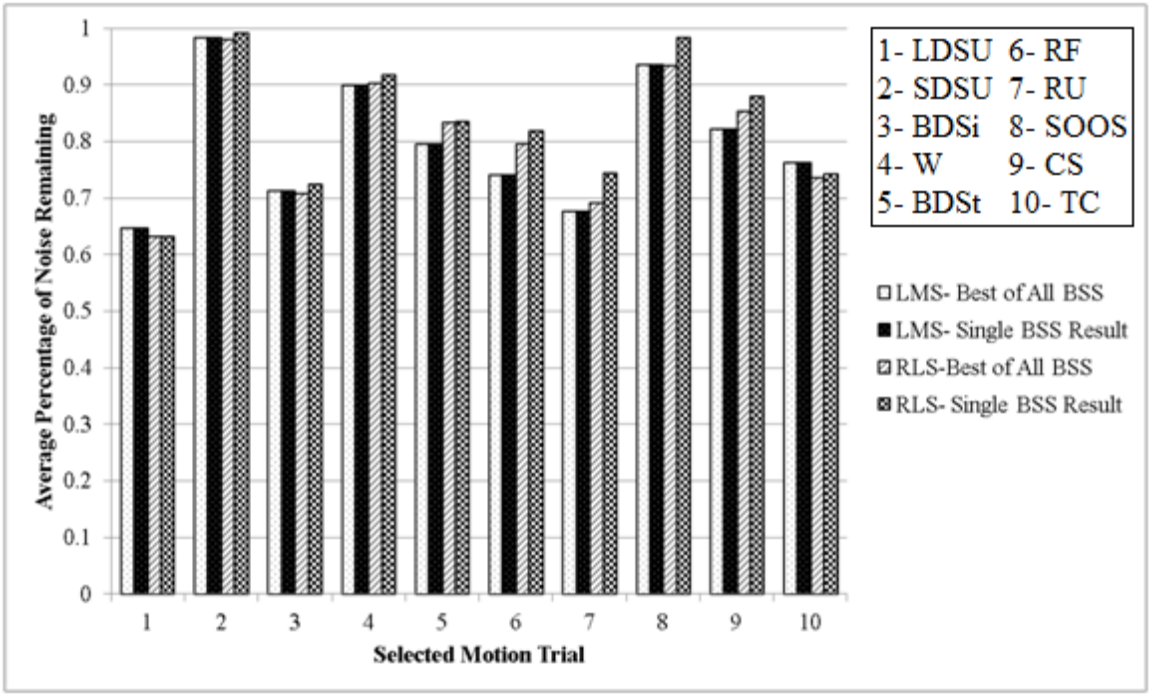

Figure 5.40: LMS vs RLS motion experiment 2, shared variables

Figure 5.39 and Figure 5.40 compare the best results of experiments 1 and 2 respectively among the combined sensor approaches for both the LMS and RLS filters under shared variables. LMS outperforms RLS in every trial of experiment 1 except motion trial 4. Trials 1 and 6 have LMS removing an additional 5% of noise compared against RLS while trials 3 and 5 have it removing an additional 10% on average. The significant difference between the two filters is due to the significant amount of additional noise left unfiltered in RLS's shared forgetting factor approach for experiment 1 compared to its optimal results, as discussed in Section 5.3.4.

LMS and RLS saw roughly equal amounts of additional noise in the shared variable approach compared to the optimal variable approach in experiment 2, leading to more equal results between them. The biggest difference is in trial 6, with LMS performing about 5% better on average compared against RLS.

Overall, the results in comparing the different combined sensor methods are inconsistent. There is no single method that consistently performs better or comparably well against the others. The LMS filter frequently performs better than RLS on average, when the opposite is expected. This indicates that the examined approaches to prepare the sensors for being combined are not suitable for use.

5.4 Comparison of Individual vs. Combined

The results for individual sensors and combined sensors have been examined individually. In order to determine the value in combining the sensor data, it must be compared against the results during the use of individual sensors. If performing as expected, the combined sensor data should consistently be performing at least as well as the best individual sensor selection. In every case, the comparison will be made between the best individual sensor and the best combined sensor result.

5.4.1 Individual vs. Combined Sensors- Optimum Variables

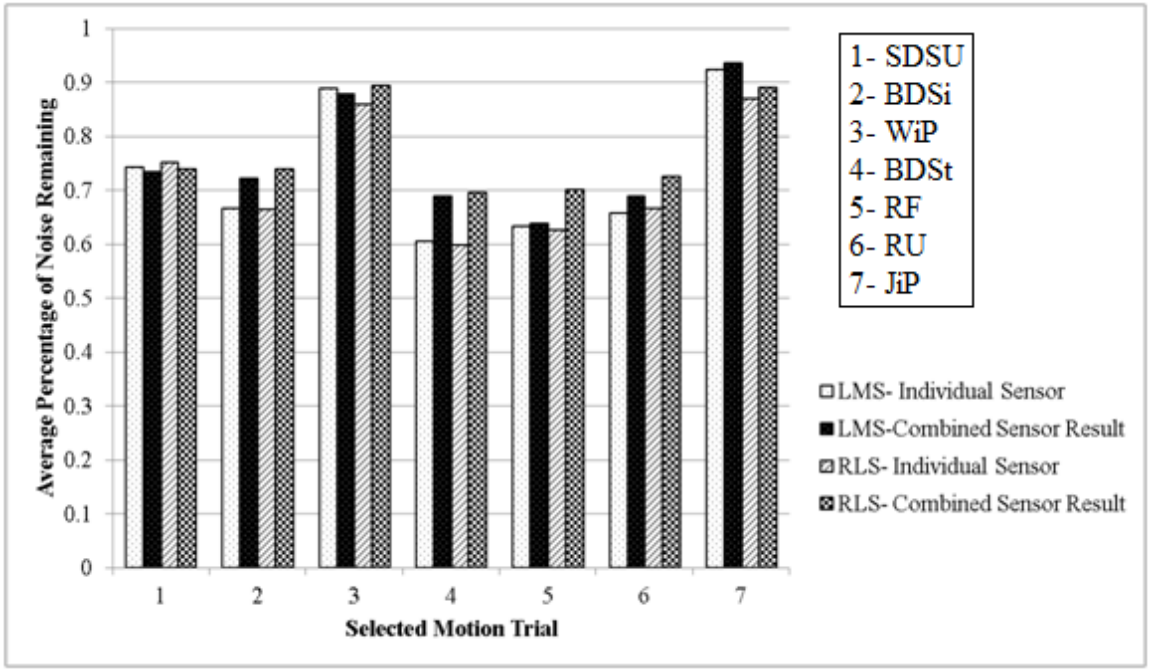

Figure 5.41: Individual vs. combined sensors experiment 1, optimum variables

Figure 5.41 demonstrates the LMS and RLS results for the best individual and best combined sensors for the motion trials of experiment 1. Contrary to expectations, the combined sensor data results are consistently performing worse than the individual sensor data approach. The exceptions are trial 1 and the LMS result of trial 3, each by a minor amount compared against the 5% to 10% differences of trials 2 and 4.

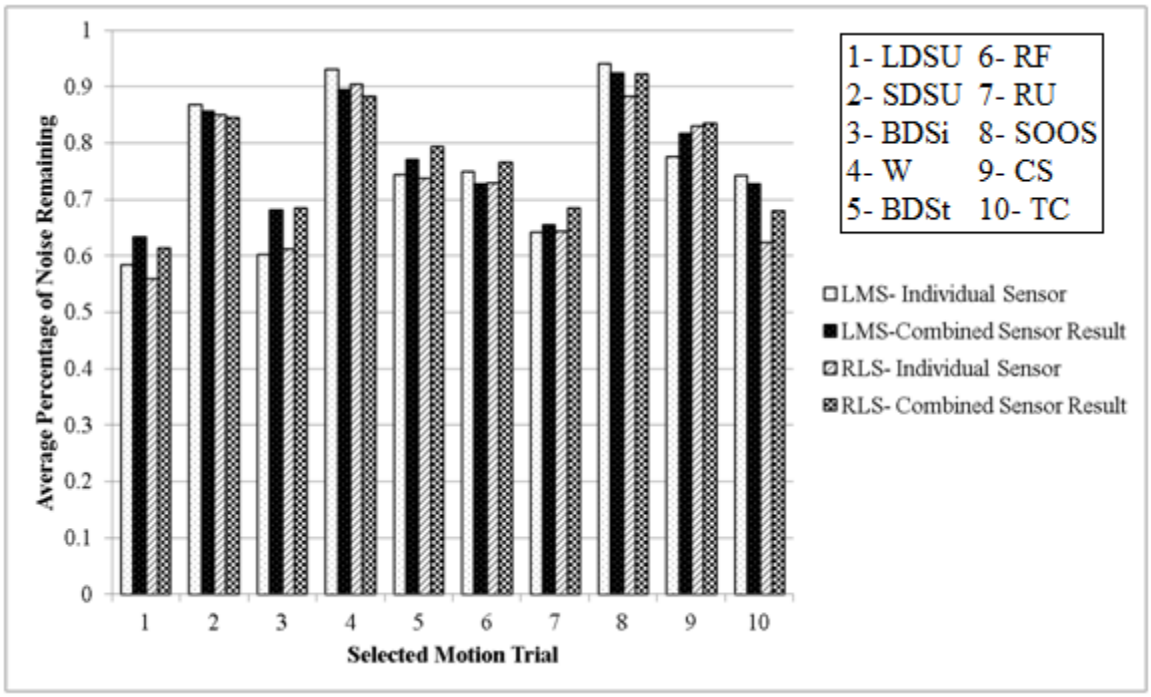

Figure 5.42: Individual vs. combined sensors experiment 2, optimum variables

Figure 5.42 demonstrates the LMS and RLS results for the best individual and best combined sensors for the motion trials of experiment 2. Overall, the combined sensor results are performing worse on average than the individual sensor results. Exceptions are in trials 2, 4, and the LMS uses of 6, 8, and 10, all by small amounts. More substantial differences are found in trials 1, 3, and the RLS uses in trials 5 and 10, where the individual sensors are removing on average an additional 5% of noise compared against the combined sensor results.

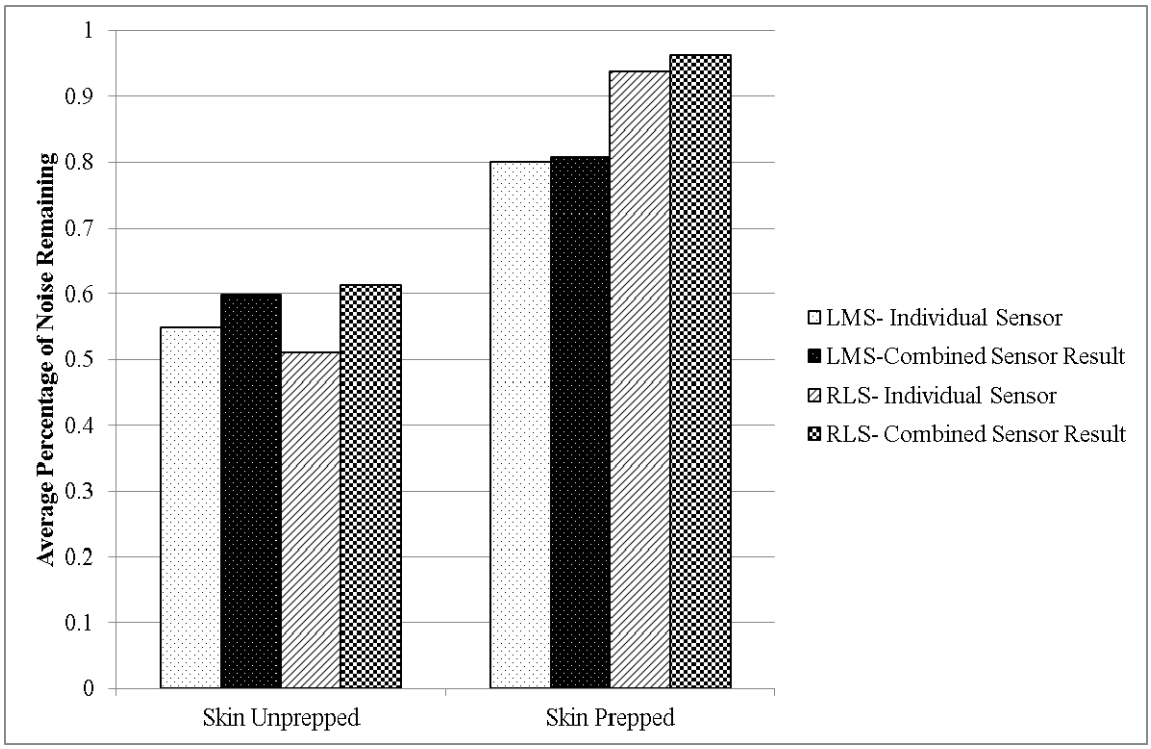

Figure 5.43: Individual vs. combined sensors skin preparation, optimum variables

Figure 5.43 demonstrates the LMS and RLS results for the best individual and best combined sensors when trials are grouped in terms of skin preparation. This gives a broader view of the results of experiment 1. The combined sensor results are worse in both cases, though the difference is far more notable in the case where skin has not been properly prepared. The best individual sensor is removing an additional 5% of noise on average compared against the best combined sensor approach when the LMS filter is used. The difference between the two increases to 10% on average when the RLS filter is used.

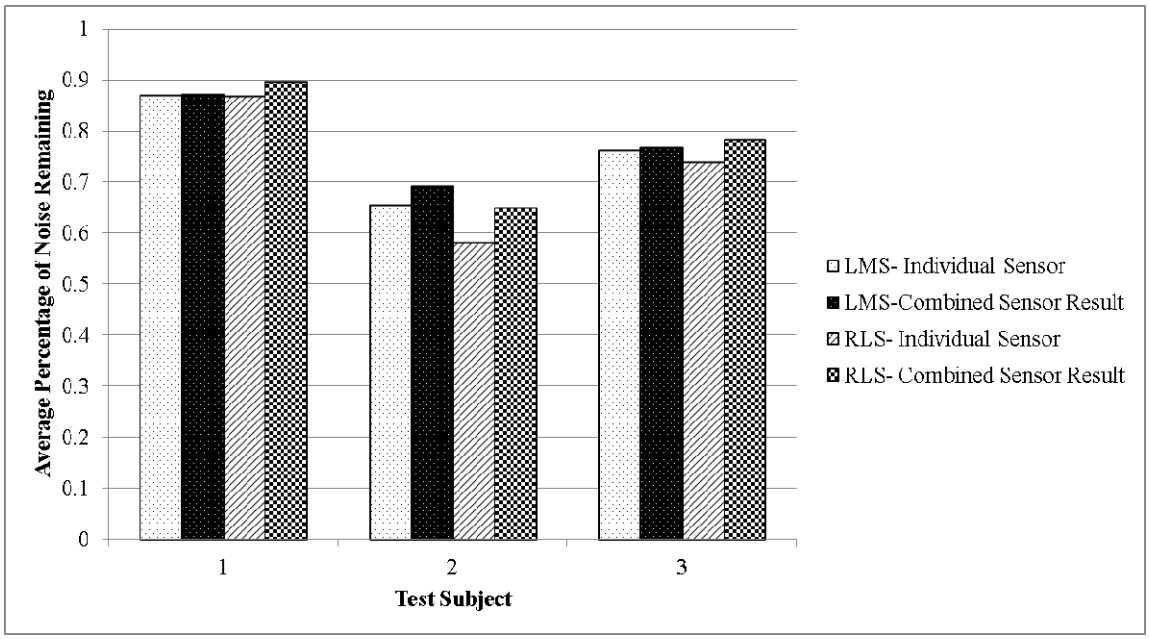

Figure 5.44: Individual vs. combined sensors multiple users, optimum variables

Figure 5.44 demonstrates the LMS and RLS results for the best individual and best combined sensors when trials are grouped in terms of the individual performing the motion trial. This gives a broader view of the results of experiment 2. Once again, the results have the best individual sensor performing better than the best combined sensor approach in every case.

As performance improves, the difference between the individual sensor and the combined sensor approach becomes more notable. Test subject 1, which sees roughly 10% to 15% of noise removed on average, has the best results roughly comparable between the individual sensor and the combined sensor approaches. Test subject 2, which sees roughly 30% to 40% of noise removed on average, has the best individual sensor performing roughly 5% better than the best combined sensor result.

Overall, the best individual sensor results perform on average better than the best combined sensor results. This indicates that none of the methods tested are suitable for the separation of motion data. This matches the expectations at the end of section 5.3, where the inconsistent results among the different separation approaches and among the LMS and RLS comparisons indicated they were ultimately unsuitable for use.

5.5 Comparisons with Other Techniques

Comparisons with other research are difficult to make as approaches in evaluation of the results vary significantly. However, there are two works that each allows for a promising basis of comparisons. The first is Liu's design and evaluation of skin stretch [50]. The second is Buxi's evaluation of the correlation between electrode-tissue impedance and ECG noise [21].

Liu used an optical sensor near the skin as a method to produce a signal that would represent the amount of skin stretch caused by motion. This signal was used as a reference signal to a LMS adaptive filter. Noiseless data was collected through a second recording immediately following a motion test where the test subject remained stationary. Results were evaluated through an analysis of the percent reduction of noise using L2-norms of the noisy, ideal, and filtered signals, reasonably similar to the evaluation method used in this work.

Liu's analysis of everyday motions led to noise reduction varying from 55% to 99% of noise removed, with an average of 85% of noise removed among all motions. Using LMS with optimal constants and assuming best motion sensor selection for experiment 1, the results with the accelerometer saw 8% to 40% noise removed, with an overall average of noise removed among all motions of 32%. Narrowing the results to those with insufficient skin prep, the accelerometer results saw a range of 9% to 68% of noise removed, with an average of 40% noise removed among all motions. Overall, Liu's use of the optical sensor outperformed the use of best accelerometer placement significantly.

Buxi collected motion artifacts by placing the electrodes on the spine in a manner that would collect a minimal amount of ECG. The data collected in this manner was considered to be motion artifacts. While data was collected for both dry and wet electrodes and through methods including both electrode/skin manipulation and real motion, the data that allows for a valid comparison are strictly the wet electrodes through real motion.

Overall, Buxi's analysis of the correlation between motion artifacts produced by real motion through wet electrodes varied between 0.25 and 0.5, depending on the type of impedance used. The average correlation of the use of a single accelerometer averaged between 0.25 and 0.3. There are differences in the approaches, but overall the comparison

indicates that the use of electrode-tissue impedance as a reference signal is more promising than the use of accelerometers.

Overall, comparing against other works demonstrates the weaknesses in the use of accelerometers as a reference signal for ECG. However, this is as expected, given the isolated results of the accelerometer tests. The expectation of this work was to improve upon the use of accelerometers in ECG adaptive filtering by combining multiple motion sensors. In the end, the approaches to prepare the motion sensors for combination in adaptive filtering did not work as expected, with individual sensors consistently outperforming the filtering performed on combined motion sensors. Without a successful combination of motion sensors, direct comparisons with recent works are bound to demonstrate the poorer results of individual motion sensor filtering.

5.6 Summary

The results in changing filter lengths across a range of gain factors and forgetting factors for LMS and RLS filtering respectively have been analyzed and a single filter length for each selected based on the results. The impact of sensor position on the body has been investigated through a comparison of adaptive filtering using the left arm, right arm, and back sensors individually. These results have been compared on the basis of motion performed, degree of skin preparation, test subject performing the motion, and the selection of sampling frequency. They have been further compared on the basis of the adaptive filtering method used and the process in selecting the gain factor and forgetting factor for use in each motion trial.

Combined sensor results have been similarly analyzed, using FastICA, Infomax, and PCA to preprocess the data before use in adaptive filtering. These results have been compared to the results using individual sensors to determine whether it can be considered a successful approach in filtering. Finally, the best results overall have been compared to the results of other literature.

6 Conclusions & Future Work

The ECG is a signal commonly used in healthcare. For the signal to be useful, it must be readable, and as such the removal of corrupting noise from the signal is of great importance. Motion artifacts are among the most problematic sources of noise in an ECG, being that it overlaps with a portion of the ECG spectrum and cannot be removed through conventional filtering without removing part of the ECG itself. Adaptive filtering is one method that can be used to solve this problem.

Chapter 1 explored background information that demonstrated the concept of a body area network, an example of its use in the FANFARE project, and a brief discussion of the importance of ECG filtering. Chapter 2 went indepth on the details of the ECG and its noise as well as exploring the technical aspects and recent relevant uses of adaptive filtering and blind source separation. Chapter 3 discussed the Shimmer node used in this work as well as the setup and performance of the experiments for data collection. Chapter 4 explored some of the decisions made to narrow the scope of the work as well as validating the use of the various adaptive filtering and blind source separation algorithms. Finally, Chapter 5 presented the results of the adaptive filtering on the experimental data that had been collected.

The use of motion sensors in adaptive filtering has been explored with respect to the use of multiple sensors in different locations on the body, specifically the left arm, right arm, and torso. From there, the possibility of combining them for simultaneous use was approached. Multiple reference single input adaptive filtering requires the signals used to be uncorrelated. To determine whether motion data can be combined prior to use in adaptive filtering, multiple methods of blind source separation were applied and compared. Results were examined with respect to the motion being performed, the preparation of the skin prior to wearing the ECG, the user wearing the ECG, and the sampling frequency of the data. Two different adaptive filters were used in collecting the results, LMS and RLS, with each being presented with both optimal results and more realistic results. FastICA, Infomax, and PCA were three different methods of separating

source signals examined. Results were compared based on the percentage of noise removed from tested data sets.

Experiments were performed with the use of Shimmer sensor nodes. Sensor nodes using the gyro expansion were placed on both upper arms, at the mid-point between the shoulder and the elbow, and on the back of the torso, specifically at the small of the back. A sensor node with a three-lead ECG expansion was placed on the chest. All sensor nodes included accelerometers, though the accelerometer data on the ECG sensor node was unused. All data was collected on local memory cards and later processed with the use of Matlab™.

Early performed tests examined the correlation between motion sensors and the noise within an ECG in order to verify their viability in adaptive filtering. Gyroscopes performed worse than accelerometer, with average correlation coefficients ranging from 0.1 to 0.15 across all three axes. Average correlation coefficients ranged from 0.15 to 0.3 on the accelerometers, with the z-axis performing the best among the three.

6.1 Conclusions

The impact of filter length on the effectiveness of filtering ECGs using motion data was investigated on both the LMS and the RLS adaptive filters. On average, LMS would provide better results at high filter lengths. RLS found the opposite result, with smaller filter lengths providing better results.

Performance of adaptive filtering was found to be related to the intensity of the motion being performed. Heavier, constant motions such as walking, jogging, and climbing stairs consistently had greater average amounts of noise remaining after filtering than lighter movements such as sitting/standing and reaching for an item. The difference ranged typically ranged between 20%-30% additional noise removed on average for both LMS and RLS adaptive filtering.

The selection of sensor position has an influence on the effectiveness of the adaptive filter, though typically not to a significant degree. The most notable difference in sensor use was found in the motions of reaching up and reaching forward, where each saw an additional 15% of noise removed when using the right arm sensor over the left arm sensor. The majority of motions otherwise tended to have all sensors perform with no

more than a 5% difference of average noise removed. Ultimately, it appears that the benefit in using multiple sensors over a single sensor integrated within an ECG device would be minimal compared to the benefits of having all needed parts readily available in a single node.

With few exceptions, the RLS filter typically performed better than the LMS filter. More often than not, the amount of improvement tended to be fairly negligible. However, most notably, the RLS filter would remove an additional 10% of noise on average over the LMS filter for trial 10 of experiment 2, where the motions being performed were constantly changing. This makes sense given RLS's faster expected speed of convergence, meaning it would be particularly significant in more realistic uses of adaptive filtering of an ECG.

Abrasion has a significant impact on filtering. Results found 35%-40% more artifacts were removed when the skin was improperly prepared compared to when the skin was fully prepared prior to applying the electrodes of the ECG. This matches expectations. As discussed in Section 2.1.2, the best way of removing motion artifacts is by preventing them through proper preparation of the skin. Filtering has less effect when skin has been properly prepared as the motion artifacts in the ECG have already been significantly reduced by the preparation.

Results can vary significantly depending on the user. Experiments were performed with three different test subjects, each instructed to prepare their skin themselves. Average results per user varied from 10%-15% noise removed in the worst case to 30%-35% removed in the best case under the use of LMS filtering. This demonstrates the need for motion artifact removal, as individual users will vary in their skin preparation before applying the ECG. Additional contributing factors to the differences are natural differences in the skin and possibly the differences in how individuals move about.

The frequency of the data does not significantly alter the capabilities of the adaptive filter, assuming the frequency is large enough such that the ECG is interpretable. Sampling frequencies were tested ranging from 50 Hz to 200 Hz. Results appeared to be improving slightly from 50 Hz to 166 Hz, though all remained within an average of 35%-40% noise removal. A drop in average performance resulted when moving from 166 Hz to 200 Hz, leaving the 200 Hz results with an average of 25% noise removed. Generally,

a higher sampling frequency would be expected to produce better results, as the adaptive filter has more opportunity to converge as necessary. The inconsistent results indicate that there is little connection in performance to frequency and implies that the filter has plenty of time to converge even at the lowest tested sampling frequency of 50 Hz.

Sharing gain factors and forgetting factors between performances of a motion trial typically saw between 0%-10% additional noise left unfiltered when compared against the use of optimal gain factors and forgetting factors for each individual performance. The worst was found in Experiment 1, likely due to the greater variety of variables that could impact the spread of optimal gain factors and forgetting factors for specific motions. Experiment 2 saw largely negligible changes in the move from optimal variables to shared variables.

FastICA, Infomax, and PCA were used on motion data prior to adaptive filtering with varying approaches. FastICA was tested using both its symmetric and its gradient approach, using two different contrast functions on each. Infomax was tested using both its subgaussian and its supergaussian approach with two different step sizes tested on each. None of the methods proved to demonstrate a consistently better performing approach, with subgaussian Infomax in particular being unable to produce results that could successfully converge when filtering for all tested data sets.

Among the tested source separation techniques, none appear to be suitable for appropriately separating the movement of individual body parts along a single axis of an accelerometer into uncorrelated source movements. Overall best performance of single sensors saw removal of, on average, an additional 5%-10% over the use of combined sensor data. This was also notable by the lack of any single consistently well performing BSS method and the inconsistent performance of RLS filtering when compared to LMS filtering during the multi-reference filtering.

Compared against recent works in adaptive filtering, the motion sensor work does not improve results. A direct comparison with the work using an optical sensor for skin stretch demonstrates significantly poorer results in the motion sensor approach. Comparisons with the correlation between motion sensor and ECG noise against the correlation between electrode-tissue impedance are similarly poor, further demonstrating

the weaknesses of the motion sensor approach. This is to be expected, due to the inconsistent results when attempting to combine data from multiple motion sensors.

There are three major conclusions to be drawn from this work. First, the goal to improve upon adaptive filtering of ECGs through the use of multiple motion sensors was not proven as a successful method to separate the motion data was not found. The likely reasons for this are that either none of the BSS methods properly prepared the motion data for combination in adaptive filtering, or multiple reference single input adaptive filtering simply isn't suitable for use. Second, the use of additional motion sensors overall led to minimal improvements over the use of a single motion sensor. The instances where the use of the right arm accelerometer provides an improvement over the use of the torso accelerometer are too infrequent and too insubstantial to warrant the additional resources in having both available for use in adaptive filtering. Finally, an analysis of the results demonstrates the importance of examining skin preparation prior to ECG application and the variety of intensities in motion selection when approaching the results of adaptive filtering. These are issues that could be given more consideration in future work.

6.2 Future Work

The area of reducing motion artifacts in ECGs is still a promising one and the area of adaptive filtering for ECGs is one that continues to be researched. There are a number of open avenues of research that can yet lead to further improvements in these areas.

One of the more notable results is the significant reduction in the effectiveness of the adaptive filter when proper skin preparation has been performed prior to applying the ECG electrodes. However, the results presented are from no preparation whatsoever to very highly prepared skin. A more careful study with granular results in between may be worth investigating. A similar note can be made for the sampling frequency results, which only had 4 different sampling frequencies to test, though the results found do not indicate a need for further study.

The other results which indicated a pattern was that of the effectiveness of the adaptive filter against the degree of motion intensity on the motion performed. The results presented in this work were rather broad, using a rough qualitative approach to differentiate lighter motions from heavier motions. A quantification of motion intensity

could allow for a more thorough study of the effectiveness of adaptive filtering of ECG against the intensity of the motion causing the noise.

All presented work was performed by processing the collected data on a computer well after the experiments had been performed. However, ECG motion artifact reduction is most useful when it can be performed while the data is being collected in order to improve ambulatory ECG monitoring. The presented work could be expanded through an investigation and application of a system that performs the analysis in real time.

The presented work aimed to combine data from multiple motion sensors, with unsatisfactory results. However, multi-reference adaptive filtering is still a largely unused area in ECG filtering that could be further explored. Instead of attempting to combine multiple data of a single type, combining entirely different varieties of reference signals may lead to more promising results.

Finally, a recurring difficulty in this work was how to quantify and present the results. Results from other works tended to vary, with no single baseline that allowed for a consistent method of comparison. An investigation into the various methods in how noise reduction in ECGs can be quantified and those which would be most useful to medical professionals would be greatly beneficial to future work in ECG noise reduction.

References

[1] M. Patel, J. Wang, "Applications, challenges, and prospective in emerging body area networking technologies," *IEEE Wireless Communications*, vol. 17, pp. 80-88, 2010.

[2] A. Dinh *et al*., "A fall and near-fall assessment and evaluation system," *The Open Biomedical Engineering Journal*, vol. 3, pp. 1-7, 2009.

[3] I. Chaikowski *et al.*, "Value of the single-lead ECG in comparison with 12-lead ECG," *Український журнал телемедицини та медичної телематики*, vol. 6, 2008.

[4] G. Moran. *ECG Scene* [Online]. Retrieved 1 May, 2013, from the University of Nottingham http://www.nottingham.ac.uk/nursing/

[5] Philips, "Improving ECG quality", *Application Note*, 2008.

[6] R.N. Subbiah *et al.*, "Ambulatory monitoring (Holter, event recorders, external, and implantable loop recorders and wireless technology)," *Electrical Diseases of the Heart,* part II, pp. 344-352, 2008.

[7] CRY. *Holter* [Online]. Retrieved 1 May, 2013, from Cardiac Risk in the Young http://www.c-r-y.org.uk/cardiac_tests.htm

[8] M.S. Thaler, *The Only EKG Book You'll Ever Need*, 6th ed. Philadelphia: Lippincott Williams & Wilkins, 2010.

[9] G. Tang and A. Qin, "ECG de-noising based on empirical mode decomposition," *9th Int. Conf. for Young Computer Scientists,* pp. 903-906, 2008.

[10] R.U. Acharya *et al*., *Advances in Cardiac Signal Processing*, New York: Springer, 2007.

[11] A. Comert, M. Honkala, J. Hyttinen, "Effect of pressure and padding on motion artifact of textile electrodes," *Biomedical Engineering Online*, pp. 12-26, 2013.

[12] D. Jeong, S. Kim, "Development of a technique for cancelling motion artifact in ambulatory ECG monitoring system," *3rd 2008 Int. Conf. Convergence and Hybrid Information Technology*, pp. 954-961, 2008.

[13] T. Pawar *et al.*, "Impact analysis of body movement in ambulatory ECG," *Proc. of the 29th Annu. Int. Conf. IEEE,* pp. 5453-5456, 2007.

[14] M.A.D. Raya, L.G. Sison, "Adaptive noise cancelling of motion artifact in stress ECG signals using accelerometer," *Proc. 2nd Joint EMBS/BMES Conf.*, vol. 2, pp. 1756 – 1757, 2002.

[15] D.A. Tong, "Adaptive reduction of motion artifact in the electrocardiogram," *Proc. 2nd Joint EMBS/BMES Conf.*, vol. 2, pp. 1403-1404, 2002.

[16] S.W. Yoon *et al.*, "Adaptive motion artifacts reduction using 3-axis accelerometer in e-textile ECG measurement system," *J Med Syst*, pp. 101-106, 2008.

[17] V.K. Pandey, "Adaptive filtering for baseline wander removal in ECG," *10th IEEE Int. Conf. ITAB*, pp. 1-4, 2010.

[18] P.S. Hamilton, M.G. Curley, "Adaptive removal of motion artifact," *Proc.19th Annu. Int. Conf. IEEE/EMBS,* vol. 1, pp. 297-299, 1997.

[19] Y. Liu, M.G. Pecht, "Reduction of skin stretch induced motion artifacts in electrocardiogram monitoring using adaptive filtering," *Proc. 28th IEEE EMBS Annu. Int. Conf.*, pp. 6045-6048, 2006.

[20] W.C. Lee, *et al.,* "Adaptive reduction of motion artifact in a portable ECG system," *IEEE Sensors 2010 Conf.,* pp. 704-707, 2010.

[21] D. Buxi *et al*., "Correlation between electrode-tissue impedance and motion artifact in biopotential recordings," *IEEE Sensors Journal*, vol. 12, pp. 3373-3383, 2012.

[22] H. Kim *et al*., "Motion artifact removal using cascade adaptive filtering for ambulatory ECG monitoring system," *IEEE Biomedical Circuits and Systems Conf*., pp. 160-163, 2012.

[23] A. Zaknich, *Principles of Adaptive Filters and Self-Learning Systems*, London: Springer, 2005.

[24] Y. Tu, "Multiple reference active noise control," M.Sc. Thesis, Dept. Mech. Eng., Virginia Polytechnic Institute and State University, Blacksburg, VA, 1997.

[25] J. Fortuna, A.M. Martinez, "A blind source separation approach to structure from motion," *Proc. 3rd Int. Symp.3D Data Processing, Visualization, and Transmission*, pp. 145-152, 2006.

[26] M. Sigalas, H. Baltzakis, P. Trahanias, "Visual tracking of independently moving body and arms," *IEEE Int. Conf. Intelligent Robots and Systems*, pp. 3005-3010, 2009.

[27] P. Gao, E. Chang, L. Wyse, "Blind separation of fetal ECG from single mixture using SVD and ICA," *Proc. 2003 Joint Conf. 4th Int. Conf Information, Communications and Signal Processing and 4th Pacific Rim Conf. Multimedia*, vol. 3, pp. 1418-1422, 2003.

[28] R. Sameni, C. Jutten, M.B. Shamsollahi, "What ICA provides for ECG processing: application to noninvasive fetal ECG extraction," *2006 IEEE Int. Symp. Signal Processing and Information Technology*, pp. 656-661, 2006.

[29] X. Wu, Z. Ye, "Online infomax algorithm and its applications to remove EEG artifacts," *Proc. 2005 IEEE Engineering in Medicine and Biology 27th Annu. Conf.,* pp. 4203-4207, 2005.

[30] M. Milanesi, *et al.*, "Multichannel techniques for motion artifacts removal from electrocardiographic signals," *Proc. 28th IEEE Engineering in Medicine and Biology Society Annu. Int. Conf.*, pp. 3391-3394, 2006.

[31] I. Romero, *et al.*, "Motion artifact reduction in ambulatory ECG monitoring: an integrated system approach," *Proc. 2nd Conf. Wireless Health*, Article 11, 2011.

[32] H. Mori, J. Hoshino, "Independent component analysis and synthesis of human motion", *2002 IEEE Int. Conf. Acoustics, Speech, and Signal Processing*, vol. 4, pp. 3564-3567, 2002.

[33] J.V. Stone, *Independent Component Analysis A Tutorial Introduction*, Cambridge: MIT Press, 2004.

[34] A. Hyvarinen, "Survey on independent component analysis," *Neural Computing Surveys*, vol. 2, pp. 24-128, 1999.

[35] D. Langlois, S. Chartier, D. Gosselin, "An introduction to independent component analysis: infomax and fastICA algorithms," *Tutorials in Quantitative Methods for Psychology*, vol. 6(1), pp. 31-38, 2010.

[36] P. Comon, C. Jutten, *Handbook of Blind Source Separation: Independent Component Analysis and Applications*, Academic Press, 2010.

[37] R. Mutihac, M.M. Van Hulle, "PCA and ICA neural implementations for source separation - a comparative study," *Proc. Int. Joint Conf. Neural Networks*, vol. 1, pp. 769-774, 2003.

[38] Shimmer Research. *Product Gallery* [Online]. Retrieved 15 July, 2013, from Shimmer Research http://www.shimmersensing.com/

[39] *Shimmer User Manual Revision 2R.f* [Online]. Retrieved 19 January, 2013, from Shimmer Research http://www.shimmer-research.com/

[40] *Shimmer Platform Key Features* [Online]. Retrieved 19 January, 2013, from Shimmer Research http://www.shimmer-research.com/

[41] *Shimmer Wireless Sensor Platform* [Online]. Retrieved 19 January, 2013, from Shimmer Research http://www.shimmer-research.com/

[42] *Shimmer MicroSD Media Guide Rev1a* [Online]. Retrieved 19 January, 2013, from Shimmer Research http://www.shimmer-research.com/

[43] *Shimmer GYRO IMU Module* [Online]. Retrieved 19 January, 2013, from Shimmer Research http://www.shimmer-research.com/

[44] *Shimmer ECG Module* [Online]. Retrieved 19 January, 2013, from Shimmer Research http://www.shimmer-research.com/

[45] *ECG User Guide Rev 1.4* [Online]. Retrieved 19 January, 2013, from Shimmer Research http://www.shimmer-research.com/

[46] TinyOS Alliance, TinyOS [Online]. Retrieved 1 May, 2013, from http://www.tinyos.net/

[47] Shimmer Research. *Multicharger* [Online]. Retrieved 22 July, 2013, from Shimmer Research http://www.shimmersensing.com/

[48] M.L. Simoons, P.G. Hugenholtz, "Gradual changes of ECG waveform during and after exercise in normal subjects," *Circulation*, vol. 52, pp. 570-577, 1975.

[49] H. Gavert *et al.*(2005). *FastICA Package for Matlab* [Online]. Retrieved 23 September, 2013, from Aalto University Department of Information and Computer Science http://research.ics.aalto.fi/ica/fastica/

[50] Y. Liu, "Reduction of skin stretch induced motion artifacts in electrocardiogram monitoring using adaptive filtering," Ph.D. dissertation, Dept. Mech. Eng., University of Maryland, College Park, MD, 2007.

Appendix A Matlab™ Code

The coding used to implement specific algorithms needed throughout this work is provided below. All coding is performed in Matlab™.

A1 LMS

```
%Inputs:
%inSignal: The noisy input signal
%refSignal: Reference signal that is well correlated with noise
%
%Output:
%outSignal: The noise-reduced signal

p = 16; %Filter Order

W(p) = 0; %Weight vector
x(p) = 0; %Vector of p most recent reference signal values

for i = 1:length(inSignal)
    x(1) = refSignal(i);
    y(i) = W*x'; %Estimated error
    outSignal(i) = inSignal(i) - y(i);
    W = W + scale*outSignal(i)*x;

    x = circshift(x, [0,1]);
end

outSignal = outSignal';
```

A2 RLS

```
%Inputs:
%FF: Forgetting Factor, a small postive constant close to one
%delta: Value to initialize P, typically a small positive constant less
%than one
%inSignal: Noisy input signal
%refSignal: Reference signal that is well correlated with noise
%
%Output:
%outSignal: The noise-reduced signal
p = 2; %Filter Order

P = (delta^-1)*eye(p,p);
W(p) = 0; %Weight vector
x(p) = 0; %Vector of p most recent reference signal values
```

```
x=x';
W=W';


for i = 1:length(inSignal)
    x(1) = refSignal(i);
    K = (P*x)/(FF + x'*P*x);

    y(i) = x'*W;
    outSignal(i) = inSignal(i) - y(i);

    W = W + K*(outSignal(i));
    P = (FF^-1)*P - (FF^-1)*K*x'*P;
    x = circshift(x, [1,0]);
end
```

A3 PCA

```
    %Input:
    %X: Mixed Signals
    %
    %Output:
    %Y: Decorrelated Signals
    %
    %The following steps are also used to whiten data prior to
    %ICA methods
    C= cov(X');
    M= mean(X');
    [V,D]= eig(C);
    P = V * diag(sqrt(1./(diag(D) + 0.001))) * V';
    W = bsxfun(@minus, X', M) * P;
    Y = W';
```

A4 Infomax

```
%Inputs:
%X: Array of m mixed signals of n samples each
%u: Step size value, typically 0.01

%Output:
%infoOut: Unmixed signals
[m n] = size(X);
W = rand(m,m); %Unmixing matrix initialization

i = 1;

while i < n

     y = W*X(:,i);
```

```
     %Comment out one of the two below lines depending on approach
     W = W + u*(eye(m,m) - tanh(y)*y')*W; %Use for supergaussian
     W = W + u*(eye(m,m) + tanh(y)*y' - y*y')*W; %Use for subgaussian

     i = i + 1;
end

infoOut = W*X;
```

Appendix B Additional Graphs

Throughout Chapter 5, the results were collected and presented based on a number of variables. After a point, graphs were left out due to the fact that they ultimately presented redundant information or led strictly to results that had already been explained previously. The graphs that were not included in Chapter 5 are presented below for reference.

B1 Adaptive Filtering of Individual Sensors

B1.1 LMS – Shared Gain Factor

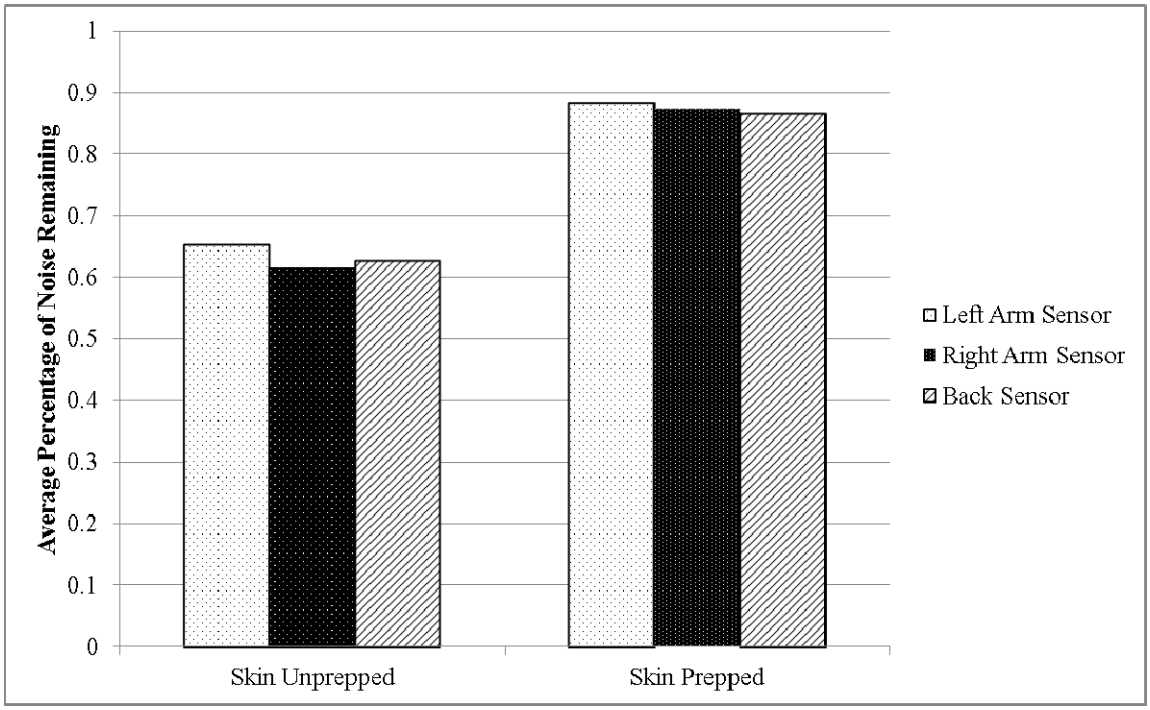

LMS Skin Preparation, Shared Variables

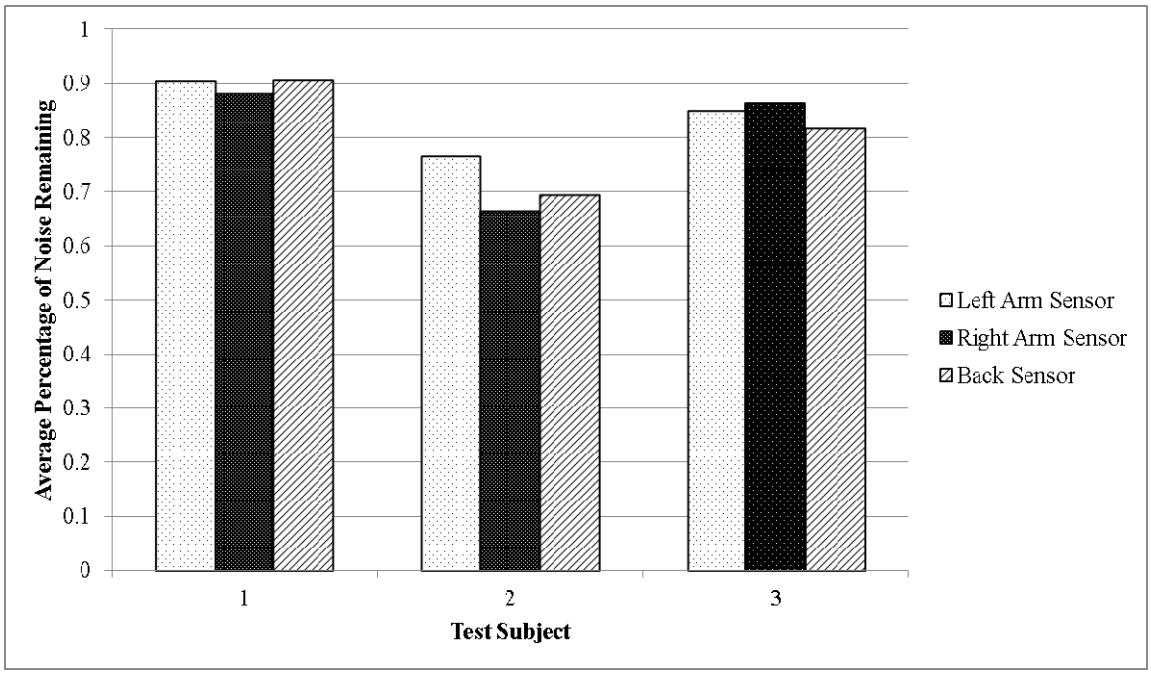

LMS Multiple Users, Shared Variables

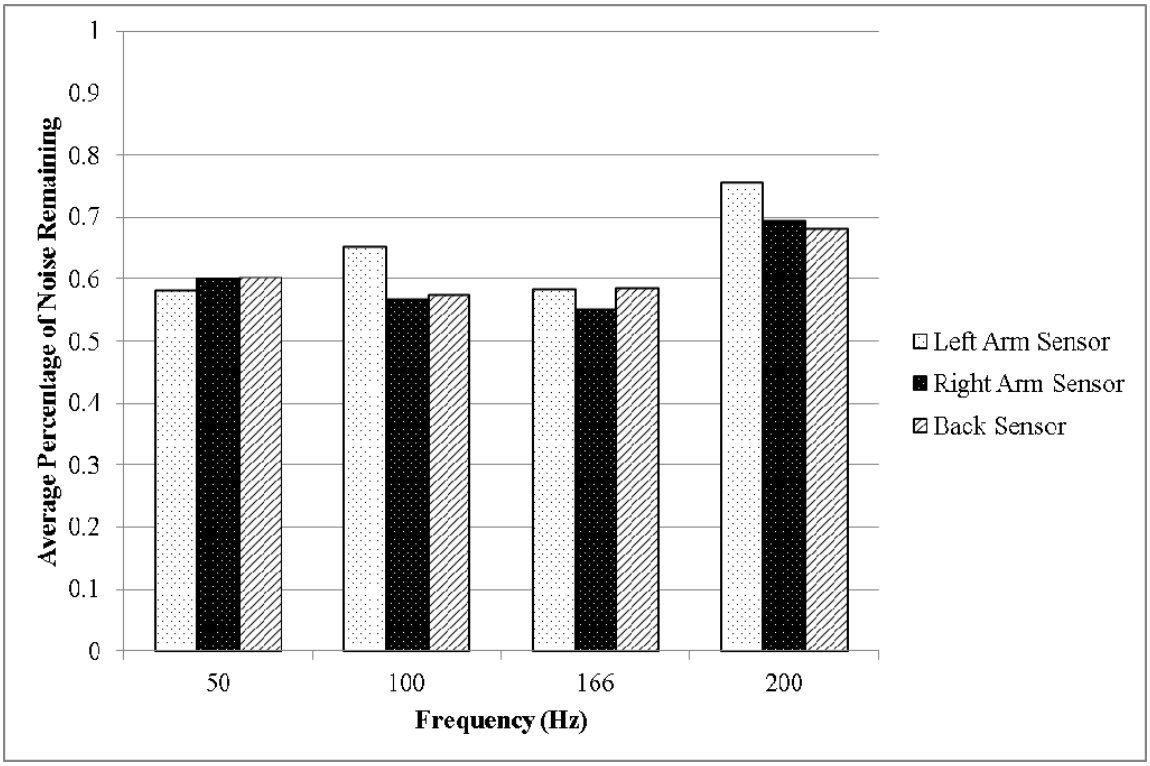

LMS Sampling Frequencies, Shared Variables

B1.2 RLS – Shared Forgetting Factor

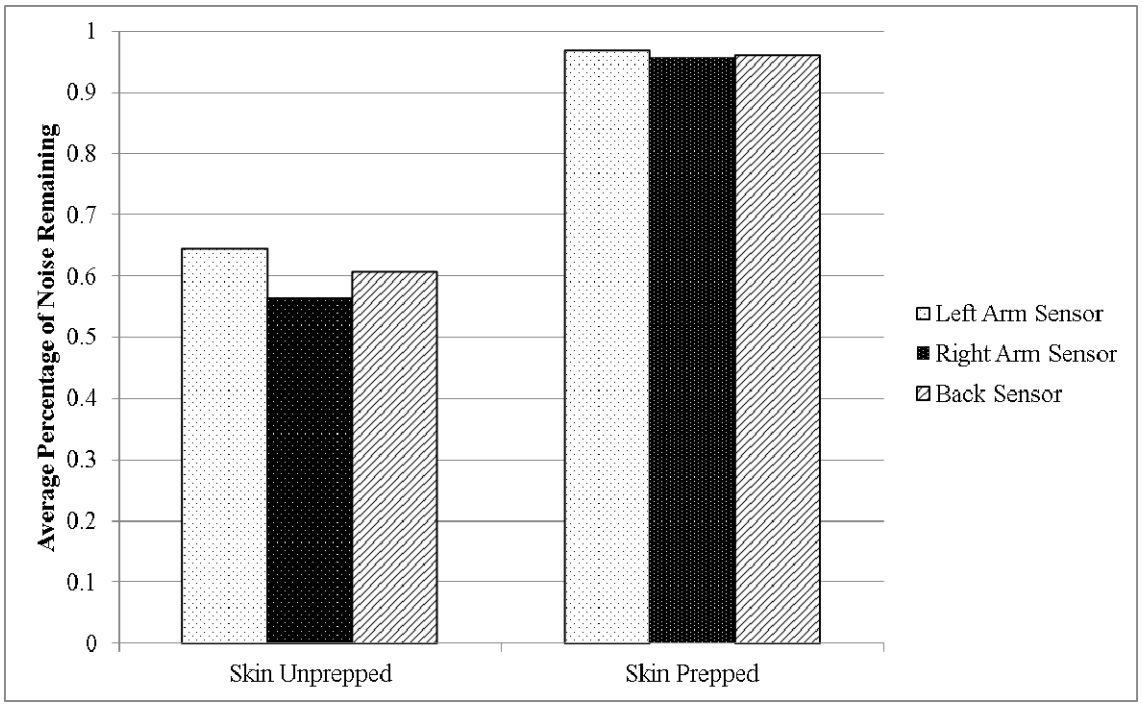

RLS Skin Preparation, Shared Variables

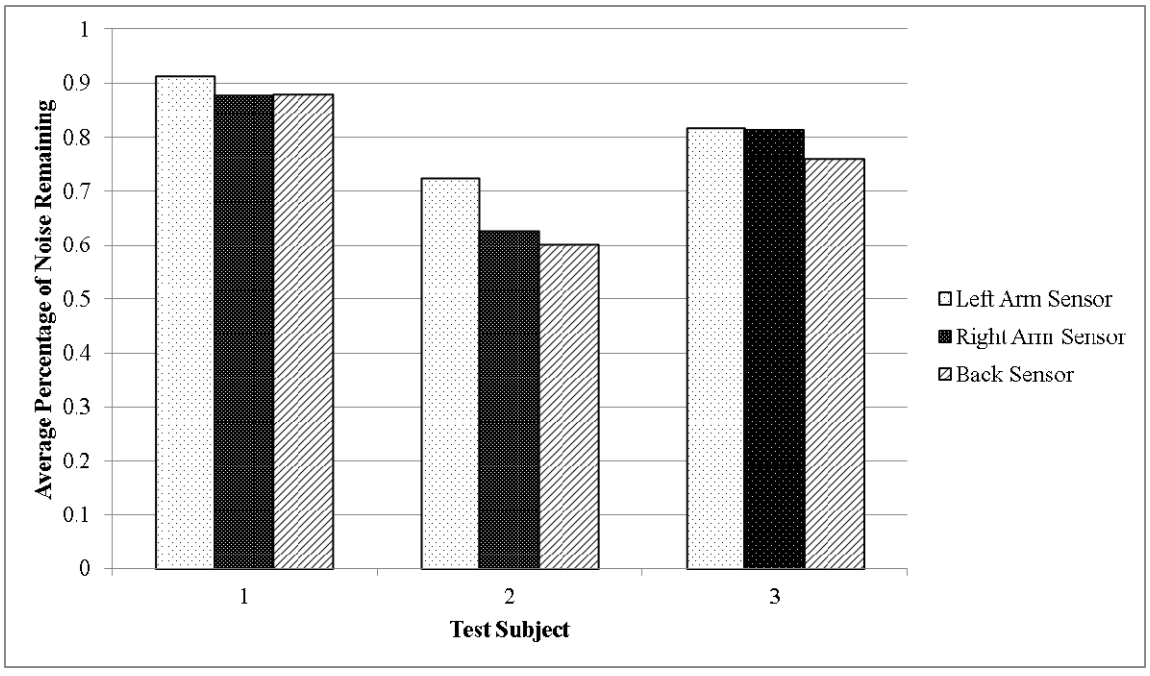

RLS Multiple Users, Shared Variables

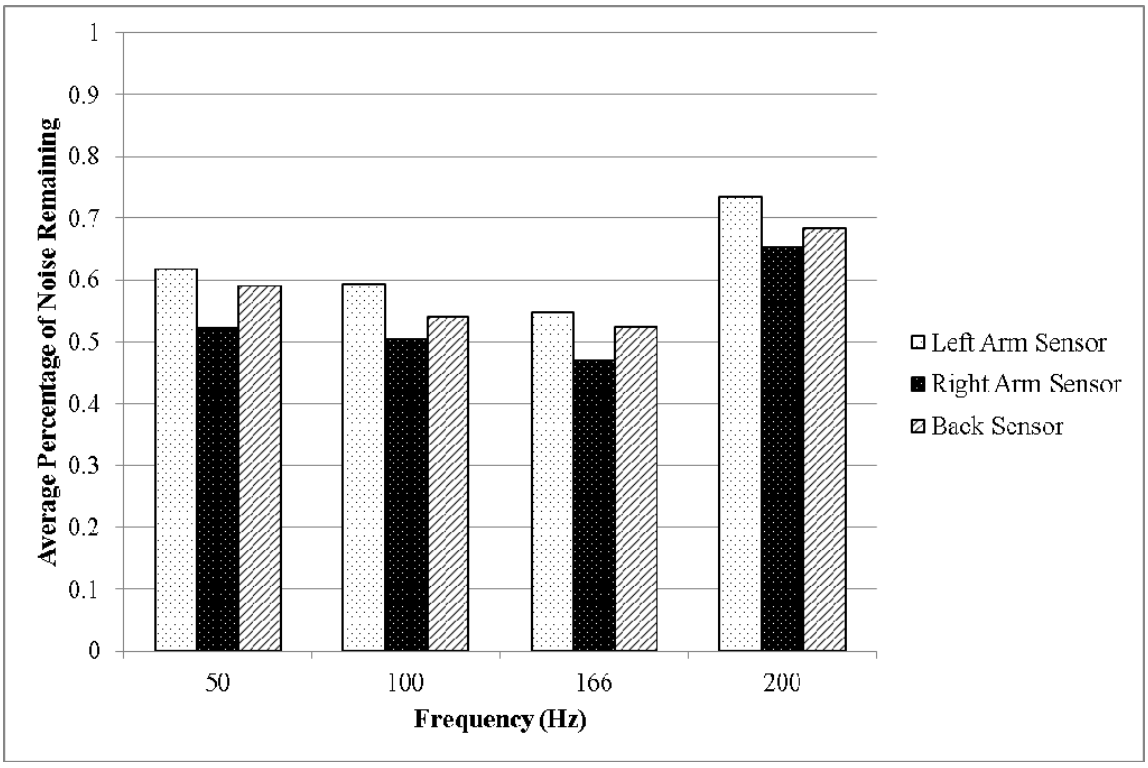

RLS Sampling Frequencies, Shared Variables

B1.3 LMS vs RLS – Optimal Variables

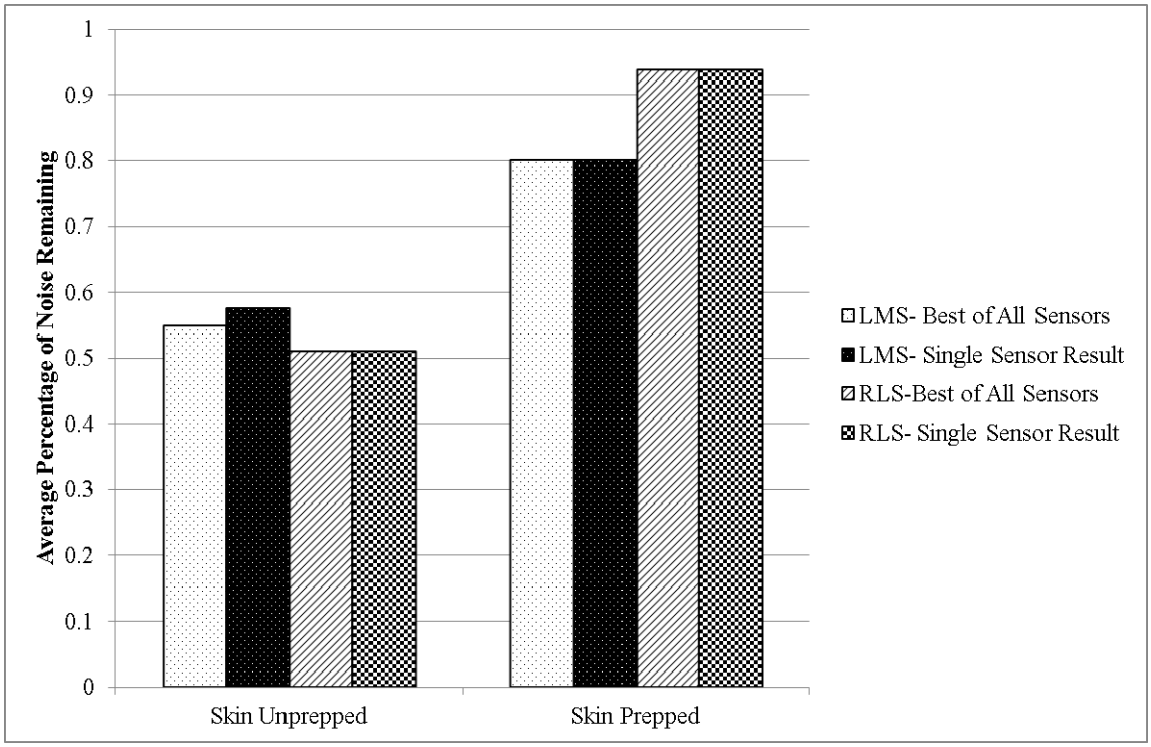

LMS vs RLS Skin Preparation, Optimum Variables

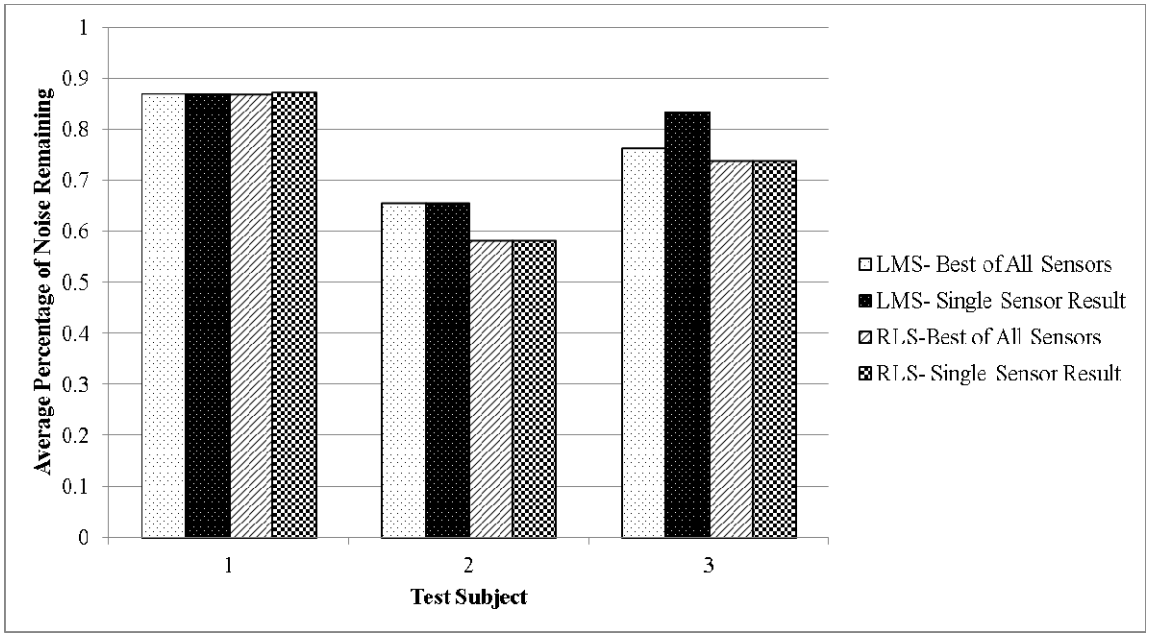

LMS vs RLS Multiple Users, Optimum Variables

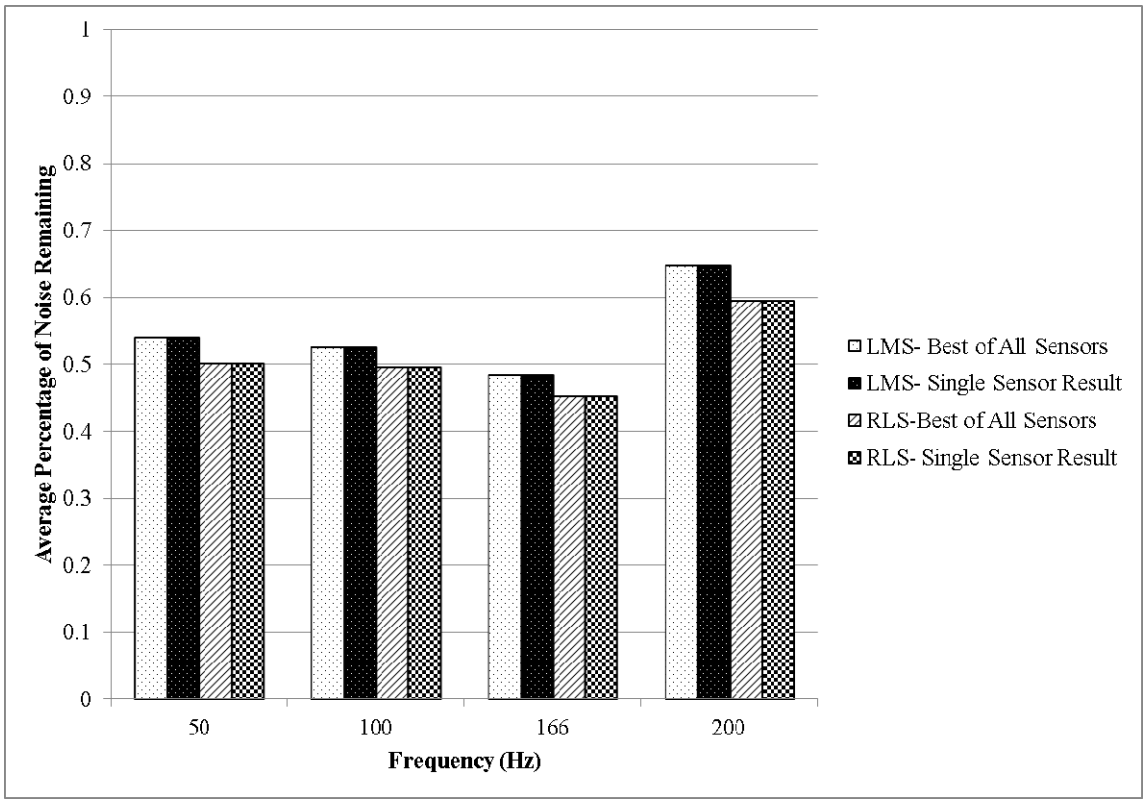

LMS vs RLS Sampling Frequency, Optimum Variables

B1.4 LMS vs. RLS – Shared Variables

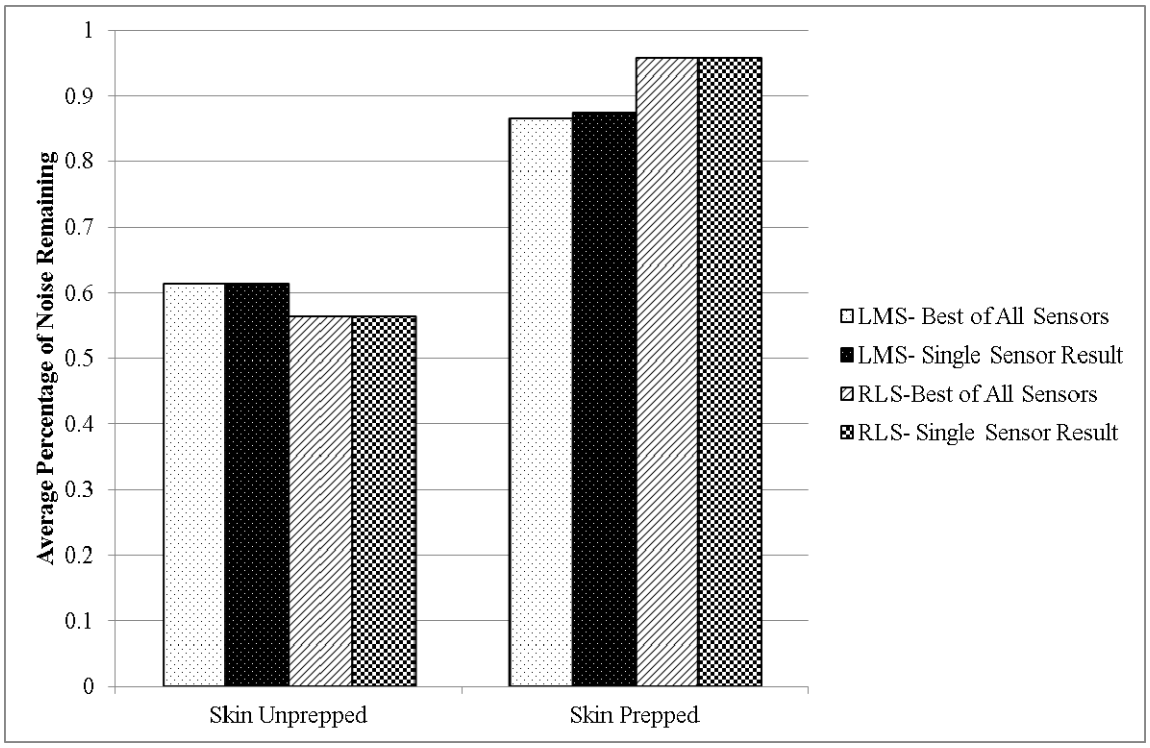

LMS vs RLS Skin Preparation, Shared Variables

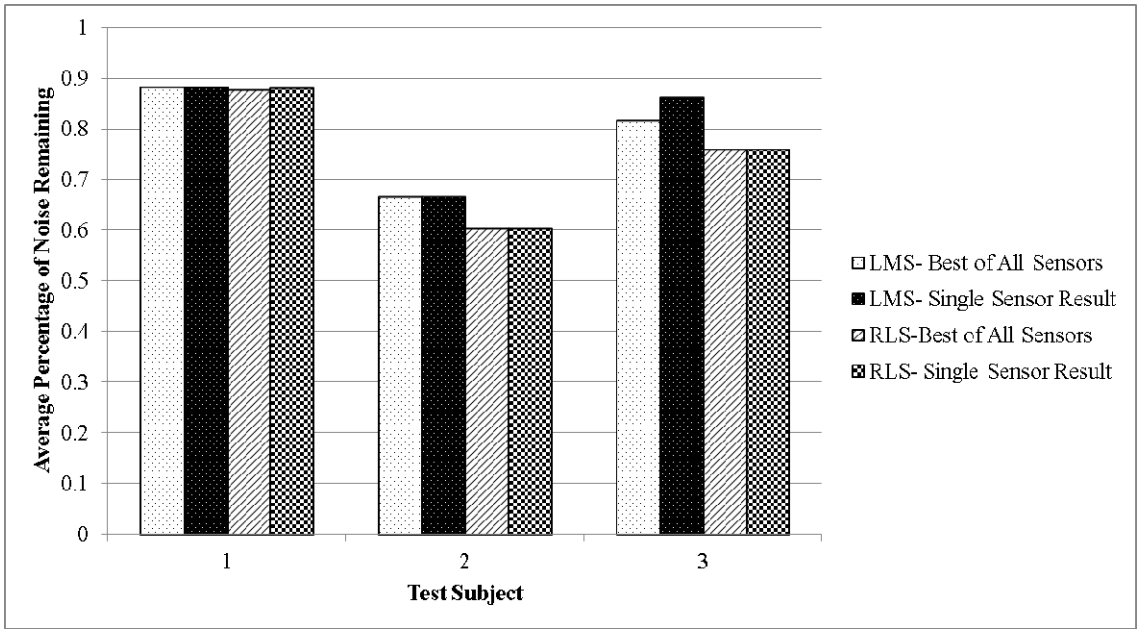

LMS vs RLS Multiple Users, Shared Variables

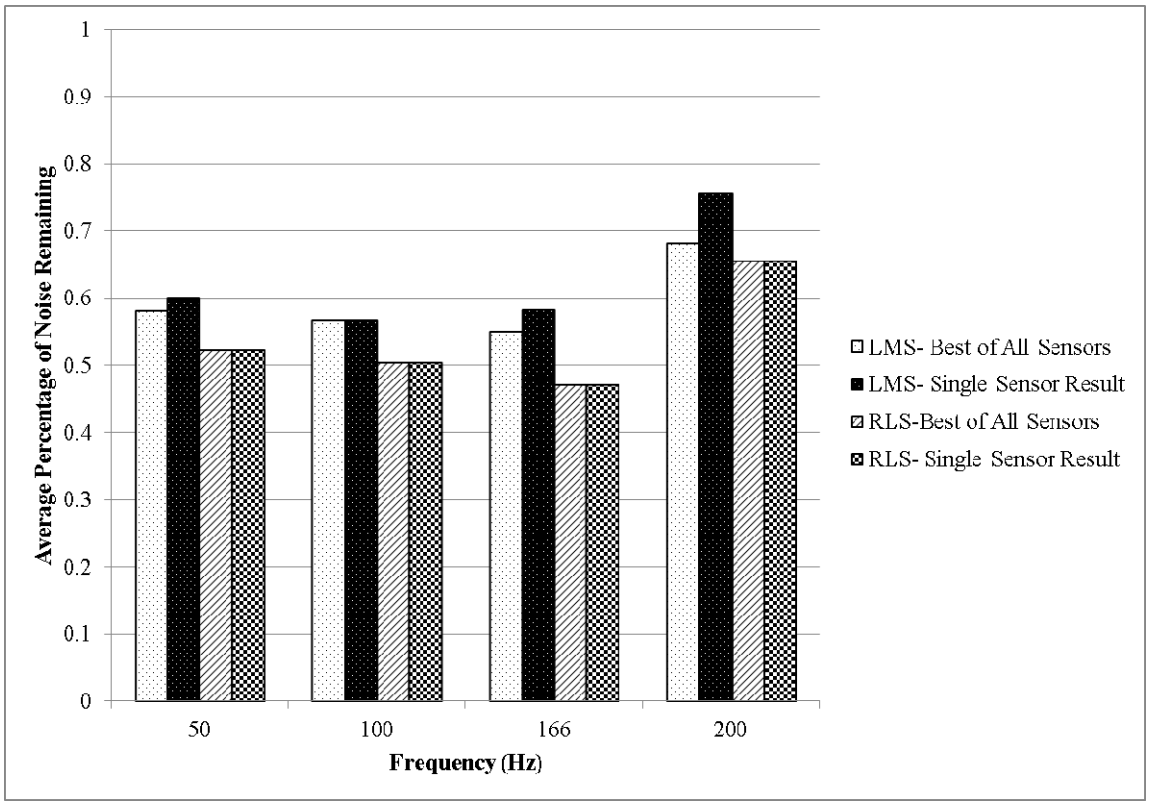

LMS vs RLS Sampling Frequency, Shared Variables

B2 Adaptive Filtering of All Sensors via BSS

B2.1 LMS Optimum Gain Factors

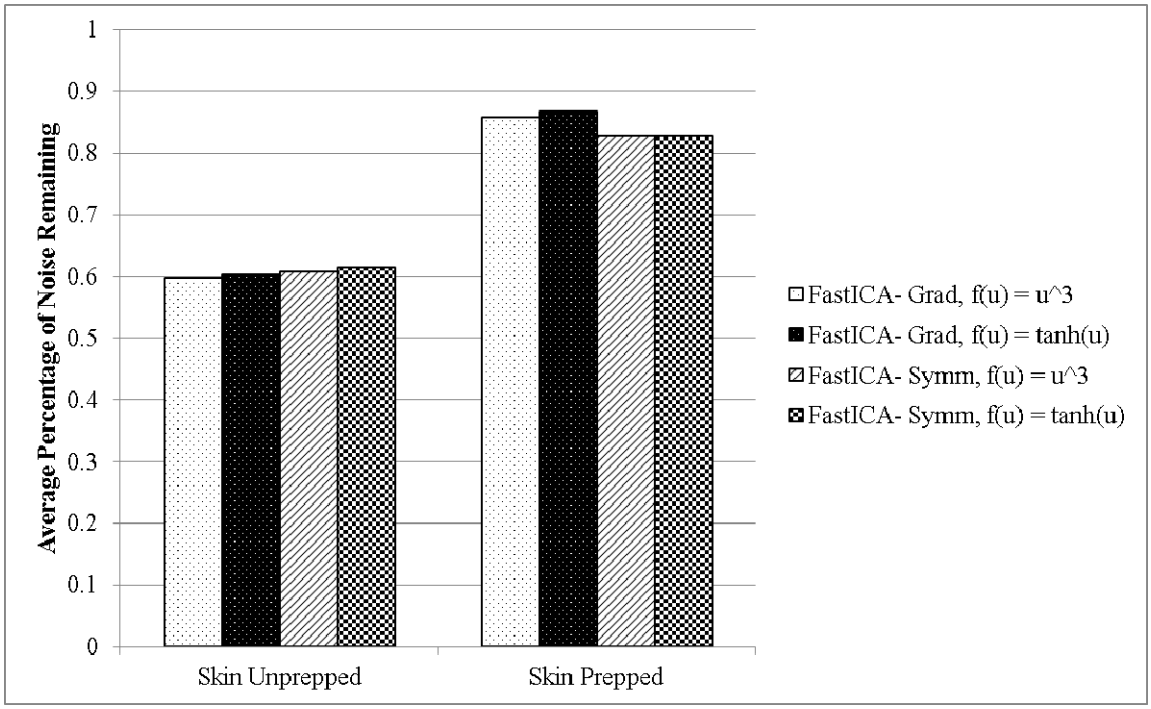

FastICA LMS Skin Preparation, Optimal Variables

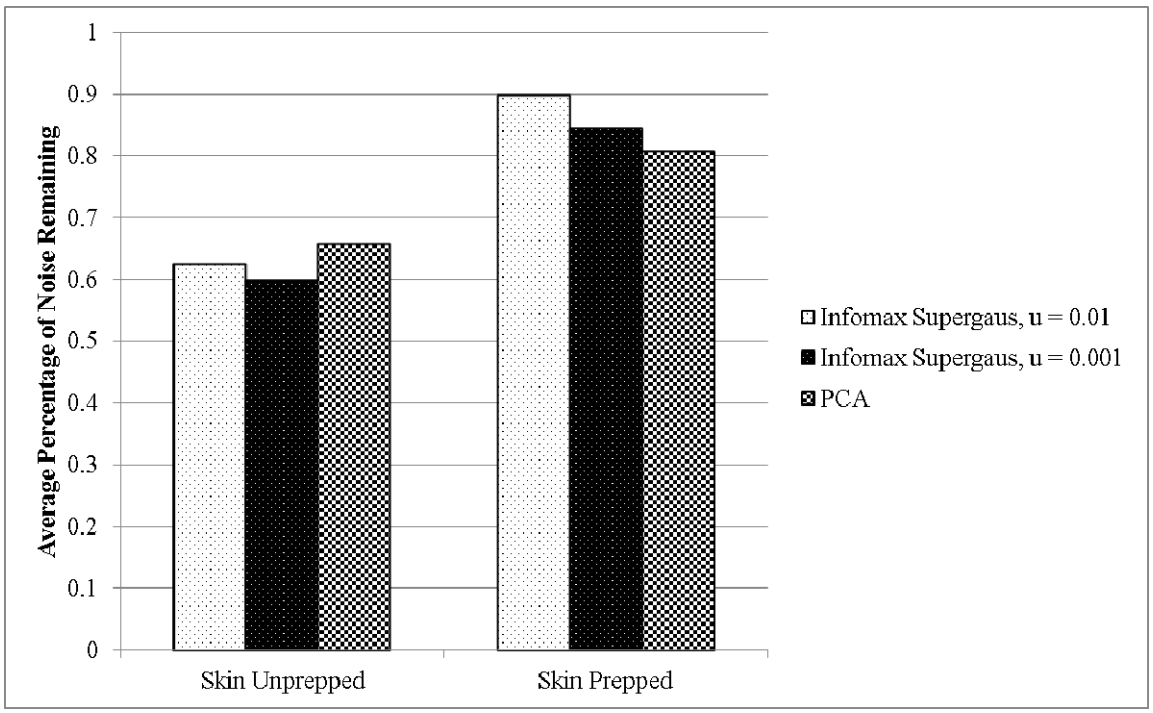

Infomax & PCA LMS Skin Preparation, Optimal Variables

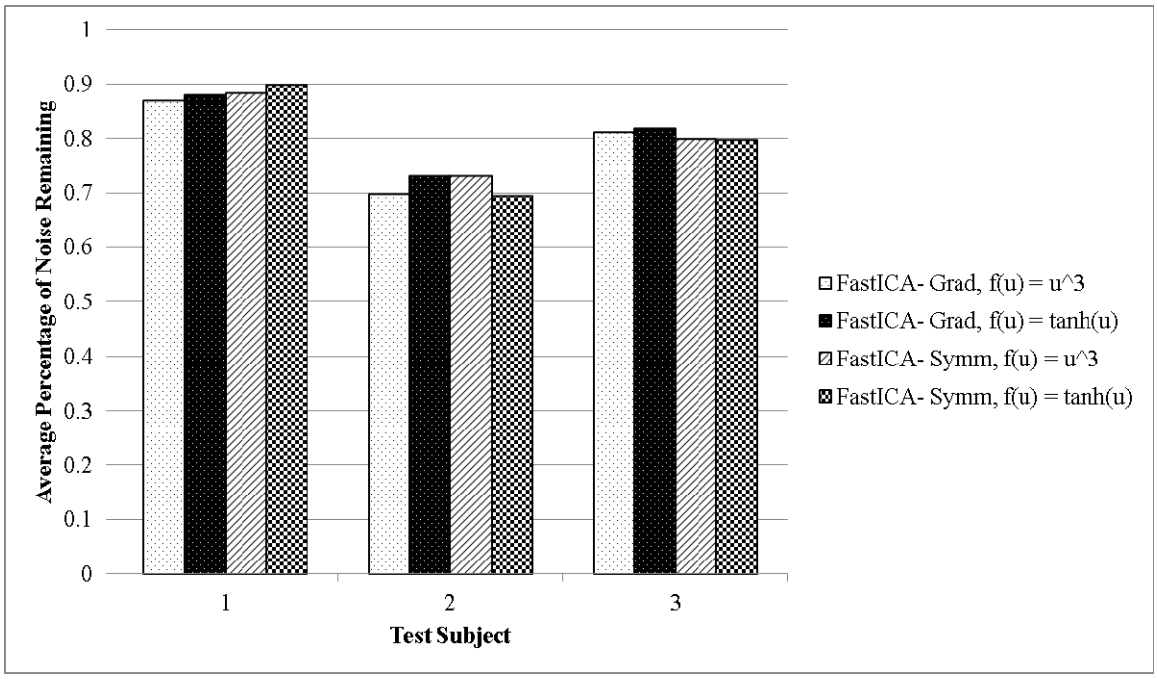

FastICA LMS Multiple Users, Optimal Variables

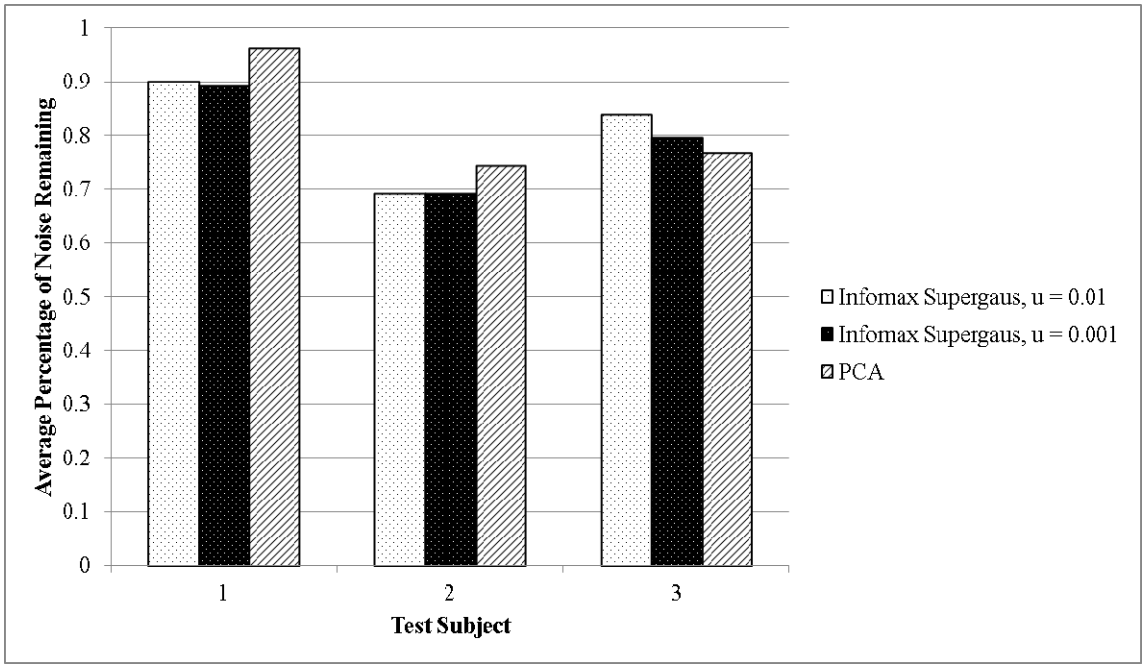

Infomax & PCA LMS Multiple Users, Optimal Variables

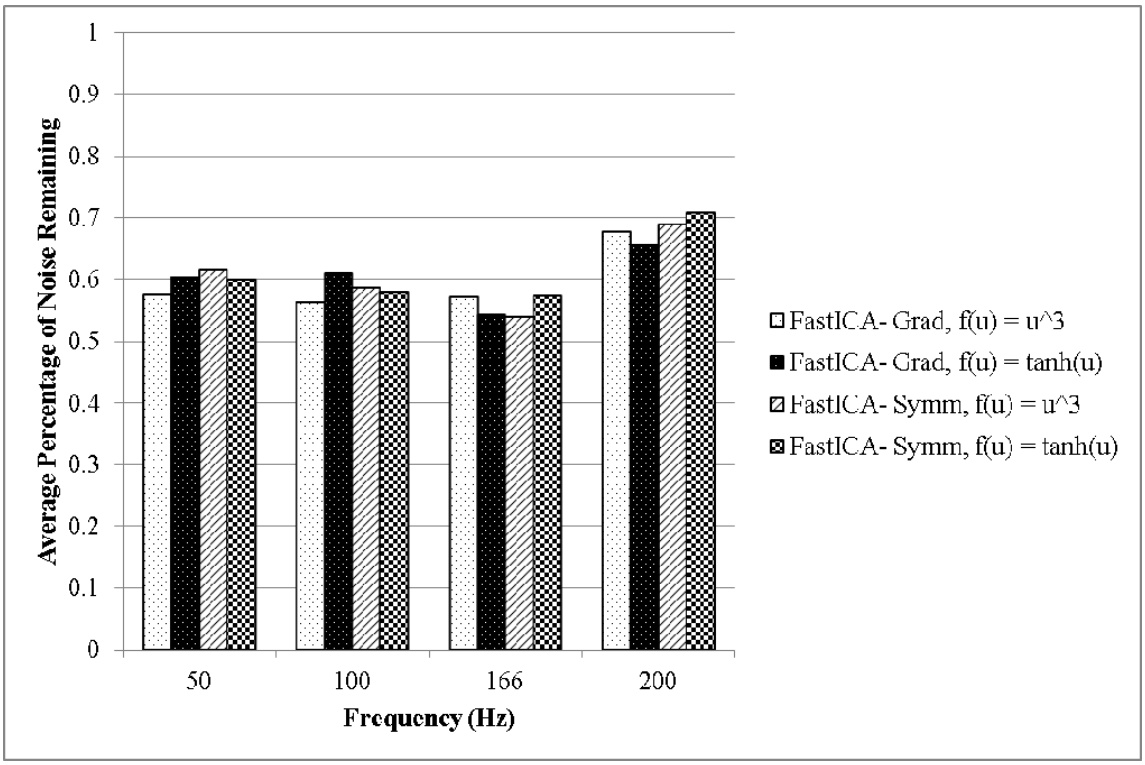

FastICA LMS Sampling Frequency, Optimal Variables

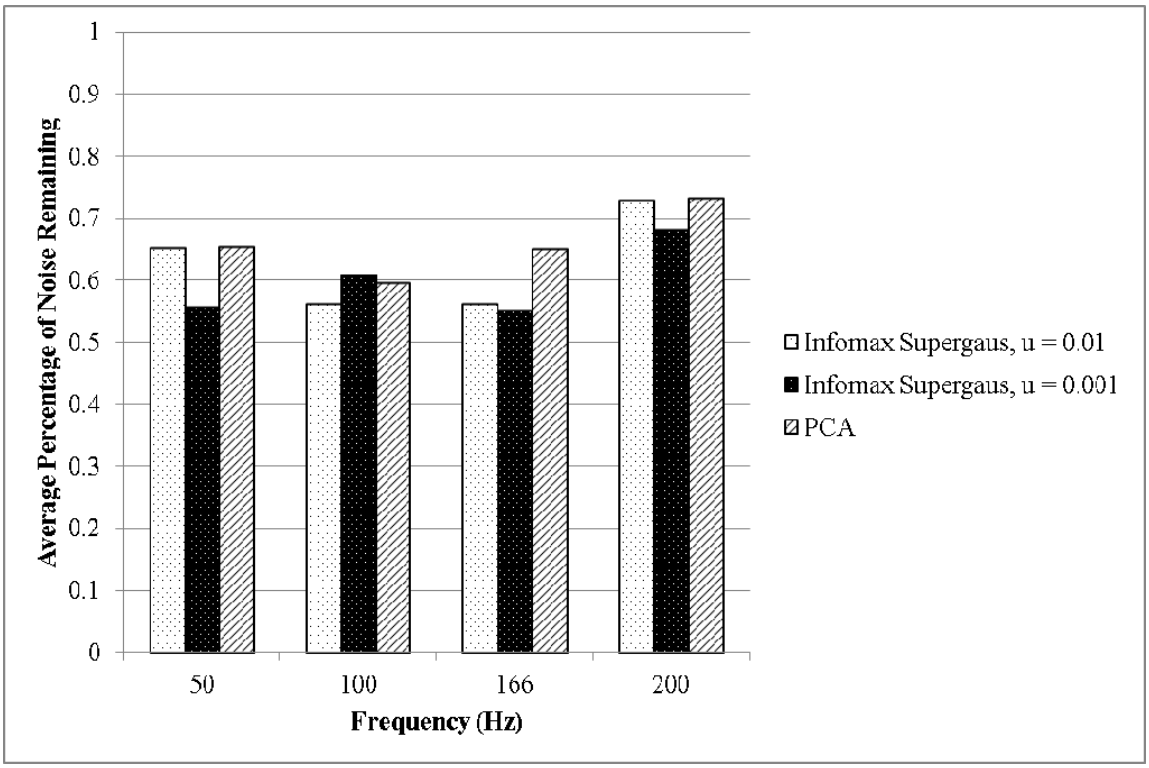

Infomax & PCA LMS Sampling Frequency, Optimal Variables

B2.2 LMS Shared Gain Factors

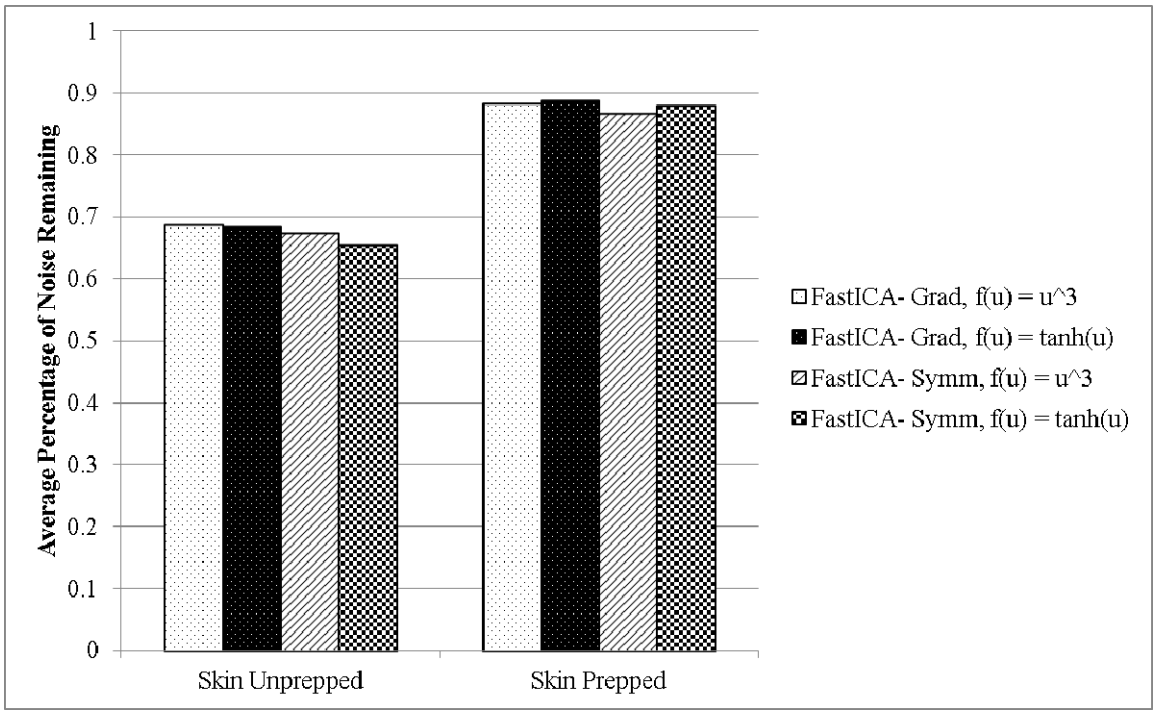

FastICA LMS Skin Preparation, Shared Variables

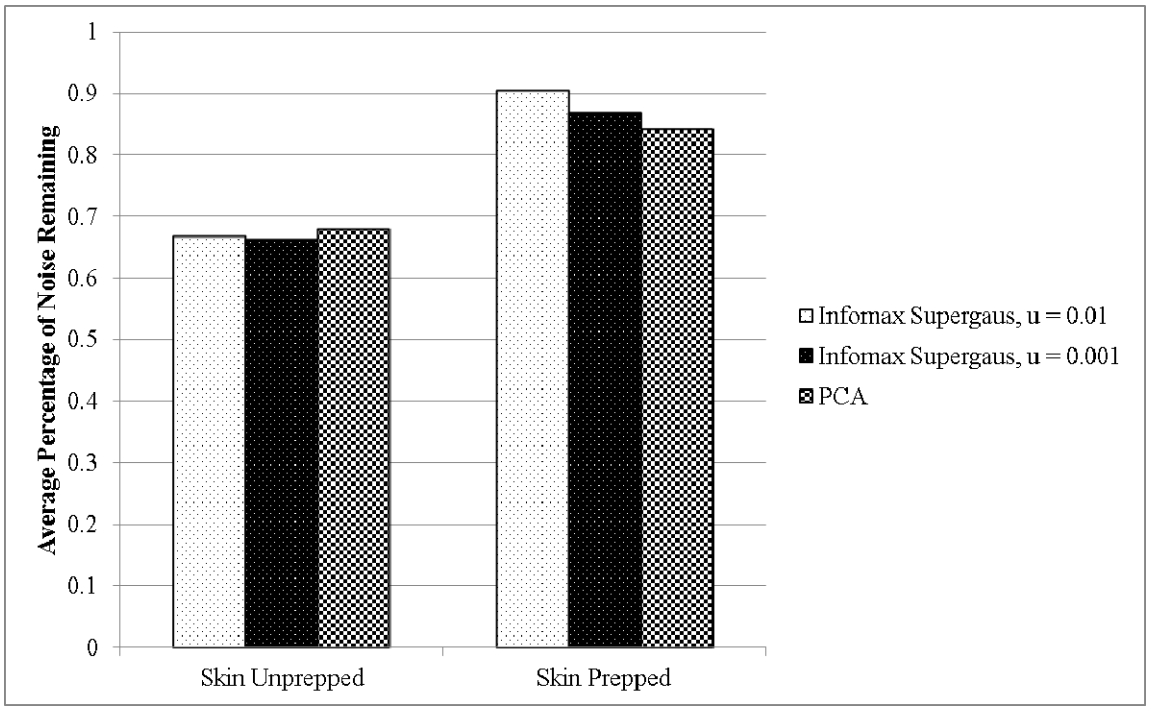

Infomax & PCA LMS Skin Preparation, Shared Variables

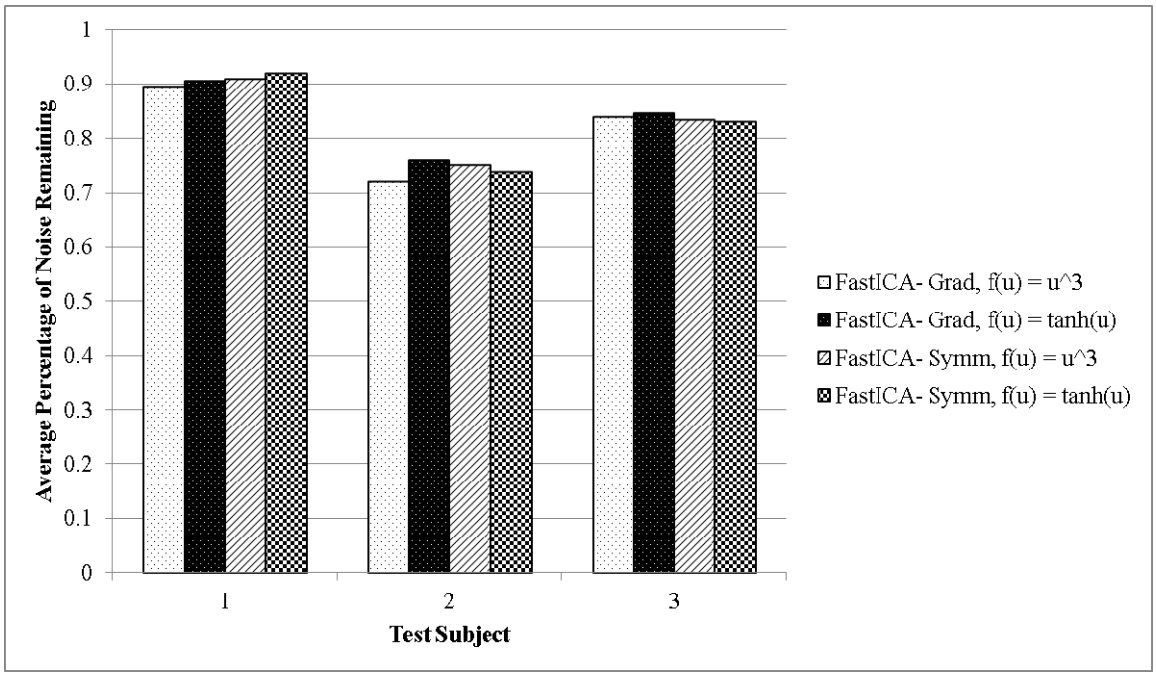

FastICA LMS Multiple Users, Shared Variables

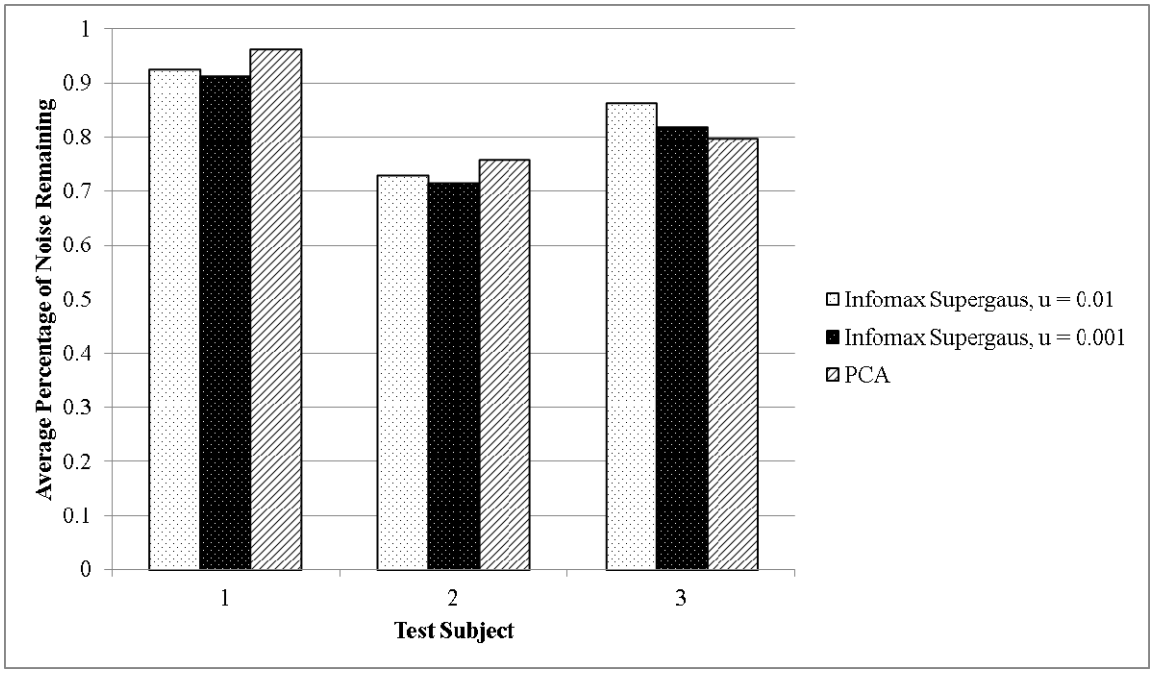

Infomax & PCA LMS Multiple Users, Shared Variables

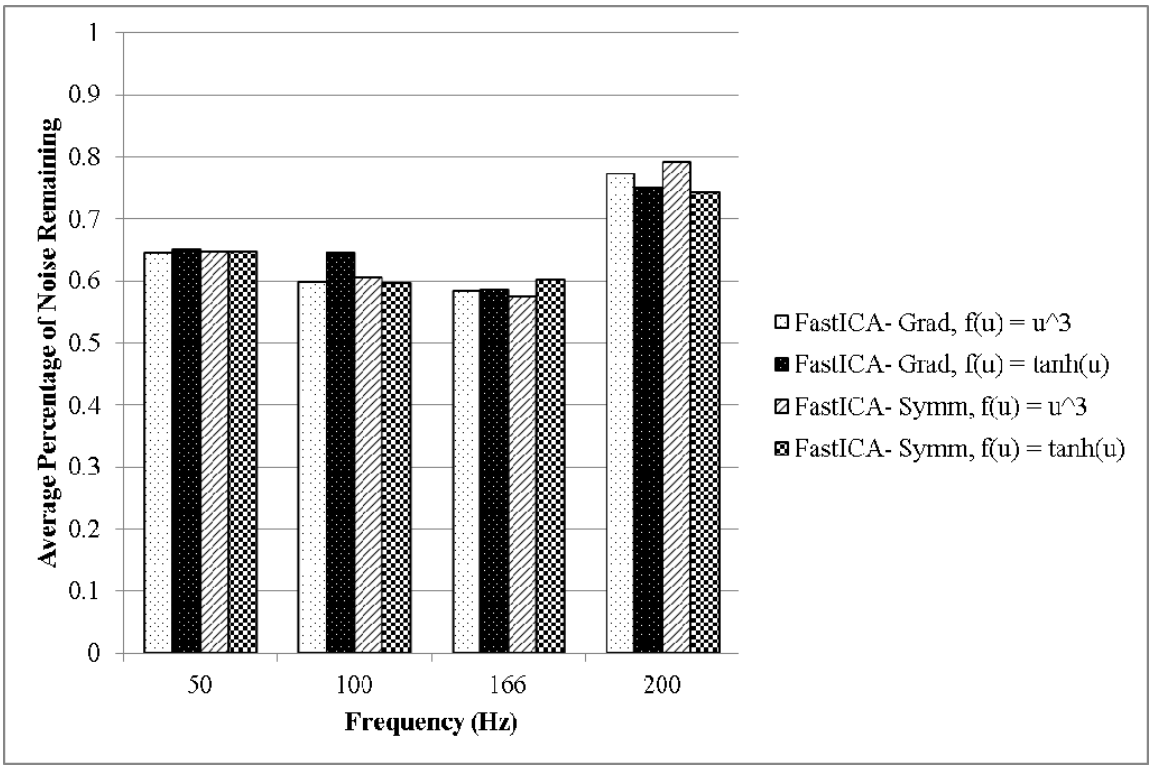

FastICA LMS Sampling Frequency, Shared Variables

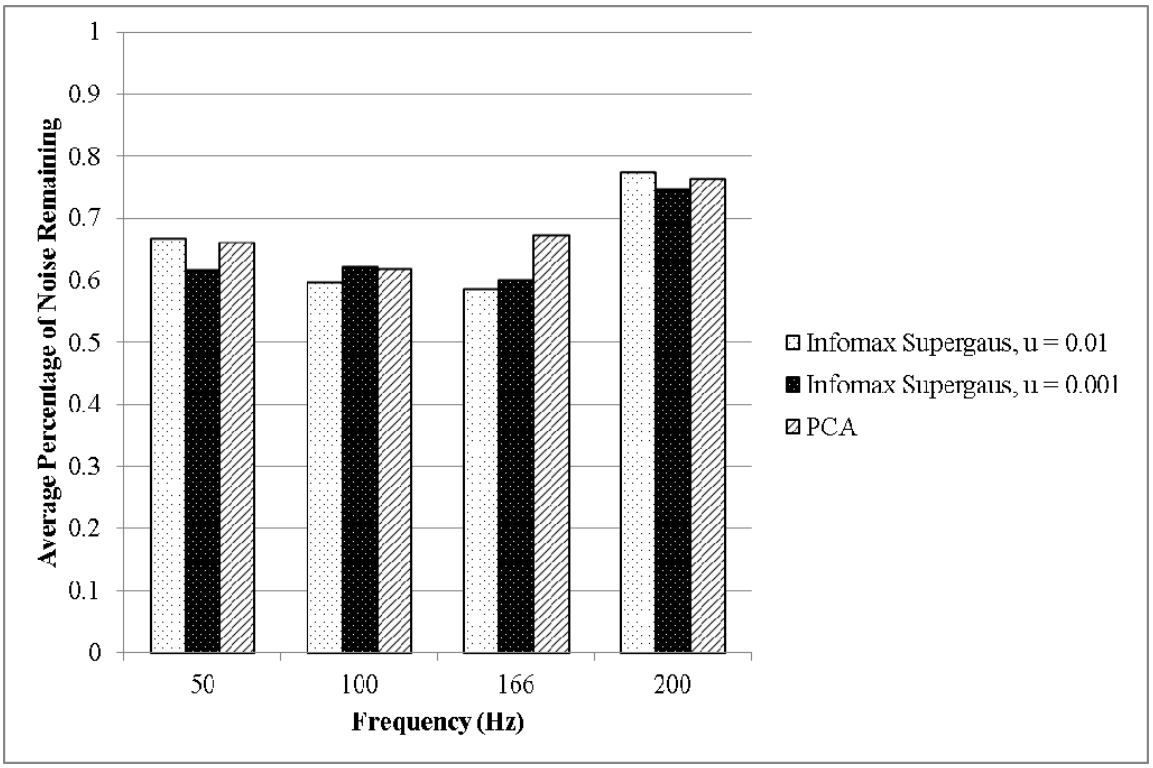

Infomax & PCA LMS Sampling Frequency, Shared Variables

B2.3 RLS Optimum Forgetting Factors

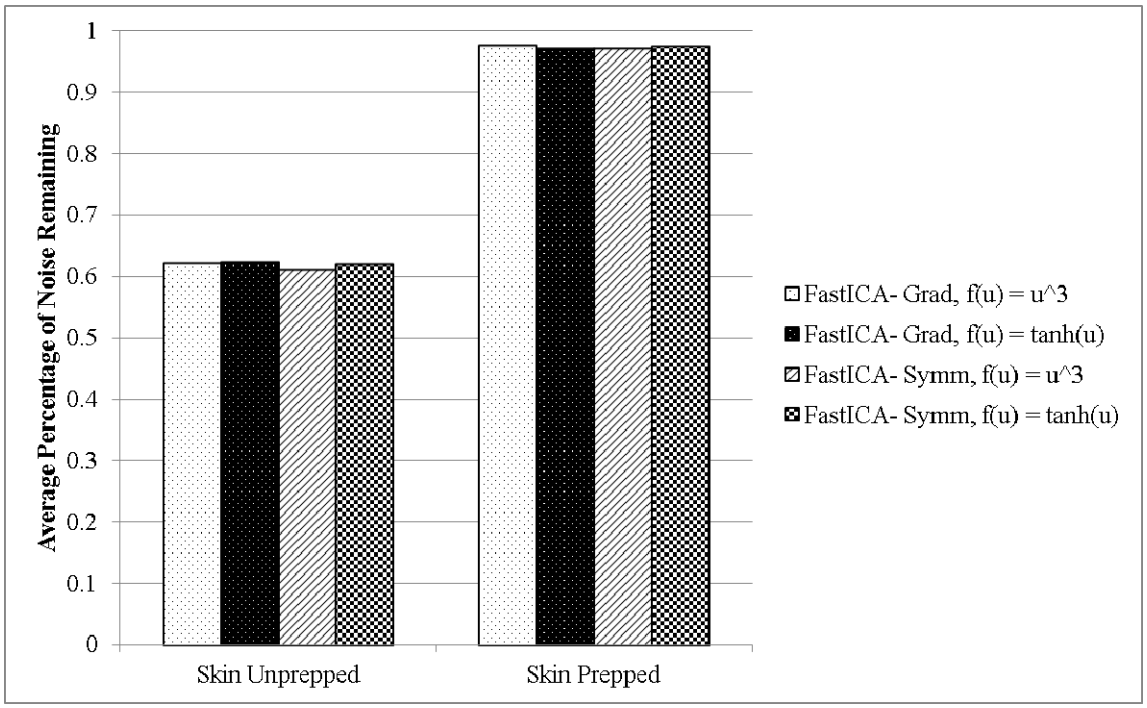

FastICA RLS Skin Preparation, Optimal Variables

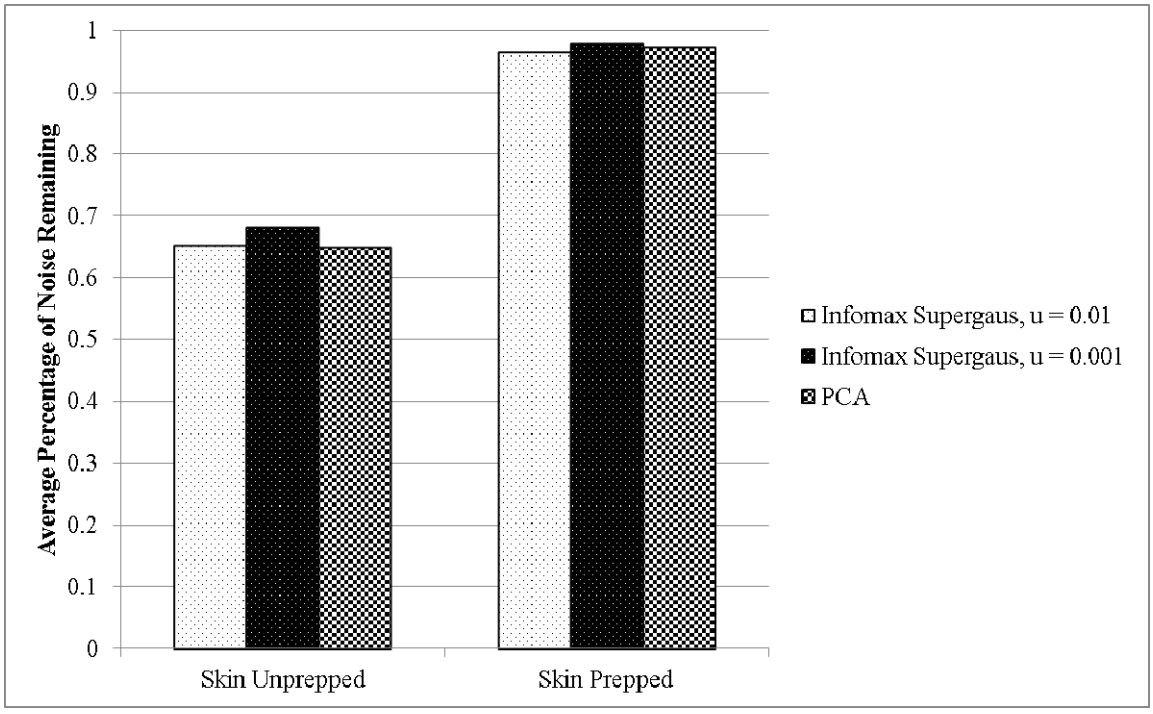

Infomax & PCA RLS Skin Preparation, Optimal Variables

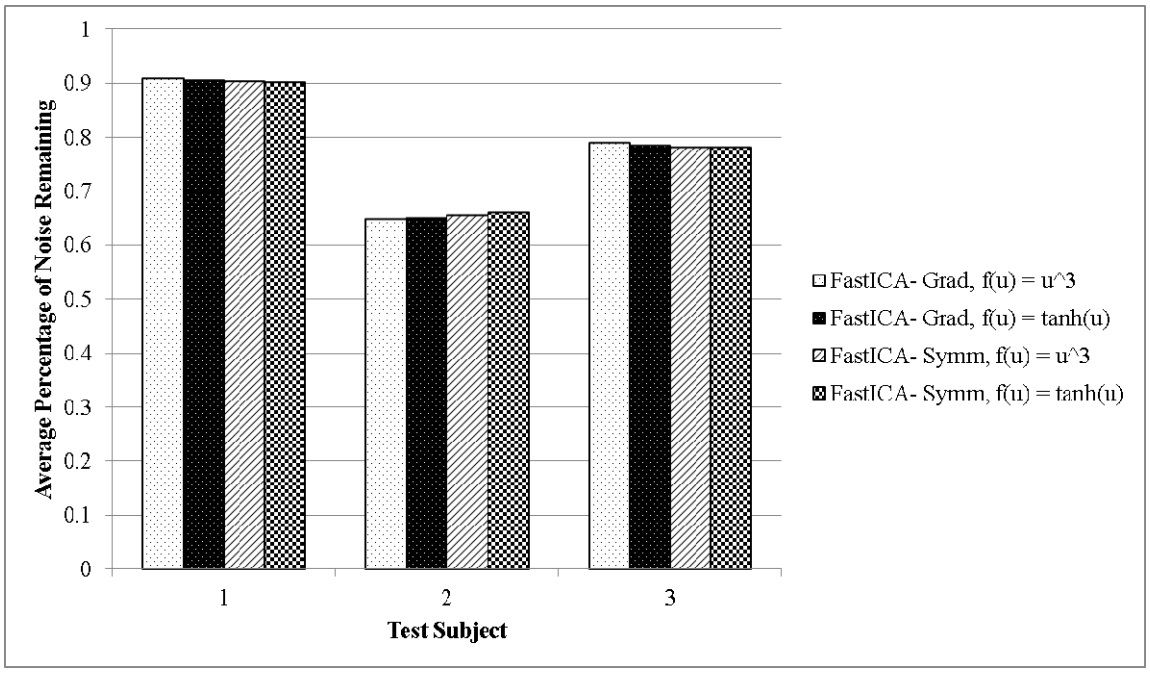

FastICA RLS Multiple Users, Optimal Variables

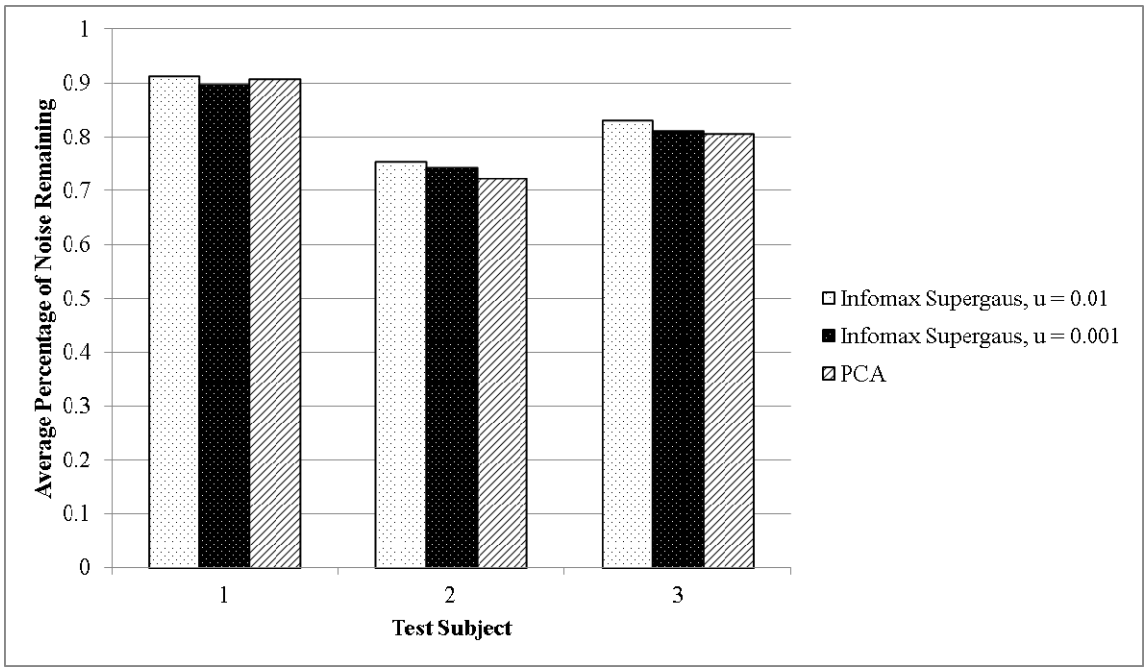

Infomax & PCA RLS Multiple Users, Optimal Variables

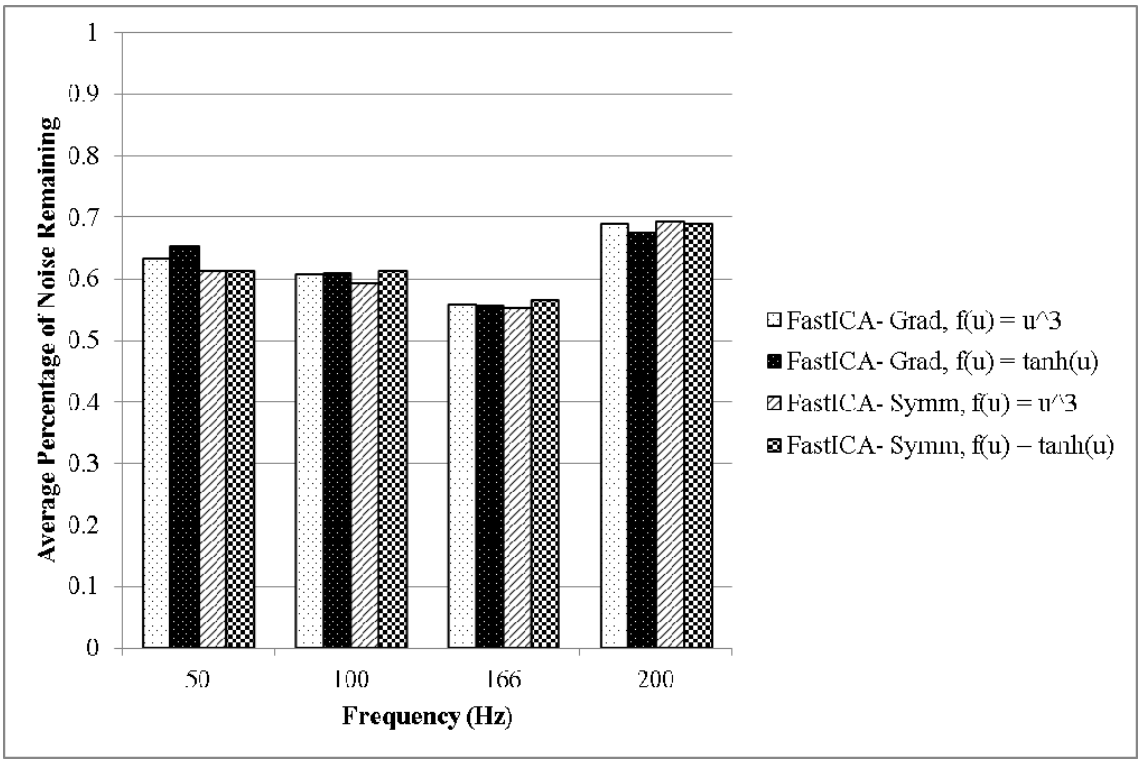

FastICA RLS Sampling Frequency, Optimal Variables

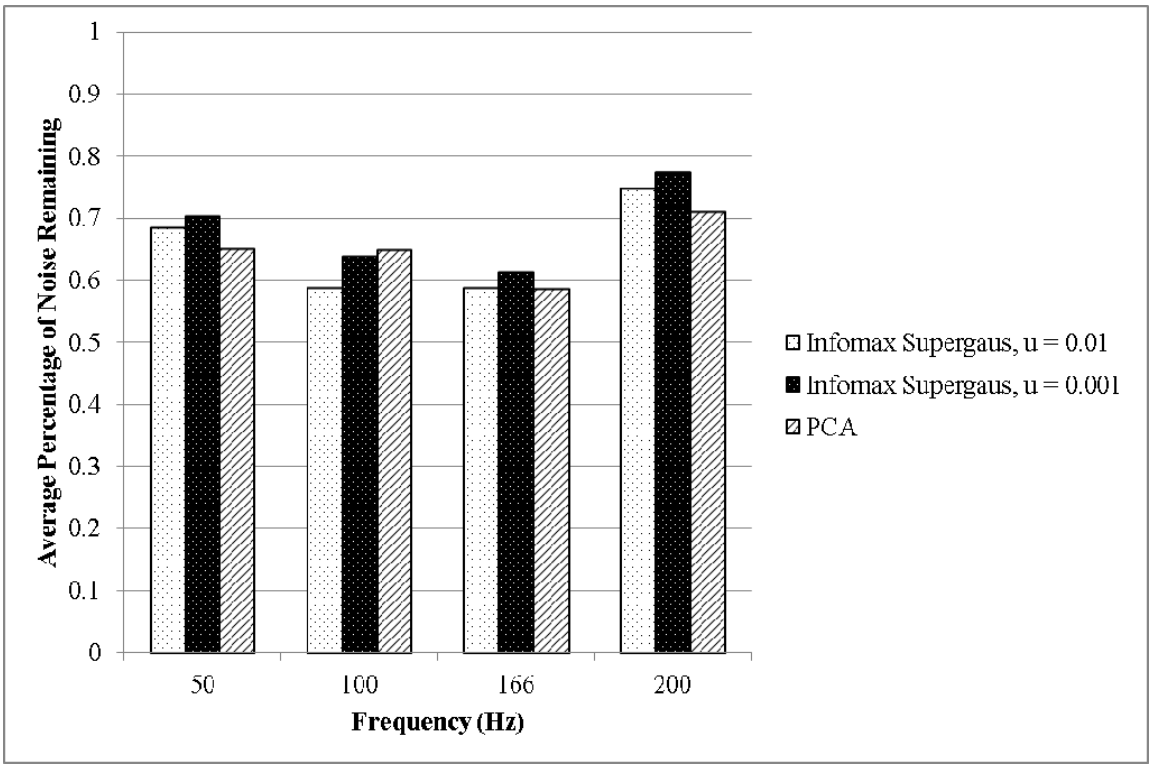

Infomax & PCA RLS Sampling Frequency, Optimal Variables

B2.4 RLS Shared Forgetting Factors

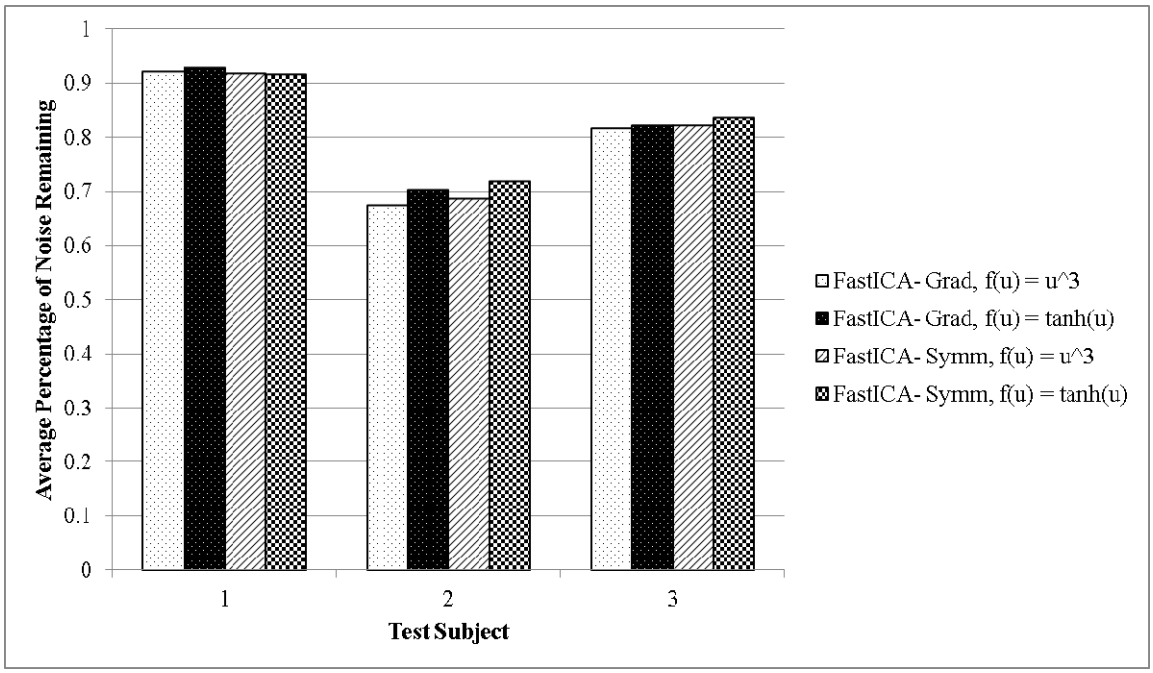

FastICA RLS Multiple Users, Shared Variables

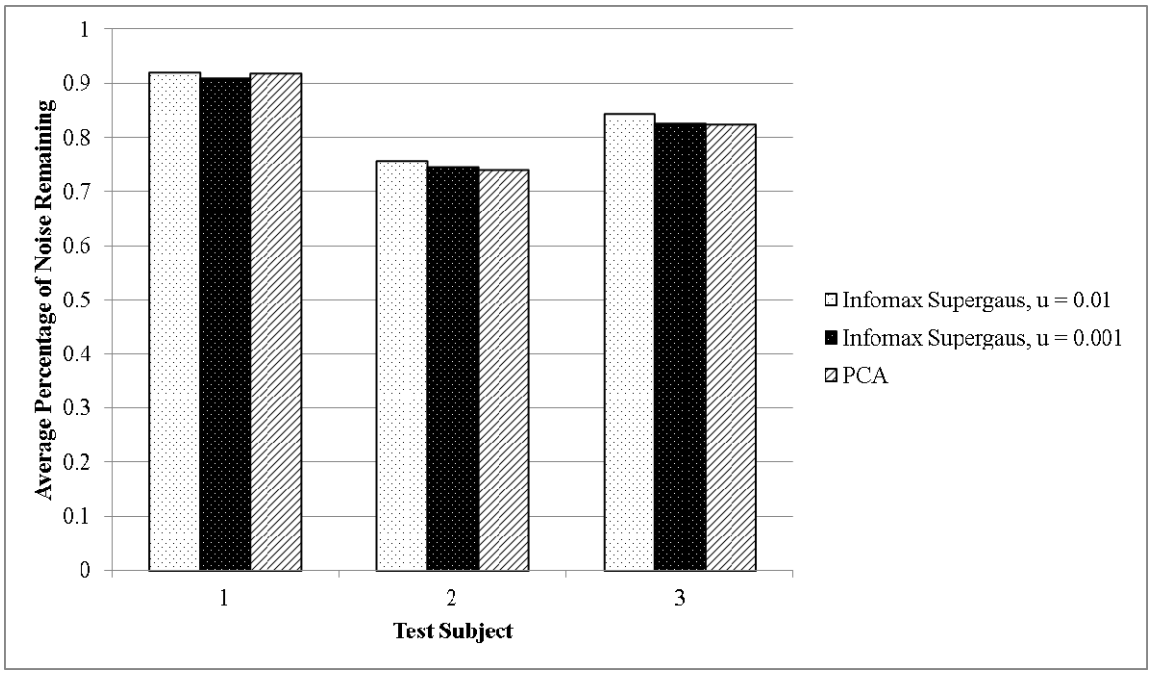

Infomax & PCA RLS Multiple Users, Shared Variables

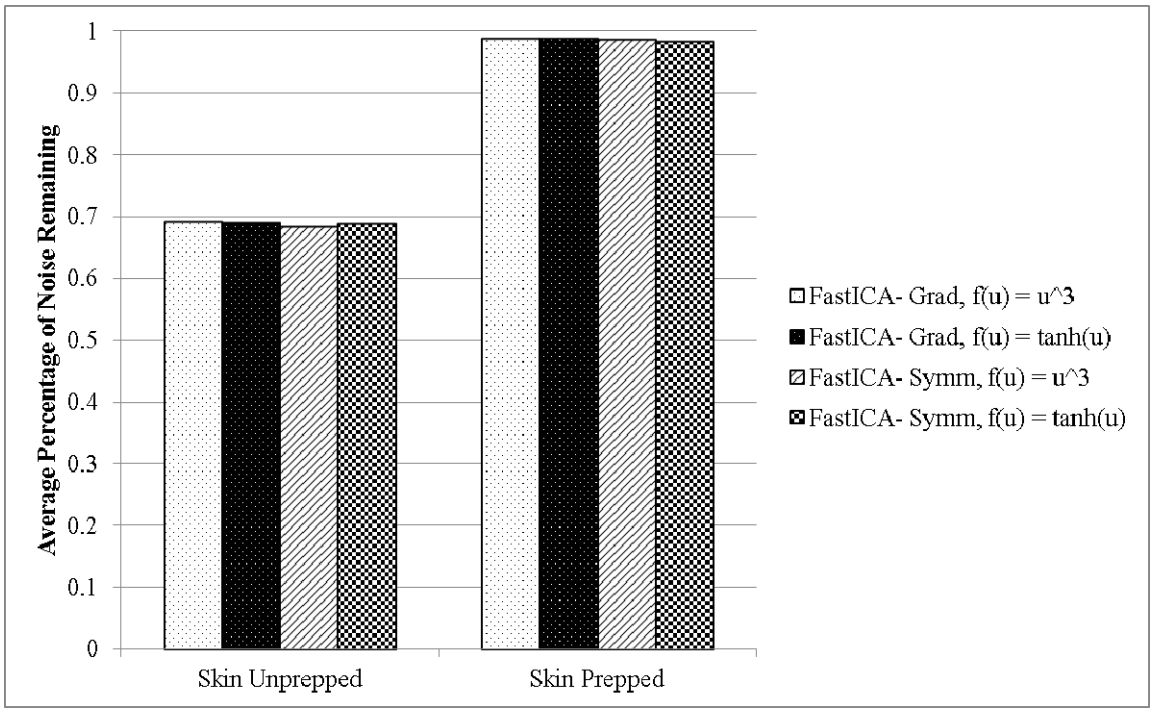

FastICA RLS Skin Preparation, Shared Variables

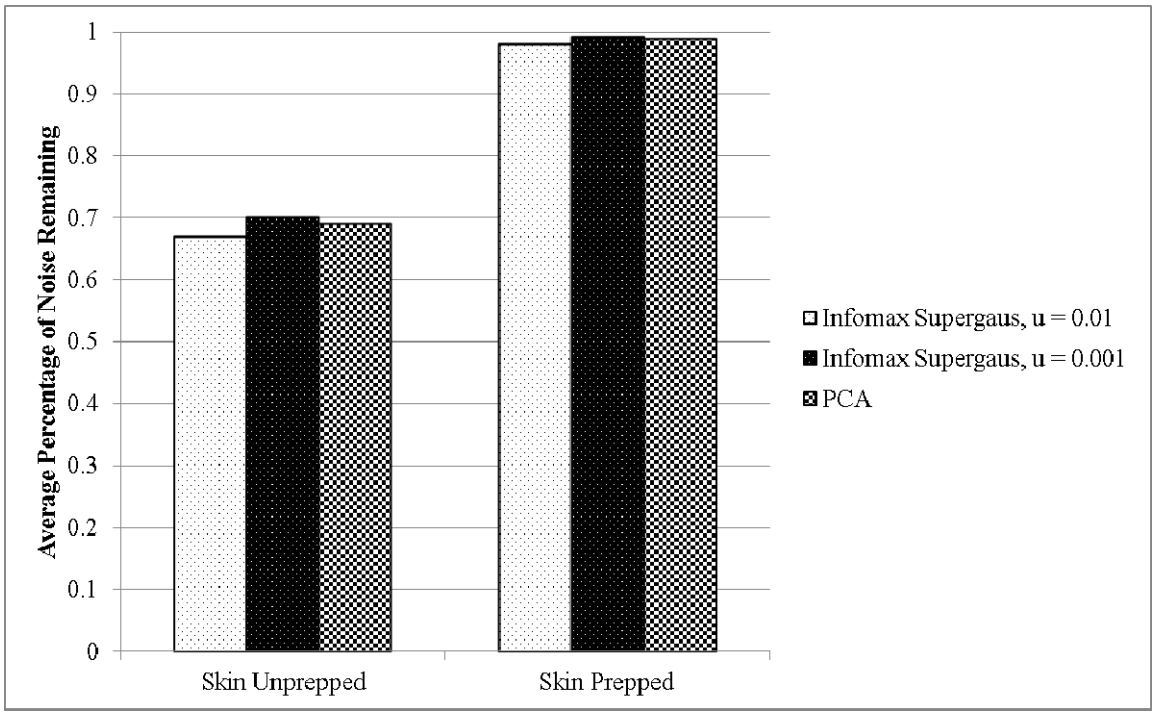

Infomax & PCA RLS Skin Preparation, Shared Variables

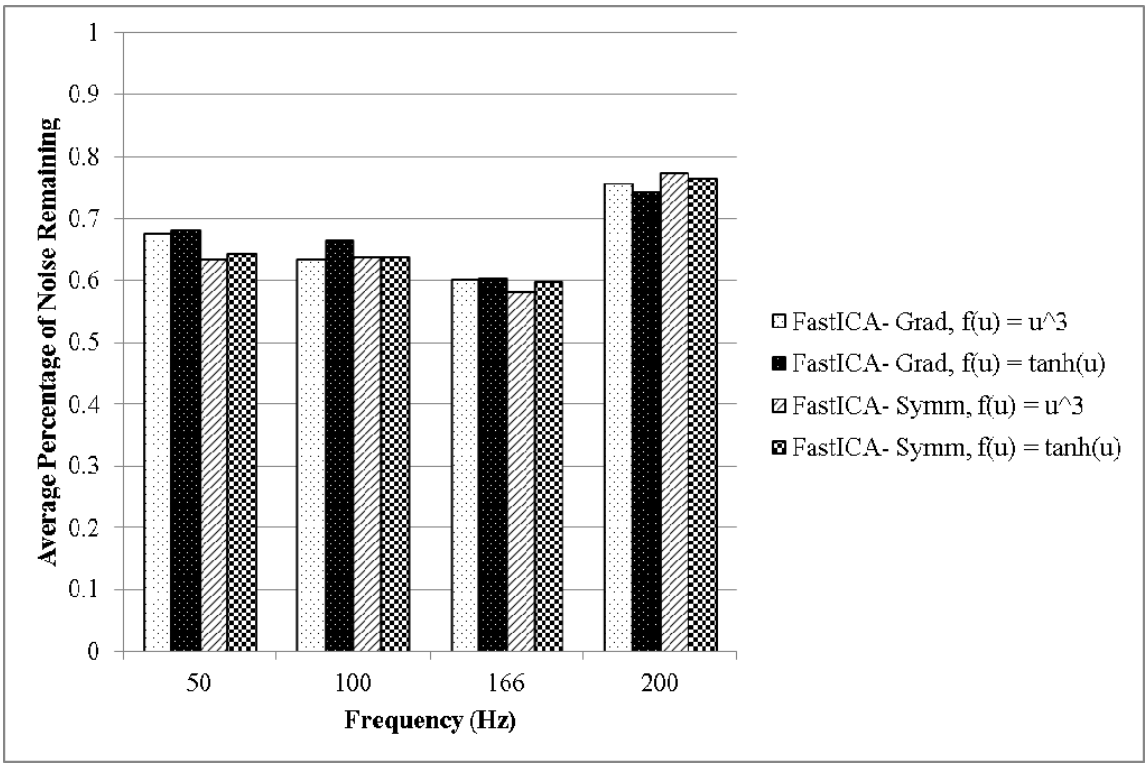

FastICA RLS Sampling Frequency, Shared Variables

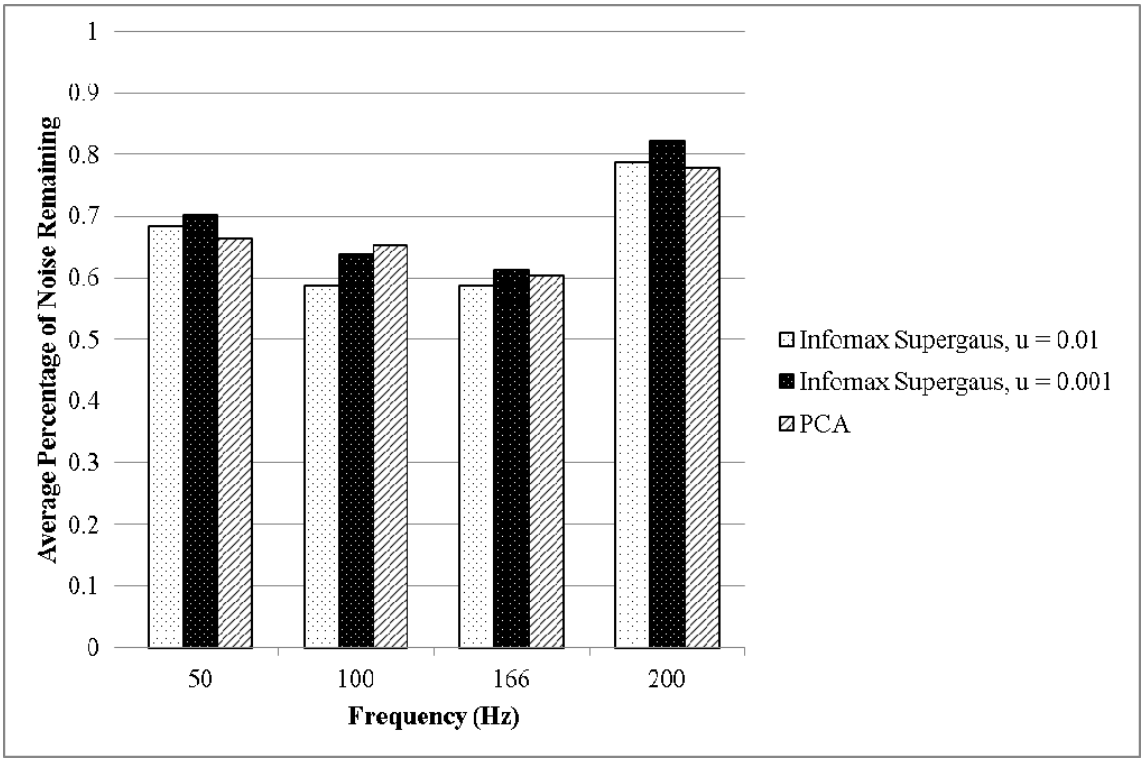

Infomax & PCA RLS Sampling Frequency, Shared Variables

B2.5 LMS vs RLS Optimum Variables

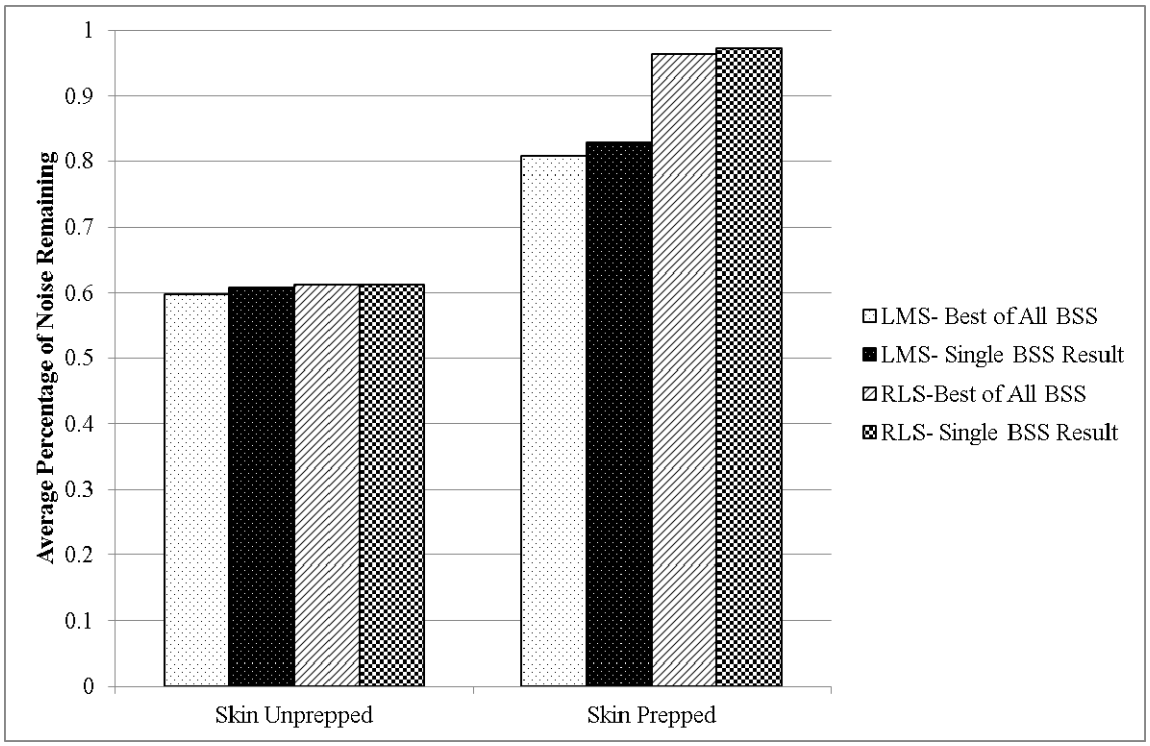

LMS vs. RLS Skin Preparation, Optimum Variables

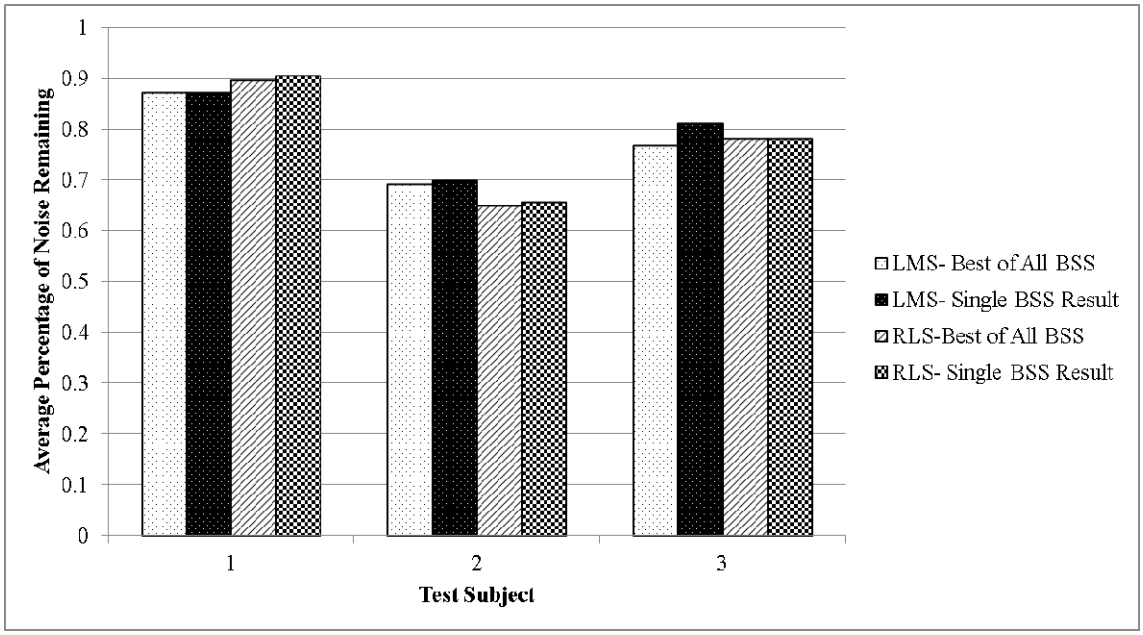

LMS vs. RLS Multiple Users, Optimum Variables

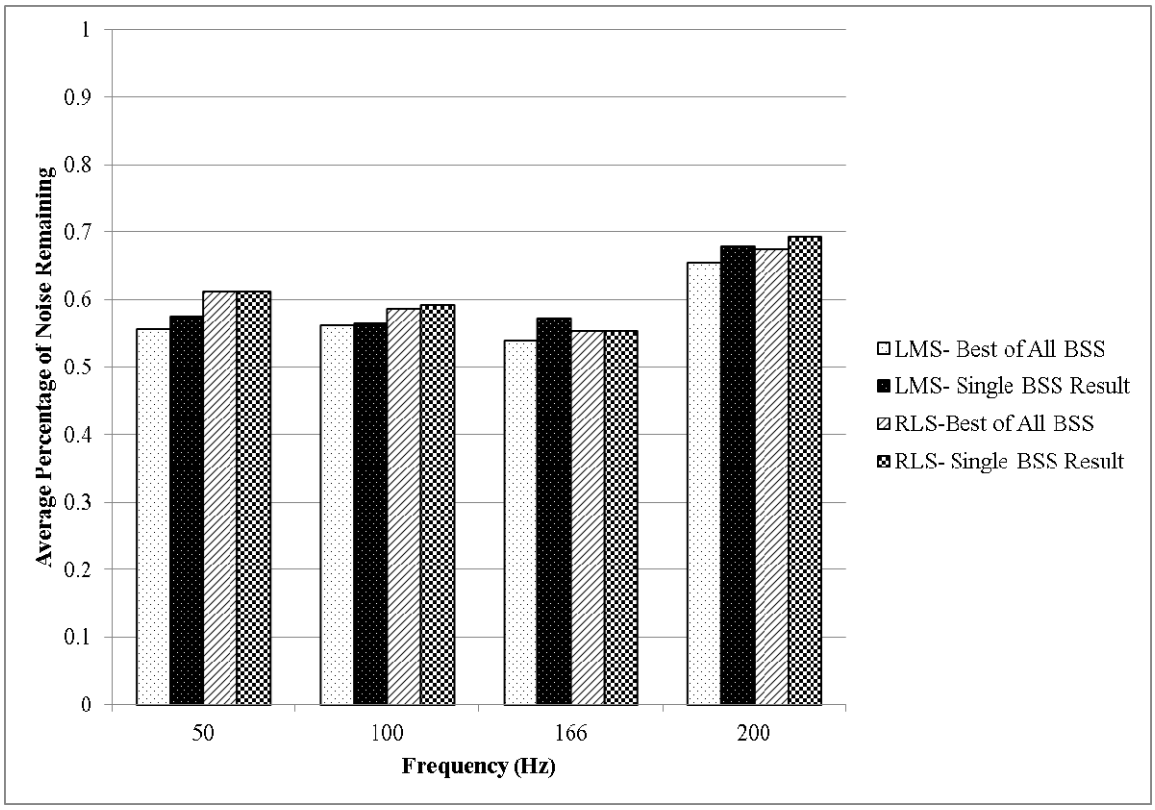

LMS vs. RLS Sampling Frequency, Optimum Variables

B2.6 LMS vs RLS Shared Variables

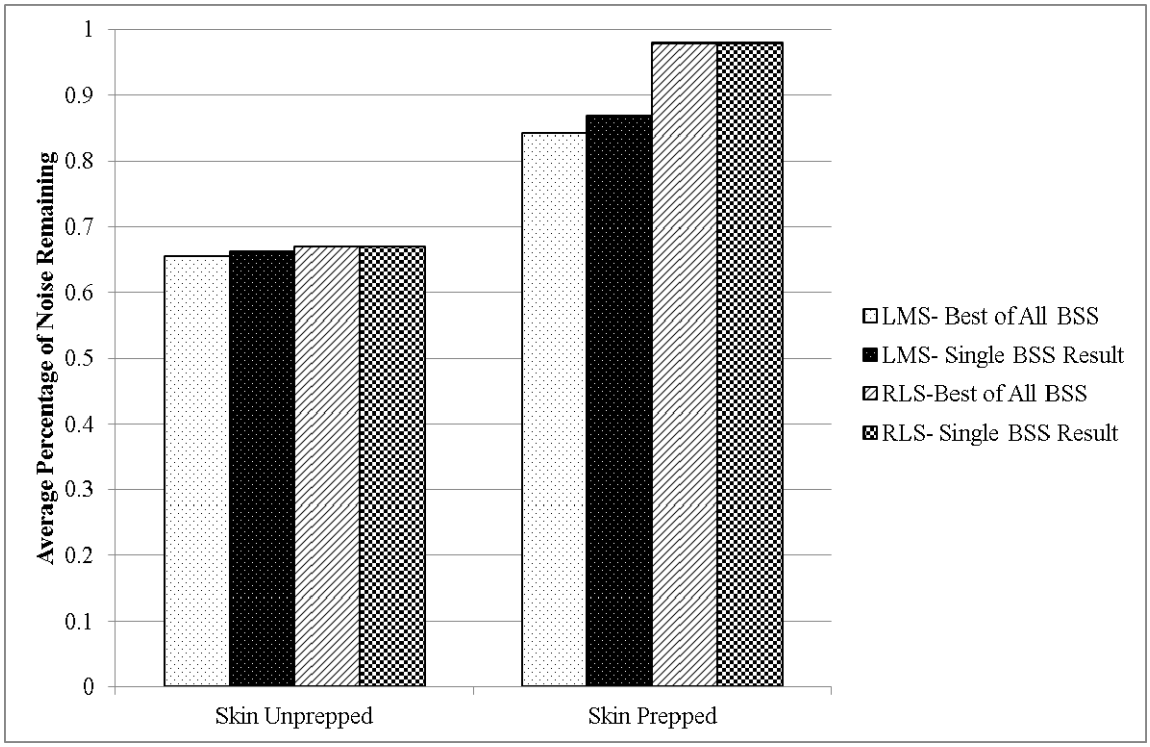

LMS vs. RLS Skin Preparation, Shared Variables

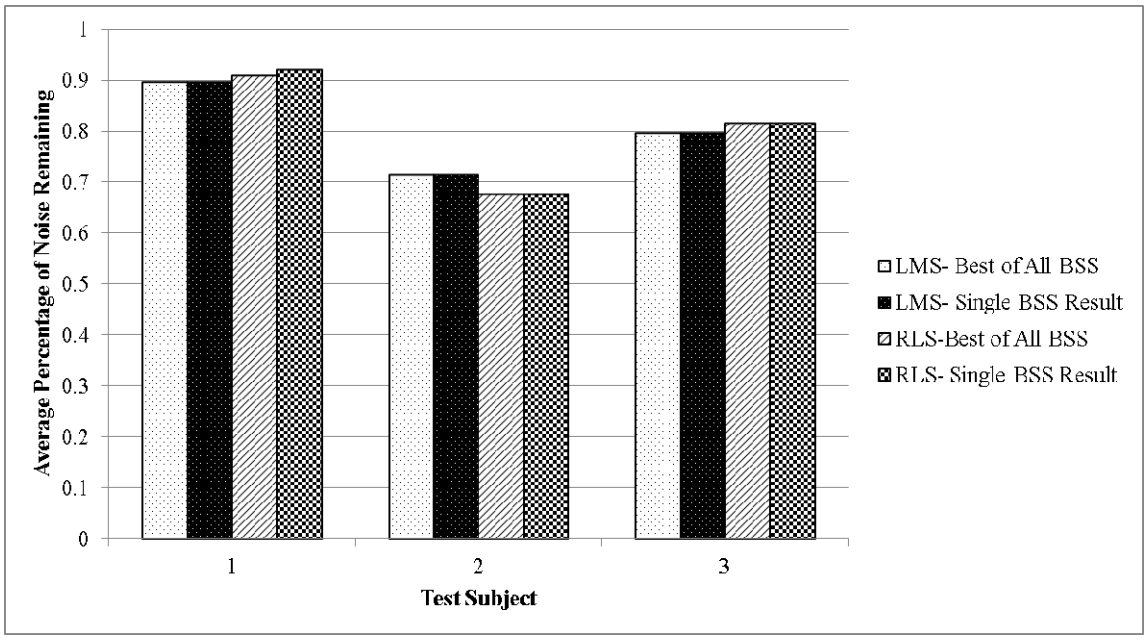

LMS vs. RLS Multiple Users, Shared Variables

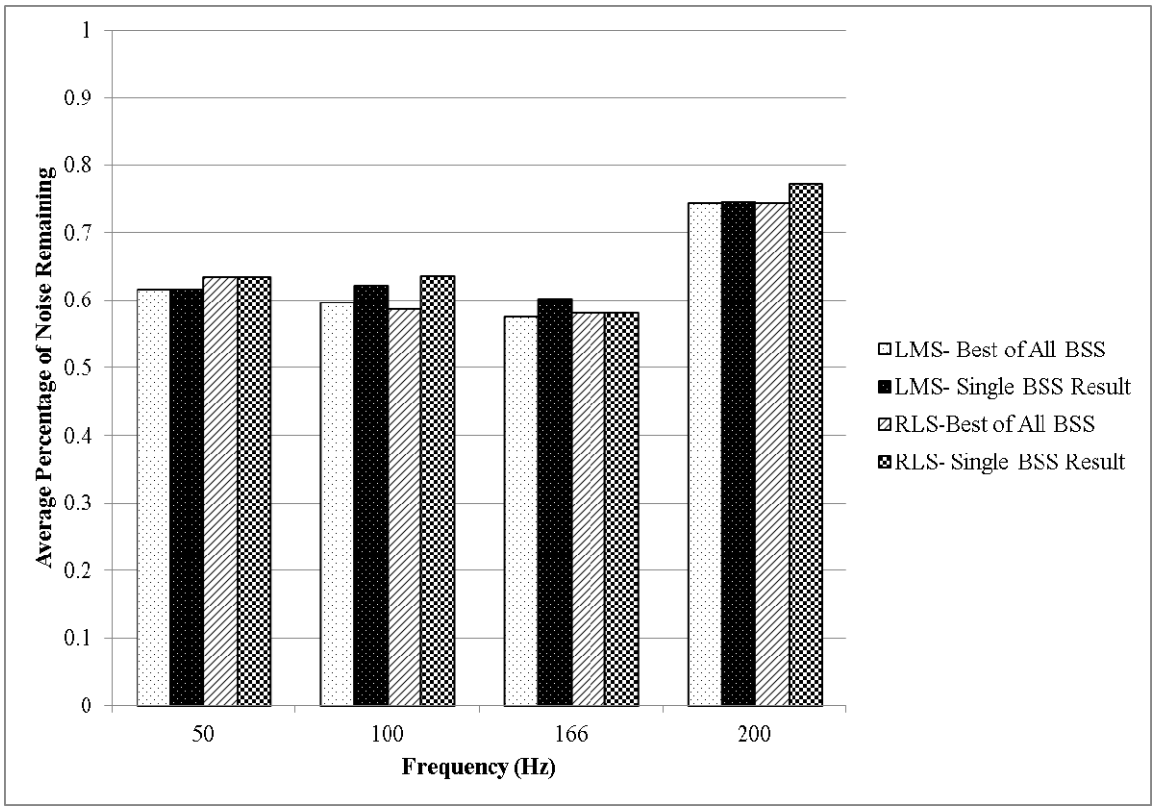

LMS vs. RLS Sampling Frequency, Shared Variables

B3 Comparison of Individual vs Combined

B3.1 Individual vs Combined Sensors – Optimum Variables

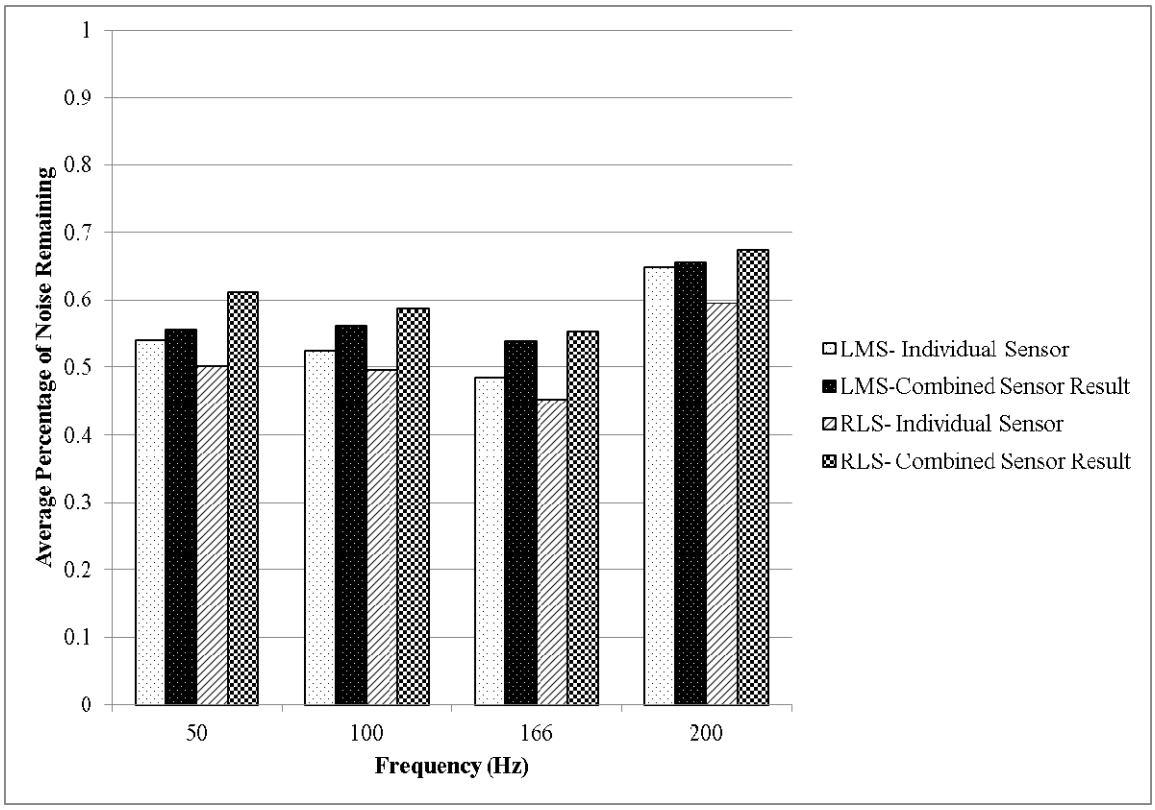

Individual vs. Combined Sensors Sampling Frequencies, Optimum Variables

B3.2 Individual vs Combined Sensors – Shared Variables

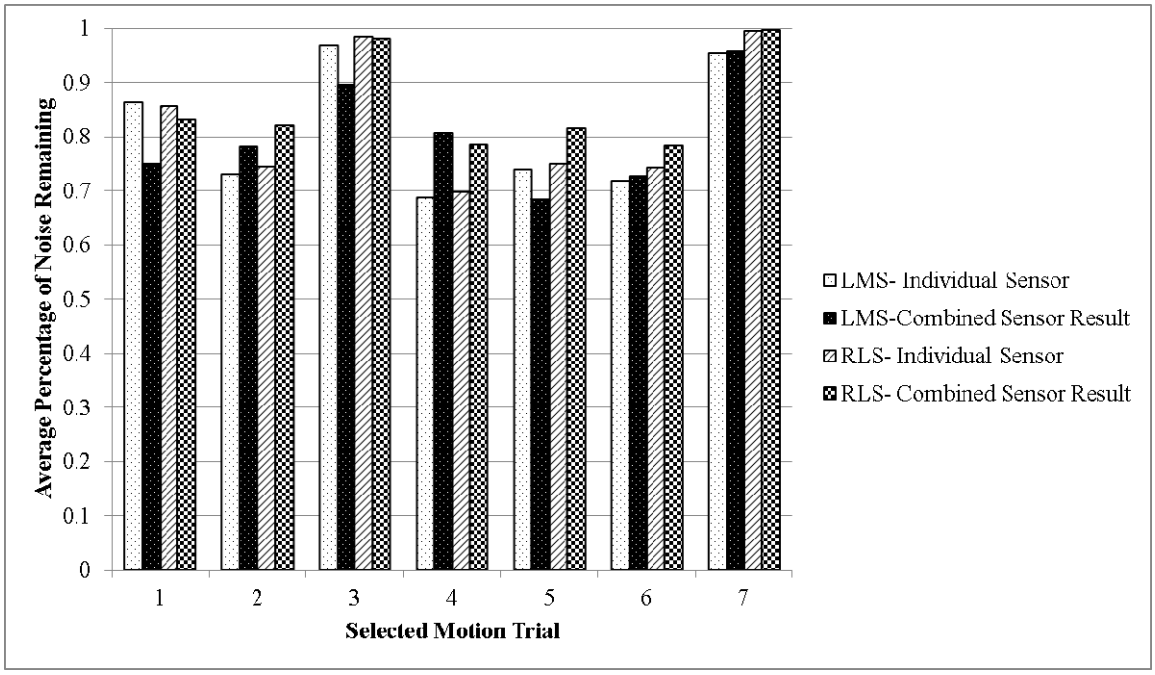

Individual vs. Combined Sensors Experiment 1, Shared Variables

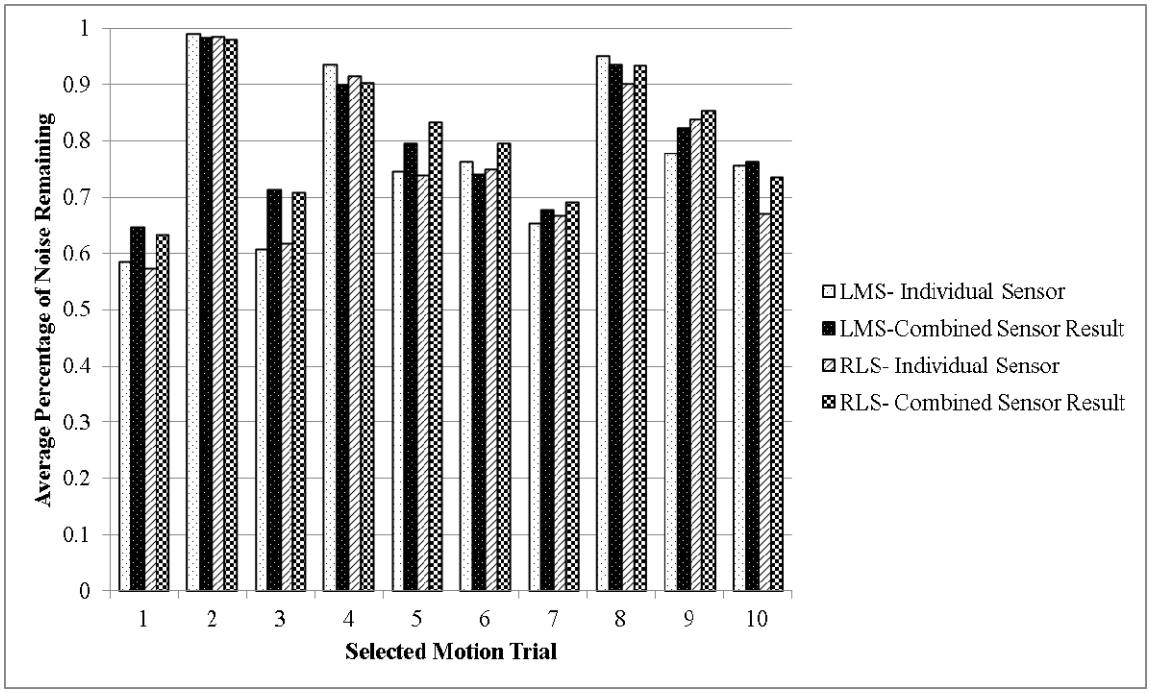

Individual vs. Combined Sensors Experiment 2, Shared Variables

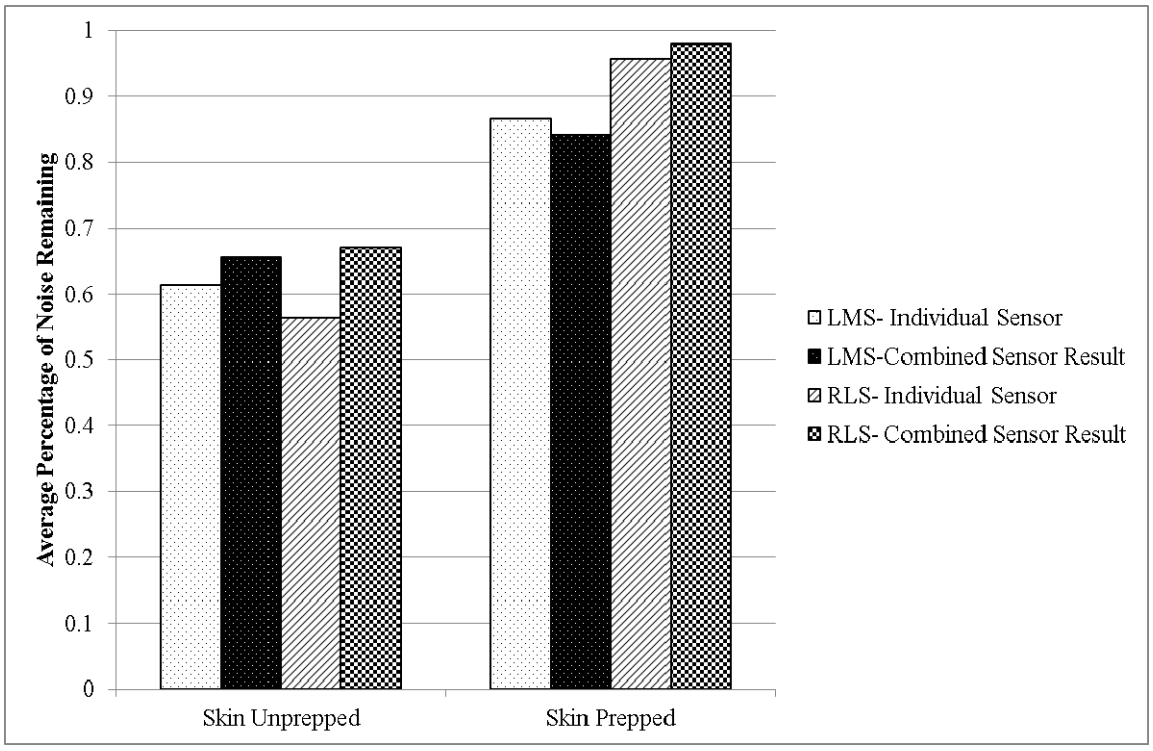

Individual vs. Combined Sensors Skin Preparation, Shared Variables

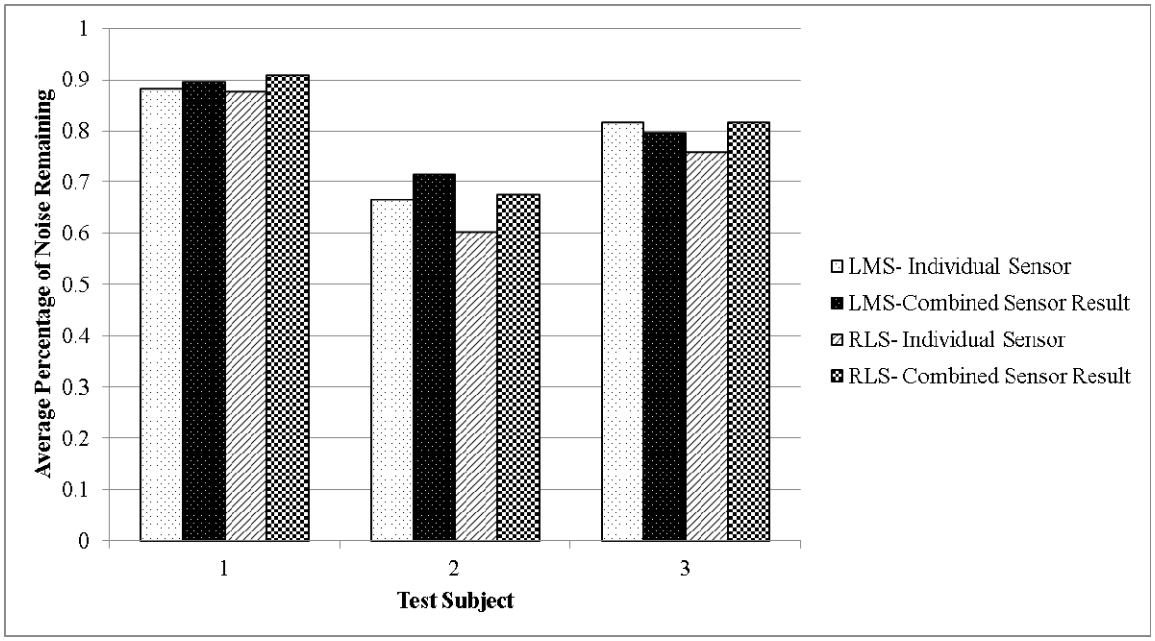

Individual vs. Combined Sensors Multiple Users, Shared Variables

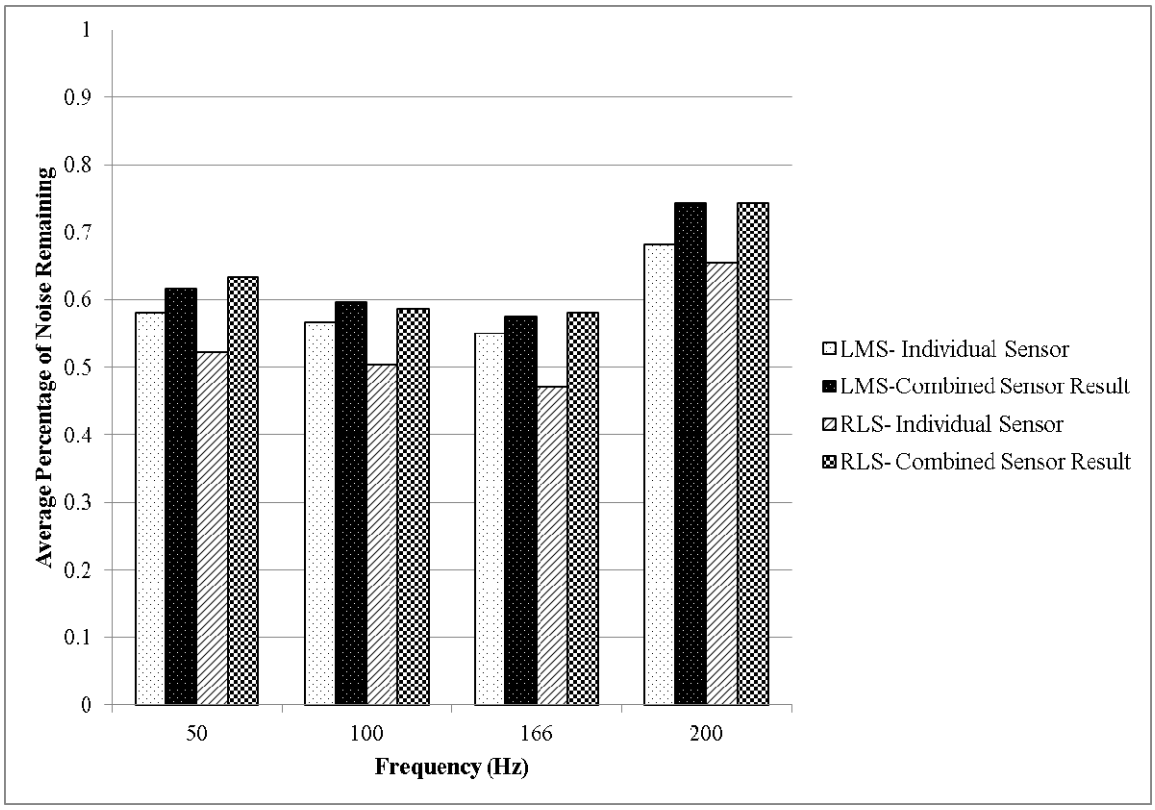

Individual vs. Combined Sensors Sampling Frequencies, Shared Variables

B3.3 Individual vs Combined Sensors – Optimum Variables, Best Average Sensor/Method

B3.3 and B3.4 compares the results using only one sensor or one BSS method for the variable in question. As an example, for Experiment 1, only one of left arm, right arm, or back sensor is selected. It must be used across all trials, even though there may be better results using a different sensor on particular trials. The sensor or BSS method selected is the one that performs best on average across all trials. These results were not included in Chapter 5 as it was already established that the combined results perform significantly worse than individual sensor results. As a comparison basis between individual and combined sensors, it would only have led to the redundant result that individual sensors were performing better than the techniques that attempted to combine the sensors.

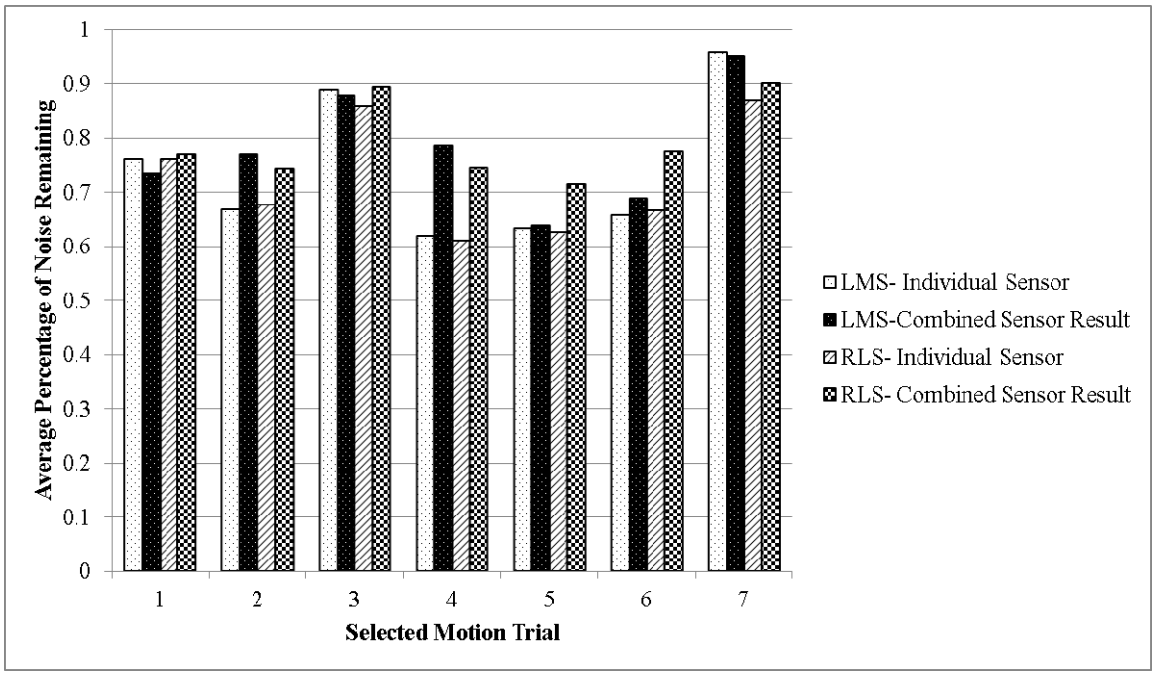

Individual vs. Combined Sensors Experiment 1, Optimum Variables

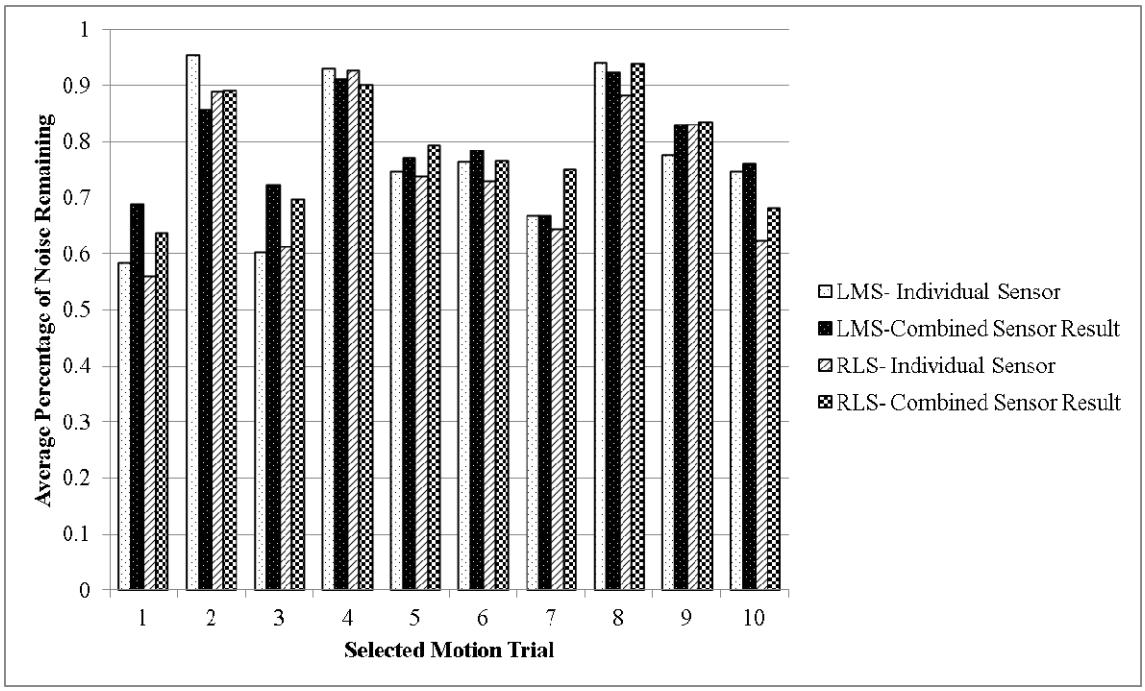

Individual vs. Combined Sensors Experiment 2, Optimum Variables

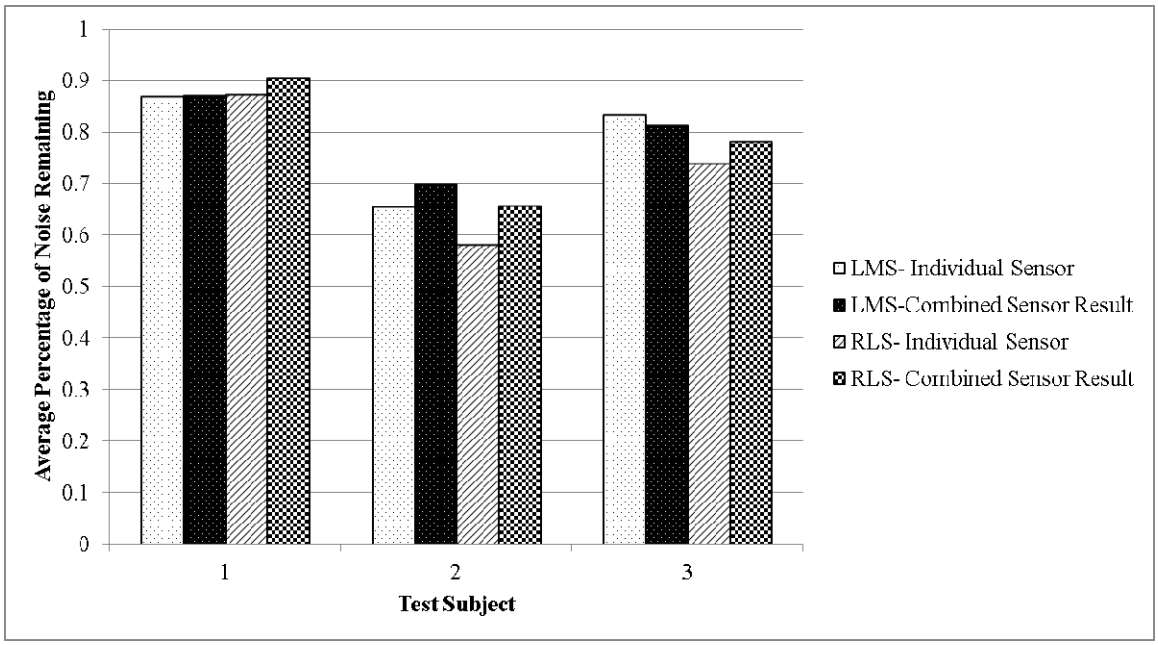

Individual vs. Combined Sensors Multiple Users, Optimum Variables

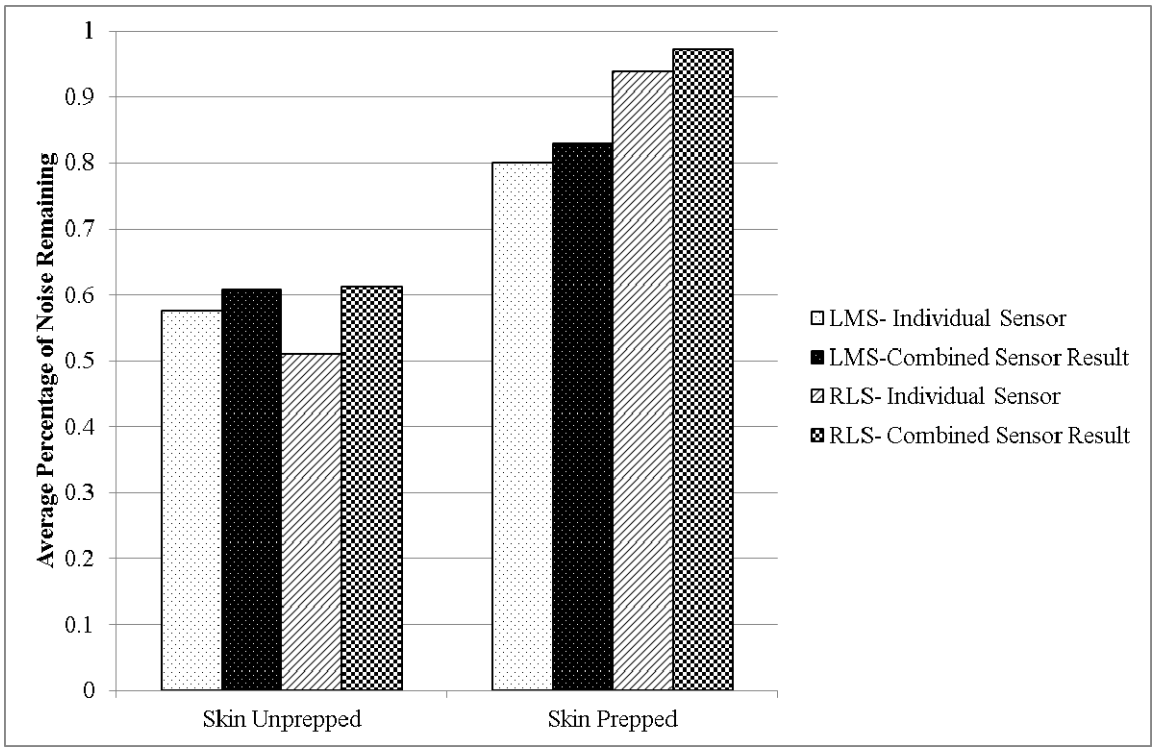

Individual vs. Combined Sensors Skin Preparation, Optimum Variables

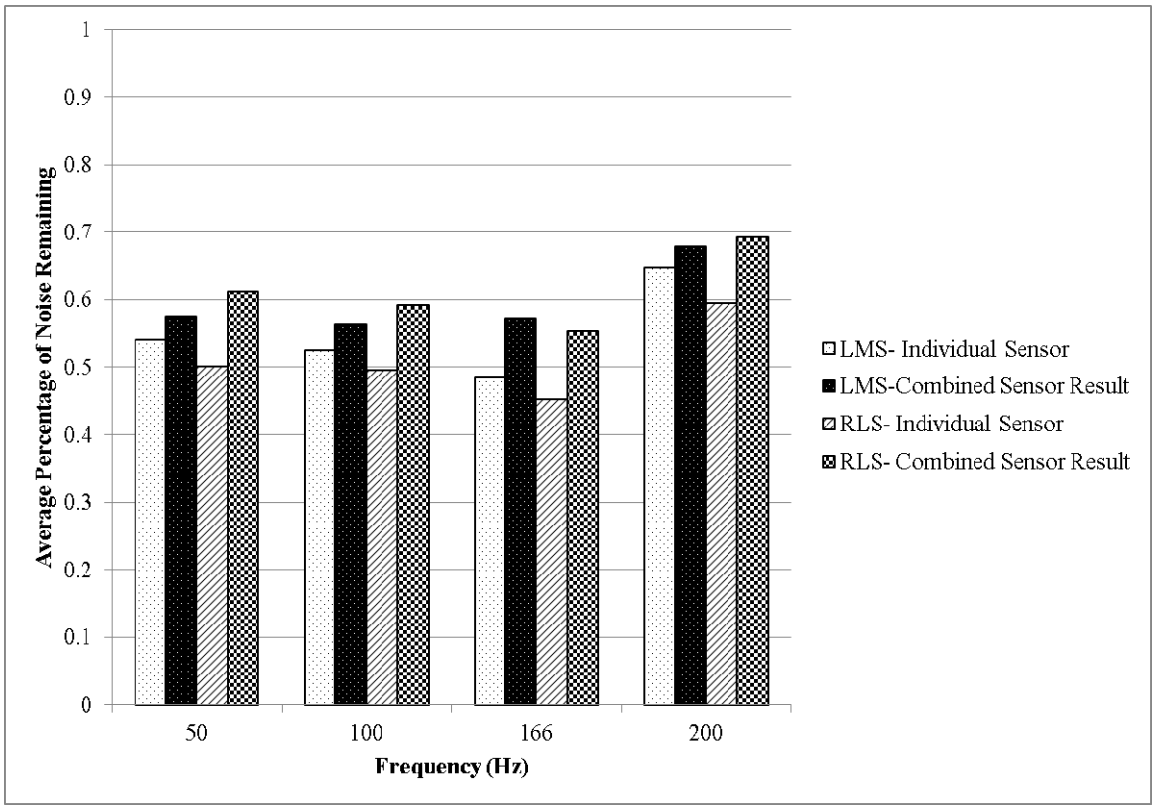

Individual vs. Combined Sensors Sampling Frequency, Optimum Variables

B3.3 Individual vs Combined Sensors – Shared Variables, Best Average Sensor/Method

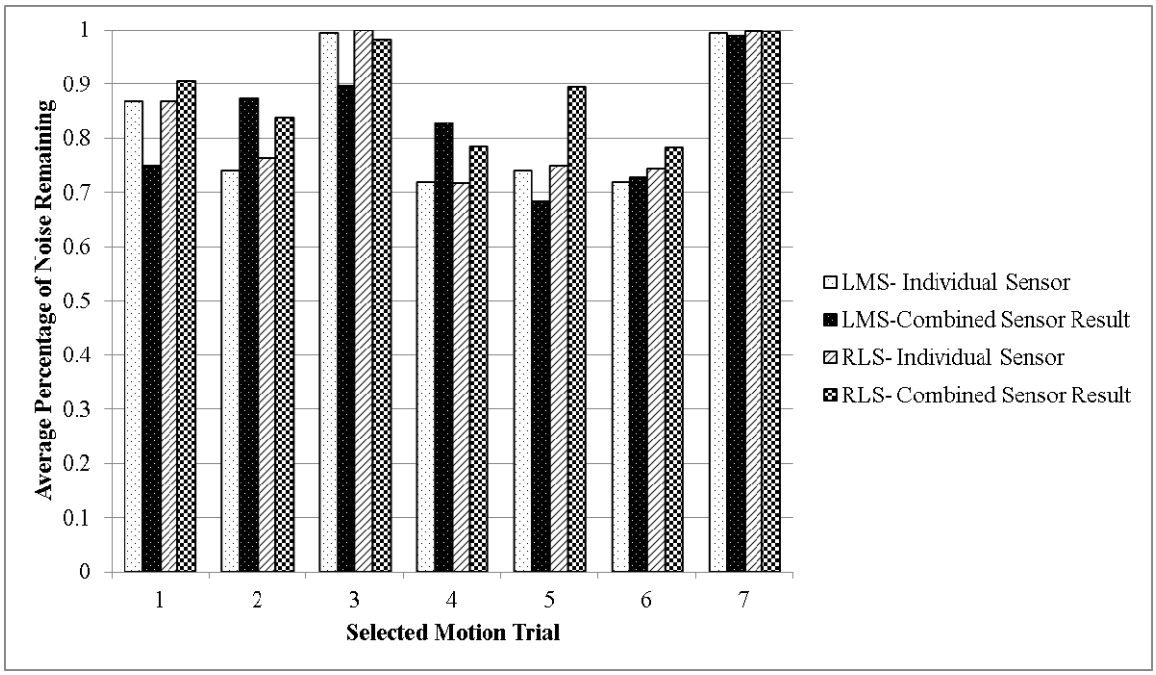

Individual vs. Combined Sensors Experiment 1, Shared Variables

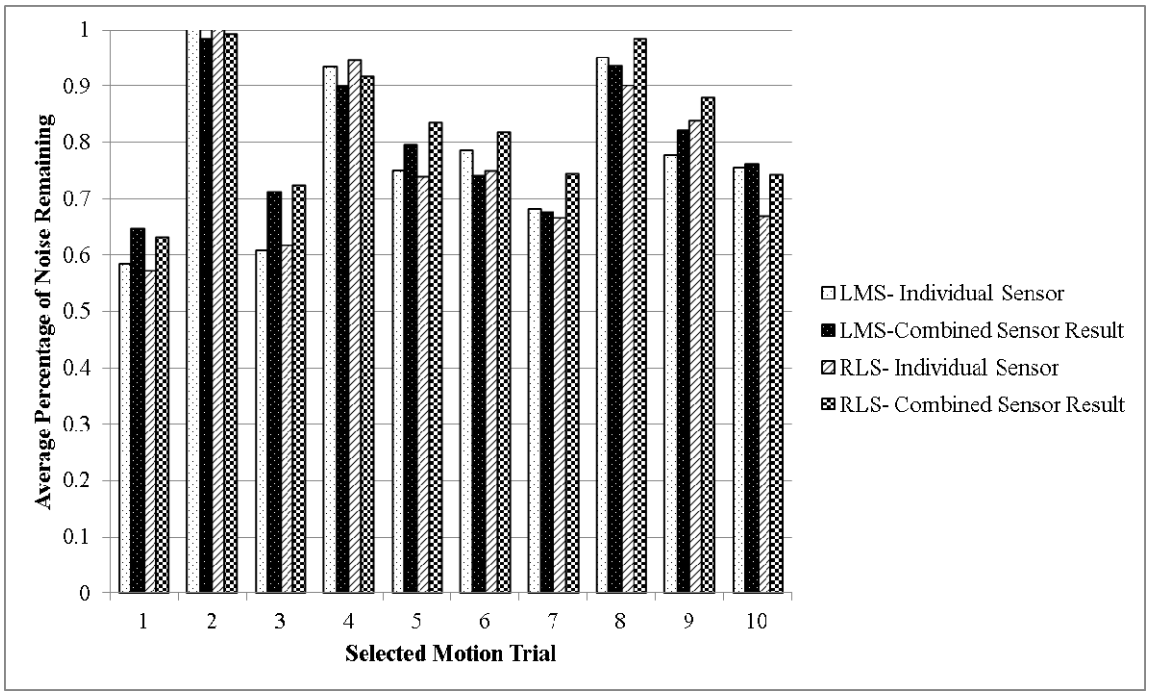

Individual vs. Combined Sensors Experiment 2, Shared Variables

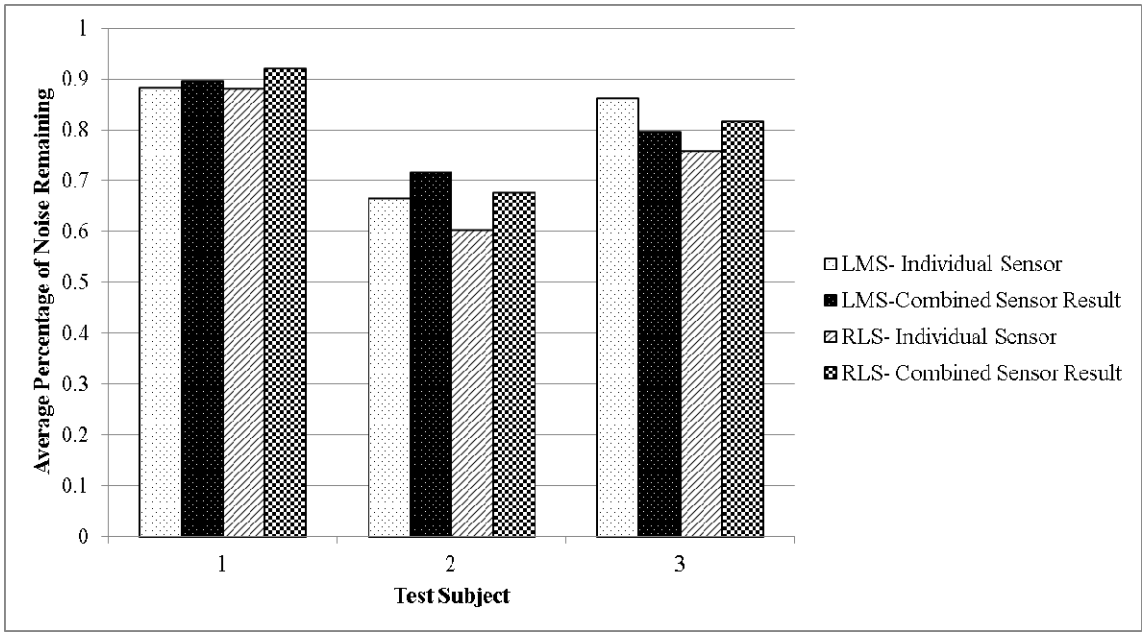

Individual vs. Combined Sensors Multiple Users, Shared Variables

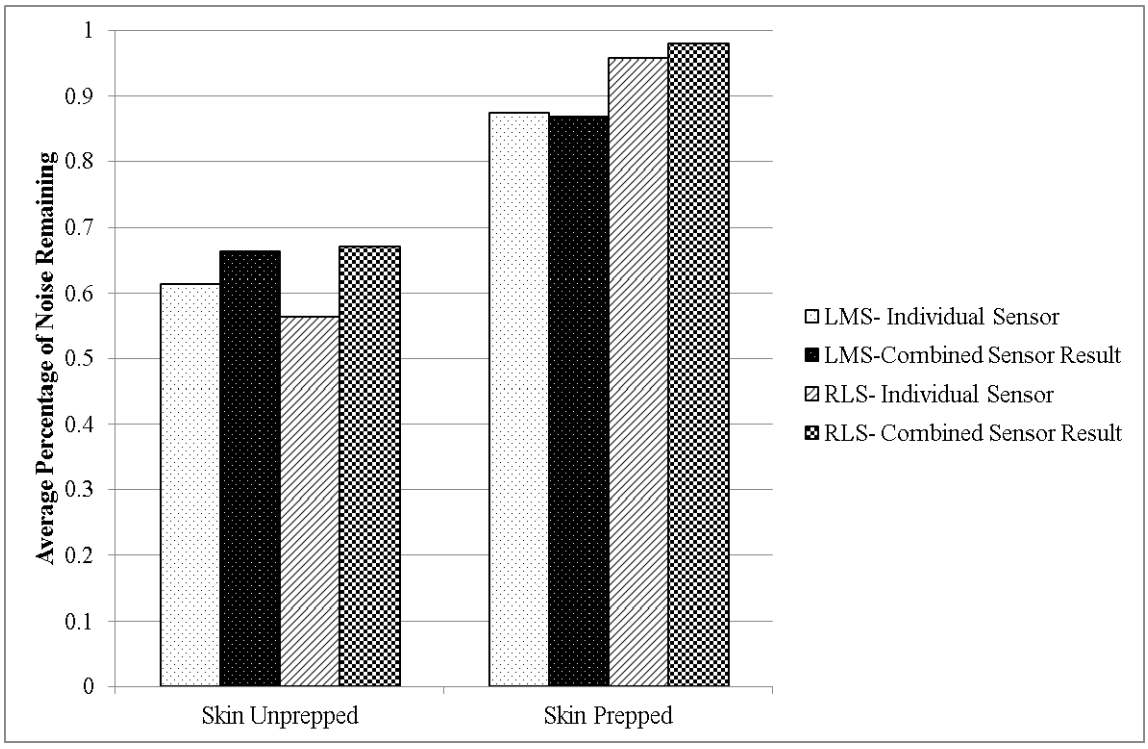

Individual vs. Combined Sensors Skin Preparation, Shared Variables

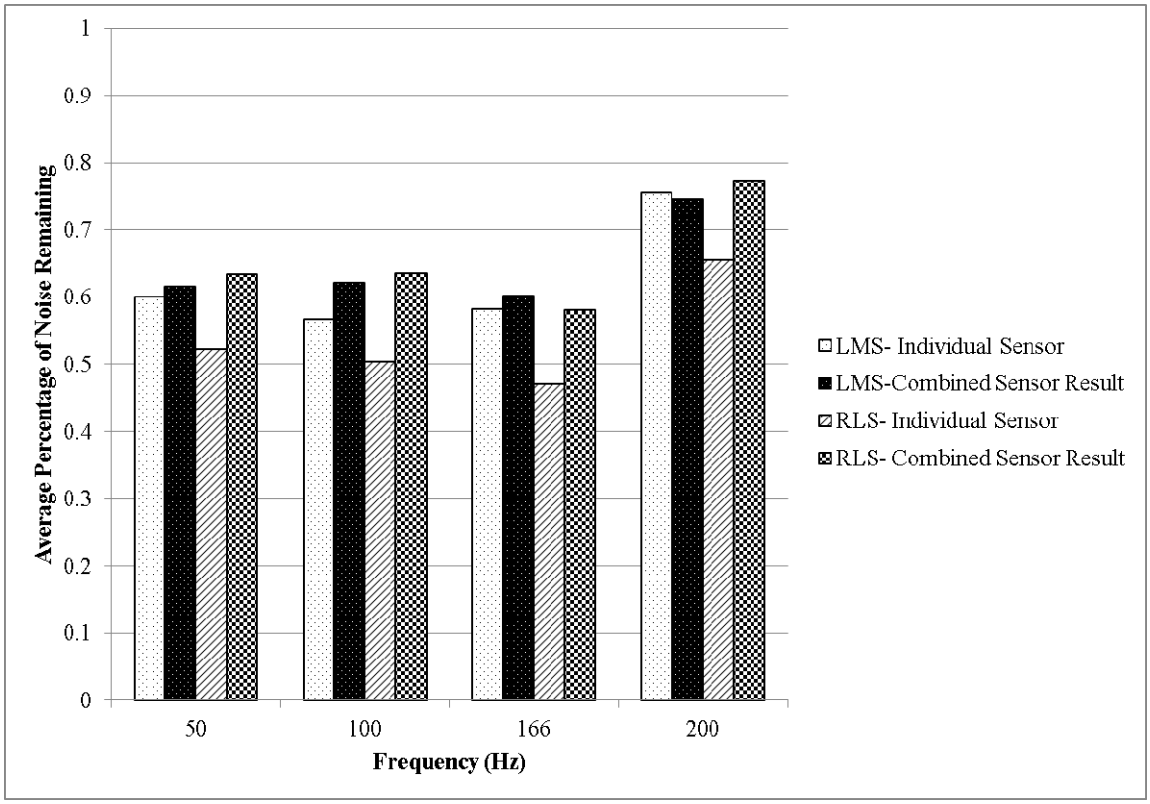

Individual vs. Combined Sensors Sampling Frequency, Shared Variables

Appendix C Motions and Trials

The collected files for analysis are listed below. Repeated motions were separated and analyzed separately. All were repeated 5 times with the exceptions of Walking for experiment 1 (eg. Motions # 1-56), Jogging, and Combination of Movements. The exceptions of Walking and Jogging were performed once at each instance, while Combination of Movements was performed three times per test subject, once per file.

Combination of Movements was performed as follows: Start from lying down. Stand up. Sit down. Bend over. Sit up. Stand up. Walk forward. Bend down from standing. Reach forward. Reach up. Step up onto stool.

Motion #	Motion Performed	Sampling Frequency (Hz)	Skin Prep	Test Subject
1	Sit/Stand	50	No	1
2	Bend (from sitting)	50	No	1
3	Walking	50	No	1
4	Bend (from standing)	50	No	1
5	Reach Forward	50	No	1
6	Reach Up	50	No	1
7	Jogging	50	No	1
8	Sit/Stand	100	No	1
9	Bend (from sitting)	100	No	1
10	Walking	100	No	1
11	Bend (from standing)	100	No	1
12	Reach Forward	100	No	1
13	Reach Up	100	No	1
14	Jogging	100	No	1
15	Sit/Stand	166	No	1
16	Bend (from sitting)	166	No	1
17	Walking	166	No	1
18	Bend (from standing)	166	No	1
19	Reach Forward	166	No	1
20	Reach Up	166	No	1
21	Jogging	166	No	1

22	Sit/Stand	200	No	1
23	Bend (from sitting)	200	No	1
24	Walking	200	No	1
25	Bend (from standing)	200	No	1
26	Reach Forward	200	No	1
27	Reach Up	200	No	1
28	Jogging	200	No	1
29	Sit/Stand	50	Yes	1
30	Bend (from sitting)	50	Yes	1
31	Walking	50	Yes	1
32	Bend (from standing)	50	Yes	1
33	Reach Forward	50	Yes	1
34	Reach Up	50	Yes	1
35	Jogging	50	Yes	1
36	Sit/Stand	100	Yes	1
37	Bend (from sitting)	100	Yes	1
38	Walking	100	Yes	1
39	Bend (from standing)	100	Yes	1
40	Reach Forward	100	Yes	1
41	Reach Up	100	Yes	1
42	Jogging	100	Yes	1
43	Sit/Stand	166	Yes	1
44	Bend (from sitting)	166	Yes	1
45	Walking	166	Yes	1
46	Bend (from standing)	166	Yes	1
47	Reach Forward	166	Yes	1
48	Reach Up	166	Yes	1
49	Jogging	166	Yes	1
50	Sit/Stand	200	Yes	1
51	Bend (from sitting)	200	Yes	1
52	Walking	200	Yes	1
53	Bend (from standing)	200	Yes	1
54	Reach Forward	200	Yes	1
55	Reach Up	200	Yes	1
56	Jogging	200	Yes	1

57	Lie/Stand	50	Yes	1
58	Sit/Stand	50	Yes	1
59	Bend (from sitting)	50	Yes	1
60	Walking	50	Yes	1
61	Bend (from standing)	50	Yes	1
62	Reach Forward	50	Yes	1
63	Reach Up	50	Yes	1
64	Step Onto Stool	50	Yes	1
65	Climb Stairs	50	Yes	1
66	Combination of Movements 1	50	Yes	1
67	Combination of Movements 2	50	Yes	1
68	Combination of Movements 3	50	Yes	1
69	Lie/Stand	50	Yes	2
70	Sit/Stand	50	Yes	2
71	Bend (from sitting)	50	Yes	2
72	Walking	50	Yes	2
73	Bend (from standing)	50	Yes	2
74	Reach Forward	50	Yes	2
75	Reach Up	50	Yes	2
76	Step Onto Stool	50	Yes	2
77	Climb Stairs	50	Yes	2
78	Combination of Movements 1	50	Yes	2
79	Combination of Movements 2	50	Yes	2
80	Combination of Movements 3	50	Yes	2
81	Lie/Stand	50	Yes	3
82	Sit/Stand	50	Yes	3
83	Bend (from sitting)	50	Yes	3
84	Walking	50	Yes	3
85	Bend (from standing)	50	Yes	3
86	Reach Forward	50	Yes	3
87	Reach Up	50	Yes	3
88	Step Onto Stool	50	Yes	3
89	Climb Stairs	50	Yes	3

90	Combination of Movements 1	50	Yes	3
91	Combination of Movements 2	50	Yes	3
92	Combination of Movements 3	50	Yes	3

Trials were grouped as follows.

Experiment 1

Trial	Motion #
1 (Sit down, stand up)	1, 8, 15, 22, 29, 36, 43, 50
2 (Bend down from sitting)	2, 9, 16, 23, 30, 37, 44, 51
3 (Walking in place)	3, 10, 17, 24, 31, 38, 45, 52
4 (Bend down from standing)	4, 11, 18, 25, 32, 39, 46, 53
5 (Reach forward)	5, 12, 19, 26, 33, 40, 47, 54
6 (Reach up)	6, 13, 20, 27, 34, 41, 48, 55
7 (Jogging in place)	7, 14, 21, 28, 35, 42, 49, 56

Experiment 2

Trial	Motion #
1 (Lie down, stand up)	57, 69, 81
2 (Sit down, stand up)	58, 70, 82
3 (Bend down from sitting)	59, 71, 83
4 (Walking)	60, 72, 84
5 (Bend down from standing)	61, 73, 85
6 (Reach forward)	62, 74, 86
7 (Reach up)	63, 75, 87
8 (Step onto stool)	64, 76, 88
9 (Climb stairs)	65, 77, 89
10 (Combination of movements)	66, 67, 68, 78, 79, 80, 90, 91, 92

Skin Preparation

Skin Prepped	Motions 1-28 inclusive
Skin Unprepped	Motions 29-56 inclusive

Test Subject

Test Subject 1	Motions 57-68 inclusive
Test Subject 2	Motions 69-80 inclusive
Test Subject 3	Motions 81-92 inclusive

Sampling Frequency

50 Hz	Motions 1-7 & 29-35 inclusive
100 Hz	Motions 8-14 & 36-42 inclusive
166 Hz	Motions 15-21 & 43-49 inclusive
200 Hz	Motions 22-28 & 50-56 inclusive